PhD-FSTC-2015-33
The Faculty of Sciences, Technology and Communication

DISSERTATION

Defense held on 09/07/2015 in Luxembourg

to obtain the degree of

DOCTEUR DE L'UNIVERSITÉ DU LUXEMBOURG

EN SCIENCE DE L'INGÉNIEUR

by

Patricia Cristina BENITO MARTIN
Born on 26th August 1979 in Madrid (SPAIN)

MESOPHILIC ANAEROBIC DIGESTION OF LIGNOCELLULOSIC SUBSTRATES UNDER DIFFERENT OPERATING MODES AND EXTREME FEEDING CONDITIONS – OPTIMISATION AND MODELLING

Dissertation defense committee

Dr. Ing. Manfred Greger, dissertation supervisor
Professor, University of Luxembourg

Dr. Stephan Leyer, Chairman
Professor, Université du Luxembourg

Dr. Ing. Stijn Van Hulle, Vice Chairman
Professor, Ghent University

Dr. Ing. Marco Ragazzi
Professor, University of Trento

Dr. Thomas Sauter
Professor, University of Luxembourg

Dr. Ing. Nonjabulo Sibisi-Beierlein
Expert

Abstract

The main objectives of this PhD project were two-fold: to perform an extensive comparative study of the effects of different operational parameters on the performance and stability of the digestion of lignocellulosic material, and to develop a model well adapted to describe this process, using the acquired experimental data, and on the basis of the widely applied ADM1 model. This model had to integrate current knowledge and previously identified limitations.

Experimental work covered a wide range of operational conditions, including batch and semi-continuous feeding conditions, increasing loading and different feedstock composition (different silages of maize and grass, and mixtures of them, different carbohydrates as cellulose, starch, and glucose, and intermediate products of the fermentation such as acetate and propionate) under mesophilic conditions.

The results highlighted the resilience of batch systems to increasing loadings. Poorer stability and performance in the fermentation process was found for the batch digestion of grass silage at extreme feeding conditions (i.e. loadings up to 46 gVS/l), but the systems could recover and failure was not observed. For semi-continuous feeding and with addition of trace elements, the performance of the process in terms of biogas production was affected to a different extent depending on the substrate. Indeed, while in the case of grass silage an increase from 1.9 to 4.7 gVS/l/d, resulted in a minor impact on the methane yield (with a decrease of approximately 13%), in the case of maize silage, an increase from 2 to 3.5 gVS/l/d resulted in an 18.2% reduction in the methane yield. Signs of overloading-induced instabilities were observed at loadings of 6 gVS/l/d, which worsen for a loading of 10 gVS/l/d, with peaks of hydrogen content in the biogas up to 5%.

The optimum organic loading rate can only be determined considering the specific feedstock and operational conditions. In semi-continuous feeding conditions, the addition of trace element solution allowed to increase the maximum organic loading rate at which stable and inhibition-free operation was feasible to 3.7 gVS/l/d for grass silage and to 3.5 gVS/l/d for maize silage (beyond levels previously suggested as problematic in literature without the addition of micro-nutrients).

The feasibility and performance of applying a pH-phased two-stage configuration to the digestion of maize silage was analysed. This type of configuration can contribute to optimise the process by compartmentalizing it and better meeting the environmental and operational requirements of the different bacterial groups. It was found that when the first reactor was operated at an average pH of 5.17, there was a significant increase of volatile fatty acids and hydrogen content in the biogas, up to an average of 35%, while the methane production ceased. Of the estimated total energy produced per kg of VS added in the two-stage system, only 5% was from hydrogen production. Therefore, there is a potential to additionally improve the H_2 production and thus the energy yield for this type of configuration when using lignocellulosic material (by regulating the pH, for example).

To monitor the advancement of the degradation process, different experimental methods, originally applied in the field of wastewater treatment had to be modified for the analysis

of certain parameters, such as the chemical oxygen demand, which is difficult to measure in the case of heterogeneous and solid substrates, including samples with high solids content. The chemical Van Soest method, commonly used in the field of animal food analysis, was found not to be applicable to monitor the digestion of the different structural carbohydrates. Alternatively, the Anthrone method was adapted to monitor the degradation of polysaccharides and monosaccharides in the biogas reactors.

Two distinct models were developed to describe the anaerobic digestion of lignocellulosic material: the Lignogas model, and the lighter version, the Lignogas-SIM. Both models address some of the known limitations of the ADM1 model, take into account specific substrate characteristics, and are intended to be applicable in a wide variety of operational conditions. These models contain the same inhibition terms than ADM1, but some were adapted to better simulate selected variables.

The Lignogas model is an extended version of the ADM1 model and tries to integrate current knowledge about the microbial composition in biogas plants. It includes acetate oxidation to promote the hydrogenotrophic methanogenesis and a dedicated variable for the decayed biomass to close the carbon and nitrogen balance. Moreover, the impact of considering the influence of the hydrolysis of carbohydrates for the fast and the slow degradable fractions was investigated with this model. The Lignogas-SIM, on the other hand, is a simplified version of the ADM1 model that does not consider the butyrate and valerate and in which all monomers produced during hydrolysis are lumped in one variable.

One of the novelties of the developed models is that they are tested and evaluated using experimental data from extreme loading or pH conditions, which helps to evaluate their strengths and weaknesses.

Both models fitted satisfactory experimental data for the lower organic loadings for a variety of substrates and feeding modes. In the case of the Lignogas-SIM, the quality of the simulations worsened for extreme loading conditions, often as a result of the simulated free ammonia inhibition of acetogens. Overall, the Lignogas model displayed better agreement between simulation results and measurements, particularly under semi-continuous feeding conditions and for extreme loadings. Considering acetate oxidation contributes to increase the share of hydrogenotrophic methanogens. Nevertheless, it is still necessary to investigate ways to modulate their presence depending on the concentration of acetate and inhibitory substances. After adapting some of the inhibition factors, the Lignogas model was capable of simulating the drop in the methane content and the increase of the H_2 content during semi-continuous digestion of maize silage, and thus the instability associated with the high loading, but it was not capable of modulating the shift. One of the main limitations to properly model and optimise the production of H_2 with the Lignogas model seems to lay in the fermentation of glucose. Indeed, the stoichiometric parameters for glucose fermentation products are fixed and should be regulated depending on the pH and H_2 concentration, although their influence is still not well understood. This could also contribute to better adapt the model to existing knowledge about microbial population abundance. Moreover, future efforts should also focus on the inhibition mechanisms and factors, particularly for acetogens.

Résumé

L'objectif principal de cette thèse de doctorat était double : effectuer une vaste étude comparative des effets de différents paramètres opérationnels sur la performance et la stabilité du processus de digestion anaérobique de matière lignocellulosique, et développer un modèle adapté décrivant le processus en utilisant des données expérimentales et sur la base du modèle ADM1 déjà largement adopté. Ce nouveau modèle a dû prendre en compte les connaissances sur le sujet et les limitations identifiées auparavant.

Le travail expérimental a couvert des conditions opérationnelles très diverses, incluant des conditions d'alimentation de type batch (par lot) et semi-continue, avec un taux de charge organique croissant et en variant la composition de matière première (différents ensilages de maïs et d'herbes différents, mélanges des deux, différents carbohydrates en tant que cellulose, amidon, et glucose, et produits intermédiaires de fermentation tel que l'acétate et propionate) sous conditions mésophiles.

Les résultats ont mis en évidence la capacité d'adaptation du system batch à des taux de charge organique très élevés. Une stabilité et une performance moindre ont été constatées pour la digestion d'ensilage d'herbe dans des conditions de charge extrême (avec charges jusqu'à 46 gVS/l), mais le système a pu se rétablir et aucune perturbation permanente n'est apparue. Pour la charge de type semi-continu avec addition de micronutriments, la performance du processus, en termes de production de biogaz, a été affectée à différents niveaux dépendants du substrat. En effet, tandis que dans le cas d'ensilage d'herbe, une augmentation de 1,9 à 4,7 gVS/l/d, a produit un impact mineur sur le rendement de production de méthane (avec une de 13%), dans le cas d'un ensilage de maïs, une augmentation du taux de charge de 2 à 3,5 gVS/l/d a produit une réduction de 18,2% du rendement. Des signes d'inhibition ont été observés avec le taux de charge de 6 gVS/l/d, qui s'aggravent pour des charges à 10 gVS/l/d, avec des pics de jusqu'à 5% de concentration d'hydrogène dans le biogaz.

Le taux de charge organique optimale ne peut être déterminé qu'en considérant la matière première spécifique et les conditions opérationnelles. Dans des conditions d'alimentation semi-continue, le rajout d'une solution avec micronutriments permet d'augmenter le taux maximal de charge organique à laquelle l'opération stable et sans inhibition fût faisable à 3,7 gVS/l/d pour un ensilage d'herbes et à 3,5 gVS/l/d pour un ensilage de maïs (plus haut que les niveaux suggérés comme problématiques sans l'addition de micronutriments).

La faisabilité et la performance d'une configuration à deux étapes différenciées par le pH pour la digestion d'ensilage de maïs a été analysée. Ce type de configuration peut contribuer à optimiser le processus en le compartimentant et en mieux satisfaisant les besoins opérationnels des différents groupes de bactéries. Lorsque le premier réacteur était opéré à un pH compris entre 5 et 5,5, il y avait une augmentation importante d'acides gras volatiles et d'hydrogène contenus dans le biogaz, jusqu'à une moyenne de 35%, tandis que la production de méthane s'était arrêtée.

Afin de surveiller l'avancement du processus de dégradation, différentes méthodes expérimentales, d'habitude utilisées dans le domaine des traitements d'eaux usées, ont dû

être modifiées pour l'analyse de certains paramètres, telle que la demande biochimique en oxygène, difficile à mesurer dans le cas de substrats hétérogènes et solides, et les échantillons avec des contenus élevés en solides. La méthode chimique Van Soest, communément utilisée dans le domaine de l'analyse de nourriture animale, n'a pas pu être applicable pour caractériser la digestion de polysaccharides et monosaccharides dans les réacteurs biogaz. En alternative, la méthode Anthone a été adaptée.

Deux modèles distincts ont été développés pour décrire la digestion anaérobique de matériel lignocellulosique : le modèle Lignogas et sa version simplifiée, le Lignogas -SIM. Les deux modèles adressent certaines des limitations du modèle ADM1, prennent en compte les caractéristiques spécifiques du substrat et sont prévus pour être applicable à une large variété de conditions opérationnelles. Ces modèles contiennent les mêmes termes d'inhibition que l'ADM1, mais certains ont été adaptés pour mieux simuler les variables.

Le modèle Lignogas est une version étendue du modèle ADM1 et essaie d'intégrer les connaissances actuelles de la composition microbienne dans les installations de méthanisation. Cela inclut l'oxydation d'acétate pour favoriser la méthanogénèse hydrogénotrophique et une variable dédiée aux microorganismes morts afin de fermer le bilan de masse du carbone et de l'azote. De plus, l'impact de la prise en compte des constantes d'hydrolyse distinctes pour les fractions des carbohydrates dégradables rapidement et lentement a été étudié dans ce modèle. D'un autre côté, le Lignogas-SIM est une version simplifiée du modèle ADM1 qui ne considère ni le butyrate ni le valérate et dans lequel tous les monomères produits lors de l'hydrolyse sont réunis en une variable. Une des nouveautés des modèles développés est qu'ils sont testés et évalués en utilisant des données expérimentales de conditions de charge ou pH extrêmes, ce qui aide à évaluer leurs forces et faiblesses.

Les deux modèles ont décrit de façons satisfaisantes les données expérimentales dans le cas de charge organiques faibles pour une variété de substrats et de modes d'alimentation. Dans le cas du Lignogas-SIM, la qualité des simulations se dégradent pour des conditions de charge extrême, souvent dû à l'inhibition simulée pour les acétogènes par la concentration d'ammoniac élevée. Le modèle Lignogas affiche de meilleure performance, en particulier en alimentation semi-continue et sous des conditions de charge extrême. La prise en compte de l'oxydation de l'acétate contribue à augmenter la part de méthanogènes hydrogénotrophiques. Cependant, il reste nécessaire d'investiguer différentes façons de moduler leur présence en fonction de la concentration d'acétate et d'inhibiteurs. Après avoir adapté certains facteurs d'inhibition, le modèle Lignogas était capable de simuler la baisse de CH_4 et d'augmenter l'H_2 lors de la digestion semi-continue d'ensilage de maïs avec les charges élevées, mais il n'était pas capable de contrôler le changement. Une des principales limitations pour modéliser et optimiser proprement la production d'H_2 avec le modèle Lignogas semble reposer dans l'acidification du glucose. En effet, les paramètres des produits de fermentation de glucose sont fixes et doivent être régulés en fonction du pH et de la concentration d'H_2, bien que leurs influences ne soient pas très bien comprises. Ceci pourrait contribuer à mieux adapter le modèle aux connaissances actuelles sur l'abondance de population microbienne. De plus, des efforts supplémentaires doivent aussi se concentrer sur les mécanismes et facteurs d'inhibition, en particulier pour les acétogènes.

Acknowledgements

I would like to express my more sincere gratitude to all the people who have contributed and helped me in one way or another during the past years to carry out the research presented in this dissertation.

I would like to thank in particular my supervisor Prof. Dr. Eng. Manfred Greger for giving me the opportunity to work in this project, for his guidance, and insightful suggestions. I am also grateful to my PhD co-supervisors Prof. Dr. Eng. Stijn Van Hulle from the University of Ghent and to Dr. Eng. Nonjabulo Sibisi-Beierlein for their most valuable advice and feedback, and the fruitful discussions during the length of this doctoral research. I also would like to extend my gratitude to Prof. Dr. Eng. Marco Ragazzi from the University of Trento, and Prof. Dr. Eng. Thomas Sauter and Prof. Dr. Stephan Leyer, from the University of Luxembourg, for their participation in the thesis defense jury.

Special thanks go to Markus Schlienz, for his technical assistance in the laboratory, his handy ideas, the interesting discussions, assistance with the data collection and analysis and deep commitment. He certainly contributed to make my work in the laboratory much easier and pleasant.

This research would have not been possible without the assistance and commitment of the technical team members from which Gilbert Klein, Marc Seil, Marco De Cillia and Vicente Reis Adonis deserve a special mention. I thanks also to the students and collaborators who contributed also with their work and projects to the advancement of this research, including Julien Marques, Veronique Welz, Alain Blouet, Charel Gleis, Mark Theisen, Johan Winkel and Denis Reiners.

I also would like to express my gratitude to Dr. Jean Mersch and his team from the Administration des services techniques de l'agriculture au Luxembourg (ASTA) in Ettelbrück for contributing to this study with the NIRS analysis, to Prof. Dr. Christiane Zell and Katharina Haas from Hochschule Offenburg in Germany for the measurements with the polymerase chain reaction technique, IGLux for providing the silages, and Constant Kieffer from Beckerich biogas plant for the inoculum used in the assays.

I would also like to thank my University (ex-) colleagues and office mates for the good moments shared and interesting discussions: Joana, Laurent, Julien, Anusha, Christof, Simon, Pascal, Stephan, Tobias, Anja, Jessica, Srivathsan, Anahita, Khadidja, Sebastian, and Christian.

A special thought to my friends and to my family both in France and Spain, who, even in the distance, have always been there for me. Especially, I would like to thank my beloved Charles, who supported me in every step of the process, and my little ones, Chloe and Selena, who inspired me for trying to be and to do better.

My final words go to my parents, for teaching me and guiding throughout my life. This work will have not been possible without you.

Patricia Benito

Table of contents

Table of figures

Table of tables

Abbreviations

ADF	Acid detergent fibre
ADL	Acid detergent lignin
ADM1	Anaerobic Digestion Model N°1
AMPTS	Automatic methane potential test system
ANOVA	One-way analysis of variance
ARC	Archaea
ASTA	Administration des services techniques de l'agriculture (Luxembourg)
BMP	Biological methane potential
BPR	Biogas production rate
CHP	Combined heat and power
COD	Chemical oxygen demand
CSTR	Continuously stirred tank reactor
DGS	Dried grass silage
DMS	Dried maize silage
EEG	Renewable Energy Sources Act (Germany)
EPS	Exopolysacharides
EU	European Union
FID	Flame ionization detector
FM	Fresh matter
GC	Gas chromatograph
GHG	Greenhouse gases
GS	Grass silage
HAc	Acetic acid
HBu	Butyric acid
HCa	Caproic acid
HPr	Propionic acid
HPR	Hydrogen production rate
HRT	Hydraulic retention time
HVa	Valeric acid
IA	Intermediate alkalinity

IC	Inorganic carbon
IN	Inorganic nitrogen
ISR	Inoculum to substrate ratio
IWA	International water association
LCFA	Long-chain fatty acids
MBT	Methanobacteriales
MEV	Methane energy value
MEVM	Methane energy value model
MMB	Methanomicrobiales
MPR	Methane production rate
MS	Maize silage
Msc	Methanosarcinaceae
Mst	Methanosaetaceae
MSW	Municipal solid waste
NDF	Neutral detergent fibre
NfE	Nitrogen free extracts
NIRS	Near-infrared spectroscopy
OL	Organic loading
OLR	Organic loading rate
Org-N	Organic nitrogen
PA	Partial alkalinity
pCH	Particulate carbohydrates
RMSE	Root mean square error
S	Concentration of soluble component (variable in models)
SBP	Specific biogas production
SBPR	Specific biogas production rate
sCH	Soluble carbohydrates
sCOD	Soluble chemical oxygen demand
SHP	Specific hydrogen production
SIR	Substrate to inoculum ratio
SMP	Specific methane production
SMPR	Specific methane production rate
SRT	Solid retention time

STP	Standard temperature and pressure
tCH	Total carbohydrates
tCOD	Total chemical oxygen demand
ThSMP	Theoretical specific methane production
TIC	Total inorganic carbon
TN	Total nitrogen
TS	Total solids
TVFA	Total volatile fatty acids
UASB	Up-flow anaerobic sludge blanket (reactor)
VFA	Volatile fatty acids
VHPR	Volumetric hydrogen production rate
VMPR	Volumetric methane production rate
VS	Volatile solids
WV	Working volume
X	Concentration of particulate component (variable in models), including bacterial biomass)
Xaa	Amino acid degraders
Xac	Acetate degraders
X_acetox	Acetate oxidising microorganisms
Xbio	Decayed biomass
Xc4	Valerate and butyrate degraders
XF	Crude fibre
Xfa	Long-chain fatty acid degraders
Xh2	Hydrogen degraders
XL	Crude fat
XP	Crude protein
Xpro	Propionate degraders
Xsu	Sugar degraders

1. Introduction

1.1 Background of this project

Primary energy consumption in the 28 member States of the European Union (EU) amounted to 1,585 Mtoe in 2012, with 73.9% being derived from fossil fuels, and 11.6% from renewable sources (European Environment Agency, 2015). In 2007, Europe adopted targets to reduce greenhouse gas (GHG) emissions by 20%, to increase the share of renewable energy to 20%, and to achieve 20% energy savings. Moreover, the focus of the energy policy was also put into minimizing the dependence from external energy sources and thus exposure to the volatility of the price of fossil fuels and the need for more competitive energy markets to stimulate technology innovation and jobs (European Commission, 2007).

In this context, biomass can play a very important role to reach these targets. Indeed, the main contributors to the gross inland consumption of renewable energy in 2012 were biomass and renewable waste (58%), followed by hydro (16%), and wind (10%) energies (European Environment Agency, 2014). Amongst the different bioenergy sources, biogas produced from the fermentation of different organic feedstock has still a large potential to contribute to replace high CO_2-emitting conventional fuels and diversify the energy supply. Indeed, with its high content of methane (CH_4) varying from 50% to 75%, biogas is a very versatile energy carrier with a variety of applications. Up to recently, biogas was produced as by-product during the wastewater treatment process or anaerobic waste treatment. But since the 2000s, dedicated plants have been put in operation with the sole purpose of biogas production.

Indeed, there is a growing number of agricultural biogas plants, a majority of which use energy crops and crop residues in mono-fermentation or as co-substrate, given their high biogas yield potential. Nevertheless, many co-digestion plants do not reach their full potential and achieve lower methane yields (Chen et al., 2008; Poeschl et al., 2010), mainly due to incomplete bioconversion or process instability. Indeed, energy crops and crops residues are lignocellulosic material, thus containing cellulose and hemicellulose, as well as lignin. While the latter is considered not to be degradable during normal anaerobic conditions, cellulose and hemicellulose degradation poses some challenges due to the structures they form and the resulting slow hydrolysis. For example, for grass silage, cellulose can represent between 20% and 40% of the Total Solids (TS) (Malherbe and Cloete, 2002; Koch et al., 2009; Wichern et al., 2009) and approximately 20% in the case of maize silage (Biernacki et al., 2013).

1.2 Motivation

It is crucial to optimize the methane yield of the process to ensure the sustainable use and the profitability of biogas plants using lignocellulosic material (i.e. energy crops and crops residues) as substrate. This can be done by further investigating optimal operational conditions, pre-treatment methods and feedstock characteristics. The impact of certain agronomic parameters on the biogas potential of different energy crops have been previously addressed in literature including the species and variety (Lehtomäki, 2006; Mähnert et al., 2005), the stage of maturity and harvesting period (McEniry and O'Kiely, 2013), the intensity of the management

(Amon et al., 2007) or the conservation methods (Pakarinen et al., 2008). Other aspects, particularly operational parameters, still need further investigation in the field of anaerobic digestion of lignocellulosic material, particularly under semi-continuous and continuous conditions and mono-digestion.

This is the case, for example, for the organic loading rate (OLR), which is an important parameter that needs to be optimised in a way that allows a maximum load and methane production, while avoiding system instability and failure due to the accumulation of intermediary products such as volatile fatty acids (VFA) and ammonia (NH_3). For energy crops and crop residues, this aspect has been investigated for certain crops but mainly under batch conditions (Hashimoto, 1989; Golkowska and Greger, 2010; Liu et al., 2009; Raposo et al., 2009; Eskicioglu and Ghorbani, 2011), which can differ from the performance and stability that could be experienced in semi-continuous and continuous mode. Continuous co-digestion of different types of grass with manure and slurry in continuously stirred tank reactors (CSTR) has been addressed in literature at loadings up to 4 g Volatile Solids (VS)/l/d (Frigon et al., 2012; Mähnert et al., 2005; Xie et al., 2012; Lehtomäki et al., 2007). Mono-digestion of grass silage has been reported to be problematic beyond an OLR of 2.5 gVS/l/d in a two-stage CSTR system due to trace elements deficiency (Thamsiriroj et al., 2012), and feasible up to an OLR of 4 gVS/l/d with addition of trace elements and recirculation in one-stage systems (Wall et al., 2014). Therefore, research analysing the effect of increasing OLR on methane yields, process stability and kinetics of anaerobic continuous systems treating energy crops is still scarce, particularly for one-stage digestion, which is the most common application at commercial scale (Nizami and Murphy, 2010), and mono-digestion, and for crops other than grass silage. Also, increasing the OLR and decreasing pH favour the production of hydrogen (H_2), which production from energy crops and crop residues has had a very limited coverage to date (Pakarinen et al., 2011; Zhang et al., 2003).

As regards the effect of the feedstock characteristics, only a handful number of papers investigate energy crops co-digestion (Comino et al., 2010; Lehtomäki et al., 2007; Cuetos et al., 2011; Bauer et al., 2009), with the main focus on the biogas production and not on the stability or dynamics. Moreover, the effect of changing feedstock characteristics during semi-continuous or continuous digestion still needs further understanding.

Furthermore, the use of process simulation models for predicting/defining plant behaviour is still very limited for agricultural biogas plants using energy crops and other lignocellulosic material, mainly because of the complexity of the process and the heterogeneity of the substrate. The Anaerobic Digestion Model No. 1 (ADM1) (Batstone et al., 2002) by the International Water Association (IWA), well-known and widely applied in the field of wastewater treatment, has been applied in recent years in the field of lignocellulosic material digestion with different modifications in order to overcome certain limitations identified, particularly in the case of particulate and heterogeneous substrates. The problems relate, for example, to the characterisation of the feedstock and its fractionation during the disintegration step, the fate of the decayed biomass, or the use of default values for certain parameters. Indeed, there is not a standard method for characterising the composite feedstock that is used in agricultural biogas plants. Moreover, the model omits certain processes and products, as they are not considered relevant during standard operational conditions. Some of these aspects have been addressed to a different extent by a handful

number of publications that applied the ADM1 to the digestion of energy crops, and in particular grass silage. These include the work of Koch et al. (2010) for mono-digestion of grass silage in loop reactors in mesophilic conditions; Thamsiriroj et al. (2012) for continuous mono-digestion of grass silage in 2-stage CSTR anaerobic system; Wichern et al. (2009) for continuous mono-digestion of grass silage under mesophilic conditions, Lübken et al.(2007) for co-digestion of liquid manure and fodder for cows in a mesophilic CSTR reactor, Biernacki al. (2013) for mono-digestion of grass, maize, green weed silage, and industrial glycerine in batch reactors, Wolfsberger (2008) for maize silage and sunflower press residues in CSTR reactors, and Schlattmann (2011) for maize silage, grass silage and rapeseed oil in CSTR reactors under mesophilic conditions. These investigations mainly focus on the calibration of the parameters, the fractionation of the substrate, and the modification of the hydrolysis steps.

Additionally, recent research highlights the importance of hydrogenotrophic groups in the methanogenesis phase, also under mesophilic conditions, opposing to what it was initially believed (Zhu et al., 2011; Demirel and Scherer, 2008; Nettmann et al., 2008; Munk et al., 2010). This would suggest that the current chemical oxygen demand (COD) flux assumed in the ADM1 might need to be modified in the case of lignocellulosic material digestion. The inclusion of the acetate-oxidisation has only been addressed by Schlattmann (2011) to date. Finally, modification might be also necessary if applying the ADM1 model to describe the fermentative H_2 production from lignocellulosic material, which up to date, has only been attempted once (Antonopoulou et al., 2012).

All these knowledge gaps and modelling limitations have hindered the improvement and further application of anaerobic digestion of energy crops and other lignocellulosic material.

1.3 Main goals of this research and approach

The present PhD research aimed at addressing before-mentioned existing gaps and modelling limitations, thus contributing to further optimise the process when applied to lignocellulosic material. The main objective of the research was twofold:

- To perform an extensive comparative study on the effect of different operational parameters, including the OLR, the feedstock characteristics, the reactor configuration and the pH, on the kinetics, stability and performance of systems digesting energy crops and crop residues under mesophilic conditions, with special focus on mono-digestion and semi-continuous feeding mode.
- To develop a model suitable for describing the anaerobic digestion of energy crops based on the ADM1, using substrate composition data, redefining the default process kinetic constants using the different experimental data sets covering a wide range of operational conditions, and adapting the necessary biochemical and physico-chemical processes to address identified shortcomings.

Thus, the thesis work covered a broad variety of topics, from the areas of optimisation and simulation of biogas production from energy crops and lignocellulosic material, with the main goal of improving biogas plant long-run operation taking into account the specific characteristics of this type of substrates.

This project used methods applied in the animal feed industry (fibre analysis of Weende and Van Soest) to characterise and determine substrate composition, which was used to define the theoretical methane yield for each substrate considered. These include complex substrates (grass and maize silages from different harvesting periods) and simple substrate such as cellulose, starch, and glucose, or gluten that can be found in lignocellulosic material, as well as other intermediate products such as acetate and propionate. A method was adopted, taking into account previous work (i.e. Koch et al., 2010), to determine feedstock fractionation during disintegration using the substrate composition in each case.

Laboratory-scale reactors with different working volumes (WV) were used to perform an extensive investigation into the effect of some operational parameters, such as the feeding mode (continuous and batch), the OLR and the pH on the kinetics of anaerobic digestion of energy crops and lignocellulosic material and the system performance, thus completing the limited knowledge about the digestion of certain crops for continuous feeding and mono-digestion in CSTR reactors and for mesophilic conditions. Moreover, different co-digestion mixtures were also evaluated for grass and maize silage. The experimental data thus obtained were used to determine the biodegradability for the substrates considered under different operational conditions (by taking into consideration the theoretical values obtained on the basis of the substrate composition data).

Using the acquired experimental data, two models were developed on the basis of the existing ADM1, to be applied in the field of anaerobic digestion of energy crops. On the one-hand, an extension and modification of the ADM1, the Lignogas model, addressing some of the limitations of the ADM1, using experimental substrate composition data, and with certain redefined process kinetic constants and biochemical processes (e.g. inclusion of the acetate-oxidising bacterial group into the model). On the other-hand, a simplified version, the Lignogas-SIM, was also developed so as to analyse the applicability of a lighter version.

Therefore, the novelties of the modelling approach are the following:

- The models were developed so as to take into account the substrate characteristics and were validated with experimental data for different substrates in mono-digestion and mixtures of co-substrates.
- The models developed are intended to be applicable under a variety of operational conditions (e.g. feeding mode or the OLR), including H2-producing systems. Therefore the models have a universal initial parameter set for energy crops and only the substrate fractionation values have to be set for each substrate applied.
- While most of the previous models are developed for standard conditions of operation, the obtained experimental data set allowed validating the models under overloading conditions.
- Parameters were validated with experimental data for intermediary products and simple substrates (e.g. starch, cellulose, glucose, gluten, etc.).
- The possibility of using different values for the hydrolysis rate constant for the easily and slowly degradable fractions of carbohydrates was analysed.

- One of the developed models was intended to integrate current knowledge about the microbial composition in agricultural digesters.
- The two developed models allowed analysing the differences, advantages and disadvantages of the two different approaches (e.g. complex vs. simplified version).

2. Background

2.1 History and status of biogas production in Europe

2.1.1 Historic development

The production of biogas by means of anaerobic digestion of organic matter and its use for energy generation has been known for a long time by human kind.

The first systematic investigations on biogas were conducted by the Italian scientist Alessandro Volta, who collected gas in marshes and lake sediments for analysis. Around 1800, Dalton proposed a chemical structure for methane and in 1821 Amedeo Avogadro elucidated the final chemical structure of this molecule. In the 19th century the development and utilisation of anaerobic digestion received great attention. For example, the famous French bacteriologist Louis Pasteur conducted experiments on biogas generation, and it was in 1907 when the German engineer Karl Imhoff developed the so-called Imhoff tank which was the first anaerobic digester in wastewater treatment. Initially triggered by the need for identifying new and alternative energy sources after World War II, agriculture was identified to be a promising supplier of organic material, mainly cattle, pig or chicken slurry and manure, to be used as feedstock in biogas plants (Deublein and Steinhauser, 2011). Since the 1950s, the evolution of biogas production and its profitability has been strongly linked to the evolution of the prices of fossil fuels. Indeed, the number of biogas plants and production increased in the 1970s with the oil crisis.

The beginning of the 1990s constituted a turning point in Germany, stimulated by the profitability of using power derived from produced biogas and by the new waste legislation, which resulted in higher cost for disposal of solid waste. At the end of the 1990s, many plants, based on anaerobic digestion with some aerobic composting, were built for the treatment of waste, particularly slurry and food residues, not only in Germany but also in other countries such as Denmark, Austria, or Switzerland (Deublein and Steinhauser, 2011).

After 2000, the continuous increase of the price of fossil fuels and the enforcement of legislation promoting renewable energies and guaranteeing remuneration from feeding-in electricity in different countries (such as the Renewable Energy Sources Act –EEG- in Germany, which first entered into force in year 2000), contributed to a steady increase in the number of facilities over the following years.

Nowadays, slurry and manure, one of the most significant agricultural waste streams, are often co-digested with other biomass, such as energy crops and other biowaste with higher methane potentials in order to increase the gas yield. This is particularly the case in countries such as Germany and Austria, where dedicated crops were grown in some areas with the sole purpose of biogas production. For example in Germany, 90-95% of the biogas plants in operation by the end of 2010 were using crops as co-substrates (between 5,400 and 5,700 plants) (Murphy et al., 2011). Consequently, research focused during the first decade of the 2000s on exploring different energy crops and investigating different agronomic aspects for optimisation of the process. Moreover, efforts were also put into the investigation of different reactor designs and

some operational conditions. This triggered the technical development in new directions. For example, while the wet digestion is the most common process, dry digestion has gained increasing popularity in recent years.

2.1.2 Combating climate change with renewable energies - The role of biogas

It has been estimated that the globally averaged land and surface temperature has increased by 0.85°C over the period of 1880 to 2012. The Intergovernmental Panel on Climate Change (IPCC) concluded in its Fifth Assessment Report that global warming since the middle of the 20th century is very likely to have been due to human influences (IPCC, 2014). Coal, natural gas and oil fired energy production plants are major contributors to CO_2 emissions in the atmosphere, which along with other GHG, are believed to be the dominant cause of the observed warming. The Kyoto Protocol, signed in 1997, aimed to reduce GHG emissions by 5.2% from the 1990 level by 2008-2012. The EU committed to an 8% emission reduction, with the obligation distributed among the Member States. More recently, during the United Nations Climate Change Conference in Lima (Peru), nations agreed on elaborating the elements of the new agreement, scheduled to be agreed in Paris in late 2015.

Substantial reduction of GHG emissions will contribute to inverse the observed trend and reduce the risks associated with climate change. These required reductions will rely on the decrease of the final energy consumption (i.e. energy efficiency), an efficient energy conversion, and the implementation of efficient, carbon neutral, and renewable energy technologies.

In 1997, the EU started working towards a target of a 12% share of renewable energy in gross inland consumption by 2010[1], which unfortunately was not achieved in spite of the important progress made. Furthermore, in March 2007, all Member States agreed on a binding target of a 20% share of renewable energies in overall EU energy consumption by 2020[2].

The use of biomass can significantly reduce GHG emissions. Biomass includes energy crops and micro and macro algae, organic material from different waste streams (such as municipal solid waste (MSW), crop residues, wastewater and manure and slurry. It has been estimated that biomass contributed in 2012 to 19.5% of the total renewable electricity generation in the 27 Member States of the EU (EurObserv'ER, 2013). It offers an enormous potential for the production of electricity and heat. Indeed, biomass can be converted into different secondary energy sources (solid, liquid or gaseous) depending of its characteristics. These transformation processes for biomass include combustion, thermochemical transformation (carbonisation, gasification, and liquefaction), physico-chemical transformation (trans-esterification and extraction) and the biochemical transformation (anaerobic digestion and alcoholic fermentation).

[1] Renewable Energy Road Map available at: http://eur-lex.europa.eu/LexUriServ/LexUriServ.do?uri=COM:2006:0848:FIN:EN:PDF

[2] European Council - Presidency Conclusions of 9 March 2007, available at www.consilium.europa.eu/ueDocs/cms_Data/docs/pressData/en/ec/93135.pdf

In particular, biogas, produced from the anaerobic digestion (biological transformation) of biomass, is a very versatile energy carrier as it allows for a variety of applications including the production of heat after burning in a boiler, heat and electricity using a Combined Heat and Power (CHP) unit, and as vehicle fuel, injection into the public grid and application in fuel cells after upgrading.

Biogas can therefore contribute to replace high CO_2-emitting conventional fuels and diversify the energy supply. However, in order to fully meet its potential to produce CO_2-neutral energy, it is important to ensure that the produced biogas meets sustainability criteria. Indeed, generating net GHG savings depends on the cultivation and fuel production processes used. A study focusing on the energy and CO_2 balance of the biogas production from maize and grass energy crops showed that, in spite of the fossil energy consumed for their production and transformation to biogas, maize and grass energy crops allow a net production of renewable energy together with a significant reduction in fossil energy related CO_2 emission (Gerin et al., 2008). Nevertheless such study also highlighted the importance of an adequate coverage of the digestate storage tank and a good agricultural practice for spreading the digestate. For example, results showed that a leakage of 5% of the methane produced could ruin efforts to reduce CO_2 emissions through the use of maize or grass as a source of renewable energy. Another study, by Pöschl et al. (2010), evaluated the energy efficiency of different biogas systems, including single and co-digestion of multiple feedstock, different biogas utilization pathways, and waste-stream management strategies. This study showed a large variability in the energy balance depending on the substrates used for biogas production, the utilization efficiency, and the energy value of fossil fuels intended for substitution. For example, obtained results suggest that the energy efficiency of the biogas system could be improved by up to 65% when natural gas was substituted instead of electricity. It was also found that the system energy efficiency could be further improved by 5.1%–6.1% with the recovery of residual biogas from enclosed digestate storage units.

2.1.3 Impacts of the biogas production process

There are a number of advantages of applying anaerobic digestion to biomass for the production of biogas, including (Wellinger, 2005; European Commission, 2005; FNR[3], 2013):

- Waste treatment benefits
  - Biogas production contributes to reduce disposed waste volume and weight.
  - Biogas production helps recycling waste as a new resource with economical values (e.g. digestate can be used to amend soils).

[3] Fachagentur Nachwachsende Rohstoffe e.V. (Germany)

- Environmental benefits
    - Biogas significantly reduces GHG emissions by replacing high-CO_2 emitting conventional fuels.
    - Anaerobic digestion contributes to eliminate odours (by treating the disposed manure and slurry thus avoiding the emission of its volatile organic compounds).
    - Anaerobic digestion closes the nutrient cycle when using the digestate as fertiliser.
- Energetic benefits
    - Biogas production is a net energy producing process.
    - Biogas is a versatile form of renewable energy that can produce heat, electricity and serve as a vehicle fuel.
    - Biogas can be stored, which can help to better balance the offer and the demand of energy.
- Social and economic benefits
    - Biogas production contributes to the diversification of energy supply and contributes to reduce energy imports and thus external dependency by using local resources.
    - Biogas production contributes to technological and added value sector development.

Nevertheless, meeting these benefits is not exempt of potential problems. There have been in the past years discussions on the possible problems regarding bioenergy production, mainly related to the potential competition for land between energy and food crops (Muller, 2008). Similar to the competition for land, there is also a potential competition for water, in the context of increasing water scarcity. One key element to face these potential issues is the sustainability of the production of the agricultural products used for biogas production. In any case, as it will be explained in sub-chapter 2.1.5, the total agricultural surface dedicated to biofuel and biogas production is still small in Europe (below 5% of the total cropping area) and it can still be enlarged without harming the environmental or impacting food production.

Different studies have analysed, compared and estimated the energy output potential and environmental impact of different crop rotation systems intended for the production of biogas. It has been suggested, for example, that sustainable energy production from agrarian biomass should not be based on single crops, but rather on site-specific and environmentally friendly crop rotation systems (Bauer et al., 2009).

Moreover, there is still a large potential for biogas production from other sources, such as manure and slurry, crop and gardening residues and household waste, largely unexploited to date.

2.1.4 Regulatory background

Although there is not a dedicated piece of legislation regulating biogas production to date at the European level, there is a wide range of agro-environmental legislation having an impact

on the feasibility and promotion of biogas technology, including the EU Nitrate Directive (91/676/EC), the Integrated Pollution Prevention and Control Directive (96/61/EC), the Sewage Sludge Directive (86/278/EC), and the Water Framework Directive (60/2000/EC). Also, land filling of untreated organic waste is gradually being reduced through the so-called Landfill Directive (1999/31/EC), which obliges Member States to reduce the amount of biodegradable waste that is landfilled, and will contribute to increase the amount of organic waste material available for digestion. Moreover, installations using certain animal-related residues are entitled to comply with the Regulation governing animal by-products not designated for human consumption (1069/2009/EC).

The EU Biomass Action Plan of December 2005 (European Commission, 2005) identified 32 key activities for boosting the bioenergy market. One of these key actions requested the Commission to encourage Member States to establish national biomass action plans. Following the Commission's Biomass Action Plan, several Member States produced their own national action plans, some of which specially refer to the promotion of anaerobic digestion and biogas production from crops (e.g., United Kingdom, Germany, Spain, etc.).

The Directive 2009/28/EC on the Promotion of the Use of Energy from Renewable Sources was adopted in 2009 by the European Parliament and the Council. It recognises that the use of agricultural material such as manure, slurry, and other animal and organic waste for biogas production has significant environmental benefits resulting from the GHG emission saving potential, and highlights the important role that it can play in the promotion of the economic development in rural areas (European Commission, 2009).

Also, the Commission conducted a study in 2009 addressing the permit application procedure for biomass installations (Ecofys and Golder Associates, 2009), and in 2010 adopted a report on sustainability requirements for the use of solid biomass and biogas in electricity, heating and cooling. The report recommends a general prohibition on the use of biomass from land converted from forest, a common GHG calculation methodology, the differentiation of national support schemes for installations that achieve high energy conversion efficiencies; and the monitoring of the origin of biomass (European Commission, 2010).

United Kingdom or the Walloon region of Belgium, for example, have implemented markets based on ‘‘green certificates’’ to support the production of green energy. Most countries have introduced policies to support the promotion of biogas, including the introduction of favourable feed-in tariffs for the produced electricity (up to 13 countries in the EU), or the introduction of tax exemptions (up to 6 countries in the EU) (Braun et al., 2010). The legislative framework for feeding bio-methane (methane-rich gas resulting from cleaning and upgrading biogas produced biologically) in the public natural gas grid is established in the Directive 2003/55/EC. However, a unified standard for the feed-in of bio-methane does not exist yet. A summary of the feed-in tariff schemes applied in Germany (as indicated in the last amendment of the EEG from 2014) and Luxembourg (Grand Ducal regulation of 1 August 2014) is presented in Annex A.

Overall, biogas is a good example showing the complexity of bioenergy systems in terms of the policies that have to be considered, including agricultural, waste, energy and human and animal health policies.

2.1.5 European situation and potential

European production of primary energy from biogas reached 12 Mtoe in 2012, i.e. a 15.7% increase compared to 2011. Landfill biogas accounted for 23.7% of the total produced biogas followed by 9.9% from waste treatment plants (urban and industrial). The other sources, mainly agricultural biogas units, and also centralised co-digestion units and solid household waste methanisation units, accounted for more than half Europe's biogas production, i.e. 66.5% in 2012, mainly due to the German contribution, country in which this type of source has the largest share. Until 2014, agricultural biogas was being increasingly based on the development of dedicated energy crops, such as maize, although this might change in the future with recent changes in national legislation (EurObserv'ER, 2013) .

Germany was by far the leading producer of biogas (49.87% of the EU total), followed by the United Kingdom and Italy in 2012. Regardless the total biogas production, it can be observed that the biogas sources vary amongst Member States. Germany, Austria and Denmark produce the largest share of their biogas in decentralised agricultural plants, MSW methanisation plants, and centralised CHP plants, whereas the main source of biogas in the UK, Italy, France and Spain is landfill gas.

According to a study by the European Environment Agency from 2006, the potential from agriculture was still largely unexploited and the sector was expected to have the highest growth rates in the coming years (European Environment Agency, 2006). Available data for the 27 Member States published in 2013 showed that agricultural land for biofuels and biogas covered approximately 5.5 Mio hectares of agricultural land in 2008, which represented 3.2 % of the total cropping area in the EU-27. Most of this land was used for dedicated biofuel cropping and only 7% for biogas. Such share for biogas is expected to increase in the future (European Environment Agency, 2013). A potential of methane derived from animal manure and energy crops and waste was estimated in the range of 40 Mtoe in 2020 as compared to a production of 7.5 Mtoe in 2008 (AEBIOM, 2009), assuming that 25 Mio ha of agricultural land (arable land and green land) could be used for energy without harming food production and the environment.

An emerging technology is the injection of bio-methane (purified biogas) into the natural gas grids. Countries where this new technology is rapidly expanding are Germany (151 plants in 2012), Sweden (53 plants in 2012), the Netherlands (23 plants in 2012), Austria (10 plants in 2012), and Finland (6 plants in 2012) and Luxembourg (3 plants in 2012) (EurObserv'ER, 2014).

In the case of Germany, the most important producer of biogas in Europe, the installation of biogas plants was largely promoted when the German EEG came into force in the year 2000. In 2008, 3 891 biogas plants were operating in Germany for energy production. In 2010, 5,905 biogas plants were operational, figure that increased to 7,515 in 2012, as it can be seen in Figure 1, with an installed capacity of 3,352 MW. Of these plants, 117 were upgrading biogas to bio-methane. The same year, 54% of the substrate input to biogas plants were energy crops (mass related), and 41% of the input were manure and slurry, while only 4% was bio-waste and 1% industrial and harvest residues. Maize silage represented 73% (mass related) of the energy crops input, with grass taking the second place with 11%. In 2012, the biogas share in electricity production from biomass sources was of approximately 50.2%, and 15.1% of that

generated by renewable sources. Biogas is mainly produced in agricultural facilities (Fachagentur Nachwachsende Rohstoffe (FNR), 2013).

The EEG has been amended in 2004, 2009, 2012, and 2014. An important change in the feed-in tariffs introduced with the 2012 amendment affected the installation of biogas plants in 2012 and 2013. Moreover, a new amendment was adopted in June 2014 which introduced additional reductions in the feed-in tariffs (see Annex A) and some additional changes. One of the changes is the elimination of the premium for using energy crops, which are widely used as co-substrate in Germany to increase the methane yield. This was done to encourage the use of farming waste, but operators and owners fear that this change will worsen the profitability of the plants. Also, there will be a restriction on the additional capacity of biogas plants installed annually to 100MW. These changes are expected to impact negatively the number of new installation from 2015 onwards.

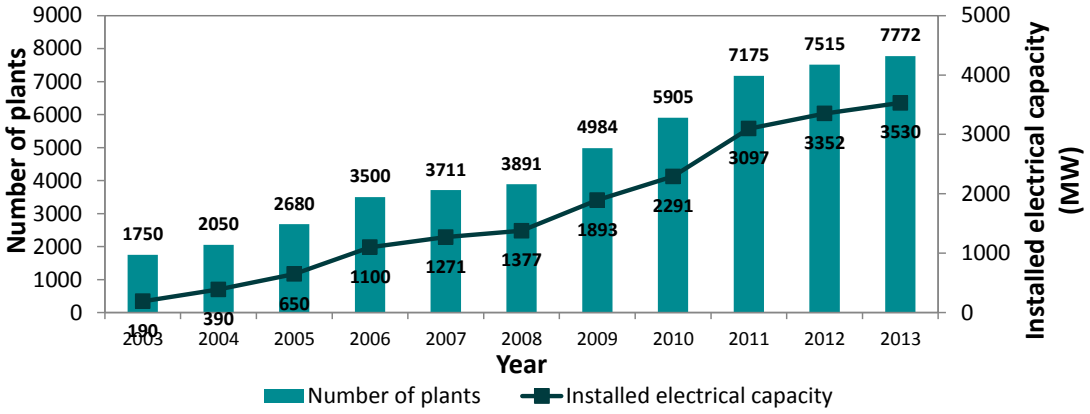

Figure 1: Number of biogas plants with their total installed electrical capacity in Germany
(Fachagentur Nachwachsende Rohstoffe (FNR), 2013)

In spite of its size, Luxembourg is one of the countries with the highest gross electricity production from biogas per capita (after Germany). There were 26 biogas plants in Luxembourg in 2010, with an installed capacity of 7.3 MW_e (Institut Luxembourgeois de Régulation, 2010). Eight biogas plants were using agricultural wastes, having a total capacity of 345 kW, while 14 were co-digestion plants, with a total capacity of 3,687 kW. In 2010, the production of electricity from biogas represented 50.4 GWh, thus representing the 36.1% of the total electricity produced in Luxembourg from renewable sources. It has been estimated that the feasible potential of energy production from biogas by 2020 for Luxembourg could be of 369 GWh/year (Biermayr et al., 2007). In recent years, stagnation in the number of plants in operation has been observed (Ministère du Développement durable et des Infrastructures - Département de l'Environnement, 2010).

In addition, three plants with injection into the natural gas grid initiated operation in the end of 2010 and in 2011 (Bakona, Minett-Kompost, and Kielen). In total, approximately 6.9 Mio m^3 can potentially be produced in these plants per year.

2.2 Biogas production and technology

2.2.1 Biogas process

Biogas production through anaerobic digestion is a complex, multi-step biological process where the organic carbon is converted into CO_2 and CH_4 as main constituents, in the absence of oxygen. It can be divided into four phases, carried out by a variety of microorganisms, with very different environmental requirements and growth optimum conditions, which makes the operation and control of this type of systems complex.

In the first step, known as hydrolysis, complex polymers with high molecular weight (i.e. carbohydrates, fats and/or proteins) are divided into soluble monomers (i.e. monosaccharides, amino acids and long-chain fatty acids - LCFA) by means of the enzymatic action of hydrolytic bacteria. Secondly, during the so-called acidogenesis or acidification phase, the products of hydrolysis are metabolised by acidogenic bacteria and broken down into short-chain VFA, including acetic acid (HAc), propionic acid (HPr), butyric acid (HBu), and valeric acid (HVa). Also different alcohols, H_2 and CO_2 are produced. During the acetogenesis, the produced organic acids and alcohols are broken down into HAc, H_2 and CO_2, which act as direct substrate for methanogenic microorganisms during the fourth and final phase, the methanogenesis. The main product of the process is biogas which is a mixture of CH_4 and CO_2, as well as trace gases such as H_2S and H_2. Figure 2 shows the diagram of the biogas production process.

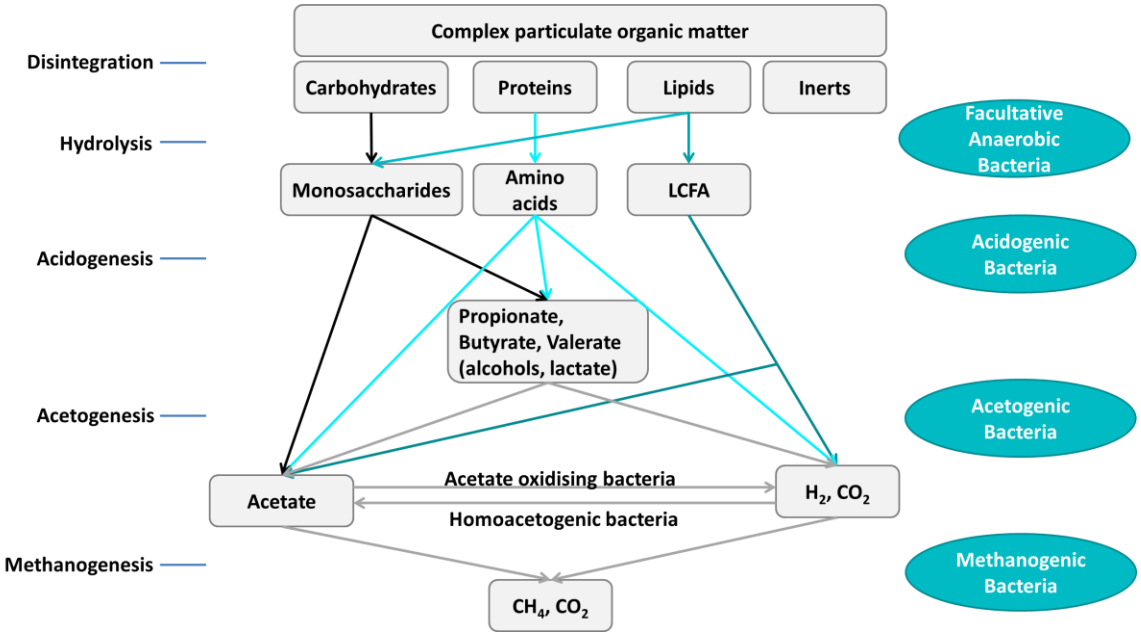

Figure 2: Main steps and pathways of anaerobic digestion. (modified from Batstone et al., 2002)

2.2.1.1 Disintegration and hydrolysis

During this extra-cellular process, polymers, which cannot be utilised by microorganisms directly, are broken down into simpler and soluble intermediates which can then pass the cell membrane and be used to provide energy and synthesise cellular components (Deublein and Steinhauser, 2008; Batstone et al., 2002; Pavlostathis and Giraldo-Gomez, 1991). The hydrolysis of carbohydrates takes place within a few hours while that of proteins and lipid

within few hours up to a few days. Lignocellulose is only degraded partially and lignin can be considered to be not degradable (unless a certain pre-treatment is applied). Microorganisms of many different genera are responsible for this process (e.g. Bacteroides, Lactobacillus, etc.), both facultative and obligatory anaerobic bacteria (Deublein and Steinhauser, 2011).

Hydrolytic enzymes include cellulase, cellobiase, xylanase and amylase for degrading carbohydrates into monosaccharides, protease for degrading protein into amino acids, and lipase for degrading lipid into glycerol and LCFA (Parawira et al., 2005).

The overall hydrolysis rate depends on several factors including the feedstock size, shape, surface area, and concentration. In spite of this complexity, in most existing models, hydrolysis is described using a first-order kinetic approach based on the substrate consumption (Batstone et al., 2002). Vavilin et al. (1996) explored 4 different hydrolysis kinetics for complex organic matter and proposed a model that considered substrate particle colonisation by bacteria and substrate degradation.

In the absence of inhibitory conditions and for particulate substrates, hydrolysis is considered as the rate-limiting step (Noike et al., 1985; Tomei et al., 2009; Vavilin et al., 1996). In the case of readily degradable substrates, on the other hand, and depending on the operational conditions, acetogenesis and/or methanogenesis could become the rate-limiting steps (Vavilin, al., 2008)

Some authors also propose to consider a disintegration step, during which complex and particulate organic material are converted into carbohydrates, proteins and lipids that will undergo the hydrolysis step (i.e. solubilisation). This preliminary step, proposed for example by Batstone et al. (2002) allows taking into consideration the different characteristics of different organic composites. It is an extracellular step and includes a number of processes, including physical breakdowns of molecules, non-enzymatic decay or bacterial lysis.

2.2.1.2 Acidogenesis

In the step subsequent to hydrolysis, referred to as acidogenesis or fermentation, the monomers are degraded to a number of VFA including HPr (CH_3CH_2COOH) and HBu ($CH_3CH_2CH_2COOH$) as well as HAc (CH_3COOH), alcohols, H_2, and CO_2.

The degradation of monosaccharides (e.g. glucose) can take place through different pathways which leads to different products (see Table 1), with different yields of energy. The dominant pathway depends on several factors, including the pH and the dissolved H_2 concentration, which is going to determine the H_2 partial pressure. These variables can in turn be affected by other operational parameters, such as the substrate loading and its bio-availability. It has been found that the lower the partial pressure, the higher the production of reduced compounds as HAc (Boe, 2006; Deublein and Steinhauser, 2008). Alternative products such as lactate or ethanol are commonly not found in reactors running under normal operational conditions. Indeed, ethanol is produced over acetate at low pH, while lactate is a key intermediate that is usually fast degraded (Batstone et al., 2002).

Table 1: Examples of glucose fermentation products (Batstone et al., 2002; Thauer et al., 1977)

Products	Reaction
Acetate	$C_6H_{12}O_6 + 2H_2O \rightarrow 2CH_3COOH + 2CO_2 + 4H_2$
Propionate + Acetate	$3C_6H_{12}O_6 \rightarrow 4CH_3CH2COOH + 2CH_3COOH + 2CO_2 + 2H2O$
Butyrate	$C_6H_{12}O_6 \rightarrow CH_3CH_2CH_2COOH + 2CO_2 + 2H_2$
Lactate	$C_6H_{12}O_6 \rightarrow 2CH_3CHOHCOOH$
Ethanol	$C_6H_{12}O_6 \rightarrow 2CH_3CH_2OH + 2CO_2$

Acidogenesis is often the quickest step in the anaerobic conversion of complex organic matter in liquid phase digestions. Therefore, in the case of process imbalance, an accumulation of fatty acids could be detected (Vavilin et al., 1996).

There are two main pathways for the amino acid fermentation: the Stickland oxidation-reduction paired fermentation and the oxidation of a single amino acid (Batstone et al. 2002), the first one being the most common, and results in the production of HAc, NH_3, and CO_2 (Deublein and Steinhauser, 2011).

Nearly all microorganisms participating in the acidogenesis phase also participate in the hydrolysis. The genera Clostridium, Paenibacillus and Ruminococcus appear in all the phases of the fermentation process but are predominant in the acidogenic phase (Deublein and Steinhauser, 2011).

2.2.1.3 Acetogenesis

During this step, long-chain VFA (such as HPr and HBu) and LCFA are oxidized to produce HAc, CO_2, and H_2. Table 2 presents the reactions for some VFAs as well as the change in the standard Gibbs free energy (ΔG°) and the Gibbs energy at low H_2 partial pressure conditions (ΔG'). Indeed, these equations are endergonic (ΔG°>0) and become thermodynamically possible only at low H_2 partial pressure (ΔG'<0). As acetogenic bacteria produce H_2, these reactions are only possible when acetogenic bacteria are living in symbiosis with hydrogen-consuming methanogenic archaea, which live only in high H_2 partial pressure conditions. Thus, these reactions can only occur simultaneously within a narrow range of very low p_{H2} (Deublein and Steinhauser, 2008; Batstone et al., 2002).

Table 2: Organic acids degradations (Thauer et al., 1977; Schink, 1997; Batstone et al., 2002)

Substrate	Reaction	ΔG°' [kJ/mole]	ΔG' [kJ/mole]
Propionate	$CH_3CH_2COOH + 2H_2O \rightarrow CH_3COOH + 3H_2 + CO_2$	+76.2	-14.6
Butyrate	$CH_3CH_2CH_2COOH + 2H_2O \rightarrow 2CH_3COOH + 2H_2$	+48	-25.6
Valerate	$CH_3CH_2CH_2CH_2COOH + 2H_2O \rightarrow CH_3COOH + CH_3CH_2COOH + 2H_2$	+48	-25.6

ΔG°' is the increment of the free energy under standard conditions (temperature of 25°C and pressure of 1 atm) but with a pH of 7. ***ΔG'*** is calculated for a temperature of 37°C, a pH 7, pH_2 10^{-5} atm and organic acids concentration of 1 mM. ΔG' is calculated from $\Delta G' = \Delta G°' + RTLn([C]^c[D]^d)/([A]^a[B]^b)$ in the reaction $aA + bB \leftrightarrow cC + dD$

For both acetogenesis and methanogenesis the neutral pH conditions of 6.8 – 7.5 are necessary. The acetogenesis phase is going to limit the rate of degradation in the final methanogenesis stage, as it provides the necessary substrates for that phase (H_2, CO_2, and HAc). It is also going to determine the quantity and composition of the obtained biogas (Deublein and Steinhauser, 2011).

2.2.1.4 Methanogenesis

During this final phase, CH_4 is formed under strictly anaerobic conditions by methanogenic archaea from the fermentation products, namely HAc, H_2, and CO_2. Two main groups of methanogenic bacteria can be distinguished according to the substrate they use. On the one

hand, the acetoclastic or acetotrophic methanogens convert HAc into CH_4 and CO_2. The hydrogenotrophic methanogens, on the other hand, use H_2 as the electron donor and CO_2 as the electron acceptor to produce CH_4. Many different species of methanogenic bacteria are known. The most commonly families of methanogenic bacteria found in biogas reactors and their optimum conditions are presented in Table 3. While most methanogens can produce CH_4 from H_2 and CO_2, only some known species can convert HAc to CH_4, i.e. Genus Methanosarcina and Methanosaeta (Deublein and Steinhauser, 2011; Batstone et al., 2002).

Table 3: Important methanogenic families (Demirel and Scherer, 2008)

Order	Families	Substrate	Optimum
Methanobacteriales (Class I)	Methanobacteriacae	H_2, CO_2, Formic acid	Temp. range: 37°C -70°C pH range: 6.6-8.5
Methanomicrobiales (Class III)	Methanomicrobiacae	H_2, CO_2, Formic acid	Temp. optimum: 40°C pH range: 6.1-6.9
Methanosarcinales (Class III)	Methanosarcinaceae	H_2, CO2, Methanol, Methylamine, HAc	Temp. range: 30°C -40°C pH range: 6-7
	Methanosaetaceae	HAc	Temp. range: 35°C - 40°C (mesophilic) and 55°C - 60°C (thermophilic) pH range: 7-7.5 (mesophilic) and 7 (thermophilic)

Moreover, during the methanogenesis phase, an inter-conversion between H_2/CO_2 and HAc takes place by the homoacetogenic bacteria. Indeed, HAc can be either oxidized or produced by homoacetogens depending on the H_2 concentration and the temperature (Schink, 1997). As it can be seen in Table 4, H_2 consumption via the hydrogenotrophic methanogenesis is more thermodynamically favourable than homoacetogenesis. Acetoclastic methanogenesis is also more favourable than HAc oxidation, and therefore, most HAc is likely to be degraded via this pathway. Nevertheless, the acetoclastic methanogenesis is more sensible to high NH_3 concentration, in which case, HAc oxidation will take over.

Table 4: Reactions related to methanogenesis (Schink, 1997; Thauer et al., 1977; Batstone et al., 2002)

Degradation pathway	Substrate	Reaction	$\Delta G^{\circ\prime}$ [kJ/mole]
Hydrogenotrophic methanogenesis	H_2/CO_2	$4H_2 + CO_2 \rightarrow CH_4 + 2H_2O$	-131
Acetoclastic methanogenesis	HAc	$CH_3COOH \rightarrow CH_4 + CO_2$	-31
Acetate oxidation	HAc	$CH_3COOH + 2H_2O \rightarrow 4H_2 + 2CO_2$	+104.6
Homoacetogenesis	H_2/CO_2	$4H_2 + 2CO_2 \rightarrow CH_3COOH + 2H_2O$	-104.6

Up to recently, it was believed that only 27-30% of the CH_4 resulted from the degradation of CO_2 and H_2, while up to 70% could be originated from acetate (Deublein and Steinhauser, 2008; Klass, 1984). However, recent studies suggest that the predominance for the different possible pathways for biogas production is greatly depending on the VFA concentration, and presence of some inhibitory substances such as NH_3 or H_2S, and so it could vary greatly depending on the type of substrate and the reactor operation. For example, Nettmann et al. (2008) evaluated in an agricultural biogas plant the Archaea diversity to find that 70% of all archaea corresponded to hydrogenotrophic methanogens, and more precisely to Methanomicrobiales, with acetotrophic methanogens constituting only a minor share. Demirel and Scherer (2008) performed a literature review focused on the evolution of acetotrophic and hydrogenotrophic methanogens during anaerobic conversion of particulate biomass to CH_4 to find that acetotrophic methanogens were more common at low HAc concentrations. On the contrary, their share decreased at high concentrations of NH_3 and H_2S, largely present in cattle and swine manure. More recently, Munk et al. (2010) monitored microbial population dynamics during mono-digestion of maize and found that obligate acetoclastic (i.e. Methanosaetaceae) bacteria were found only at acetate concentrations below 1g/l, while at an OLR of 1 gVS/l/d and without acidification, strict hydrogenotrophic Methanobacteriales,

and hydrogenotrophic and acetoclastic Methanosarcinaceae were dominant. These results were in line with results from Zhu et al. (2011), who found that 90% of the methanogenic Archaea in a mesophilic biogas reactor fed with swine manure were hydrogenotrophic methanogens, and that Methanobacteriales instead of Methanomicrobiales were the most predominant methanogenic archaea.

In any case, the latest research highlight the importance that the hydrogenotrophic pathway plays in the overall control of the CH_4 production process, given its role to regulate the H_2 partial pressure. An imbalance in this pathway, resulting from the presence of certain inhibitory substances or a drop in the pH, can result in an accumulation of HAc and H_2, which in turn can affect negatively the uptake of HPr during the acidogenesis step (Demirel and Scherer, 2008).

2.2.2 Agricultural substrates for anaerobic digestion

All types of organic substrates can be used for biogas production as long as they contain degradable fractions (i.e. carbohydrates, proteins, and fats) that are bioavailable to bacteria. A general distinction can be made between substrates from agriculture, like by-products (manure), grass or dedicated crops for biogas, and from various waste streams (e.g. landfill, sewage sludge, MSW, industrial wastes, etc.). In farm-based plants, it is mainly animal manures and slurries that are used (e.g. cattle and pig liquid manure) as the main substrate. Other organic materials, such as energy crops or household organic waste, are used as co-substrates to increase the biogas yield.

The value of a substrate depends on its potential biogas yield and quality, i.e. CH_4 content. The theoretical biogas yield of a substrate is determined by its composition in terms of the degradable fractions (i.e. protein, lipids and carbohydrates) and not bio-available fractions (i.e. part of the hemicellulose and cellulose, and the lignin). Table 5 summarises the theoretical biogas yield and composition for carbohydrates, proteins, and lipids on the basis of the stoichiometric conversion of each element. Lipids have the highest biogas yield, but their degradation takes longer given its poor bioavailability. Carbohydrates and proteins show faster conversion rates but lower gas yields (Deublein and Steinhauser, 2011; Weiland, 2010). Given the fact that lignin presents a very low bioavailability, its methane potential is generally considered to be null. Thus substrate having high lignin content will display a lower methane and biogas yields. On the other hand, certain treatments are possible to alter the lignin structure and improve accessibility to hydrolytic enzymes (e.g. thermal and acid pre-treatment), although they have an impact on the overall cost of the process. Hendriks and Zeeman (2009) performed an extensive review of pre-treatments to enhance the digestibility of lignocellulosic biomass.

Table 5: Maximal gas yields and theoretical CH_4 contents (Weiland, 2010)

Substrate	Biogas (Nm^3/t TS)	CH_4 (%)	CO_2 (%)
Carbohydrates	790-800	50	50
Proteins	700	70-71	29-30
Lipids	1,200-1,250	67-68	32-33
Lignin	0	0	0

Table 6 presents the range of energy yield for various plants and plant materials, as reported in selected literature. In general, it is possible to observe a wide range of CH_4 yields for energy crops, between 120–658 m^3t^{-1} VS for different crops. A comprehensive data bank on crop

yields, appropriate climate and growth conditions, based on literature and own investigations, was elaborated in the recent EU funded "CROPGEN" project[4].

Table 6: CH_4 yields from digestion of various plants and plant materials as reported in literature (Braun et al., 2010; Weiland, 2010)

Plant and plant material	Methane yield (m^3 per tonne of VS)
Maize (whole plant)	205-450
Wheat (grain)	384-426
Oats (grain)	250-295
Rye (grain)	283-492
Grass	298-467
Clover grass	290-390
Red clover	300-350
Clover	345-350
Hemp	355-409
Sunflower	154-400
Oilseed rape	240-340
Potatoes	276-400
Sugar beet	420-500
Barley	353-658
Alfalfa	340-500
Leaves	417-453

As the nutritional composition of substrates changes as the plant matures, the harvesting time and frequency of a crop are going to be thus most relevant in the determination of the biogas yield. For example, Amon et al. (2007) have shown that maize crops harvested after 97 days of vegetation at milk ripeness produced up to 37% greater CH_4 yields when compared with maize at full ripeness. Research has also addressed the species and variety (Lehtomäki, 2006; Mähnert et al., 2005), the stage of maturity and the harvesting period (McEniry and O'Kiely, 2013).

To increase the degradation rate of a substrate, a pre-treatment can be applied by mechanical, thermal, chemical, or enzymatic processes. The decomposition process is faster with decreasing particle size, although this does not necessarily increase the CH_4 yield (Mshandete et al., 2006).

Energy crops and crop residues can be stored after undergoing an ensilaging process, which is a biochemical process that converts the monosaccharides contained in the plant matter to lactic acid, acetate, propionate, and butyrate, thus making the pH drop to values between 3 and 4, which in turn inhibits the growth of detrimental microorganisms (Weiland, 2010). For optimal ensiling conditions, the energy crops should have a specific particle size (e.g. 10–20 mm) and have TS between 25% and 35% (Braun et al., 2010). Lehtomäki (2006) investigated the influence of storage on the CH_4 potential of different crops, and found that ensiling with additives can increase the anaerobic biodegradability of certain energy crops and crop residues, and that the duration and temperature of storage can also play an important role for certain substrates.

[4] Website available at: www.cropgen.soton.ac.uk

2.2.3 Biogas plants configuration

Anaerobic digesters can be designed and operated under different configurations, according to which they can be classified, as illustrated in Figure 3.

According to their **TS content**, it is possible to distinguish between wet and dry digestion. Although there is not an unanimous definition, a process operating with a TS concentration below 10% can be considered as wet fermentation, while if operating with a TS between 15% and 35%, the process can be considered as dry digestion (Weiland, 2010). Wet digestion is thus observed in the digestion of manure and slurries, while in the case of solid substrates, such as energy crops or crop residues, the mixing with slurries or recycled liquid fraction from the fermenter's digestate will be necessary. The TS concentration is going to have major implications for the reactor type and operation, in terms, for example, of the type of mixing and the feedstock loading (also referred to as feeding mode). In certain countries, such as Germany, there has been in recent years an increasing interest in the mono-digestion of certain energy crops. Regardless, about 70% of biogas plants in Germany are based on wet digestion (Fachagentur Nachwachsende Rohstoffe (FNR), 2013).

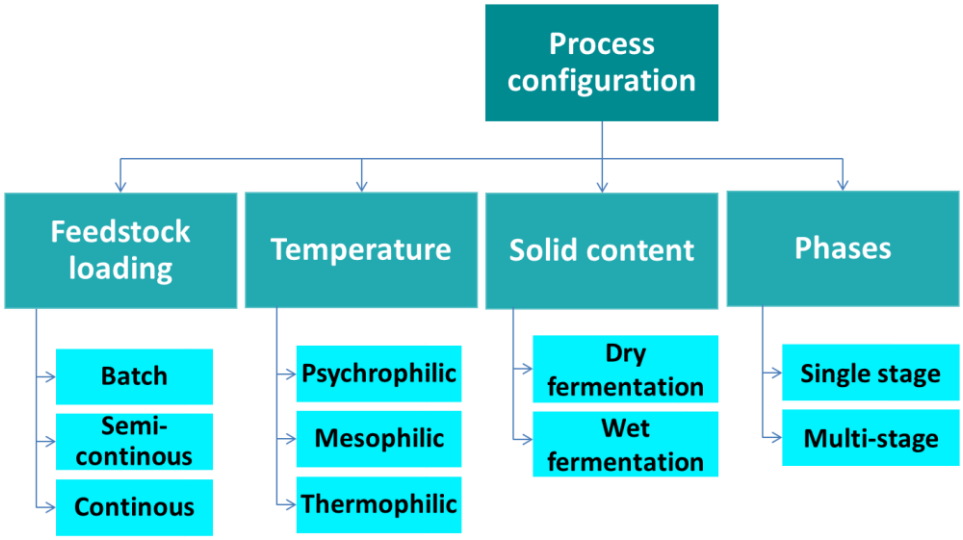

Figure 3: General possible configurations for the anaerobic digestion process

It is also possible to distinguish between **one-stage and multi-stage** (generally two-stage) configurations, depending on the number of reactors applied. In the first case, all the steps of the degradation of the organic substrates take place in a single reactor simultaneously, while in the case of a multi-stage system, the phases take place in different reactors, which run in series. The idea of the multi-stage configuration, usually with a separation of the hydrolysis and acidogenesis steps on the one hand, and the acetogenesis and methanogenesis on the other hand, is to optimise the digestion performance, given the different environmental requirements and kinetics, i.e. ideal pH range for hydrolysis (5.5–6.5) and methanisation (6.8–7.2) is different (Weiland, 2010). Nevertheless, the operation of this type of configuration can be more complicated, as it requires for controlling the characteristics of the feed to the methanogenic reactor. Boe and Angelidaki (2009) compared a single thermophilic CSTR with a serial CSTR configuration digesting cattle manure and found that the serial CSTR could obtain 11% higher biogas yield compared to the single CSTR. Indeed, the results suggested that the second reactor in serial CSTR configuration helped utilizing VFA produced from overloading in

the first reactor, which improved the effluent quality and conversion efficiency of the serial CSTR.

Depending on the type of feedstock to be used and the configuration of the reactors, different **feeding modes (or feedstock loading)** can be considered. In the batch process, the digester is completely filled at once with the substrate, which is consumed progressively without anything being added or discharged until the end of the residence time (Deublein and Steinhauser, 2011). Gas production begins after loading the digester and decreases again after the maximum value is reached. In a continuously fed reactor, the organic material is going to be introduced constantly or regularly (for semi-continuous systems), and reactor content (effluent) is going to be extracted at similar or the same rate, while biogas is going to be produced continuously. Semi-continuous at particularly continuous feeding modes display a stable production of biogas at steady-state conditions and microorganisms present maximum growth rates permitted (in the absence of inhibition), thus presenting faster kinetics (Klass, 1984). In batch system, the concentrations of components in the digester are changing with time and therefore, the steady-state can only be reached after the complete degradation has finished.

While most wet digestion systems are operated under continuous feeding conditions, both batch or continuous can be found in the case of dry digestion systems (Weiland, 2010). Continuous feeding mode can be applied in CSTR and up-flow anaerobic sludge blanket reactors (UASB). The selection of the type of reactor will depend on the type of substrate, and in particular, on the content of particulate solid content.

As regards **temperature**, the anaerobic digestion process can be operated in a wide range of temperatures, including psychrophilic (<20°C), mesophilic (20-45°C), and thermophilic (45-70°C) conditions. Most of German's farm biogas plants operate in the mesophilic range (between 32°C and 42°C), while only a few run at the thermophilic range (Weiland, 2010). The necessary heat is usually produced in the installation through boilers or CHP units.

In the last years, different concepts for the organisation of biogas plants have been suggested and implemented, in response to the feedstock availability and the access to the grid. An example of configuration of an agricultural biogas plant is presented in Figure 4.

A simpler and often applied differentiation based on the management and organisation of the plants can be made between decentralised farm-scale and centralised large-scale plants. Farm-scale digestion plants are usually simple stirred tanks that use long retention times to digest agricultural by-products and that either use the generated heat (and electricity) on-site, or use pipelines to transport biogas to cogeneration units located nearby. The hydraulic retention time (HRT) of the waste in the digester can vary between 15 to 50 days. Longer HRT are applied when lignocellulosic material is used as co-substrate or in mono-digestion (Wellinger, 2005).

The obtained gas can either be used directly in the CHP unit (to produce heat and electricity) or burned in boilers, or it can be upgraded to natural gas standard, so it can be injected in the natural gas grid. In any case, raw biogas is usually further treated (e.g. cooled, drained, dried and cleaned from H_2S because of its corrosive effect), before it can be used (Wellinger, 2005).

Regarding the produced digested material, it can be easily spread on fields for fertilization. The anaerobic digestion process is able to inactivate weed seeds, bacteria (e.g., Salmonella, Escherichia coli, Listeria), viruses, fungi, and parasites in the feedstock which is of great importance if the digestate is used as fertilizer (Weiland, 2010).

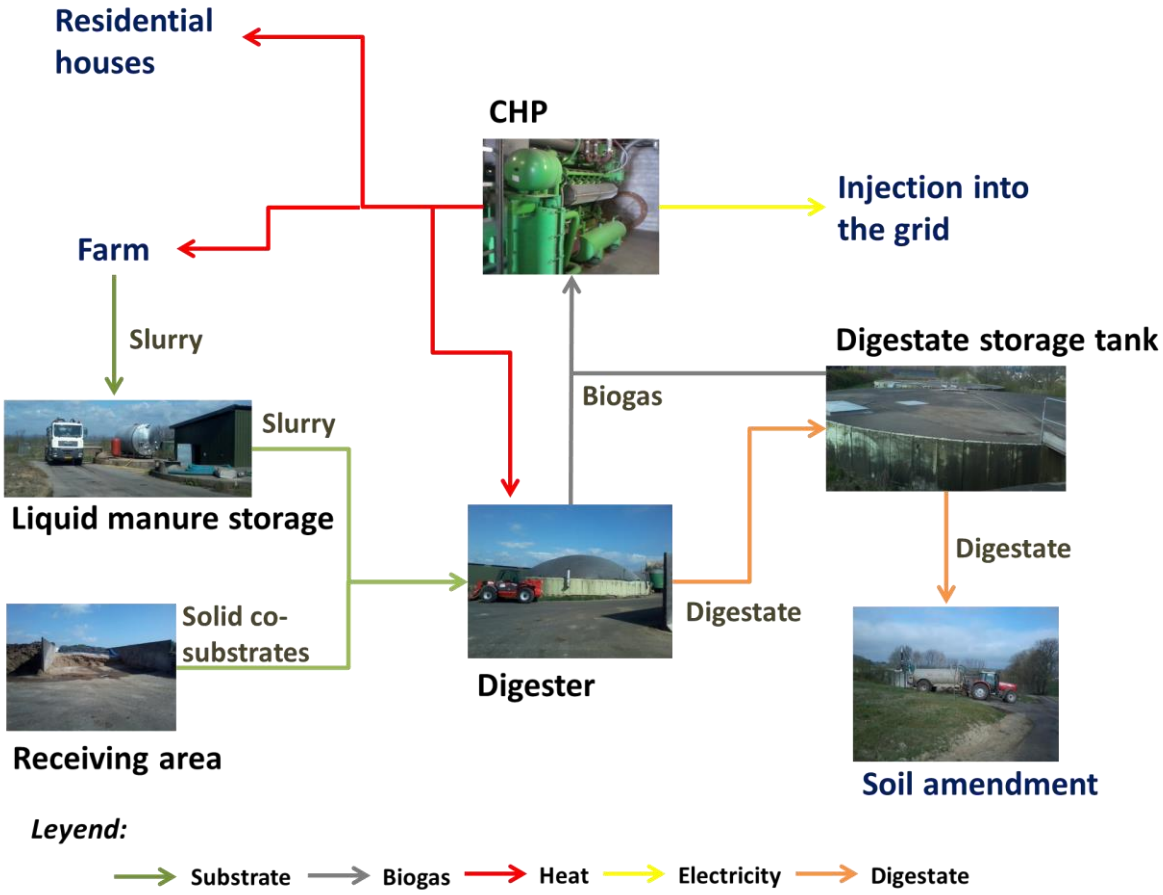

Figure 4: Example of agricultural biogas plant for co-digestion (pictures from the biogas plant in Beckerich in Luxembourg)

2.2.4 Process parameters and process stability

The factors affecting the biogas production are mainly related to the operating conditions (e.g. temperature, pH, retention time, etc.) and the feedstock characteristics, which can affect the different groups of bacteria involved, thus producing imbalance in the process. The main reasons for process imbalance are presented in the following sub-sections.

2.2.4.1 Feedstock characteristics and nutrients

The characteristics of a feedstock, in terms of its content of proteins, lipids, and carbohydrates (both the easily degradable and the slowly degradable fractions), is going to determine not only the final biogas yield and composition, but also the level of degradation and the rate. Also, certain fractions such as the lignin will not be degradable under normal conditions, or will present a very low availability for bacteria without treatment.

Cellulose is an important component of plants and thus it is significantly present during the anaerobic digestion of energy crops and agricultural waste for biogas production. In grass

silage, for example, cellulose can represent between 20% and 40% of the TS (Malherbe and Cloete, 2002; Koch et al., 2010; Wichern et al., 2009) and approximately 20% in the case of maize silage (Benito et al., 2012; Biernacki et al., 2013). Nevertheless, its degradation poses some challenges due to its structure and resulting slow hydrolysis (Noike, 1985). Indeed, cellulose is a polysaccharide consisting of a chain of glucose units forming complex arrangements and associated with other polymers such as hemicellulose and lignin (Malherbe and Cloete, 2002). Starch is another polysaccharide also present in certain crops, particularly maize in a proportion that can range from 25 to 32%. Finally, a small proportion (0-15%) of the TS can be constituted by easily degradable sugars such as glucose.

Moreover, the presence of certain macro and micro nutrients is important for the microbial growth. Macro-nutrients include carbon (C), nitrogen (N), phosphorus (P) and sulphur (S). The C/N ratio of the substrate should be in the range of 16:1 to 25:1. A low C:N ratio could result in a release of NH_3, which in turn could inhibit CH_4 production (Deublein and Steinhauser, 2011). Sulphur, phosphorus, potassium, calcium, magnesium and iron are required for specific cellular functions. These macro-nutrients should be present in the cell in concentrations around 10^{-4}M. Micro-nutrients (or trace elements) include iron, nickel, cobalt, and copper, which are required in smaller amount.

On the other hand, the lack of certain micro-nutrients during operation can also have significant impact on the biogas production. While nutrients are generally present in sufficient quantities in slurries and manure, trace elements can be problematic during the mono-digestion of certain energy-crops and crops residues. For example, Lebuhn et al. (2008) showed that mono-digestion of maize could present process instability in biogas production already at a low OLR (i.e. 2 gVS/l/d) during long-term digestion due to the lack of certain trace elements, with methanogens being particularly affected. The most limiting element seemed to be cobalt, but with molybdenum and selenium being also required. In this sense, Munk et al. (2010) found a threshold of approximately 0.03 mgCo/kgFM for mono-digestion of maize, below which process breakdown could occur. A study of Wall et al. (2014) suggested that stable digestion of grass silage was possible at high OLRs when trace elements are added. Indeed, it was found that the addition of cobalt, iron and nickel, during long term mono-digestion of grass silage could contribute to a stable CH_4 yield even at a high OLR of 4 gVS/l/d (with recirculation of effluent).

2.2.4.2 Inhibitory substances

An inhibitory substance can either be present in the substrate or be formed during digestion under certain conditions. Certain heavy metals and antibiotics, which can have inhibitory effect and be toxic at certain concentrations, can be present in industrial and domestic wastewater, but are rarely present in agricultural biogas plants. The most common inhibitory substances in this type of plants are produced during degradation and include VFA, NH_3, and hydrogen sulphide (H_2S).

In the case of VFA, particularly the undissociated acid can have an inhibitory effect, as they can penetrate into the cells and denature the cell proteins. Some authors used HPr as a sole process indicator (Nielsen et al., 2007) while others suggested to use the variation in the HPr to HAc ratio as an indicator for impending failure (Marchaim and Krause, 1993). Hill and Holmberg (1988), for example, concluded that a HAc concentration greater than 0.8 g/l,

together with a sum of all the VFAs concentration (here after referred to as TVFA) greater than 2 g/l, and a HPr to HAc ratio greater than 1.4 were efficient indicators of failure during digestion. Nevertheless, these parameters were not found to be reliable to predict failure in advance and proposed using the concentration of iso-HBu and/or iso-HVa instead, with values between 5 and 15mg/l as indicator of approaching failure and above 15mg/l to indicate occurring failure. More recently, it has been proposed that the anaerobic fermentation can be considered to run optimally if the TVFA amounts to less than 1g/l and the concentration of HPr is lower than 0.25 g/l. Values above 4g/l of TVFA and of HPr above 1g/l could be considered as highly likely unstable process (Drosg, 2013).

During the digestion of energy crops, N can be released during the degradation of plant protein. Inside the reactor, N can appear in the forms of free NH_3 and ammonium (NH_4^+). The free NH_3 concentration, which is pH dependent (see Figure 5), has been suggested to be the active component causing inhibition (Koster and Koomen, 1988; Zeeman et al., 1985). Angelidaki and Ahring (1994) showed that relatively stable process was possible at high levels of NH_3 with well adapted microorganisms, although with reduced CH_4 yield. More recently, a decrease up to 50% in CH_4 production have been found for total NH_3-N concentrations between 1.7 g/l and 14 g/l, although the inhibitory effect can vary depending on the system (Chen et al., 2008).

H_2S is produced through degradation of sulphur containing compounds, and, as it happens with NH_3, it is the undissociated form (see Eq. 1), in the liquid phase, that is known to be inhibitory. As such, it can be considered as toxic for bacteria even at small concentrations (ca. 50 mg/l) (Deublein and Steinhauser, 2011). However, the microbial population can reach a certain degree of adaptation.

$$H_2S \leftrightarrow HS^- + H^+ \leftrightarrow S^{2-} + 2H^+ \qquad \text{Eq. 1}$$

Moreover, the undissociated form can also contribute to the precipitation of certain ionic species, thus reducing the bioavailability of trace elements including iron (Drosg, 2013). Finally, the presence of sulphates can also contribute to the growth of sulphate-reducing microorganisms, which can compete with methanogenic archaea for HAc and H_2 (Batstone et al., 2002).

2.2.4.3 pH and the buffering system

Each bacterial group has different operational pH ranges, with methanogenic groups having a pH optimum range between 6.8 and 7.2 (Gerardi, 2003) and fermentative bacteria with a wider pH range from 4.5 to 6.3, although also being able to function at neutral pH conditions. If the pH decreases below 6.8, the methanogens will be affected and thus the uptake of acids will be decreased, which in turn will result in an additional drop of the pH. Moreover, the pH value affects acid-base equilibrium of different compounds in the digester. At low pH, free acids (e.g. associated VFA) can cause inhibition, while at high pH, NH_3 can also result in inhibition.

The buffering capacity present in the reactor contributes to avoid pH drops due to the accumulation of VFA, and to keep it within a neutral range that allows the functioning of all bacterial groups. There are several buffering systems that allow for this natural regulation of the pH, with the bicarbonate (CO_2/hydrogen carbonate-HCO_3^-/carbonate-CO_3^{2-}, pka1=6.34 and

pKa2=10.32) and the NH_3 (NH_4^+/NH_3, pKa=9.3) being the most important buffering systems. In the case of the first system, CO_2 is continuously produced during the digestion and released into the gas phase. For a pH between 6.5 and 8.5, CO_2 will be increasingly being converted into HCO_3^- (see Figure 5, left), which will react with available protons (H^+) being released (e.g. during the acidogenesis phase), thus avoiding a decrease in the pH value (Eq. 2) (Deublein and Steinhauser, 2011). HCO_3^- alkalinity should in any case exceed 1 $gCaCO_3/l$ and preferably be in the range 2 to 3 gCaCO3/l for high rate systems (Pind et al., 2003).

$$H_2O + CO_2 \leftrightarrow H_2CO_3 \leftrightarrow H^+ + HCO_3^- \leftrightarrow 2H^+ + CO_3^{2-} \quad \text{Eq. 2}$$

As for the NH_3 buffering system (Eq. 3 and Eq. 4), approximately 99% of the NH_3-N is present in its dissociated form at a pH of 7.3, percentage that increases with decreasing pH (Figure 5, right).

$$NH_3 + H_2O \leftrightarrow NH_4^+ + OH^- \quad \text{Eq. 3}$$

$$NH_3 + H^+ \leftrightarrow NH_4^+ \quad \text{Eq. 4}$$

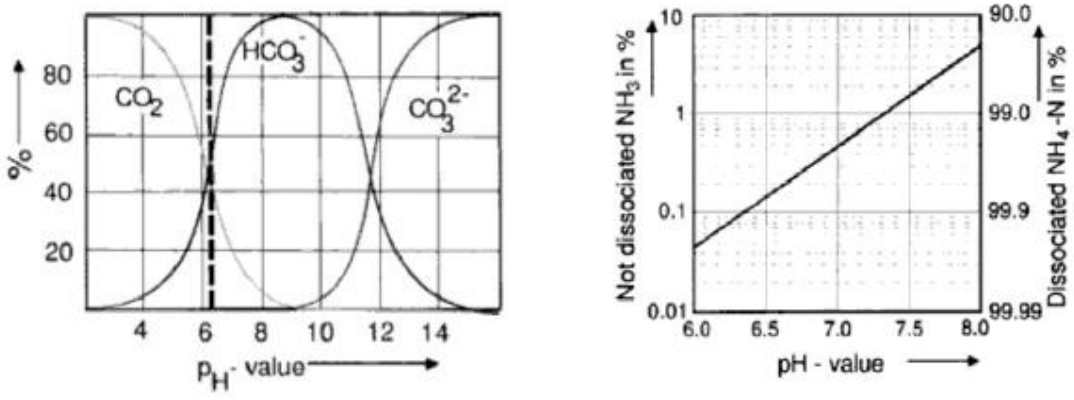

Figure 5: CO_2/ HCO_3^-/ CO_3^{2-} buffer system (left) and NH_3/NH_4^+ dissociation system (right) in aqueous media depending on the pH (Deublein and Steinhauser, 2011)

Manure and slurry commonly supplied into the digesters have a sufficient buffering capacity coming from the $CO_2/HCO_3^-/CO_3^{2-}$ and NH_3/NH_4^+ systems, which contributes to balance increasing concentrations of VFA. In the case of mono-digestion of certain solid lignocellulosic material, an external addition of buffering capacity would be necessary, with the recirculation of the liquid fraction of the effluent being an option.

Nevertheless, it is important to highlight that in well buffered systems, high VFA concentrations have to be attained in order to get a well detectable pH drop, thus probably being too late to determine imminent acidification or failure of the process. Consequently, although the pH can provide very useful information about the process, it cannot be considered as an early indicator of process imbalance (Pind et al., 2003; Drosg, 2013; Deublein and Steinhauser, 2011).

Alkalinity measures the ability of a solution to neutralize acids and it is usually expressed as grams of calcium carbonate $CaCO_3$ (Pind et al., 2003 a). The so called partial alkalinity (PA) represents the alkalinity, mainly due to the HCO_3^- buffering system. The intermediate alkalinity (IA) represents the sum of the VFA present in the reactor. An important indicator of stability of a process is the so-called alkalinity ratio, which is the IA/PA ratio, also known as TVFA/alkalinity ratio, the Ripley ratio or TVFA/total inorganic Carbon (TIC). In German, this parameter is

referred to as FOS/TAC. FOS stands for Flüchtige Organische Säuren, i.e. volatile organic acids, and is measured in mg HAc_{eq}/l, while TAC stands for Totales Anorganisches Carbonat, i.e. total inorganic carbonate (alkaline buffer capacity), and is measured in mg $CaCO_3$/l. In this work, this ratio is referred to as TVFA/TIC. The method applied for the measurements of these parameters is described in sub-chapter 3.5.

Cecchi et al. (2003) proposed to keep the TVFA/TIC ratio below 0.3 in order to ensure the good stability of the process. Nevertheless different values have been proposed in literature, for different substrates. For example, Lebuhn et al. (2008) found that a TVFA/TIC threshold of 0.5 should not be exceeded for the mono-digestion of maize silage. Overall, the maximum limits reported in literature for stable processes range from 0.3 to 0.8 (Drosg, 2013).

2.2.4.4 Temperature

Constant temperature conditions are important, as fluctuations can affect significantly the biogas production through a complex system. On the one hand, temperature is going to influence the growth rate of bacteria, which is going to be higher at thermophilic conditions, which in turn makes the process faster under these conditions. This means that a well-functioning thermophilic digester can be operated at a higher OLR or at a lower HRT than at mesophilic conditions. For example, a study by Cavinato et al. (2010) analysed the benefits of applying to the anaerobic co-digestion of cattle manure with agro-wastes and energy crops a temperature of 55°C instead of 47°C. The experimental work pointed out that biogas production improved from 0.45 to 0.62 m^3/kg VS operating at proper thermophilic conditions. Moreover, also the CH_4 content increased from 52% to 61%.

On the other hand, methanogenic diversity is in general lower in plants operating at thermophilic temperatures as most of the methanogenic microorganisms belong to the mesophilic range. Therefore, at the thermophilic range, methanogens are going to be more sensitive to changes in temperature and other operational parameters (Deublein and Steinhauser, 2011; Weiland, 2010).

Furthermore, temperature has direct effect on physical-chemical properties of most components in the digester. For example, temperature has an important effect on NH_3 content. Indeed, it has been observed that both acidogenesis and methanogenesis are negatively affected by increased NH_3 concentrations at the thermophilic range, which prevail when the operational temperature is increased (El-Mashad et al., 2004). Angelidaki and Ahring (1994) studied the combined effect of temperature and NH_3 and for high free NH_3 loads, the results clearly showed a higher sensitivity to inhibition with higher temperatures. Thus, lowering the process temperature could be a good option in the case of NH_3-induced inhibition in anaerobic reactors. Poor process performance was observed for a concentration of NH_3-N exceeding 0.7 g-N/l.

2.2.4.5 Mixing

If taking into considering the mixing inside the digester, it is possible to have completely stirred, percolation and plug-flow reactors. Active stirring can be obtained by using mechanical, hydraulic, or pneumatic mixing with up to 90% of biogas plants using mechanical stirring equipment (Weiland, 2010). An effective mixing system is critical for a stable and

efficient operation of an anaerobic process, as it allows for a better contact of the microorganisms with the substrate and also to maintain the homogeneity inside the reactor (in terms of temperature and solids mixture throughout the tank). It also facilitates the release of gas and it helps to prevent solids' deposition and scum formation (Schön, 2009; Rojas et al., 2010). Poor mixing could lead to stratification within the digester, hence only partially digested sludge being withdrawn with effluent.

Several studies showed that the mixing intensity in a CSTR reactor has an effect on the inhibition process and the recovery from overload (Vavilin and Angelidaki, 2005; Rojas et al., 2010).

Vavilin and Angelidaki (2005) investigated the effect of mixing intensity in CSTR digesters treating MSW and manure. They found that when the organic loading (OL) was high, intensive mixing resulted in acidification and process failure, while low mixing intensity was crucial for stable digestion. It was hypothesized that mixing was preventing establishment of methanogenic zones in the reactor space (Vavilin and Angelidaki, 2005).

Rojas et al. (2010) analysed the biogas yield of lipid-rich waste and corn silage under the effect of stirring in batch and semi-continuous reactors. The results showed a significant effect of stirring on the anaerobic digestion when using sludge from a biogas plant to inoculate the reactor. The addition of slurry improved the biogas production. This suggested that the more diluted the media in the reactor, the better the contact between the bacteria and the substrates, thus making stirring not as critical for digestion performance.

Overall, a certain level of mixing is required to ensure a successful operation of the reactor; nevertheless it should not disrupt the microbial community structure and functioning. For example, it has been observed that continuously mixed conditions could inhibit the syntrophic interactions in a reactor (McMahon et al., 2001). Also, mixing consumes energy, and thus can have an impact on the overall profitability of a plant. Therefore, the praxis in biogas plants is that mixers rotate slowly, with a rotating speed between 15 and 50 rpm (Wellinger, 1999), although specific guidelines in this respect do not exist.

2.2.4.6 Retention time and organic load

One further important parameter is the HRT, which indicates the average time that the added feedstock remains in the fermenter before being removed. This is calculated from the utilisable volume of the fermenter and the amount of biomass loaded daily, according to Eq. 5. It is also the reciprocal of the dilution rate (D) in continuous systems.

$$HRT = \frac{\text{Capacity of the fermenter V}\,(\text{m}^3)}{\text{Flow of feedstock added Q}\,(\text{m}^3 d^{-1})} \qquad \text{Eq. 5}$$

In the absence of recirculation of liquid, the CSTR have the same HRT and solid retention time (SRT).

Methanogenic microorganisms have a long regeneration time, between 5 and 16 days, and therefore it is necessary to have HRT of at least 10-15 days to avoid washing out without systems for retaining and returning biomass. In the case of thermophilic systems, HRT down to 4-6 days are feasible (Deublein and Steinhauser, 2011; Pind et al., 2003).

Also, it is important to take into account the type of material that is to be digested. The rate-limiting step for agricultural systems digesting composite material usually is the hydrolysis. The degradation rate of the different components present in lignocellulosic material increases in the following order: cellulose, hemicellulose, proteins, fat, and easily degradable carbohydrates (Wellinger, 1999), and therefore, the required retention time can be decreased in that order. Energy crops digestion requires prolonged HRT of several weeks to achieve complete degradation given its high content in lignocellulosic fractions.

The OLR is used to characterise the loading on anaerobic treatment systems and is a measure of the biological conversion capacity of the anaerobic digestion system. Feeding a system above its sustainable OLR could result in a decrease of the biogas production and acidification, and ultimately in a cessation of the process (Golkowska et al., 2012). It can be expressed in terms of the mass of VS applied and is calculated as follows:

$$OLR\,(gVS/l/d) = \frac{Q \times C}{V} = \frac{C}{HRT} \qquad \text{Eq. 6}$$

where OLR is expressed in kgVS/m^3/d, Q is the influent flow rate [m^3/d], C the concentration of VS in the feedstock [kgVS/m^3] and V the reactor WV [m^3].

The typical loading rate for wet fermentation processes is usually between 2 and 4 kg VS/m^3/d without the addition of trace elements (Weiland, 2010), although threshold values might change depending on the specific feedstock and reactor configuration. This aspect was further investigated in this research.

2.2.4.7 Current research gaps

Overall, while the impact of certain agronomic parameters on the biogas potential of different energy crops have been previously addressed and are well known (e.g. grass species, harvesting period, ensiling phase, etc.), others, particularly operational parameters, still need further investigation. This is the case, for example for the OLR, which has to be optimised in a way that allows a maximum CH_4 yield and volumetric CH_4 production, while avoiding system instability and failure due to the accumulation of intermediary products such as VFA, which can potentially affect the stability of the process. The impact of the OLR in the process stability and performance have been investigated in the field of energy crop and crop residues for wheat straw (Hashimoto, 1989), for cellulose (Golkowska and Greger, 2010), food and green wastes (Liu et al., 2009), maize silage (Raposo et al., 2006), sunflower oil cake (Raposo et al., 2009), and whole stillage from a dry-grind corn ethanol plant (Eskicioglu and Ghorbani, 2011). But these studies were conducted in batch feeding conditions, which results can be different to that of semi-continuous or continuous feeding conditions due, for example, to the different acclimation of the bacteria and the maximum uptakes and growth that is possible in each case.

Different authors have investigated the continuous co-digestion of different types of grass with manure and slurry (Frigon et al., 2012; Mähnert et al., 2005; Xie et al., 2012; Lehtomäki et al., 2007) in CSTR at loadings up to 4 gVS/l/d. The same type of analysis, to investigate the response of anaerobic systems to increasing loading rates during continuous mono-digestion is still needed for different crops. Moreover, literature is scarce on one-stage digestion, which is the most common application at commercial scale (Nizami and Murphy, 2010).

Finally, as regards the effect of the feedstock characteristics on the process performance, some recent publications have reported on the co-digestion of manures and various agricultural by-products, including crop residues, MSW and slaughterhouse waste (Pagés Díaz, et al., 2011), cattle manure, maize, fruit-processing waste and bread (Cavinato et al., 2010), or various animal manures and olive husk (Fantozzi and Buratti, 2009). But there are still very few studies examining different mixing ratios for energy crops co-digestion. Some examples include the work of Comino et al. (2010) for cow manure with a crop silage mix, Lehtomäki et al. (2007) for cow manure with grass silage and crop residues, by Cuetos et al. (2011) for swine manure with energy crops residues, and by Bauer et al. (2009) for a mix of different crops (maize, barley, sunflower, lucerne, and sorghum). In most cases, the experiments are performed under batch feeding conditions. Knowledge regarding the optimum mixture and resulting synergies for lignocellulosic material is still limited, especially regarding maize and grass silages, crops with increasing popularity in Central Europe's agricultural biogas plants (Amon et al., 2007; Gerin et al., 2008; Resch et al., 2008). Moreover, the effect of changing feedstock characteristics during semi-continuous or continuous digestion still needs further understanding.

2.3 Anaerobic digestion modelling

Numerical modelling allows investigating and predicting the static and dynamic behaviour of a system beforehand, without the need of experimental work, or with a very limited number of trials. Consequently, it can play a most important role, not only in the understanding of the process, but also on its optimisation and control.

While in wastewater, complex models have been developed at laboratory scale and are widely applied at large scale, in anaerobic digestion of energy crops and other lignocellulosic material this is not the case. Modelling in this field has not received the attention required to improve and ensure its wider application, especially in design, although since 2010 a handful of publications address this issue.

This sub-chapter describes in brief different models that have been proposed to date that are of relevance for this work, the fundamentals and principles of the ADM1 that, as explained earlier, is the starting point of the current research project, and different existing modelling applications in the field of energy crops and crop residues.

2.3.1 Relevant models proposed in the literature

Different types of model can be distinguished in literature for describing the anaerobic digestion of organic substrates. While the purpose of some is merely to predict the final CH_4 production given the biochemical composition of the substrates used, other models intend to describe the microbial kinetics with different levels of detail, which determines their level of complexity. Some of the most known models are described in brief below.

2.3.1.1 Models for calculating biogas production

On the basis of the known elemental composition of the substrates, and using the stoichiometry of the reactions, Buswell and Mueller (1952) proposed an empirical equation to

determine the theoretical biogas yield. It was further modified by Boyle in 1977 to include N, according to the following equation:

$$C_aH_bO_cN_d + \left(a - \frac{b}{4} - \frac{c}{2} + \frac{3d}{4}\right) \times H_2O \rightarrow \left(\frac{a}{2} - \frac{b}{8} + \frac{c}{4} + \frac{3d}{8}\right) \times CO_2 + \left(\frac{a}{2} + \frac{b}{8} - \frac{c}{4} - \frac{3d}{8}\right) \times CH_4 + d \times NH_3 \quad \text{Eq. 7}$$

Kleerebezem and van Loosdrecht (2006) also proposed a method for an initial analysis of the biogas production and composition as well as the reactor pH on the basis of the substrate characterization.

More recently, Amon et al. (2007) developed the methane energy value model (MEVM) for different energy crops, particularly grass and maize, which estimates CH_4 yield from the nutrient composition. The MEVM considers the impact of the content of crude protein, crude fat, crude fibre, N-free extracts (NfE) to determine the so-called methane energy value (MEV), with Eq. 8 (Amon et al., 2007). The coefficients of regression (i.e. x1, x2, x3 and x4) were determined for each case through batch experiments.

$$\begin{aligned} \text{MEV}(l_N CH_4 kg^{-1} VS) &= x1 \times \text{crude protein (XP) (content in \% TS)} \\ &+ x2 \times \text{crude fat (XL) (content in \% TS)} \\ &+ x3 \times \text{crude fibre (XF) (content in \% TS)} \\ &+ x4 \times \text{N-free extracts (XX) (content in \% TS)} \end{aligned} \quad \text{Eq. 8}$$

2.3.1.2 Models with reaction kinetics

When addressing the kinetics of anaerobic digestion of biomass, three different aspects can be considered: the growth of the microorganisms involved, the degradation of the substrate and the product formation (Garcia-Heras, 2002; Gerber and Span, 2008). It is important to take into account that bacterial growth is limited by the amount of available substrate and by certain conditions in the media such as the presence of inhibitory substances, the pH or the temperature. Moreover, microorganisms have a limited life span, and after their death, they are reincorporated into the degradation process (Garcia-Heras, 2003).

First-order kinetics is the simplest model to describe substrate uptake, without considering the growth of microorganisms. It can be expressed according to Eq. 9.

$$\frac{dS}{dt} = -k \times S \quad \text{Eq. 9}$$

where S represents the substrate concentration and k the first-order constant. Monod kinetics consider the growth of microorganism, and has been extensively used in anaerobic digestion (Eq. 10).

$$\mu = \mu_{max} \times \frac{S}{S + K_s} \quad \text{Eq. 10}$$

Where μ is the bacterial growth rate, μ_{max} is the maximum bacterial growth, and K_s is the half saturation constant, which expresses the value at which μ reaches the value of $\mu_{max}/2$. This

expression can be modified to include inhibition by product or substrate concentration. This expression can also be expressed in terms of the substrate degradation rate (dS/dt) as follows:

$$\frac{dS}{dt} = -\frac{\mu_{max}}{Y} \times \frac{S}{K_s + S} \times X \quad \text{Eq. 11}$$

where Y is the biomass yield coefficient and X is the concentration of microorganisms.

However, some limitations to Monod kinetics have been highlighted in the past. For example, it has been suggested that it does not describe satisfactorily the degradation of complex substrates (Pfeffer, 1974) or the lag phase that can be observed for certain substrates (Strigul et al., 2009). Thus, some modifications were proposed, such as considering the biomass concentration with the Contois model (Contois, 1959) or including the influence of the initial concentration of substrate (Chen and Hashimoto, 1978), to mention a few.

These kinetics have been chosen by authors in models more or less complex depending on their purpose. For example, first-order kinetics were used by Hashimoto for determining the CH_4 production from straw degradation (Hashimoto, 1989). Eastman and Ferguson also proposed a model for describing primary sewage sludge digestion, using first-order kinetics for the description of hydrolysis, and Monod for the substrate utilisation phase (Eastman and Ferguson, 1981). Monod kinetics were also used by Hill in 1983 to describe the fermentation of animal wastes (swine, poultry, beef and dairy manures) (Hill, 1983). First-order kinetics have been used for describing the disintegration, the hydrolysis phase and the bacterial biomass decay in multispecies models (taking into account several bacterial groups) such as the model proposed by Angelidaki et al. (1999) or in the ADM1, proposed by the IWA in 2002 (Batstone et al., 2002), which will be further described in the next sub-section. Chen and Hashimoto used a modified version of the Contois kinetics for describing the degradation of organic waste successfully, by including a coefficient to take into account for the non-biodegradable part of the substrate (Chen and Hashimoto, 1980). Vavilin et al. (1996) investigated the application of different types of kinetics to the degradation of particulate organic matter and found that surface related kinetics (surface colonisation of particles by the hydrolytic bacteria) were more adequate to describe the process. Alternatively, Song et al. (2005) proposed to consider an area specific hydrolysis rate, although the possibility of determining the surface in a substrate could be difficult in practice.

Table 7 present a selection of values for the disintegration and/or hydrolysis constant from literature proposed for different agricultural substrates, as calculated applying different kinetic models (i.e. first-order, Monod, and Contois) for these steps.

Table 7: Selection of disintegration/hydrolysis rate values for different agricultural substrates estimated according to different kinetic models

Kinetic model	Parameter	Substrate	Parameter value	Temperature (°C)	Feeding mode	Reference
First-order	K (d^{-1})	Cellulose	0.1	35	Batch	Vavilin et al. (1996)
			0.10-0.15	38	Batch	O'Sullivan et al. (2006)
			0.45	38	Semi-Continuous	Song and Clarke (2009)
			0.123	37	Batch	Wall et al. (2014)
		Cattle manure	0.25	35	Batch	Vavilin et al. (1996)
		Maize	0.36	55	Batch	Golkowska et al. (2012)
			0.23- 0.24	55	Semi-Continuous	
			0.26 – 0.60	55	Continuous	
		Straw	0.08 – 0.24	35	Batch	Hashimoto (1989)
		Ryegrass silage	0.107	37	Batch	Wall et al. (2014)
		Napier grass	0.05- 0.16	35	Batch	Chynoweth et al. (1993)
		Sugar cane	0.05 – 0.016	35	Batch	
		Carbohydrates	0.5 - 2			Garcia-Heras (2003)
		Lipids	0.1 – 0.7			
		Proteins	0.25 – 0.8			
Monod	v_{max} (d^{-1})	Cellulose	1.25	35	Batch	Vavilin et al. (1996)
		Cattle manure	3	35	Batch	Vavilin et al. (1996)
		Starch	37.5	35	Continuous	Noike et al. (1985)
		Glucose	66.2	35	Continuous	Noike et al. (1985)
Contois	v_{max} (d^{-1})	Cellulose	1.25	35	Batch	Vavilin et al. (1996)
			1.25	35	Batch	Noike et al. (1985)
		Cattle manure	3	35	Batch	Vavilin et al. (1996)

Up to date, a large variety of models of varying complexity have been proposed, depending on the bacteria groups, reactions considered and parameters included. The different existing models have been reviewed extensively in literature and classified according to different criteria (Lyberatos and Skiadas, 1999; Tomei et al., 2009; Lübken et al., 2010; Pavlostathis and Giraldo-Gomez, 1991; Gerber and Span, 2008).

One of the most comprehensive models to date in the field of anaerobic digestion is the ADM1 (Batstone et al., 2002), proposed in 2002 by the IWA Task Group for Mathematical Modelling of Anaerobic Digestion Processes to overcome some of the limitations of previous existing models (mainly their specificity to certain process and substrates). In particular, the ADM1 model was intended to be a common tool that could be applied to a large variety of processes. Given the fact that part of the PhD work involves the development of a model based on the ADM1, it is briefly described in the following sub-section.

2.3.2 The ADM1 model

The ADM1 (Batstone et al., 2002) is a highly complex model which describes the evolution of 32 dynamic state variables, including 7 groups of bacteria and archaea, and considers 19 biochemical kinetic processes coupled to 105 kinetic and stoichiometric parameters.

Overall, two types of processes take place during the conversion of the organic matter, namely the biochemical and the physico-chemical reactions, described below. Biochemical reactions are considered as irreversible processes, while physico-chemical reactions are considered as reversible.

2.3.2.1 Biochemical reactions

In the ADM1, two extracellular steps (disintegration and hydrolysis) and three intracellular steps (acidogenesis, acetogenesis and methanogenesis) are considered (Batstone et al., 2002). All the extracellular steps are assumed to be first-order. Death of biomass is also represented by first-order kinetics, and dead biomass is maintained in the system as composite particulate material (Batstone et al., 2002).

For all intracellular biochemical reactions, Monod-type kinetics are used. These are expressed in terms of the substrate uptake rather than the bacterial growth, according to Eq. 12.

$$\rho = k_m \times \frac{S}{K_S + S} \times X \times I_1 \times I_2 \times \ldots \times I_N \qquad \text{Eq. 12}$$

where ρ is the substrate uptake rate [kgCOD/m^3/d], k_m is the maximum specific uptake rate [kgCOD/kgCOD/d], S is the substrate concentration [kgCOD/m^3], K_S is the half-saturation coefficient [kgCOD/m^3], and X is the substrate-specific biomass concentration [kgCOD/m^3], and $I_1 \ldots I_n$ are factors to describe inhibition by, for example, H_2 (on the acidogenic groups), free NH_3 (on the acetoclastic methanogens), or pH (all groups).

2.3.2.2 Physico-chemical reactions

Physico-chemical reactions are not biologically catalysed and essentially include the processes of ionic association/dissociation and gas-liquid mass transfer phenomena. Solid precipitation is not included in ADM1. Dissociation/association processes are often referred to as acid/base equilibrium processes, and refer to the couples NH_4^+/NH_3, CO_2/HCO_3^-, VFA/VFA^- and H_2O/OH^-.

2.3.2.3 Modelling within the ADM1 model

The modelling concept in the ADM1 model is expressed using the Peterson matrix format, which presents, in a structured manner, all the model components, with processes organised in rows and model variables in columns. A process rate ρ is formulated for each process used. The respective rate equation matrices for dissolved and particulate compounds involved in the biological processes as presented in the ADM1 are reported in Annex B, Table B.1 and B.2.

For each component, the mass balance within the system boundary can be expressed via liquid phase equations as expressed in Eq. 13 (assuming a constant reactor volume).

$$\frac{dS_{liq,i}}{dt} = \frac{q_{in} \times S_{in,i}}{V_{liq}} - \frac{q_{out} \times S_{liq,i}}{V_{liq}} + \sum_{j=1-19} \rho_j \times \nu_{i,j} \qquad \text{Eq. 13}$$

Accumulation= Input- Output + Reaction

where the reaction term is the sum of the kinetic rates ρ_j for process *j* [kgCOD/m^3/d] multiplied by the stoichiometric coefficients $\nu_{i,j}$. $S_{liq,i}$ is the concentration of component i [kgCOD/m^3], q is the flow [m^3/d], and V_{liq} is the volume of the reactor [m^3].

COD [kgCOD/ m^3] was chosen as the chemical component base unit for ADM1, with inorganic carbon (IC) (HCO_3^- and CO_2) and IN (NH_4^+ and NH_3) in (kmoleC/m^3) and (kmoleN/m^3), respectively.

The acid-base reactions involved in the anaerobic digestion can be described, depending on the chemical process rates, in terms of algebraic or differential equations. In both cases it is necessary to express the charge balance as follows:

$$S_{Cat^+} + S_{NH_4^+} + S_{H^+} - S_{HCO_3^-} - \frac{S_{Ac^-}}{64} - \frac{S_{Pr^-}}{112} - \frac{S_{Bu^-}}{160} - \frac{S_{Va^-}}{208} - S_{OH^-} - S_{An^-} = 0 \quad \text{Eq. 14}$$

where S_{Cat}^+ and S_{An}^- are the metal ionic concentrations that behave like bases and strong acids, respectively. These components are considered as inert substances and therefore their concentration is assumed to be constant.

The Henry´s law is applied to describe the gas–liquid equilibrium. On this basis, the mass transfer rates of the gaseous components (referred to the liquid volume unit, $\rho_{T,i}$ and expressed as kmole/m^3/d), are included in the rate equation matrix reported for each gas in Annex B, Table B.3.

Overall, the gas phase rate equations are very similar to the liquid phase equations (Eq. 13), except there is no advective influent flow. They can be expressed with Eq. 15 (assuming a constant gas volume).

$$\frac{dS_{gas,i}}{dt} = -\frac{q_{gas} \times S_{gas,i}}{V_{gas}} + \rho_{T,i} \times \frac{V_{liq}}{V_{gas}} \quad \text{Eq. 15}$$

where $S_{gas,i}$ is the gas concentration of gas *i* [kmole/m^3], q_{gas} is the gas flow [m^3/d], and V_{liq} and V_{gas} are the volumes of the reactor and the headspace [m^3], respectively (Batstone et al., 2002). The gas transfer rates $\rho_{T,i}$ (in kgCOD/m^3/d) are estimated according to Eq. 16, with the $p_{gas,i,}$ being the partial pressure of component i (bar), K_La is the gas-liquid transfer coefficient (d^{-1}), $S_{liq,I}$ is the concentration of component i in the liquid phase [kgCOD/m^3], and $K_{H,I}$ being the Henry's law coefficient of gas i [kmole/m^3/bar].

$$\rho_{T,i} = k_L a \times \left(S_{liq,i} - K_{H,i} \times p_{gas,i}\right) \quad \text{Eq. 16}$$

2.3.2.4 Model inhibition terms

In the ADM1 model (Batstone et al., 2002) different inhibition terms are suggested with emphasis in the effects of pH (on all the bacterial groups), insufficient N concentration and H_2 inhibition. pH inhibition is implemented as an empirical equation, while H_2 and free NH_3 inhibition are represented by non-competitive functions. The other uptake-regulating functions take the form of Monod kinetics for IN (NH_3 and NH_4), to prevent growth with low N concentration, and competitive uptake of HBu and HVa by the single group that utilises these two organic acids. The inhibition terms implemented in ADM1 are listed in Annex B.4.

2.3.2.5 Limitations in the ADM1 model and problems identified

The ADM1 does not include certain processes such as homoacetogenesis and acetate oxidation, sulphate reduction and sulphide inhibition, nitrate reduction, weak acid and base inhibition, and LCFA inhibition (Batstone et al., 2002). Perhaps, and according to the results of

recent research, the omission of the syntrophic acetate oxidation might be one of the most relevant. ADM1 considers that the majority of acetate will be degraded via the acetoclastic pathway, for mesophilic conditions. As explained in sub-chapter 2.2.1.3, acetate oxidation, performed by acetate-oxidising bacteria, produces H_2 and CO_2, which are subsequently converted into CH_4. Therefore, there is a syntrophic association between acetate-oxidizing and hydrogenotrophic methanogens. The ADM1 recognises that under certain conditions (e.g. extreme thermophilic processes, or for low acetate concentrations at thermophilic conditions), the acetate oxidation pathway might be necessary. Nevertheless, as explained in the aforementioned sub-section, recent research highlights the importance of hydrogenotrophic groups in methanogenesis phase, also under mesophilic conditions (Zhu et al., 2011; Demirel and Scherer, 2008; Nettmann et al., 2008; Munk et al., 2010). This would suggest that the current COD flux assumed in the ADM1 might need to be modified in the case of lignocellulosic material digestion.

Another important aspect is the fact that the degradation of glucose, which is used as the model saccharide, is not well described for all conditions. Indeed, two important products of glucose fermentation, namely, ethanol and lactate, are not considered in the ADM1 due to the fact that they are present in very low concentrations during normal digestion conditions (Batstone et al., 2002). Lactate is an important intermediate but it is quickly degraded and thus only present during transient or overloading conditions. Ethanol is produced mainly at low pH (below 5). ADM1 recognises that it should be desirable to include these intermediates in the case of substrates yielding high glucose concentrations, transient conditions or when operating at low pH (e.g. to promote the production of ethanol).

Moreover, problems have been found when closing the C and N balances (Ersahin et al., 2007; Blumensaat and Keller, 2005), as there are discrepancies between the N and C content proposed for the bacterial biomass and the composite material, in which decayed biomass is converted to. This makes it necessary to introduce stoichiometric coefficients for the biomass decay process expressing N and C release due to biomass decay (Ersahin et al., 2007; Blumensaat and Keller, 2005).

The ADM1 application has also been reported to have practical problems in the case of heterogeneous and particulate wastes related to the characterization of the feedstock and the associated model definition of the disintegration and hydrolysis steps (Zaher et al., 2009; Lübken et al., 2007). Indeed, the ADM1 assumes default values for the fractionation of the composite material during the disintegration, without considering the actual characteristics of the substrate in terms of the main components (carbohydrates, proteins, and lipids).

Finally, because ADM1 is currently the most comprehensive description of anaerobic degradation, it is a highly complex model, with many different parameters and therefore, difficult to properly calibrate with experimental data.

2.3.3 Application of the ADM1 to anaerobic digestion of agricultural waste

The ADM1 model has been applied previously for the simulation of the anaerobic degradation of different substrates, including waste activated sludge (Ramirez et al., 2009), sewage sludge (Blumensaat and Keller, 2005), or distillery vinasse (Ramirez et al., 2009 b). In recent years there has been an increasing interest on the digestion of agricultural substrates, and

consequently on the modelling of this type of substrates. Accordingly, some studies were published addressing the ADM1 application to the digestion of agricultural by-products and residues such as manure (Palatsi et al., 2010; Schoen et al., 2009), corn processing wastewater (Ersahin et al., 2007), olive mill solid waste (Fezzani and Cheikh, 2008) or different agro-waste (Galí et al., 2009). Since 2007, and in parallel to the increasing share of this type of substrate in the feedstock of many biogas plants, a handful of studies have addressed the modelling of the fermentation of energy crops, in mono or co-digestion. These are the work of Koch et al. (2010) for mono-digestion of grass silage in loop reactors in mesophilic conditions; Thamsiriroj et al. (2012) for continuous mono-digestion of grass silage in 2-stage CSTR anaerobic digester; Wichern et al. (2009) for continuous mono-digestion of grass silage under mesophilic conditions, Lübken et al.(2007) for liquid manure and fodder for cows in a mesophilic CSTR reactor, Biernacki al. (2013) for mono-digestion of grass, maize, green weed silage, and industrial glycerine in batch reactors, by Wolfsberger (2008) for maize silage and sunflower press residues in CSTR reactors fed continuously, and by Schlattmann (2011) for maize silage, grass silage and rapeseed oil in CSTR reactors in mesophilic conditions. It is worth mentioning as well the work of Antonopoulou et al. (2012), who adapted the ADM1 so as to describe the fermentative H_2 production from the extractable sugars of sweet sorghum biomass (i.e. soluble carbohydrates). To the knowledge of the author, this work was one of the first attempts to apply the ADM1 model to describe H_2 production in continuous systems (in this case using monosaccharides as substrates).

All the above mentioned studies have changed, to a different extent, the original ADM1 so as to adapt it to the digestion of lignocellulosic material and address previously mentioned limitations. For example, the inflow fractioning of the total COD is of highest importance for the calibration of the ADM 1 and is strongly affecting the gas composition. In this regard, one option was to do it based on detailed measurement data from the Weende and Van Soest analysis (Koch et al., 2009; Wichern et al., 2009; Lübken et al., 2007). On the basis of this analysis, Koch et al. (2010) proposed a method to determine the stoichiometric f-factors (e.g. fPr_Xc – protein content), to define the disintegration of the composite material into carbohydrates, proteins, and lipids and also into a no-degradable inert fraction.

As indicated in sub-chapter 2.3.2.1, disintegration and hydrolysis are modelled in ADM1 according to first-order kinetics assuming that their rates do not depend on disintegration/hydrolytic biomass concentrations. It has been suggested to modify first-order kinetics to account for slowly degradable material (Wolfsberger, 2008) or to use Contois kinetics to describe the disintegration and hydrolysis steps (Ramirez et al., 2009). Koch et al (2010) also integrated the influence of solids on hydrolysis in ADM1.

Table 8 summarises some changes that have been introduced to date in the ADM1 for better adjustment to the characteristics of lignocellulosic material.

Table 8: ADM1 applications to the fermentation of lignocellulosic material and modifications

Publication	Substrate	Experimental data used	Software used	Modifications implemented
Lübken et al. (2007)	Liquid manure and fodder for cows	Semi-continuously-fed reactor	SIMBA 4.0 based on MATLAB/SIMULINK	• Modified pH inhibition terms. • Parameter calibration (including calibration of hydrolysis kinetic constants). • Influent COD according to substrate characteristics.
Wolfsberger (2008)	Maize, sunflower/whole crop maize silage	Continuous and batch experiments digestion	Based on the existing MATLAB/SIMULINK file of the original ADM1 by Rosen et al.	• Second hydrolysis rate for slow degradable carbohydrates. • Parameter calibration. • Addition of the Sulphate reduction process.
Wichern et al. (2009)	Mono-digestion grass silage	Semi-continuously-fed reactor	SIMBA 4.2 based on MATLAB/SIMULINK (Version 7.0)	• Influent COD according to substrate characteristics. • Parameter calibration (modified NH_3 and H_2 inhibition constants)
Thamsiriroj et al. (2012)	Mono-digestion grass silage	Continuously-fed 2-stage CSTR anaerobic digester	MATLAB/SIMULINK	• Uptake and decay of lactate degraders. • Parameter calibration. • Substrate fractionation according to substrate characteristics.
Koch et al. (2010)	Mono-digestion grass silage	Continuous experiments digestion	SIMBA 4.2 based on MATLAB/SIMULINK (Version 7.0.4)	• Substrate fractionation adapted to substrate characteristics. • Function to describe the influence of solids on the process of hydrolysis. • Dedicated variable for biomass decay products. • Parameter calibration (modified H_2 inhibition constants)
Biernacki et al. (2013)	Grass, maize and green weed silage	Batch experiments	MATLAB (own implementation) and IFAK's SIMBA	• Substrate fractionation • Calibration of disintegration and hydrolysis kinetic constants.
Schlattmann (2011)	Grass silage, maize silage, rapeseed, saccharose	Batch and semi-continuous experiments	AQUASIM	• TS-based input. • Substrate fractionation adapted to substrate characteristics. • Integration of the acetate oxidation. • Decayed biomass constitutes a separate variable. • 2-sided pH inhibition. • Parameter calibration.

Overall, the sources addressing the modelling of energy crop digestion to date are still scarce (7 in total), with most focusing on the mono-digestion of grass silage in CSTR reactors and for mesophilic conditions. Furthermore, there is no extensive comparative study on influence of changes in different operational parameters (e.g. feeding mode, OLR, or pH) on the kinetics of anaerobic digestion of energy crops and lignocellulosic material.

3. Materials and methods

3.1 Overview of experimental work

One of the objectives of the PhD research was to get a better insight into the impact of certain operational parameters not well addressed in literature to date on the biodegradability of selected energy crops, namely the OLR, the feedstock characteristics, and the feeding mode. In order to address existing research gaps, the focus was set on the mono-digestion of energy crops and on semi-continuous feeding conditions (once a day). A total of 31 experiments were conducted, which can be classified in 6 groups according to their main objective:

1. Experiments to investigate the impact of increasing loading on the process stability and performance during digestion of different substrates (grass silage, maize silage, and cellulose) for different feeding modes (batch and semi-continuous feeding).
2. Experiments to investigate the impact of the feedstock characteristics for different feeding modes, including different co-digestion mixtures of grass and maize silages for batch and semi-continuous feeding, and different types of carbohydrates (glucose, starch, and cellulose) during batch digestion.
3. Experiments to investigate the degradation of intermediary products, namely acetate and propionate.
4. Experiments to get a better insight into the impact of the feeding mode on the biogas performance.
5. Experiments to explore the feasibility and performance of a pH-phased 2 stages system for maize silage digestion.
6. Experiments to determine the biodegradability and methane potential of the different substrates and mixtures applied in the different experiments.

The experimental work allowed acquiring data for a variety of operational conditions and substrates, which were used for model calibration and validation. To this end, a variety of parameters were monitored. Some of the experiments also contributed to explore the applicability of certain methodological aspects in the field of lignocellulosic material digestion. Table 9 overviews the experiments and the different operational conditions that were applied in each case. A more exhaustive chronological summary of the operational conditions for each experiment is presented in Annex F. Additionally, and in order to get a better insight into the population diversity during the anaerobic digestion of energy crops, samples from two batch experiments and one semi-continuous experiment were sent to an external laboratory to quantitatively analyse the abundance of major Archaea groups, by means of real-time polymerase chain reaction (PCR) analysis[5].

[5] Performed in an external lab in Hochschule Offenburg, Germany. Prof. C. Zell.

Table 9: Experimental set-up overview

Temp.	WV (l)	Substrate	Mixing ratio (%MS/%GS)	Batch Digestion															Semi-continuous Digestion								
				OL (gVS/l)															OLR (gVS/l/d)								
				0.5	1	2	4	5	6	7	8	12	14	17	18	24	35	46	1	1.5	2	2.5	3	3.5	4.7	6	10
38 °C	0.4	MS, GS, Co-digestion	100, 30/70, 70/30, 40/60, 50/50									X															
	0.75	MS	-						X			X															
		GS	-						X		X			X	X	X	X	X									
		Co-digestion MS/GS	30/70									X															
			70/30									X															
			50/50									X															
			40/60									X															
		Cellulose	-						X																		
		Starch	-						X																		
		Glucose	-						X																		
		Sodium acetate	-	X	X	X	X																				
		Sodium propionate	-	X	X	X																					
		Gluten	-					X																			
	10	GS	-									X															
		MS	-									X															
		Cellulose	-		X														X	X							
	11.5	DGS	-																		X	X	X		X		
	6.675	DMS	-			X															X	X		X		X	X
		Co-digestion DMS/DGS	50/50																		X						
			30/70																		X						
		DGS	-																		X						
55°C	0.75	GS	-							X			X		X	X											

3.2 Origin of materials

3.2.1 Substrates

Two complex substrates were used in the experiments, namely perennial ryegrass (*Lolium perenne*) silage and maize (*Zea mays*) silage (whole crop) (see Figure 6). These two substrates were chosen because they are popular crops in agricultural biogas plants in Central Europe (Amon et al., 2007; Gerin et al., 2008; Resch et al., 2008). Given the influence of the harvesting period on the composition and thus on the methane potential, silages from different harvesting periods and years were used in the experiments. In total, four different grass silages (GS 1: late harvesting 2008, GS 2: mid harvesting 2011, GS 3: late harvesting 2012, and GS 4: early harvesting 2014) and two maize silages (MS 1: mid harvesting 2009 and MS 2: late harvesting 2011) were used in the experiments.

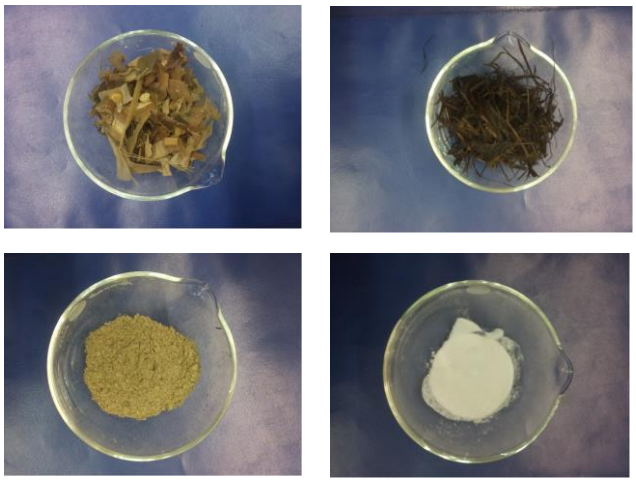

Figure 6: Substrates used in the experiments: whole plant maize silage (top left), grass silage (top right), maize silage dried at 60° and milled (bottom left), and microcrystalline cellulose (bottom right)

Upon delivery, each silage was finely cut (average particle size ≤ 5mm) and stored frozen (kept at -20 °C) until use (see sub-chapter 3.4). In the case of those substrates used in semi-continuous experiments, the unfrozen silage was subsequently dried at 60° and milled (particle diameter of approximately 0.75 mm) by means of a cutting mill (Pulverisette 15, Fritsch, Germany) to facilitate the feeding procedure. Depending on the drying temperature, the concentration of different volatile fractions could be reduced. The influence of the substrate drying temperature on the biogas production and quantity was evaluated in the beginning of this research project. The detailed results of this analysis can be found in Annex C. Up to 10% difference in the methane biogas yield was observed when comparing the performance of fresh and substrate dried at 60°C and up to 20% difference for substrate dried at 105°C. This was mainly due to the loss of the VFAs during the drying process. Therefore, the temperature of 60° was chosen for drying the substrates in the semi-continuous digestion experiments. Hereafter, when a dried substrate has been used in the experiments, it is denoted as dried grass silage (DGS) or dried maize silage (DMS).

Moreover, simple substances such as cellulose, starch, and glucose, or gluten (in some cases) are important constituents of lignocellulosic materials, and are therefore present during their digestion. Microcrystalline cellulose powder of pharmaceutical grade (Euro OTC Pharma

GmbH, Germany) with a particle size of 50 µm, was used in the experiments, along with glucose (purity ≥ 99.5%, Sigma–Aldrich, USA) and corn starch (Sigma–Aldrich, USA) to investigate the difference in the kinetics of these simple constituents. Additionally, the uptake of intermediate products such as acetate and propionate was also investigated at different concentrations. Sodium propionate (Sigma–Aldrich, USA) and sodium acetate (VWR, USA) were used in order to avoid problems with the CO_2 stripping with the addition of the ionised corresponding acids, which in turn could affect the measurement of the biogas.

3.2.2 Inoculum

The inoculum used in the experiments was obtained from Beckerich agricultural biogas plant in Luxembourg, from the post-digesters storage tanks. This plant, in operation since 2004, uses animal manure and a mix of grass and maize silages and cereals, and operates under mesophilic conditions.

The inocula were prepared following the German guideline Verein Deutscher Ingenieure (VDI) 4630 (*VDI,* 2006) for the degradation of organic matter. Before the beginning of each experiment, the inoculum was acclimated to the specific substrate in order to ensure a bacterial adaptation to the feed. To this end, either grass or maize silage was fed on a weekly basis (OL of 6 gVS/l) during the acclimation phase, which generally ran for 5 weeks in total. During this period, and after 2 feedings, 3 weeks without feeding were allowed to remove degradable components. The inoculum thus prepared was then filtered through a strainer (2mm mesh size) to remove remaining fibres and mixed to ensure homogenous conditions prior to the beginning of each test. In the case of batch experiments, the inoculum was reused in several tests before disposal. The influence of the inoculum characteristics and the conditioning phase on the biogas and methane production was investigated in batch tests with cellulose (see Annex D). The results suggested that while the final methane yield can be very similar for experiments using inocula with different history (observed difference of 0.3%), the evolution of the methane production can indeed differ, depending on the level of activation of the bacterial biomass.

The TS of the inoculum ranged from 3.15% up to 6% (of fresh matter - FM), and the VS between 1.75% and 3.65% (of FM). The detailed history of the inocula that was used in the experiments and the main characteristics are presented in the Annex E.

3.3 Substrates characterisation

3.3.1 Main characteristics

The substrates used in the experiments were characterised according to their TS and VS content (in the case of grass and maize silages determined for both the fresh and the dried silage). Moreover, complex substrates were also characterised according to their nutritional composition, in terms of protein and fat and the fibrous and non-fibrous carbohydrates.

The substrates were thus characterised using well established animal fodder analysis, namely the Weende and Van Soest methods. The Weende method is a feed characterisation method to determine the amount of biodegradable material in animal feeds. From this method crude fibre (XF), protein (XP) and fat (XL), and NfE can be obtained. The sum of the NfE and the XF

correspond to the carbohydrates present in the feedstock. This method was further developed by Van Soest to divide the fibre composition into biodegradable and non-biodegradable components. From this analysis, the neutral detergent fibre (NDF) (corresponding to the cellulose, hemicellulose, and lignin), acid detergent Fibre (ADF) (constituted by the cellulose and lignin) and acid detergent lignin (ADL) (lignin) are measured (as a percentage of TS). The procedures are detailed in different sources (Van Soest and Wine, 1967). Figure 7 outlines the biomass composition and the correspondence with the Weende and van Soest fractions. Both Weende and Van Soest fractions were determined through near-infrared spectroscopy (NIRS) by the Luxembourgish Administration for agricultural technical services (ASTA). The results from the analysis were calibrated on the basis of a database for crops, soils and organic waste, REQUASUD, from an association of nine Belgian agricultural laboratories. The content of the different VFAs was also determined in each case.

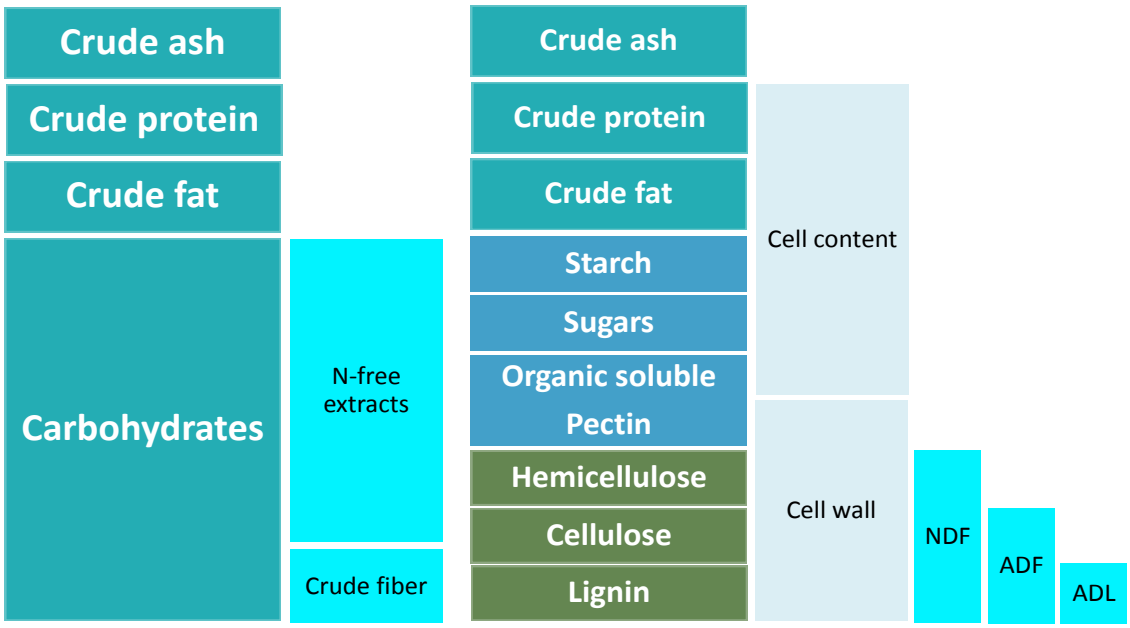

Figure 7: Biomass compositions and corresponding Weende (left) and Van Soest (right) fractions

Table 10 presents the characteristics of the fours grass silages and the two maize silages used in this research (both fresh and dried when applicable). The observed differences in composition are a result of the different levels of maturity (for the different harvesting periods and years). The obtained values are in line with those found in literature for equivalent harvesting periods for maize (Amon et al.,2007, b) and grass silage (Wichern et al., 2009; Koch et al., 2010).

Table 10: Characteristics of the complex substrates used in the experiments

Parameter	Units	GS 1	GS 2	GS 3	GS 4	MS 1	MS 2
TS	% Fresh Matter (FM)	34.7±1.08	n.d.	35.60	n.d.	34.55	n.d.
VS	% FM	31.38±0.74	n.d.	30.40	n.d.	33.13	n.d.
TS when dried at 60°C	% FM	n.d.	94.7±1.30	94.3±2.50	92.51±0.49	95.82±0.00	95.21±0.03
VS when dried at 60°C	% FM	n.d.	85.6±2.20	80.5±2.20	81.98±0.56	92.73±0.00	92.36±0.13
pH	(-)	n.d.	5.31±0.03	5.32±0.01	5.16±0.07	3.77±0.92	3.96±0.20
sCOD	g/gTS	n.d.	0.36	0.17±0.01	0.04±0.01	0.13	0.13
COD	g/gTS	1.03	1.38	1.19±0.05	1.26±0.04	1.27	1.17
TVFA	mg/gTS	34.67*				30.19*	
TVFA when dried at 60°C	mg/gTS		5.36	27.02	1.30±0.04	1.48	1.77
N Total	mg/gTS	n.d.	25.75	17.15±1.70	28.11±2.33	9.61	8.80
NH_4-N	mg/gTS	n.d.	1.64	2.96±0.34	1.43±0.46	1.17	0.94
XP	%TS	14.69	17.51±0.38	12.96±0.61	15.42	8.05	7.62±0.17
XF	%TS	30.46	23.40±0.3	30.02±1.74	23.40	20.28	17.14±0.35
XL	%TS	2.91	3.67±0.31	4.77±0.37	3.55	3.23	3.85±0.01
NDF	%TS	57.84	37.73±2.78	55.63±1.98	44.05	37.31	37.05±0.96
ADF	%TS	34.1	28.25±0.84	36.94±1.51	25.80	22.20	19.15±0.30
ADL	%TS	3.86	3.84±0.13	6.46±0.40	2.53	2.44	1.70±0.12
Cellulose	%TS	30.24	24.40	30.48	23.27	19.76	17.45

n.d.: Not determined

* Calculated from average values reported by average values reported by Weiβbach and Strubelt (2008 a; 2008 b).

The main characteristics of the cellulose, corn starch, and glucose used in this research are summarised in Table 11.

Table 11: Characteristics of the different carbohydrates used in the trials

	Units	Glucose	Starch	Cellulose
Chemical formula		$C_6H_{12}O_6$	$(C_6H_{10}O_5)n$	$(C_6H_{10}O_5)n$
TS	%FM	99.83	91.90	97.54
VS	%FM	99.83	91.89	97.52

3.3.2 Determination of the biological methane potential

The biological methane potential (BMP) of a substrate is an important characterisation parameter as it describes its potential performance and profitability during digestion. It refers to the methane yield that can be biologically achieved for a substrate in the absence of inhibitory conditions. A batch process is applied to determine this parameter at lab scale. Guideline to perform BMP assays for solid organic substrates are provided in the VDI 4630 or by Angelidaki et al. (2009). The assays to determine the BMP value of the different substrates used were performed in 1 litre PET bottles (WV of 0.75 l) for mesophilic conditions (38-39°C). They were conducted in accordance with the guideline VDI 4630, which recommends, for example, keeping the substrate to inoculum ratio on a VS basis (hereafter referred to as SIR) below 0.5 to avoid inhibitory effects. The assays ran in duplicates with one control (“blank”) reactor without addition of substrate running in parallel. BMP tests ran for 30 days, and were

performed for both fresh substrates but also substrates dried at 60°C and milled, as used in the semi-continuous experiments.

Additionally, in the case of the analysis of feedstock mixtures during the co-digestion of maize and grass silage, BMP tests were also performed for the silages in mono-digestion and for different co-digestion mixtures. These tests were carried out with the Automatic Methane Potential Test System (AMPTS) (Bioprocess Control AB, Sweden), which consisted on 15 glass bottles with a total capacity of 650 ml each. The test ran with 400 ml of inoculum and the appropriate amounts of substrate to achieve the desired OL in duplicate for each mixture tested and in mono-digestion. The temperature was kept constant at 39 °C by means of a temperature controlled water bath. This system has been previously used to analyse different co-digestion mixtures for food waste in municipal wastewater treatment plants (Koch et al., 2015). Figure 8 illustrates the two systems applied for the BMP determination.

Figure 8: BMP test carried out in 1l PET reactors (left) and 0.5 l reactors in the AMPTS system (right)

3.3.3 Determination of the theoretical methane production

The theoretical specific methane production (ThSMP) was calculated for all the experiments on the basis of the stoichiometric conversion of proteins, lipids, and carbohydrates. Knowing the elemental composition for each fraction, the amount of CH_4 can be calculated using the Buswell formula (Eq. 7, in chapter 2).

To calculate the specific CH_4 yield (in Nl_{CH4}/gVS), the following equation can be applied.

$$For\ \ C_nH_aO_bN_c,\ B_{o,th} = \frac{22.4\left(\frac{n}{2}+\frac{a}{8}-\frac{b}{4}-\frac{3c}{8}\right)}{12n+a+16b+14c}\left[Nl_{CH4}/gVS\right] \qquad \text{Eq. 17}$$

The values thus obtained for different components that can be found in lignocellulosic material according to their elemental composition are presented in Table 12.

Table 12: Theoretical methane yield for pure substances as determined using Eq. 17

Fraction	Formula	Nl/gVS
Carbohydrates	$C_6H_{10}O_5$	0.415
Proteins	$C_5H_7NO_2$	0.496
Lipids	$C_{57}H_{104}O_6$	1.014
Starch	$C_6H_{12}O_5$	0.415
Glucose	$C_6H_{10}O_6$	0.373
Cellulose	$C_6H_{10}O_5$	0.415

Once the composition was determined for each substrate or co-digestion mixture in terms of the content of proteins, lipids, and carbohydrates, and the non-degradable fraction lignin

through NIRS, the ThSMP was estimated with Eq. 18. A similar approach was applied, for example, by Bruni et al. (2010) for maize. The lignin content was not considered within the carbohydrates fraction (NfE+ XF - ADL), as it is assumed not to be degradable.

$$ThSMP = 0.415 \times Xch + 0.496 \times Xpr + 1.014 \times Xli \quad \text{Eq. 18}$$

Where Xch represents the amount of degradable carbohydrates, Xpr the amount of proteins, and Xli the amount of lipids in one gram of the feedstock VS (in g/gVS), as calculated converting the different fractions estimated through NIRS (in %TS) using the ratio VS/TS ($i_{VS/TS}$, see Table 10). For fresh substrates (not dried), 10% was added to the estimated values to take into account for the TVFA present in the substrate (see Annex C). This method allowed determining the ThSMP for all the complex substrates (i.e. grass and maize silages) used in the experiments, which are presented in Table 13. The estimated ThSMP values are therefore higher than the BMP values, as they do not take into account for the carbon losses during conversion and the bacterial growth.

Table 13: Calculated theoretical methane yield for the different complex substrates used in the experiments

Substrate	ThSMP (Nl/gVS)
GS 1	0.473
DGS 2	0.432
DGS 3	0.433
DGS 4	0.440
DMS 1	0.427
DMS 2	0.434

3.4 Experimental set-up and operational procedure

3.4.1 Batch experiments

Batch experiments to analyse the impact of the loading or substrate characteristics on the process dynamics and performance were conducted in 1l PET bottles filled with 750g of acclimated and well homogenised inoculum. In those cases where a high OL was being applied, 2 litre bottles were used instead in order to avoid overflowing going into the gas collecting tubing system. Each experimental series counted with 10-11 reactors running in parallel with 750g of inoculum (taking into account the sampling volume requirements), and the appropriate amount of substrate to achieve the desired OL. This experimental set-up was intended to avoid the digestate being exposed to oxygen during sampling. Indeed, every time that the analyses were performed on the digestate, one of the 11 reactors was removed from the experiment and its content used for sampling. Thus, this configuration allowed sampling the digestate 11 times. Four to three reactors for each experimental set were connected to gasometers to measure the gas production and composition (when gas produced above 300 ml), while the remaining 7 reactors were connected to gas bags. In addition, 1 reactor for each experimental series had an online pH sensor. Finally, a blank with the inoculum but without any feed was connected to a gasometer to establish the baseline gas production. The general set-up for each reactor in each series and the monitoring plan is illustrated in Figure 9. The VS content of the inoculum for each experiment is summarised in Annex E. The specific operational conditions, including the applied OLs are overviewed in Annex F.

In the case of the analysis of different mixtures for co-digestion, tests were carried out for each silage individually (mono-digestion of maize and grass silages –MS 1- and GS 1-) and for 4 different mixtures (in % of VS substrate added): 70%MS1/30%GS1 (mixture 1), 50%MS1/50%GS1 (mixture 2), and 30%MS1/70%GS1 (mixture 3), and 40%MS1/60%GS1 (mixture 4).

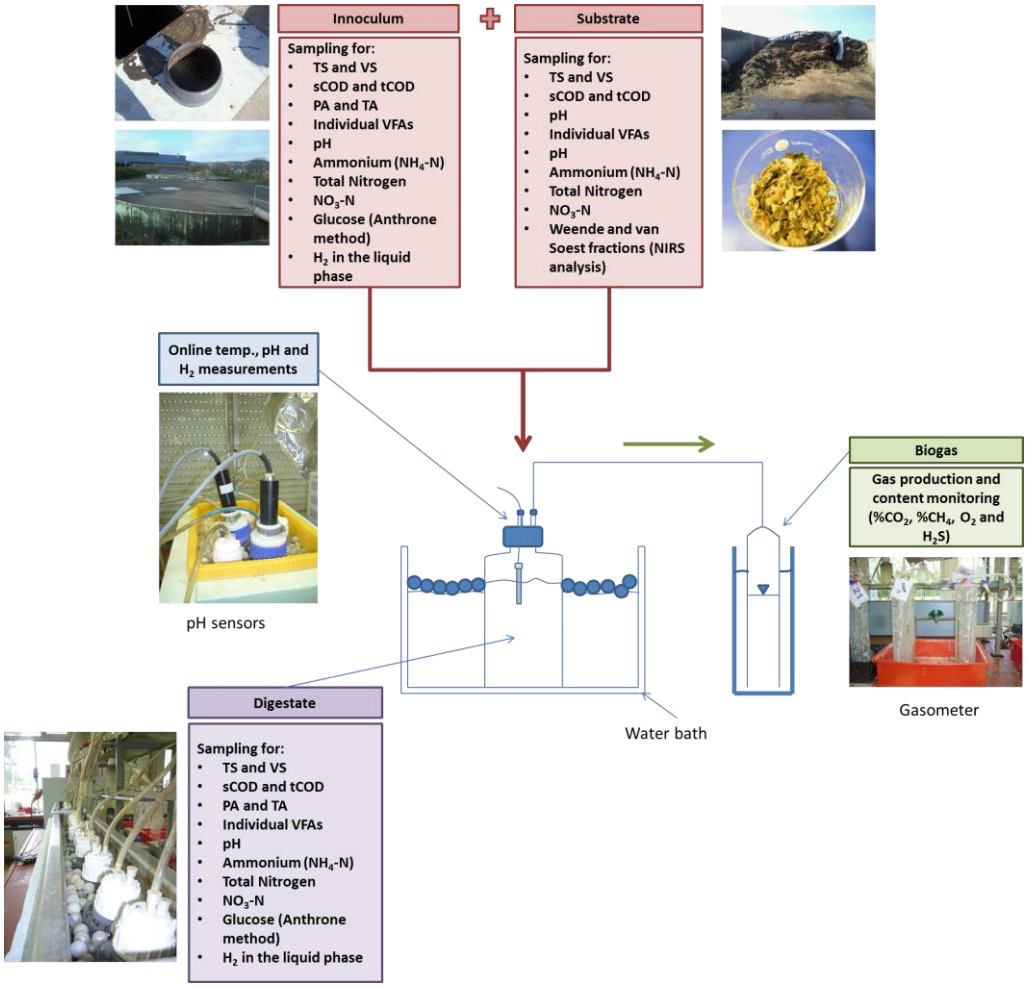

Figure 9: Schematic set-up for reactors in batch series and monitoring plan

During the investigation period for all the batch experiments, of 21 days on average, the reactors were kept in water baths at 39°C and shaken manually once a day. A complete set of parameters were monitored on a daily basis, with some modifications depending on the type of substrate being digested (i.e. not all parameters were measured for each experimental series). Chapter 3.4 describes in more detail the methods applied for measuring the different parameters considered.

Two batch experiments (with cellulose and dried maize silage - DMS 2) were performed in a larger scale reactor, to investigate the impact of the feeding mode on the biogas performance under the same operational conditions (thus implementing batch experiments in the same reactor used for semi-continuous experiments). The reactors used are described below, in sub-chapter 3.4.2. The reactors were inoculated with the same volume of inoculum than the analogous semi-continuous experiment (with WV from 6.7 litres up to 10 litres) and fed in the

beginning of the experiments with the same loading. Biogas quantity and quality was measured on a daily basis, as well as the pH and VFA, and for experiment with dried maize silage (DMS 2) also soluble and total COD (sCOD and tCOD), ammonium-nitrogen (NH_4^+-N), total nitrogen (TN), nitrate-nitrogen (NO_3^--N), TVFA, and TIC. The digesters were sampled daily by taking a volume of 25 to 40 ml of digestate for analysis. The WV of the reactor tests allowed this relative high volume to be taken out, as the total volume sampled never represented more that 5% of the total volume of the reactor.

3.4.2 Semi-continuous experiments

The semi-continuous mono-digestion of cellulose, dried grass silage (DGS 2 and DGS 3), and co-digestion of dried maize silage (DMS 2) and grass silage (DGS 4) were investigated using a double-jacket glass CSTR (Hitec Zang, Germany) with a total capacity of 16.25 litres, which set-up is presented in Figure 10. The reactor's temperature was maintained at 39°C by an external heating coil connected to a thermo-bath (CC-202C, Huber, Germany). The content of the reactor was mixed continuously by means of a propeller-like stirrer (3 levels) driven by an overhead stirrer (RTR 2051 control, Heidolph, Germany) rotating at 50 rpm, and 80 rpm for the experiments with cellulose to avoid sedimentation in the reactor.

Investigations of the mono-digestion of maize silage (DMS 1 and DMS 2) under semi-continuous feeding conditions were carried out in a double-jacket glass CSTR reactor (Glasgerätebau OCHS, Germany), with a total capacity of 8.9 litres and a WV of 6.675 litres, stirred continuously at 50 rpm by means of an anchor-type stirrer driven by an overhead stirrer (RZR 2021, Heidolph, Germany). The reactor's temperature was maintained at 39°C by an external heating coil connected to a thermo-bath (E5, Medingen, Germany). The configuration of the reactor can be seen in Figure 11.

Figure 10: Set-up of the lab-scale CSTR reactor with 16.25 l capacity used for semi-continuous mono-digestion of cellulose, grass silage (DGS 2 and DGS 3), and co-digestion of grass silage (DMS 2) and grass silage (DGS 4). Legend: 1: double-jacket glass CSTR; 2: monitoring computer; 3: overhead stirrer; 4: thermo-bath; 5: valve and level sensor system; 6: temperature sensor; 7: pH sensor; 8: feeding and sampling port

For all experiments, the digester was inoculated the first day with pre-acclimatized inoculum. The required amount of feedstock to reach the desired loading was re-suspended in double distilled water and then fed semi-continuously with a syringe (once a day, 5 days a week for the mono-digestion of grass, maize and co-digestion experiments and 7 times a week for the cellulose experiment). Prior to feeding, an equivalent volume of digester content was removed via the same port and with the syringe used for feeding. As regards the feeding and monitoring, this is specified in more detail for each experiment below.

3.4.2.1 Semi-continuous digestion of grass silage

Two ensilaged grasses dried at 60 °C (DGS 2 and DGS 3) were used, milled to ease the feeding. The amount of milled grass needed to attain the desired loading was re-suspended in double distilled water and injected daily into the reactor (5 times per week). The applied feedstock was prepared daily. The DGS 2 was used until the 41st day of digestion with an OLR of 1.9 gVS/l, and DGS 3 from the 42nd day onwards, at first with the same OLR, which was increased gradually overtime. The different feeding regimes are presented in Table 14. A trace element solution (as described Mata-Alvarez, 2002 and used by Raposo al., 2006) was added once a week after the 85th day of digestion. The composition of this stock solution is presented in Annex G. Indeed, problems with the mono-digestion of grass silage have been reported previous for long-term operation (Thamsiriroj et al., 2012; Wall et al., 2014).

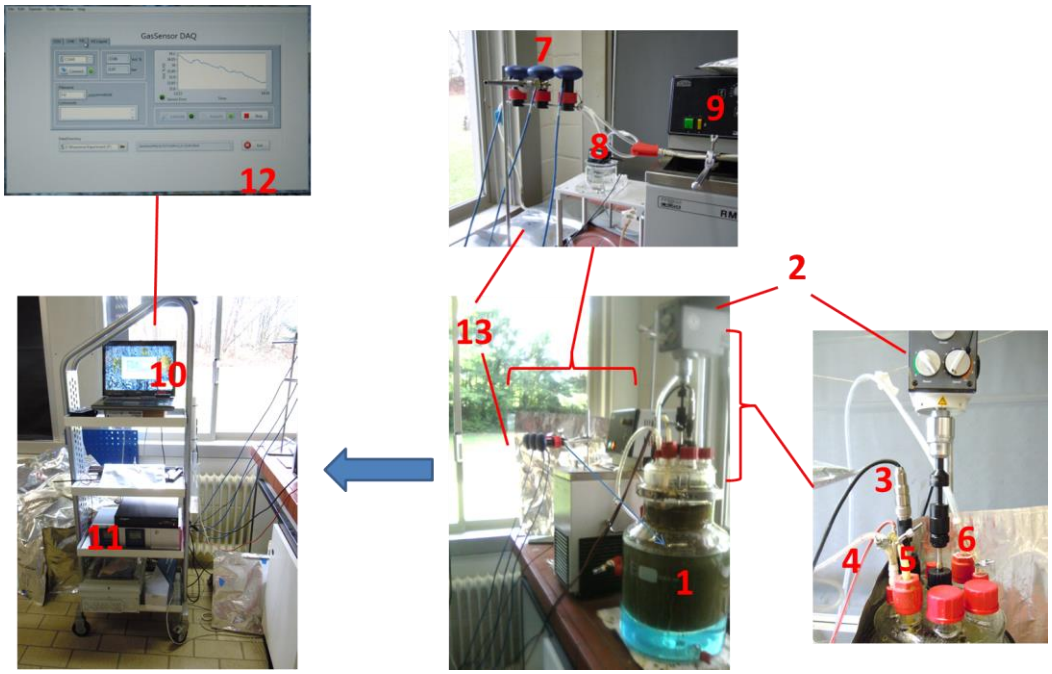

Figure 11: Set-up of the lab-scale CSTR reactor with 8.90 l capacity used for semi-continuous mono-digestion of dried maize silage (DMS 1 and DMS 2). Legend: 1: double-jacket glass CSTR; 2: overhead stirrer; 3: pH sensor; 4: temperature sensor; 5: feeding/sampling port; 6: gas outlet; 7: online gas composition sensors; 8: gas counter; 9: monitoring computer; 10: analog monitor for pH; 11: screen display with gas composition; 12: gas bags

Besides the online measurement of the biogas production, pH and temperature, off-line measurements for the collected effluent included sCOD and tCOD, VS, TS, VFA, TN, NH_4^+-N, and TVFA and TIC.

Table 14: Feeding regimes for the semi-continuous mono-digestion experiment for grass silage

		Feeding regime				
	Units	1	2	3	4	5
DGS		DGS 2	DGS 3	DGS 3	DGS 3	DGS 3
OLR	gVS/l/d	1.9	1.9	2.7	3.3	4.7
HRT	days	17.7	17.7	17.7	17.7	17.7
Duration	days	42	62	34	14	17

3.4.2.2 Semi-continuous digestion of maize silage

For the study of the mono-digestion of maize silage under semi-continuous feeding conditions, two maize silages were dried at 60°C (DMS 1 and DMS 2) and milled (Ø <1mm) and re-suspended in double distilled water for injection into the reactor. A 8.9 litres bench reactor was used in this experiment, with a working capacity of 6.7 litres. The HRT was kept constant along the experiment (i.e. 16.69 days), which ran for 185 days. The feeding regimes applied are summarised in Table 15. The reactor first operated in a single-stage configuration producing CH_4 and CO_2, with an increasing OLR from 2 gVS/l/d to almost 10 gVS/l/d (i.e. 9.83 gVS/l/d). During this period (up to day 125th of digestion), buffering capacity (a mix of $NaHCO_3$ and Na_2CO_3) was added on a daily basis, to keep the pH above a value of 7.0. Additionally, a trace element solution (as described Mata-Alvarez (2002) and used by Raposo et al.(2006)) was added once a week after day 31 on a weekly basis. Indeed, Lebuhn et al. (2008) reported process instability for mono-digestion of maize silage due to the deficiency of trace elements

already at low OLRs. After the feeding regime 5, with an OLR of 9.83 gVS/l/d, buffering capacity addition was removed, with a consequent drop in the pH. This triggered the H_2 production, from the 126th day of digestion onwards (feeding regimes 6 and 7). The pH was then kept at values above 5.

At day 131st of digestion, the system started to run as a two-stage system, with a CH_4-producing reactor being fed with part of the hydrolytic reactor effluent (for feeding regimes 6 and 7), and running in series at mesophilic range. The methanogenic reactor ran for 53 days in total and its objective was to allow for the study of the performance of this type of configuration from a biogas performance perspective. Half of the effluent of the first reactor was used for parameter analysis, and the other half (on average 200.9g) was mixed with double distilled water and introduced in the second reactor as feedstock, keeping the same HRT than the first reactor (16.69 days). The average OLR for the CH_4-producing reactor was 3.14±0.19 gVS/l/d (if considering the totality of the effluent of the first reactors is fed into the second-stage reactor).

Table 15: Feeding regimes for the semi-continuous mono-digestion experiment for maize silage (DMS 2 and DMS 1) with one-stage configuration

		Feeding regime						
		One stage – CH4 producing reactor					Two- stage – H_2 producing reactor	
Parameter	Units	1	2	3	4	5	6	7
OLR	gVS/l/d	2.00	2.51	3.50	6.00	9.83	5.86	5.64
pH	-	7.03	7.00	7.01	7.04	6.70	5.08	5.27
Substrate	DMS 2	DMS 2	DMS 2	DMS 2	DMS 2	DMS 2	DMS 2	DMS 1
HRT	days	16.69	16.69	16.69	16.69	16.69	16.69	16.69
Duration	days	33.78	20.97	31.02	27.99	21.00	27.97	31.97

In addition to the online measurement of the pH, temperature in the reactor, and produced biogas volume and composition, off-line measurements in the digestate were also performed for the effluent of both the CH_4-producing and the H_2-producing reactors, for sCOD and tCOD, VS, TS, VFA, NH_4^+-N, NO_3^--N, TN, and TVFA and TIC.

3.4.2.3 Semi-continuous digestion of cellulose

Microcrystalline cellulose was re-suspended in double distilled water and then added in the reactor daily as the sole carbon source at different OLRs (1 gVS/l/d and 1.5 gVS/l/d). The OLR was maintained at 1 gVS/l/d for 35 days and increased up to 1.5 gVS/l/d onwards. The HRT was kept at 25 days during the whole digestion period (i.e. 60 days) with a slight increase in days 28 and 58 due to mechanical problems for the feeding. Given the substrate characteristics and the duration of the experiment, the trace element solution previously described for the other semi-continuous experiment (see Annex G) was added once a week after day 25. A buffering solution containing sodium bicarbonate was also added regularly in order to maintain the pH value above 7. This value was chosen based on the results by Hu et al. (2005) showing that any decrease in pH below 7.0 could result in a longer lag-time and a reduction in hydrolysis rate during cellulose fermentation. Besides the gas production rate and composition, sCOD and tCOD, VS, TS, VFA, pH, NH_4^+-N, TVFA and TIC (titrimetrically) were monitored over a period of 60 days in the digestate.

3.4.2.4 Semi-continuous co-digestion of grass and maize silages

In the experiment to investigate the influence of the mixture of maize and grass silages, added as feedstock, on the methane yield and on the process dynamics during semi-continuous digestion, dried maize silage (DMS 2) and grass silage (DGS 4) were used. The amount of grass and maize needed to attain the desired loading and mixture was re-suspended in double distilled water and fed into the reactor once a day (5 times a week). The OLR and HRT were kept at 2 gVS/l/d and 16.69 days respectively during the whole duration of the experiment (88 days), but the mixture of the two substrates was changed, as shown in Table 16. Buffering capacity was added on a daily basis after the 42nd day of digestion to keep the pH above 7, and a trace elements solution was added on the 73th day of digestion (feeding regime 3). Online measurements included the produced biogas volume, the pH and the digestate temperature (see sub-chapter 3.5 for more detailed description of the equipment and reactor used). Off-line measurements included gas composition, sCOD and tCOD, VS, TS, VFA, NH_4^+-N, NO_3-N, TN, sTN, and TVFA and TIC. The measurements of the TN, NO_3^--N and the NH_4-N allowed for determination of the protein content in the reactor, which was considered to be relevant when using grass silage in the feedstock (due to its protein content).

Table 16: Feeding regimes in the semi-continuous digestion experiment for DMS 2 and DGS 4

		Feeding regime			
Parameter	Units	1	2	3	4
Grass silage ratio	%	0.00	50	70	100
OLR	gVS/l/d	2.00	2.13	2.13	2.13
HRT	days	16.69	16.69	16.69	16.69
Duration	days	26.94	20.01	19.99	20.01

3.5 Analytical methods

Biogas volume and composition

In the case of the batch experiments, the produced gas volume was measured according to the water displacement principle in glass gasometers filled with a highly concentrated salt solution (30g/100ml) to prevent gas solubilisation. The biogas gas volume was measured and expressed at standard temperature and pressure (STP) conditions (1013 hPa and 273.15 K). At the beginning of the experiments, the biogas components were diluted in the headspace. The measured concentrations were thus corrected for the components considered (i.e. CH_4, CO_2 and H_2), using Eq. 19, as recommended by the guideline VDI 4630 (VDI, 2004).

$$c_{corr} = c_{CH_4(CO,H_2)} \times \frac{100}{c_{CH_4} + c_{CO_2} + c_{H_2}} \qquad \text{Eq. 19}$$

The gas collected in the gasometers was then analysed to determine its composition. CH_4, H_2S, CO_2 and O_2 were determined with a Biogas Monitor BM 2000 (Geotechnical Instruments, United Kingdom) equipped with an infrared cell (for CH_4 and CO_2) and internal electrochemical cells (for O_2 and H_2S measurement). This instrument requires a minimum volume of 250-300 ml for reliable measurements, and has an accuracy of ±3% for CH_4 and CO_2.

For determining the BMP values of the different mixtures tested for co-digestion of maize and grass silage, the AMPTS system (Bioprocess Control AB, Sweden) was used. In this system, the biogas produced passes through a CO_2 fixing unit with an alkaline solution (NaOH) that absorbs

CO_2, and then the remaining volume is measured in the gas measuring unit through water displacement. Methane was then automatically normalised to STP and corrected taking into account the headspace and recorded in an Excel file for visualisation.

In the case of the semi-continuous experiments, the produced biogas was systematically collected in foil gas bags (Supel, 2-10 l, Supelco Analytical, USA) for daily analysis in terms of the compositions (by means of the Biogas Monitor BM 2000) and volume by means of a drum chamber gas meters (T6 1/5, Ritter, Germany) with a working range between 2 and 120 l/h (off-line measurements).

For the semi-continuous experiments with cellulose and maize, biogas production was also monitored online by means of a gas flow meter (MilliGascounter® MGC-10, Ritter, Germany), with a working range between 0.5 and 6.0 l/h and with a measuring error of ±1% across the full flow rate range. The difference between the volumes measured with the gas meter and the gas bags was of ±3% on average. The outlet of the gas counter was connected to Bluesense online gas sensors (Sensor PA H2, Sensor PA CH4 and Sensor PA CO2, Bluesense, Germany), with a measurement accuracy of ±3% (drift of ± 2% value/year), so as to be able to monitor the gas composition on-line in terms of CH_4, CO_2 and H_2. Correction factors were applied to correct for the cross interference between these gases (for H_2 determination).

In order to remove the water vapour from the gas, which could have an impact on the volume and composition measurements, the gas was cooled to room temperature by means of long gas tubing from the gas port of the reactor into the gas meter (minimum 1.5m). Additionally, in the case of the semi-continuous experiments with maize silage (with a very high loading at the end of the experiments and thus gas production rate), the inlet tubing was also put into a water bath at a temperature of 10°C and calcium chloride ($CaCl_2$) was introduced inside a portion of the tubing (due to its hygroscopic nature). In the case of the batch experiments, in-house condensation traps were used. The equipment used for biogas analysis is shown in Figure 12.

Figure 12: Gasometer used in batch experiments (top left), gas counter used in semi-continuous experiments (top centre), offline gas analyser (top right), on-line gas sensors, gas meter and water bath for cooling gas (bottom left) and detail of the cooling bath (bottom right)

Measurement of the pH and temperature

In batch reactors, pH and temperature were measured by means of a SensoLyt SEA electrode (WTW, Germany) and PtA sensor (WTW, Germany), connected to a Quadroline pH 296 analog monitor.

On-line pH and digestate temperature data were measured for the experiments implemented in the 16.25 litres reactor (with cellulose, grass silage, and co-digestion of grass and grass silage) by means of an electrode (SI Analytics, Germany) and sensor (Bola, Germany) respectively. Collected data was visualised and registered by means of a LabVision® software.

For the experiments implemented in the 8.9 litres reactor (semi-continuous digestion of maize silage) on-line pH and digestate temperature data were measured by means of an electrode (PL82-325 pHT VP, SI Analytics, Germany) and sensor (Pt100, JUMO Germany). Collected data were visualised and registered by means of an in-house made software.

TS and VS measurements

The VS and TS were determined on the basis of the standard methods 2540 B and 2540 E, respectively, detailed in APHA (1998). The samples (minimum of 60 ml in duplicate) were dried 24h (for TS) at 105°C and incinerated for 24h at 550°C for VS determination.

Individual VFA

The concentration of individual VFA was measured by means of gas chromatography (GC). The acids measured were HAc, HPr, iso- and n-HBu, iso- and n-HVa, and n-caproic acid (n-HCa).

The VFA purification method implemented was proposed by Golkowska (2011) as an adaptation to existing methods by Pecher (1989) and Pind et al. (2003). Samples of digestate for analysis were first centrifuged at 12,100xg (Minispin, Eppendorf, Germany) for 20 minutes. 3.6 ml of the supernatant was then mixed with 400 µl of an acid solution for pre-treatment (0.1 ml of methyl pentanoic acid, 15 ml of concentrated phosphoric acid, and acetone (Roth, 98.8%) to a total volume of 50 ml). After gassing out, the sample was pressed with a syringe through a 0.45 µm sterile filter (Rotilabo, Carl Roth) and stored at -20 °C prior to analysis. The 4-methylpentane acid was applied as a standard, to determine the recovery of the measurements being taken.

The samples thus prepared were analysed using a "FOCUS" GC instrument (Thermo Fisher Scientific, Italy) with a Econo-CapTM-1000 capillary column (15m, Ø 0.53 mm) (Grace, United States) using Helium as a carrier gas and a flame ionization detector (FID). The GC oven temperature was programmed to increase from 60 to 210°C in 15 min, with a final hold time of 3 min. The temperatures of injector and detector were 200 °C and 250 °C, respectively. The accuracy of the measurements varies from ±0.77% up to ±1.29% depending on the VFA (C2 to C6). The average concentration recovery was estimated to be of 99%.

When necessary, the concentrations for each acid were converted to COD units using stoichiometric factors (see Table 17) and summed up to determine TVFA.

Table 17: Summary of conversion factors and assumptions for the COD balance

VFA	Conversion factor	Unit	Source
HAc	1.07	grCOD/gHAc	*Stoichiometrically*; 64g COD/mole
HPr	1.51	grCOD/gHPro	*Stoichiometrically*; 112g COD/mole
HBu	1.82	grCOD/gHBu	*Stoichiometrically*; 160g COD/mole
HVa	2.04	grCOD/gHVa	*Stoichiometrically*; 208g COD/mole
Lactic acid	1.07	gCOD/gHLac	*Stoichiometrically*; 96g COD/mole

Measurement of alkalinity, TVFA and determination of the TVFA/TIC ratio

TVFA concentration can be measured by titration (Feitkenhauer et., 2002), which is cheaper and faster and thus widely used in commercial biogas plants. Several titration methods for determination of TVFA have been proposed, including a simple titration, a 4-point titration, and an 8-point titration (Lahav and Loewenthal, 2000; Lahav and Morgan, 2004).

TIC and TVFA concentration were measured by manual titration (PH3210 with SenTix 41, WTW, Germany) of the samples using 0.25M H_2SO_4 to end-points of pH 5.0 and 4.4, following the Nordmann method (Nordmann, 1977). TIC and TVFA were then calculated applying Eq. 20 and Eq. 21.

$$TIC\ (\mathrm{mgCaCO_3/l}) = \frac{20}{V} \times A \times 250 \qquad \text{Eq. 20}$$

$$TVFA\ (\mathrm{mgHAc_{-eq}/l}) = \left(\frac{20}{V} \times B \times 1.66 - 0.15\right) \times 500 \qquad \text{Eq. 21}$$

Where V represents the volume of the sample (usually 20 ml), A the volume of the H_2SO_4 solution needed to reach a pH of 5.0 (in ml) and B the volume needed for passing from a pH 5.0 to pH 4.4. Given the fact that the H_2SO_4 was 5 times more concentrated that in the proposed standard (to reduce analysis time), the volumes were corrected accordingly.

COD measurements

COD is the oxygen equivalent of the organic matter content of a sample susceptible to be oxidized by a strong chemical oxidant. It is an important water quality parameter at many wastewater treatment facilities as it is an indirect measurement of the organic content potentially susceptible to be degraded.

For the measurement of the sCOD, the ISO 15705 standard method was modified, given the relatively high suspended solids concentration in the digestate. The samples were first sieved through 1mm sieve and then centrifuged at 12,100xg (Minispin, Eppendorf, Germany) for 20 minutes. The aliquot was then filtered through a 0.45µm membrane filter and the required volume pipetted into the test cuvettes.

For measuring the tCOD, samples were first mixed for 20 minutes in a Beaker glass with the help of a magnetic stirrer, and then a volume (2ml) passed into an Eppendorf tube for

thorough mixing with a test tube mixer (Labdancer V, IKA, Germany), before the necessary volume of the suspension was added into the cuvette test.

For the substrate, samples were dried at 105°C and grinded with the help of a grinder (A10, Janke and Kunkel, Germany) to particle size below 500 µm, re-suspended in 10 ml of double distilled water and mixed during 15 minutes, before being added in the test cuvette for analysis.

The test cuvettes (LCK-914 and LCK-514 depending on the concentration range needed) were then heated at 148 °C in a heating block (Model LT 200, Hach Lange, Germany) for 2 h. After cooling the cuvette at room temperature, the sample was measured with the spectrophotometer (DR 3900 Spectrophotometer, Hach Lange, Germany). The measurement accuracy was estimated to be of ±4.9% and the recovery of the measurements was of 95.76%[6].

A difference was observed in the measured COD values when drying the substrates at 105°C and 60°C, likely corresponding to the loss of certain VFAs during drying (see Annex C). For example, such difference was of up to 17% for GS III and up to 26% for GS II for these two drying temperatures.

Measurement of N components

TN is the sum of NO_3^--N, nitrite-nitrogen (NO_2-N), ammonia-nitrogen (NH_3-N), NH_4^+-N and organic nitrogen (org-N), which can be biodegradable or not, and soluble or particular, as expressed by equation Eq. 22.

$$TN = NO_3^-\text{-}N + NO_2\text{-}N + NH_3\text{-}N + NH_4^+\text{-}N + Org\text{-}N \quad \text{Eq. 22}$$

Depending on the temperature and pH, inorganic nitrogen (IN) can exist in a fermenter in two different forms, i.e. free NH_3-N and its ionized form NH_4^+-N. With a pH of approximately 7, most NH_3 in the reactor is present as NH_4^+. NH_4^+-N analysis was performed with Hach Lange kit LCK-305 (0.015-2.0 mg/L NH_4^+-N), the TN was determined using the LATON TN cuvette test LCK338 (20-100 mg/L TN, according to EN ISO 11905-1, digestion with Peroxodisulphate), and for the NO_3^--N, the cuvette test LCK340 (5-35 mg/l NO_3^--N). The Org-N amount was estimated as the difference between the TN and the inorganic fractions (measured as NH_4^+-N and NO_3^- N). The protein amount was estimated by multiplying the Org-N by 6.25.

The sample treatment for the measurement of the NH_4^+-N and NO_3^--N consisted of centrifugation at 12,100xg (Minispin, Eppendorf, Germany) for 20 minutes followed by filtration through 0.45 µm filter.

Measurement of particulate and soluble carbohydrates

The total carbohydrates (tCH) can be estimated as the sum of the soluble fraction (sCH) and the particulate fraction (pCH). The sCH represents the monosaccharides, which are water-soluble crystalline compounds; pCH are the polysaccharides, which are high molecular weight

[6] For solid samples in comparison with the theoretical value calculated on the basis of the measured Weende and Van Soest fractions (nutritional composition)

polymers of monosaccharides (e.g. cellulose, starch, etc.). Considering that 162g of cellulose is equivalent to 180g of glucose (on the basis of the molecular weight), the concentration of insoluble saccharides (i.e. cellulose and corn starch) can be calculated by subtracting the concentration of soluble saccharides from the concentration of total saccharides and multiplying by 0.9.

Carbohydrate concentration was determined using the Anthrone method, which is a colorimetric method using the so-called “Anthrone”-solution as a test reagent with glucose as standard and distilled water as reference.

In brief, first the “Anthrone”-solution was prepared by dissolving 0.2 g Anthrone (purity ≥97%, Sigma–Aldrich, USA) in 100 ml concentrated sulphuric acid and the calibration curve for different concentrations was generated using a photometer (DR 3900 Spectrophotometer, Hach-Lange). The diluted samples were mixed with the Anthrone reagent (0.5 ml of diluted sample for 1 ml of “Anthrone”-solution), mixed and placed in the oven at 105°C for 20 minutes.

Afterwards, the samples were left to cool down for 30 minutes at room temperature and a volume of approximately 1 ml was introduced into the cuvette, which was then placed in the spectrophotometer for measuring the absorbance at 625 nm and analysed using the calibration curve. The results were obtained in grams glucose per litre. Figure 13 illustrates the changes in the colour for samples with different glucose concentrations after reacting with the Anthrone solution.

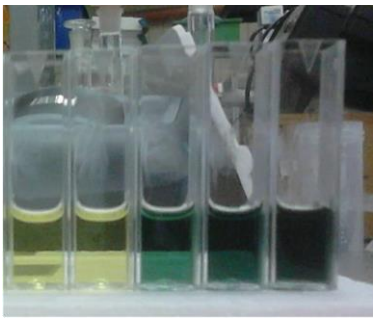

Figure 13: Difference in the intensity of the colour for different concentrations of glucose, with the blank sample on the left

Depending of the type of sample to be measured (either sCH or tCH), the sample preparation differed. For sCH, a volume of the sample was centrifuged at 13,400 rpm (rcf: 12,100 x g) (Minispin, Eppendorf, Germany) and the aliquot then filtered through a 0.45 µm membrane filter and diluted, prior to the analysis. As for measuring the tCH, a pre-hydrolysis step was required so as to be able to convert available polysaccharides into glucose. The samples were first placed with water and sulphuric acid (each representing 1/3 or the total volume) in sample tubes, which were well mixed before being placed for 10 minutes in the oven at 105°C. Samples were then allowed to cool for 30 minutes at room temperature. The samples followed then the same treatment than the one applied for measuring the sCH (given that at that moment all the saccharides were present in soluble form), with a filtration, dilution and subsequent mixing with the “Anthrone”-solution, explained above.

3.6 Data evaluation

3.6.1 Determination of performance and process stability during digestion

The main indicators used to assess the performance and the stability of the anaerobic systems analysed and to compare the impacts of the different operational conditions applied are explained in this chapter.

For the semi-continuous experiments, the OLRs and HRTs were calculated on the basis of the daily additions. Values for gas production and operational parameters are presented as averages for each feeding regime applied. The measured daily values are also displayed for some parameters.

It is important to highlight that for some feeding regimes (such as the feeding regime 4 for semi-continuous digestion of dried grass silage with an OLR of 3.3 gVS/l/d), the duration of the test might be considered to be too short (usually 2 to 3 times the HRT is required to consider that the system has reached steady-state conditions). Unfortunately, logistical considerations prevented in some cases having longer periods for each tested OLR. From a modelling perspective this did not have any negative effect, as the data from the semi-continuous experiments were mainly used for validations purposes, and the models developed had to be able to predict rapid changes (transient conditions). It was generally observed that the semi-continuous systems analysed reached stable conditions relatively fast after changes in the feeding regimes were introduced, usually 10 days after. The preliminary acclimation phase could have been beneficial in this regard. The averages presented in this work were thus performed on data over the last weeks of each feeding regime, when reactor performance was considered to be adapted to the respective operational conditions. Given the objective of the research, which focused on testing certain extreme loading conditions, in some cases, it was not possible to observed such stable conditions (such as in the case of the highest loading tested of 10 gVS/l/d for the semi-continuous digestion of dried maize silage, or 1.5 gVS/l/d for cellulose) within the duration of the test. Such transient dynamic conditions were thus preferably described through the evolution of daily values for the different parameters considered. The presented averages should be considered with caution, and are only intended to illustrate the overall trend.

3.6.1.1 Process performance indicators

The specific methane production (SMP) for a given feedstock and under specific operational conditions is used to describe the performance of a system and corresponds to the methane yield. It was estimated by dividing the daily methane production or methane production rate (MPR) (Nl/d) by the VS added daily to the reactor (W_{VS}) (gVS/d), according Eq. 23, and was expressed in Nl/gVS. In the case of batch experiments, the SMP was estimated dividing the accumulated volume of methane by the amount of substrate added for a given digestion time. For certain batch experiments, the parameter specific methane production rate (SMPR) was used to allow for comparison between different trials in terms of the process kinetics, with a focus on the methanogenic step. It corresponded to the daily methane production reported to the amount of substrate added for each experiment, and was expressed in Nl/gVS/d.

In the case of semi-continuous experiments, the volumetric methane production rate (VMPR) was calculated as the ratio between the MPR and the reactor WV (V_{liq}, in l), according to Eq. 24.

$$SMP\left(Nl/gVS\right)=\frac{MPR}{W_{Vs}} \quad \text{Eq. 23}$$

$$VMPR\left(Nl/l/day\right)=\frac{MPR}{V_{liq}} \quad \text{Eq. 24}$$

The specific biogas production (SBP) and the volumetric biogas production rate (VBPR) were calculated likewise using the daily biogas production (referred to as biogas production rate – BPR, in Nl/d), mainly consisting of CH_4 and CO_2. When necessary, the hydrogen performance was also evaluated by means of the specific hydrogen production (SHP), the hydrogen production rate (HPR) and the volumetric hydrogen production rate (VHPR), calculated in the same manner than for methane.

Moreover, the CH_4 content in the biogas was also considered to assess the performance of the process.

3.6.1.2 Process stability and degradability indicators

Different parameters were monitored during digestion in order to determine the overall stability of the process under the different operational conditions tested. The main process parameters and stability indicators were explained in sub-chapter 2.2.4. The parameters considered the TVFA/TIC ratio, the concentration of individual VFAs, the pH, or the biogas composition. Additionally, the level of degradability and the removal efficiency (mainly in terms of VS) were also estimated in each case. The estimation of the overall first-order constant also allowed getting a better insight into the kinetics of the process.

Degradability indicators

The **level of degradability** was estimated by comparing the measured CH_4 yield with the estimated BMP value for feedstock substrates (determined as described in sub-chapter 3.3.2). This indicator was mainly used for semi-continuous experiments to determine deviations from the biological potential for given operational conditions.

The efficiency of removal, in terms of COD or VS, was estimated according to Eq. 25.

$$\eta\left(\%\right)=\frac{\left(S-Se\right)}{S} \quad \text{Eq. 25}$$

Where S represents the concentration of organic matter (in VS or COD) in the inlet flow rate (g/l) and Se the concentration of organic matter (expressed as VS or COD) in the effluent flow rate (in g/l).

Determination of the first-order constant

If assuming that hydrolysis is the rate limiting step, the overall process can be described through first-order kinetics using Eq. 9 (chapter 2). If considering the existing relation between the substrate and the methane generated, this equation can be expressed in terms of the methane production according to Eq. 26.

$$B = B_{end} \times \left[1 - e^{-k \times t}\right] \quad \text{Eq. 26}$$

where B is the volume of methane accumulated (Nl) at time t (d), B_{end} is the maximum volume produced (Nl) and k is the observed first-order specific rate constant of the overall process (per day). Thus the first-order kinetic constant describes the velocities of degradation and methane production. This was the expression proposed by the ‘‘Task Group for the Anaerobic Biodegradation, Activity and Inhibition of the Anaerobic Digestion’’ of the IWA (Angelidaki et al., 2009). A non-linear least square method was used for the optimisation of “k” with the help of the Microsoft Excel Solver tool.

For a CSTR reactor operating at steady-state, a mass balance can be applied, from Eq. 9, which allows estimating the value of the substrate concentration S at steady state as a function of the SRT, according to Eq. 27. This was the approach taken by of Eastman and Ferguson (1981) for CSTRs.

$$S = So \times \frac{1}{1 + k \times SRT} \quad \text{Eq. 27}$$

which can also be expressed according to Eq. 28.

$$\frac{So}{S} = 1 + k \times SRT \quad \text{Eq. 28}$$

By plotting So/S versus SRT, it is possible to determine k, as the slope of the line.

3.6.2 Statistical analysis

Summary statistics were used to describe the observations made for the different parameters considered in the experiments, mainly the average and the standard deviation. For the semi-continuous experiments, one-way analysis of variance (ANOVA) was applied to determine whether there were significant differences between the means of different variables for the OLRs and feedstock mixtures tested. A post-hoc test was then used to specify which groups differed from each other. Additionally, correlation analyses were performed for some experimental sets in order to evaluate possible dependences between several variables.

These statistical analyses were performed using IBM SPSS 21 for Windows (SPSS Inc., Chicago, IL, USA), and are further described below.

3.6.2.1 Variance analysis

Variance analysis, namely the one-way ANOVA, was applied for the analysis of the experimental data from semi-continuous experiments in order to determine whether there were statistically significant differences in the average of different performance indicators for the different OLRs and mixtures tested. The parameters that were considered were SMP, MPR, and the CH_4 content. There are certain conditions that need to be met for this analysis to be applicable:

- Independence of the observations, which is very much dependent on the appropriated experimental design.

- The variables considered have to present a normal distribution, i.e. the distribution of the residuals is normal.
- Homogeneity of the variance. The variances of the population for each group are equal.

The homogeneity of variances was analysed with the Levene test statistic ($p<0.05$). As for the normality, it was tested by means of the Kolmogorov-Smirnov and the Shapiro-Wilk tests (depending on the size of the population and number of samples), with a confidence interval of 95%.

When both conditions were met, the ANOVA test was performed, which indicated whether there was a significance difference between means of different groups, followed by a post-hoc Tukey analysis to identify which groups were different. In the case the assumption of equal variances was not met, the Welch test was performed to test for the equality of group means, followed by the Games-Howell test. The same approach was followed by Ramos Suarez (2014) to analyse experimental data from the production of biogas from microalgae.

3.6.2.2 Correlation analysis

Correlation analyses were performed for semi-continuous experiments to explore the possible linear dependence between different variables and operational parameters considered. The Pearson correlation coefficient (r) was chosen (Eq. 29), being one of the most commonly applied. This parameter is a measure of the linear correlation (dependence) between two variables X and Y, having a value between +1 and −1, where 1 is total positive linear correlation, 0 is no correlation, and −1 is total negative linear correlation. Correlations are to be considered statistically significant with a 95% probability level ($p<0.05$). The variables considered included the BPR, the MPR, the VS removal, the sCOD, TVFA, the TVFA/TIC ratio, and the CH_4 content. Operational conditions considered included the OLR, and the feedstock mixture.

$$r(X,Y)) = \frac{\mathrm{cov}(X,Y))}{\sigma_X \times \sigma_Y} \qquad \text{Eq. 29}$$

Where cov is the variance, σ_X the standard deviation of variable X, and σ_Y the standard deviation of variable Y.

For some of the variables for which a linear correlation was found, a regression was performed to determine the coefficients of the linear equation and the coefficient of determination (R^2) was used to illustrate the quality of the fit.

3.7 Model development and implementation

3.7.1.1 General modelling approach

One of the main objectives of the present research was to develop a model, based on the ADM1 (described in Chapter 2) addressing previously detected limitations in existing models and capable of describing the degradation of lignocellulosic material (e.g. energy crops and crop residues). To this end, it was decided to have two distinct approaches:

- ***Lignogas model***: extended ADM1 model to address previously highlighted shortcomings of the ADM1 and adapted to the nature of lignocellulosic material. The identified limitations are summarised in Chapter 2, e.g. uncertainty of the parameters, incomplete description of the fermentation of sugars, and the exclusion of some related processes. The following changes were introduced:
    - Substrate characterisation according to Weende and Van Soest fractions measured experimentally and estimation of the f-factors for disintegration.
    - Parameter estimation after sensitivity analysis.
    - Decayed biomass constitutes a new variable (X_{bio}), with a different composition to that of composite material (X_c). It is recycled into the process and undergoes hydrolysis with its own fractionation factors.
    - Use of different hydrolysis rate for slowly and readily degradable carbohydrates.
    - Inclusion of acetate oxidation, to promote the hydrogenotrophic methanogenesis, pathway that can be important for certain operational conditions (e.g. high HAc concentrations).
- ***Lignogas-SIM model:*** Simplified version of the Lignogas model, developed with experimental confidence, with the following characteristics and assumptions:
    - Substrate characterisation according to Weende and Van Soest fractions measured experimentally and estimation of the f-factors for disintegration.
    - Parameter estimated after sensitivity analysis.
    - HBu and HVa are not included (modified fractionation of the monosaccharides during acidogenesis).
    - All monomers lumped in one variable (S_{mo}).
    - Homoacetogenesis and acetate oxidation are not considered.
    - Decayed biomass is recycled as composite material. Incorporation of stoichiometric coefficients for the biomass decay process expressing N and C release due to biomass decay (to address the discrepancies between the C and N content in the biomass and the composite material)

These models were implemented in AQUASIM, and compared with ADM1 (also implemented with this software). The Lignogas-SIM model was also implemented in MATLAB/SIMULINK for benchmarking purposes. To the knowledge of the author, a similar bivalent and comparative approach has not been attempted to date in the field of anaerobic digestion of lignocellulosic material.

Experimental data used for the calibration and validation of the models were obtained in the University of Luxembourg and are presented in sub-chapter 4.1. The procedure followed is illustrated in Figure 14.

Prior to the parameter estimation, an exhaustive sensitivity analysis was performed over all the parameters to identify those having a significant influence on the simulation results. After the sensitivity analysis and the parameter estimation tasks, the calibrated models were validated in each case with independent data, e.g. different loadings and feedstock. Finally,

different scenario analysis were analysed with the developed models in order to investigate the outcome for different feeding regimes.

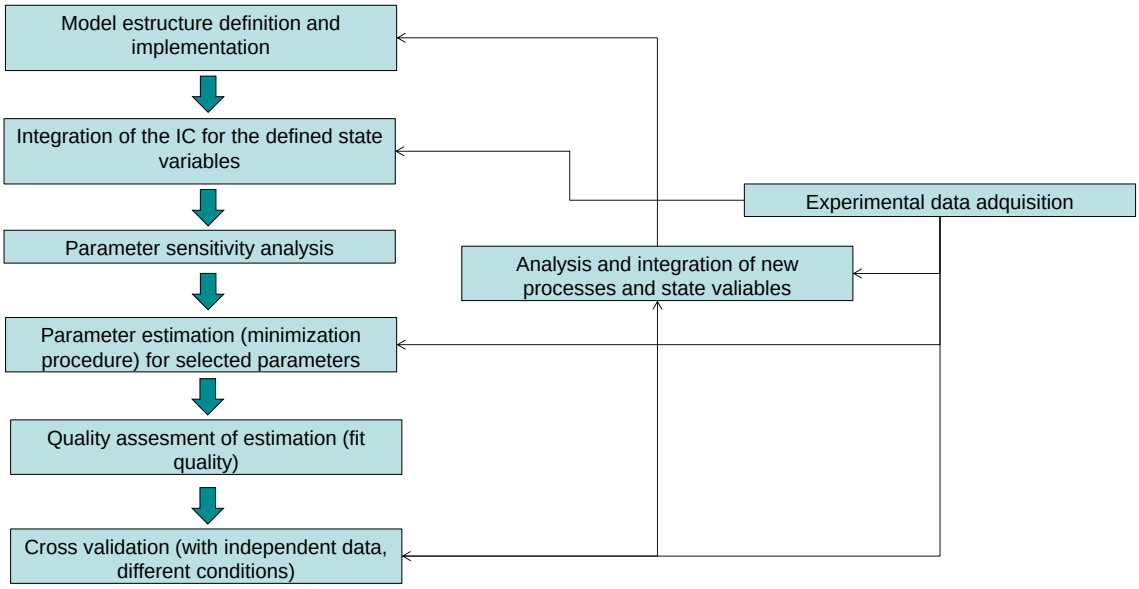

Figure 14: Modelling development steps

3.7.2 Model development

3.7.2.1 Substrate fractionation

The composite material (Xc) is going to be divided during disintegration into carbohydrates (Xch), proteins (Xpr), and lipids (Xli) according to fixed stoichiometric factors (f-factors). The inflow fractionation is thus of highest importance for the calibration of the ADM 1 and is strongly affecting the gas composition.

Different approaches have been applied to date to address substrate fractionation. Some authors proposed methods based on elemental analysis to deduce the biochemical fractionation, such as Zaher et al. (2009) or Kleerebezem and van Loosdrecht (2006). The latter work proposed using common analytical measurements such as COD, total organic carbon, or total Kheldal nitrogen to determine the elemental composition of the lumped substrate and the influent composition as required for input in the ADM1 model.

Other authors, such as Lübken et al. (2007), Wichern et al. (2009), and Koch et al. (2010), used physico-chemical analysis to characterise the substrate and determine the split of the added COD into each ADM1 f-factor.

In the present research, instead of using the default stoichiometric values given by the ADM1 model (Table 6.1 in Batstone et al., 2002), the idea was to use the characterisation of each substrate in terms of the Weende and Van Soest fractions (as measured through NIRS) to determine the fractionation. In particular, the method proposed by Koch et at. (2010) was applied with some modifications. Carbohydrates were divided into a degradable (d) and a non-degradable fraction (1-d), as proposed by Koch et al. (2010). The degradable fraction is constituted by non-structural carbohydrates (XF + NfE - NDF) and the degradable part of

cellulose and hemicellulose ((NDF - ADL)*d). The non-degradable fraction of carbohydrates is constituted by lignin (ADL) and the non-degradable part of cellulose and hemicellulose (NDF - ADL)*(1 - d)), and is allocated to the inert fraction. Dividing all fractions (calculated in terms of gVS by multiplying with the TS/VS ratio of each substrate, denoted as $i_{TS/VS}$) by the VS content allows determining the f-factors in each case, according to Eq. 30 to Eq. 33.

$$f_{Pr\_Xc} = \frac{XP(gTS) \times i_{VS/TS}(gVS/gTS)}{VS(gVS)} \quad [gVS/gVS] \qquad \text{Eq. 30}$$

$$f_{Li\_Xc} = \frac{XL(gTS) \times i_{VS/TS}(gVS/gTS)}{VS(gVS)} \quad [gVS/gVS] \qquad \text{Eq. 31}$$

$$f_{Ch\_Xc} = \frac{[NfE + XF - (NDF + (NDF - ADL) \times d)](gTS) \times i_{VS/TS}(gVS/gTS)}{VS(gVS)} \quad [gVS/gVS] \qquad \text{Eq. 32}$$

$$f_{i\_Xc} = \frac{[ADL + (NDF - ADL) \times (1-d)](gTS) \times i_{VS/TS}(gVS/gTS)}{VS(gVS)} \quad [gVS/gVS] \qquad \text{Eq. 33}$$

"d" is the percentage of the degradable part of hemicellulose and cellulose, and is estimated on the basis of the degradation level (D). Koch et al (2008) estimated D taking into account the degradation rate of VS. For the current work, D was calculated taking into account the measured methane yield in comparison with the maximal theoretical methane yield (i.e. ThSMP), estimated as explained in sub-chapter 3.3.3. The ThSMP was thus corrected by subtracting 10% of its value in order to take into account for the carbon losses during conversion and microbial growth. The equation for calculation of the degradable part of cellulose and hemicellulose "d" at a known level of degradation D is obtained through Eq. 34 (Koch et al., 2010). The calculated values are presented in Table 18.

$$d = \frac{NDF - VS \times VS(1-D)}{NDF - ADL} \quad [\%] \qquad \text{Eq. 34}$$

Applying Eq. 30 to Eq. 33, and using the calculated values of "d", the f-factors for the disintegration of the composite material were calculated for each substrate considered, and are presented in Table 19.

Table 18: Estimated degradation level (D) for the substrates used in the experiments and the degradable part of cellulose and hemicellulose "d" in each case. Note that the silages applied in most experiments used for the optimisation and calibration of the models were dried at 60°C

Substrate	D	d
GS 1	90.0%	90.4%
DGS 2	83.1%	67.6%
DGS 3	57.7%	39.8%
DGS 4	81.0%	65.5%
DMS 1	83.0%	60.0%
DMS 2	79.2%	48.2%

Table 19: Substrate fractionation during disintegration according to the f-factors determined for each substrate

Parameter	Unit	Description	GS 1	GS 2	GS 3	GS 4	MS 1	MS 2
fpr_Xc	-	Proteins from Xc	0.1632	0.1999	0.1490	0.1728	0.0831	0.0789
fli_Xc	-	Lipids from Xc	0.0323	0.0419	0.0548	0.0398	0.0333	0.0399
fch_Xc	-	Carbohydrates from Xc	0.7040	0.5889	0.3816	0.5984	0.7143	0.6736
fxi_Xc	-	Inerts	0.1005	0.1693	0.4146	0.1889	0.1693	0.2075

When using a mixture of several substrates (i.e. case of co-digestion) it is necessary to take into account the fractionation and the amount of composite material that is introduced in each case, to determine the amount of carbohydrates, lipids, proteins, and inert that will result from the disintegration phase, as illustrated in Figure 15.

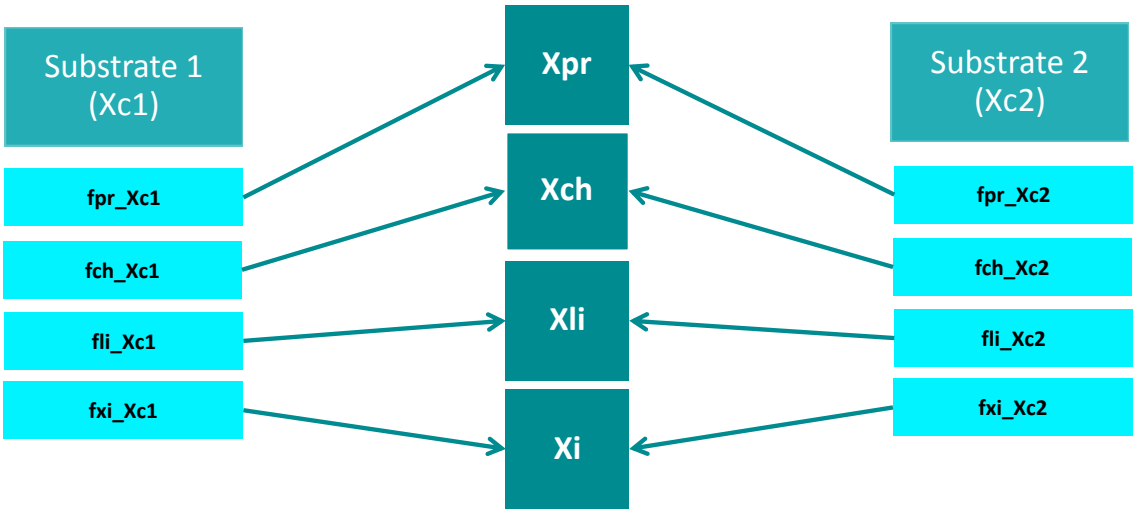

Figure 15: Fractionation during disintegration during digestion of several substrates

The coefficients, process and rates that are necessary to be considered in the case of co-digestion are presented in Table 20.

Table 20: Coefficients and kinetic rate equations for the disintegration during co-digestion of different substrates

Component →	i	1.1	1.2	…	1.i	2	3	4	5	***Rate (ρj)***
j	Process ↓	Xc1	Xc2		Xci	Xch	Xpr	Xli	Xi	
1_1	Disintegration substrate 1	-1				fch_Xc1	fpr_ Xc1	fli_ Xc1	fxi_ Xc1	K_d*X_{c1}
1_2	Disintegration substrate 2		-1			fch_Xc2	fpr_ Xc2	fli_ Xc2	fxi_ Xc2	K_d*X_{c2}
..										
1_i	Disintegration substrate i				-1	fch_Xci	fpr_ Xci	fli_ Xci	fxi_ Xci	K_d*X_{ci}

One option explored was to take into account the presence of carbohydrates with a different degree of bioavailability, and thus degradation rates, in lignocellulosic material, as proposed by Myint et al. (2007). Taking into account the results from the experiment analysing the kinetics in the degradation of different carbohydrates, the following distinction was made:

- Readily degradable carbohydrate: Glucose (non-structural carbohydrates, monosaccharides)
- Carbohydrates resulting from disintegration:
  - Starch (non-structural carbohydrates) - quickly degradable
  - Degradable part of cellulose and hemicellulose ((NDF - ADL)*d) – slowly degradable

The quantity of starch, glucose, and other fractions was determined on the basis of the Van Soest fractions measured with NIRS for each substrate, as summarised in Table 21.

Table 21: Composition of structural and not structural carbohydrates for each substrate used in the experiments

Parameter	Units	GS 1	GS 2	GS 3	GS 4	MS 1	MS 2
Total carbohydrates	%TS	72.42	66.43	69.28	70.25	85.61	85.00
Non-structural CH	%TS	14.58	28.70	13.65	26.20	48.30	47.95
Starch	%TS	0.00	18.39	12.19	15.23	35.86	36.58
Glucose	%TS	14.58	10.31	1.46	10.97	12.44	11.37
Structural carbohy-drates	%TS	57.84	37.73	55.63	44.05	37.31	37.05

On this basis, and using the methods previously explained, f-factors were estimated to define the fraction of starch (f_ch_Xc_f) and cellulose and hemicellulose (f_ch_Xc_s) in the polysaccharides for each substrate. The glucose content in the substrate (in %TS) does not undergo the hydrolysis, as it is readily available monosaccharide (S_{su}) which undergoes directly the acidogenesis step. The other fraction (starch and cellulose-hemicellulose) undergo hydrolysis with different hydrolysis constants estimated in each case through dedicated batch experiments (see Chapter 4.2). This approach was tested for the Lignogas model.

3.7.2.2 COD, C and N balance

The ADM1 include the soluble fractions IC (S_{IC}) and IN (S_{IN}). These variables can be used as a sink or a source to close mass balances in order to ensure that the conservation law is fulfilled. This is also applicable in the Lignogas-SIM and Lignogas models, which are based on the ADM1.

Rosen et al. (2006) highlighted problems with the N and C balances in the original ADM1. One of the issues related, for example, to the discrepancies between the N and C contents in the biomass and the composite material. Also, problems were detected for the disintegration step when using default values. Different adjustments have been proposed in this regard to close the mass balances for the different processes and fulfil the conservation law.

In the case of the **Lignogas-SIM model** (simplified version), stoichiometric coefficients were incorporated to express the N and C release during the biomass decay process, as suggested by Rosen et al. (2006), and applied by Ersahin et al. (2007). The following terms were introduced to the model matrix consequently:

$C_{bac} – C_{xc}$ (i = 6, j = 9–12 in the model matrix (see Table H.4 in Annex H))

$N_{bac} – N_{xc}$ (i = 7, j = 9–12 in the model matrix (Table H.4 in Annex H))

C_{bac} and N_{bac} represent the C and N content in bacteria respectively, while C_{xc} and N_{xc} represent the N and C content in composite material. The values used are summarised in Annex H. The death biomass became part of the particulate composite material.

Similarly, the C and N balances were checked for all the processes considered in the Lignogas-SIM model, and stoichiometric coefficients added when necessary to ensure that all the balances were closed. For example, a stoichiometric coefficient was added for the disintegration process expressing N and C release, as suggested by Rosen and Jeppsson (2008). The following stoichiometric terms were added to the original matrix:

$IC = -(C_{xc} – f_{xl\_xc}*C_{inert}– f_{ch\_xc}*C_{mo} – f_{li\_xc}*C_{li} – f_{pr\_xc}*C_{pr})$

$IN = - (N_{xc} – f_{xl\_xc}*N_{inert} – f_{pr\_xc}*N_{pr})$

Also, with the introduction of the variable S_{mo}, which is the sum of all the monomers originated from the hydrolysis, a new imbalance was created, given the different content in C and N of carbohydrates, proteins and lipids. Therefore, as it was done for the disintegration step, stoichiometric coefficient expressing the different N and C releases were added for the hydrolysis of proteins and hydrolysis of lipids steps.

For the **Lignogas model**, the discrepancy between the C and N contents in the biomass and the composite material was solved with the introduction of a dedicated variable for the dead biomass (X_{bio}), which became substrate to the process and had to undergo its own disintegration (different composition of proteins, lipids and carbohydrates in the death biomass). The coefficients and kinetic rate equations that were introduced with the new variable X_{bio} are presented in the Petersen matrix format in Table 22.

Table 22: Coefficients and kinetic rate equations introduced with the introduction of the new process "Disintegration of biomass" and variable X_{bio} in the Lignogas model

Component →	i	…	14	15	16	17	18	19	20	21	22	***23***	***25***	***Rate (pj)***
j	Process ↓	…	Xch	Xpr	Xli	Xsu	Xaa	Xfa	Xc4	Xpro	Xac	Xh2	Xbio	
1_0	**Disintegration biomass**		**fch_Xb**	**fpr_Xb**	**fli_Xb**								**-1**	K_d*X_{bio}
….	….													
13	Decay of Xsu					-1							1	$K_{dec,\ Xsu}*X_{su}$
14	Decay of Xaa						-1						1	$K_{dec,\ Xaa}*X_{aa}$
15	Decay of Xfa							-1					1	$K_{dec,\ Xfa}*X_{fa}$
16	Decay of Xc4								-1				1	$K_{dec,\ Xx4}*X_{x4}$
17	Decay of Xpro									-1			1	$K_{dec,\ Xpro}*X_{pro}$
18	Decay of Xac										-1		1	$K_{dec,\ Xac}*X_{ac}$
19	Decay of Xh2											-1	1	$K_{dec,\ Xh2}*X_{h2}$

The fractionation of the recirculated biomass (X_{bio}) for the disintegration of the decayed biomass are those proposed by Schlattmann (2011), who applied a similar approach, and can

be seen in Table 23. As for the Lignogas-SIM model, stoichiometric relationships were checked and coefficients added when necessary for all the processes considered.

For both models, the values for the N and C content in the different variables are the default values proposed by Batstone et al. (2002) for the ADM1 (see Annex B), except for certain variables for which the values proposed by Rosen et al. (2006) were used (see Table H.1 and I.1 in Annex H and Annex I respectively for the Lignogas-SIM and Lignogas models).

Table 23: f-factors for decayed biomass during disintegration (from Schlattmann (2011))

Parameter	Unit	Description	Value
fpr_X_b	-	Proteins from decayed biomass	0.783
fli_X_b	-	Lipids from decayed biomass	0.102
fch_X_b	-	Carbohydrates from decayed biomass	0.115

3.7.2.3 Lignogas-SIM model

The Lignogas-SIM model was developed with experimental confidence to describe the digestion of lignocellulosic material, and addresses some of the shortcomings of the ADM1 model. The main purpose of this model was to explore the possibility of applying a lighter model to the degradation of this type of particulate and heterogeneous substrate. Indeed, it is a simplified version of the ADM1, and thus there might be advantages in terms of calibration and operation. The following assumptions were made:

- Homoacetogenesis and acetate oxidation are not considered (as in the ADM1).
- Inert soluble substrate is not considered in the model, only particulate inert.
- The model considers the death of bacterial biomass (decay rates) and the decayed products become composite material.
- The growth of hydrolytic bacteria producing enzymes hydrolysing the substrate is not considered in the hydrolysis steps. Therefore, the hydrolysis step assumes first-order kinetics (as in ADM1).
- The acidogenic step of anaerobic digestion produces different VFA. In this model, butyrate and valerate were not included since more than 90% of total VFA are made up of acetate and propionate under mesophilic conditions (under not overloading conditions).
- All monomers resulting from the hydrolysis step, namely monosaccharides, amino acids and LCFA are lumped into one variable (S_{mo}). The initial value of S_{mo} (Smo_in) corresponds to the soluble sugars present in the substrate.

The process and variables taken into account are illustrated in Figure 16. The model consisted of:

- **A set of 14 differential equations for the liquid-phase, presented below.**

$$\frac{dX_c}{dt} = \frac{q_{in}}{V_{liq}}\left(X_{c\_in} - X_c\right) - \rho_1 + \rho_9 + \rho_{10} + \rho_{11} + \rho_{12} \qquad \text{Eq. 35}$$

$$\frac{dX_{ch}}{dt} = \frac{q_{in}}{V_{liq}}\left(X_{ch\_in} - X_{ch}\right) + f_{ch\_Xc} \times \rho_1 - \rho_2$$ **Eq. 36**

$$\frac{dX_{pr}}{dt} = \frac{q_{in}}{V_{liq}}\left(X_{pr\_in} - X_{pr}\right) + f_{pr\_Xc} \times \rho_1 - \rho_3$$ **Eq. 37**

$$\frac{dX_{li}}{dt} = \frac{q_{in}}{V_{liq}}\left(X_{li\_in} - X_{li}\right) + f_{li\_Xc} \times \rho_1 - \rho_4$$ **Eq. 38**

$$\frac{dX_{i}}{dt} = \frac{q_{in}}{V_{liq}}\left(X_{i\_in} - X_{i}\right) + f_{xi\_Xo} \times \rho_1$$ **Eq. 39**

$$\frac{dS_{mo}}{dt} = \frac{q_{in}}{V_{liq}}\left(S_{mo\_in} - S_{mo}\right) + \rho_2 + \rho_3 + \rho_4 - \rho_5$$ **Eq. 40**

$$\frac{dS_{ac}}{dt} = \frac{q_{in}}{V_{liq}}\left(S_{ac\_in} - S_{ac}\right) + (1 - Y_{mo}) \times f_{ac\_mo} \times \rho_5 + (1 - Y_{pr}) \times 0.57 \times \rho_6 - \rho_7$$ **Eq. 41**

$$\frac{dS_{pro}}{dt} = \frac{q_{in}}{V_{liq}}\left(S_{pro\_in} - S_{pro}\right) + (1 - Y_{mo}) \times f_{pr\_mo} \times \rho_5 - \rho_6$$ **Eq. 42**

$$\frac{dS_{H2}}{dt} = \frac{q_{in}}{V_{liq}}\left(S_{h2\_in} - S_{h2}\right) + (1 - Y_{mo}) \times f_{h2\_mo} \times \rho_5 + (1 - Y_{pr}) \times 0.43 \times \rho_6 - \rho_8 - \rho_{T,H_2}$$ **Eq. 43**

$$\frac{dS_{CH_4}}{dt} = \frac{q_{in}}{V_{liq}}\left(S_{ch4\_in} - S_{ch4}\right) + (1 - Y_{ac}) \times \rho_7 + (1 - Y_{h2}) \times \rho_8 - \rho_{T,CH_4}$$ **Eq. 44**

$$\frac{dX_{mo}}{dt} = \frac{q_{in}}{V_{liq}}\left(X_{mo\_in} - X_{mo}\right) + Y_{mo} \times \rho_5 - k_{dec} \times \rho_9$$ **Eq. 45**

$$\frac{dX_{pr}}{dt} = \frac{q_{in}}{V_{liq}}\left(X_{pr\_in} - X_{pr}\right) + Y_{pr} \times \rho_6 - k_{dec} \times \rho_{10}$$ **Eq. 46**

$$\frac{dX_{ac}}{dt} = \frac{q_{in}}{V_{liq}}\left(X_{ac\_in} - X_{ac}\right) + Y_{ac} \times \rho_7 - k_{dec} \times \rho_{11}$$ **Eq. 47**

$$\frac{dX_{h2}}{dt} = \frac{q_{in}}{V_{liq}}\left(X_{h2\_in} - X_{h2}\right) + Y_{h2} \times \rho_8 - k_{dec} \times \rho_{12}$$ **Eq. 48**

For q_{in} being the feedstock flow into and out the reactor in l/d (the flow in and out are assumed to be the same), V_{liq} is the WV of the reactor in l, X_{i_in} is the inflow concentration of particulate component i in gCOD/l, X_i is the outflow concentration of particulate component i (which is the same than inside the reactor) in gCOD/l, S_{i_in} is the inflow concentration of soluble component i (gCOD/l), S_i is the outflow concentration of soluble component i (in gCOD/l), Y_i is the yield of biomass on uptake of i (in gCOD/gCOD), ρ_i is the reaction rate for component i (in gCOD/d), the f_{i_xc} represents the f-factors and is the production of fraction i during disintegration of the composite material (gCOD/gCOD), f_{i_j} represents the yield of i from j (in gCOD/gCOD), and $\rho_{T,i}$ is the gas transfer rates (in gCOD/d).

⇨ **3 liquid-gas dynamic equilibrium equations for CH_4, CO_2 and H_2:**

$$\frac{dG_{CH4}}{dt} = \rho_{T,CH4} \times \frac{V_{liq}}{V_{gas}} - \frac{G_{CH4} \times q_{gas}}{V_{gas}} \quad \text{Eq. 49}$$

$$\frac{dG_{H_2}}{dt} = \rho_{T,H2} \times \frac{V_{liq}}{V_{gas}} - \frac{G_{H2} \times q_{gas}}{V_{gas}} \quad \text{Eq. 50}$$

$$\frac{dG_{CO2}}{dt} = \rho_{T,CO2} \times \frac{V_{liq}}{V_{gas}} - \frac{G_{CO2} \times q_{gas}}{V_{gas}} \quad \text{Eq. 51}$$

Where the V_{gas} in the volume of the gas phase (headspace) and the gas transfer rates $\rho_{T,i}$ are estimated according to Eq. 16 in sub-chapter 2.3.2.3. The related stoichiometric coefficients are presented in Appendix G. The gas flow rate was calculated using the alternative expression proposed by Rosen et al. (2006) that assumes overpressure in the headspace. Accordingly, the flow rate at atmospheric pressure is calculated according to Eq. 52.

$$q_{gas} = k_p \times \left(P_{gas} - P_{atm}\right) \times \frac{P_{gas}}{P_{atm}} \quad \text{Eq. 52}$$

Where P_{gas} is the total pressure in the headspace, P_{atm} the atmospheric pressure (1.013 bar), and k_p the pipe resistance coefficient (in m^3/l/d). The value of k_p was set at a large value (50,000 m^3/l/d) to induce the overpressure being flowed out immediately from the reactor.

⇨ **A set of algebraic equations corresponding to the acid-base equilibrium for OH^-, acetate, propionate and NH_4^+. The CO_2/HCO_3^- acid-base pair is implemented as dynamic processes (stoichiometric coefficients are presented in Annex H). The set of acid-base equilibrium algebraic equations was reduced to a single H^+ equation for dynamic pH calculation (Eq. 53).**

$$S_{H+} + S_{cat^+} + S_{NH_4^+} - S_{HCO_3^-} - \frac{S_{HAc^-}}{64} - \frac{S_{Hpr^-}}{112} - S_{OH^-} - S_{ani^-} = 0 \quad \text{Eq. 53}$$

The reactions rates ρ_i considered in the Lignogas-SIM model and the stoichiometric and kinetic parameters are presented in Annex H for both the liquid and gas phases. The default values suggested for the ADM1 model (Batstone et al., 2002) were used as starting point for parameter estimation tasks. The inhibition terms considered in the Lignogas-SIM model are the same than in the ADM1 model (for the processes considered, the inhibition factors are indicated in Annex H).

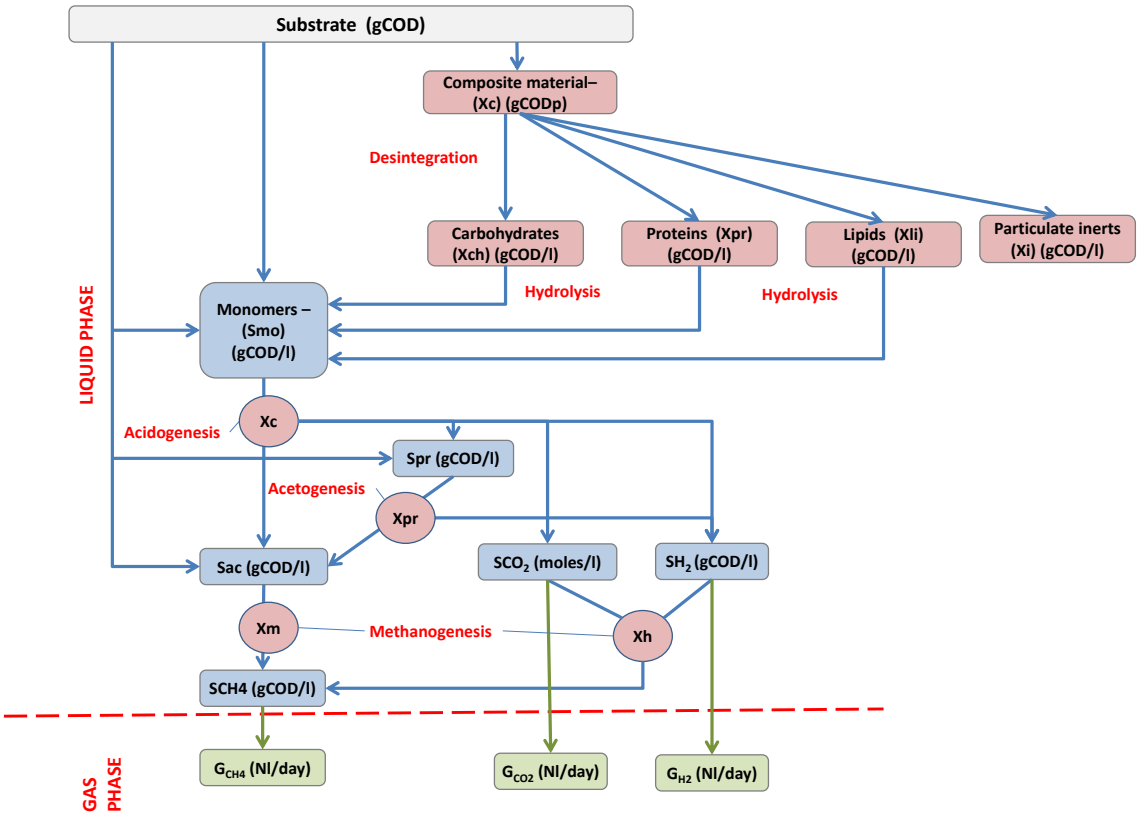

Figure 16: Model configuration (components and processes) in the Lignogas-SIM model

The fractionation method to determine the f-factors used during disintegration is explained in sub-chapter 3.7.2.1. As regards the fractionation of the monosaccharides (assumed to be glucose) during acidogenesis step, the ADM1 considers the equations mentioned in sub-chapter 2.2.1.2, Table 1, with η_1, η_2 and η_3 being the fraction that degrades via the first, second and third reactions. For the Lignogas-SIM, it was assumed that only HPr, HAc and H_2 are released, and no HBu (η_3=0), as summarised in Table 24. The amino acid fermentation is not considered in the Lignogas-SIM model.

The modifications that were introduce to close the N and C balances are explained in sub-chapter 3.7.2.2.

Table 24: Determination of the stoichiometric parameters for glucose degradation in the Lignogas-SIM model (without considering HBu production)

Stoichiometric parameter	Description	Default values in ADM1	Lignogas-SIM model	Estimation
fh2_mo	hydrogen from sugars	0.1906	0.1945	0.33*η1 +0.17*η3
fbu_mo	butyrate from sugars	0.1328	0	0.83*η3
fpro_mo	propionate from sugars	0.2690	0.3204	0.78*η2
fac_mo	acetate from sugars	0.4076	0.4852	0.67*η1 +0.22*η2

3.7.2.4 Lignogas model

The Lignogas model was developed as an alternative to the simplified version (Lignogas-SIM), thus being an extended version including some of the processes omitted in the ADM1. Some of the modifications implemented to the original ADM1 are explained elsewhere in this chapter. The fractionation method to determine the f-factors used during disintegration is explained in sub-chapter 3.7.2.1. The modifications that were introduce to close the N and C balances are explained in sub-chapter 3.7.2.2.

One of the modifications implemented in this model was the inclusion of the acetate oxidation, in an attempt to address recent research results about the important role of hydrogenotrophic methanogens under certain conditions. The acetate oxidation takes place according to the 3rd reaction in Table 4, in sub-chapter 2.2.1.4. The coefficients and kinetic rate equations that were introduced with the new variable X_{acetox} and process (acetate oxidation) are presented in the Petersen matrix format in Table 25. This approach is similar to that applied by Schlattmann (2011). pH inhibition for acetate oxidizing bacteria and growth limitation due to low concentration of IN were included as inhibitory factors. In order to achieve N and C balance, the following terms were introduced:

$IC = -(C_{ac} - Y_{acetox} * C_{bac})$

$IN = -(N_{bac} * Y_{acetox})$

Annex I summarises the reactions rates ρ_i and related stoichiometric parameters considered in the Lignogas model using the Petersen matrix format, as an extension of the ADM1 model. The adopted values for the different parameters are also stated in this Annex.

Table 25: Coefficients and kinetic rate equations introduced with the introduction of the new process "acetate oxidation" and variable X_{acetox} in the Lignogas model

Component →	i	...	*7*	*8*	..	*25*	*26*	*Rate (ρj)*
j	Process ↓	...	Sac	Sh2	..	X_{bio}	Xacetox	
..	..							
11	Acetate oxidation		-1	$(1-Y_{acetox})$			Y_{acetox}	$K_{m\_acetox} \times \frac{S_{ac}}{K_{s\_acetox} + S_{ac}} \times X_{acetox} \times I_{pH,acetox} \times I_{IN,\lim}$
...	...							
21	Decay of Xacetox					1	-1	$K_{dec,\ Xacetox} * X_{acetox}$

3.7.2.5 Initial conditions

Both models allow simulating a larger number of variables, for many of which experimental data were collected, through methods described in previous sub-chapters. Table 26 summarises the different variables in the models for which experimental data was collected and how the initial conditions were determined.

As regards the bacterial biomass, 4 bacterial groups are considered in the Lignogas-SIM model (monomers degraders, HPr degraders, HAc degraders and H_2 degraders) and 8 in the Lignogas model. The initial concentrations were determined by curve fitting during calibration and compared with values previously suggested in literature (see Table 27). It was decided to use the same concentration for all the bacterial groups considered (set to be 0.04 gCOD/l, calculated by dividing the estimated total bacterial concentration, 0.29gCOD/l by the 7 bacterial groups considered in the ADM1).

Table 26: Correspondence of measured parameters and variables in Lignogas-SIM

Variable in the model	Name	Initial values	Measured variable
S_{pro}, $S_{ac,}$	HAc and HPr	Inoculum[1]: S_{pro_in}, S_{ac_in} Substrate[2]: S_{pro_feed}, S_{ac_feed}	HAc and HPr concentrations measured through GC in substrate and feed
$GCH_{4,}$ GCO_2, GH_2	Components in the biogas (gas phase): $CH_{4,}$ CO_2, H_2	0	Accumulated volumes of CO_2, H_2 and CH_4 (in Nl), Biogas composition (in %) Production rate (Nl/d)
Xch_xc	Particulate carbohydrates from disintegration	0	-
Xpr_xc	Particulate proteins from disintegration	0	NH_4^+, TN, NO_3^- Protein= Org-N x 6.25 $g_{protein}/g_{organicN}$
Xli_xc	Particulate lipids from disintegration	0	-
Xi_xc	Particulate inerts from disintegration	0	-
Sh_2	Hydrogen concentration in the liquid phase	Inoculum: Sh_{2_in}	Concentration of H_2 in the liquid phase
Smo	Monomers	Readily available monomers, mainly sugars in the substrate (S_{mo_feed}). S_{mo_feed} (gCOD/l)= FM added (gFM) x Sugar content (%TS)[3] x TS content (%FM)[2] /180g.mole^{-1}*196gCOD.mole^{-1}	Glucose measured through the Anthrone method
S_{IC}	IC	Inoculum: S_{ic_ini}	TIC measured through manual titration
SH^+	H+ concentration	Concentration corresponding to initial pH in the inoculum (S_{H+_ini}) S_{H+_ini} =10^{-pH}	pH
Xc	Solid composite particulate matter	Inoculum: X_{c_ini} Substrate: X_{c_feed} X_{c_feed}=(100-Soluble sugar (g/gTS)[3]-TVFA (g/gTS)[2])x gTS added x COD (g/gTS)[2]	tCOD, sCOD
S_{IN}	IN	Inoculum: S_{NH4_in}	Measured NH_4^+ and NO_3^-

[1] Measured values are converted into gCOD/l using the conversion factors in Table 17.
[2] From Table 10
[3] From Table 21.

Table 27: Summary of initial microbial concentrations in different sources

Source	Inoculum Source	Biomass Concentration	Biomass Determination Method
Lübken et al. (2007)	Slurry	Bacteria = 2.47 gCOD/l Methanogens = 0.029 gCOD/l	FISH
Thamsiriroj at al. (2010)	Source unknown (not mentioned)	Monosaccharides degrades = 0.42 gCOD/l Acetate degraders = 0.4 – 0.7 gCOD/l	Model fitting
Schoen et al. (2009)	Wastewater Treatment	Total Biomass = 0.095 gCOD/l	Model fitting
Nopharatana et al. (2007)	Solid Waste treatment plant	Acetate degraders = 0.06 gCOD/l	Model fitting
Uni Luxembourg (2011)	Agricultural Biogas plant	Total Bacteria = 0.16 – 0.23 gCOD/l	FISH (internal data)
Uni Luxembourg (2011/2012)	Agricultural Biogas plant	Hydrolysing Bacteria = 0.025 gCOD/l Monosaccharides degraders = 0.16 gCOD/l Acetate degraders = 0.106 gCOD/l Total Bacteria = 0.291 gCOD/l	Model fitting

3.7.3 Model implementation

Both models were implemented in AQUASIM 2.0 (Reichert, 1998) using the ADM1 model as a starting point (Batstone et al., 2002), and introducing the modifications previously described in each case. The stoichiometric coefficients and process rates are presented in Annex H for

the Lignogas-SIM model and in Annex I for the Lignogas model. The equations implemented correspond to that of a fully mixed reactor compartment. The changes in the concentrations of any given substance are determined according to Eq. 13 in sub-chapter 2.3.2.3. A second compartment represented the headspace, connected to the first one by means of a diffusive link, to transfer the produced gasses (i.e. CH_4, CO_2 and H_2) following the Henry's law.

3.7.4 Sensitivity analysis

A sensitivity analysis was performed in order to identify those parameters having the largest impact on the modelling outcome. To this end, the absolute-relative sensitivity function (Eq. 54) provided in the AQUASIM package was applied, which is partial derivatives of the variables to the parameters, evaluated at a certain point in parameter space (local sensitivity) (De Pauw, 2005).

$$\delta_{y,p}^{a,r} = p \times \frac{\delta y}{\delta p} \qquad \text{Eq. 54}$$

Where y represents an arbitrary variable and p is a model parameter. This equation allows estimating the absolute change in y for a 100% change in p. It is most useful as it does not depend on the unit of the parameters. The changes are calculated as linear approximations (Reichert, 1998)

The error contribution of each parameter is estimated according to Eq. 55 (Reichert, 1998) .

$$\delta_{y,p}^{err} = \frac{\delta y}{\delta p}\sigma_p \qquad \text{Eq. 55}$$

Where σ_p represents the standard deviation of the parameter p considered.

3.7.5 Simulation, calibration and validation

In AQUASIM, differential and algebraic equations are integrated with the differential algebraic system solver (DASSL) algorithm, which is based on the Gear integration technique. One of the advantages of this type of technique for the solution of ordinary differential equations is that it can address stiff systems, which is the case in the ADM1 model. Parameter estimation was performed in AQUASIM by minimising the sum of the squares of the weighted deviations between measurement and modelled values according to the simplex method (Reichert, 1998), which is a type of direct-search method, thus local and derivate-free (Donoso-Bravo et al., 2011). Table 28 summarises the approach for the simulation and parameter estimation tasks.

Table 28: Parameter estimation task approach in AQUASIM

Implementing software	AQUASIM	
Optimization approach	Method	Nonlinear least squares
	Algorithm	Simplex
Simulation options	Solver type	Variable step
	Solver	DASSL implementation of the Gear integration technique

Differentiated sets of batch experimental data for intermediaries, simple and complex substrates were used to target the parameter estimation and validation. After the sensitivity analysis and the parameter estimation tasks, the calibrated models were validated in each case with independent data, and compared with the ADM1, also implemented in AQUASIM. Table

29 illustrates the experimental data sets that were used in each modelling task. One of the novelties of the present study is the validation of the models with experimental data for different operational modes and substrates, which allowed for a better identification of the strengths and weaknesses of the developed models. Scenario analysis was also performed to investigate the impact of changing certain operational conditions on the system performance and the accuracy of the predictions of each model (i.e. comparing with experimental data). The scenario analysed are summarised in Table 30.

Table 29: Data used in the calibration and validations tasks

Task	Substrate	Feeding mode	Loading
Calibration	GS 1	Batch	6 gVS/l
Cross validation	Glucose	Batch	8 gVS/L
	Starch	Batch	8 gVS/L
	Cellulose	Batch	8 gVS/L
	Acetate	Batch	0.5 g/l
	Propionate	Batch	0.5 g/l
	GS 1	Batch	46.37 gVS/l
	MS 1	Batch	6 gVS/l
	Cellulose	Semi-continuous	1 and 1.5 gVS/l/d
	DGS 3	Semi-continuous	1.9, 2.7, 3.3, 4.7 gVS/l/d
	DGS 2	Semi-continuous	2, 3.5, 6, 9.83, 5.83 gVS/l/d

Table 30: Scenarios analysed with the models

Objective	Substrate	Feeding mode	Loading
Change of the grass silage characteristics	DGS 2 and DGS 3	Semi-continuous	1.9 gVS/l/d
Semi- and batch digestion	DMS 2	Batch and Semi-continuous	2 gVS/l – 2 gVS/l/d
Increasing the HRT	DMS 2	Semi-continuous	6 gVS/l/d

3.7.6 Model performance evaluation

The quality of the simulation or model performance can be evaluated using different statistical indicators, such as the Mean Error (ME), the absolute Maximum Error (AME), the Mean Square Sorted Errors (MSSE), the coefficient of Efficiency (Nash-Sutcliffe), the Index of Agreement, to mention a few (Hauduc et al., 2011). For the purpose of this work, the Root Mean Square Error (RMSE), which is often used in environmental science, was chosen. It is an absolute criterion that indicates the overall agreement between observed and predicted data. It is calculated through the following expression:

$$RMSE = \sqrt{\sum_{i=1}^{n} (Oi - Pi)^2 / n} \qquad \text{Eq. 56}$$

where, Oi and Pi are the observed and predicted values respectively at time step i, and n is the number of data.

4. Results and discussion

4.1 Influence of different operational parameters on the performance of anaerobic digestion of energy crops

4.1.1 Impact of the organic loading

The objective of this part of the research was to investigate the influence that the loading could have on the process stability and performance during digestion. The loading (expressed either as OL for batch systems or as OLR for semi-continuous systems) is an important parameter that needs to be optimised in a way that allows a maximum methane yield and volumetric production, while avoiding system instability and failure due to the accumulation of intermediary products such VFA and free NH_3.

In spite of its importance, research on the influence of this factor on the methane production potential and the operation stability is still limited for energy crops. Some examples for lignocellulosic biomass include the research of Golkowska and Greger (2010) for cellulose under batch conditions, of Lebuhn et al. (2008) for maize silage under semi-continuous digestion, and Comino et al. (2010) for the co-digestion of energy crops and manure. Different authors have investigated the continuous co-digestion of different types of grass with manure and slurry (Frigon et al., 2012; Mähnert et al., 2005; Xie et al., 2012; Lehtomäki et al., 2007) in CSTR at loadings up to 4 gVS/l/d. Mono-fermentation of grass silage for semi-continuous feeding conditions has also been addressed by some scarce publications (Koch et al., 2009; Thamsiriroj and Murphy, 2010; Wichern et al., 2009) in different reactor types and configurations, hence up to a maximum OLR of 3.5 gVS/l/d (in a loop reactor) without the addition of trace elements, before the biogas performance and stability could be affected. Therefore, most research to date focused on co-digestion, and up to relatively low OLRs due to the deficiency of trace elements during long term operation. The present sub-chapter aimed to get a better insight into the impact of the loading during anaerobic digestion of certain energy crops under certain operational conditions not addressed to date with special focus on dynamics and stability in addition to performance. Moreover, the limits of digestion of these substrates with the addition of trace elements were also explored.

4.1.1.1 Influence of the organic loading and the substrate to inoculum ratio on the batch digestion of grass silage

The experiments described hereafter aimed at analysing the response of a system anaerobically digesting grass silage to increasing loading rates under batch conditions, which up to date, has not been investigated. Two different parameters describing the loading were considered. On the one hand, the OL (gVS/l), which represents the amount of VS introduced in the reactor related to the WV. On the other hand, the SIR (relating the substrate to the inoculum on a VS basis) was also taken into account in the analysis. Some previous research analysing the effect of the SIR or the inoculum to substrate ratio (ISR) include Hashimoto (1989) for wheat straw, Liu et al. (2009) for food and green wastes, Raposo et al. (2006) for maize silage, and Raposo et al. (2009) for sunflower oil cake, Eskicioglu and Ghorbani (2011)

for whole stillage from a dry-grind corn ethanol plant and González-Fernández and García-Encina (2009) for swine slurry.

Seven different batch series were presented comparing the performance and stability for GS 1 digestion (used fresh) at different OLs (5.99, 8.42, 16.84, 18.07 and 24.09 gVS/l, 35.78 and 46.37gVS/l) corresponding to different SIRs (0.17, 0.35, 0.70, 0.53, 0.70, 1.83, 1.88 respectively). The SIR of 0.5, suggested in the VDI guidelines 4630 (VDI, 2004) to rule out overloading-driven inhibitory conditions in batch tests was therefore exceeded in 5 of the 7 experimental sets. As it can be observed, the 7 different OLs investigated corresponded to 5 SIRs. These allowed to perform the analysis using these two parameters and to assess their relevance.

The digestion process was characterised for the different SIRs and OLs by assessing the biogas and CH_4 yields and the evolution of intermediary products, and determining the first-order rate constant (k). The net conversion of substrate (on a COD basis) was estimated as well.

4.1.1.1.1 Biogas performance

Table 31 presents main results related to the biogas quantity and quality. Figure 18 shows the CH_4 yield (1.A), the SMPR (1.B), and the CH_4 content in the biogas (1.C) respectively, as a function of time for the different OLs and SIRs tested. The SMP ranged between 0.42 Nl_{CH4}/gVS for the assay with the OL of 5.99 gVS/l to 0.30 Nl_{CH4}/gVS for the assay with the OL of 46.37gVS/l. CH_4 content in total biogas varied between 70.7% and 81.1%. For the first four OLs, the CO_2/CH_4 ratio (data not shown) increased with the loading rate but remained in a range of 0.5-2.1 the first 3 days and then decreased gradually to similar value of 0.5. Also for the last two OLs of 35.78 and 43.37 gVS/l the ratio remained above 3 until the 2nd day and then decreased to background values around 0.5 from the 6th day of digestion on. This indicator suggested important instabilities taking place the first 6 to 7 days of digestion for the two highest values, related to the important production of VFA during that period, as it can be seen in Figure 18.

As it can be observed, overall, the higher the OL and the SIR, the lower the SBP and the SMP, which suggest inhibition related to substrate overloading for the highest loadings. The difference in the SBP and SMP after 21 days of digestion between the highest and lowest OL (and SIR) was 20% and 28% respectively. A similar trend was also observed for maize silage under batch conditions (Raposo et al., 2006). Opposite to this trend, Eskicioglu and Ghorbani (2011) did not found significant differences in the methane yield for dry-grind corn ethanol plant in an SIR range of 0.27–2.17.

The same general trend was observed for the other parameters describing biogas performance, such as the SMPR. It is worth mentioning that the experimental trials with the OL of 18.07 gVS/l and 35.78gVS/l (SIR of 0.53 and 1.83) did not follow exactly the observed trend (see Table 31). This could be explained by a different activation of the inoculum or different media conditions. In the case of the trial with an OL of 35.78gVS/l, for example, it is the CH_4 content in the biogas that presents discrepancies with the observed trend.

Three different clusters in terms of their evolution could be distinguished for the different parameters monitored (see Figure 18). Cluster 1 was formed by series with the OL of 5.99 and

8.42 gVS/l (SIR of 0.17 and 0.35), cluster 2 with series with an OL from 16.84 to 24.09 gVS/l (SIR of 0.53 and 0.70) and cluster 3 with series with an OL above 35 gVS/l (SIR of 1.83 and 1.88).

Table 31: Summarised biogas results for the batch experiments digesting GS 1 at different OLs and SIRs after 21 days of digestion

Parameter	Units	Experimental series						
OL	gVS/l	5.99	8.42	16.84	18.07	24.09	35.78	46.37
SIR		0.17	0.35	0.70	0.53	0.70	1.83	1.88
gVS added	gVS	4.49	6.31	12.63	13.37	17.83	26.64	34.30
SBP	Nl/KgVS	673.97 ± 18	583.49±3	581.68±4	539.28±3	588.38±5	588.36±2	536.29±6
SMP	Nl/KgVS	425.25±11	361.47±6	350.07±6	317.90±4	322.89±8	325.65±1	305.19±1
SBPR max	Nl/KgVS/d	128.8	139.1	176.2	140.9	110.6	110.9	102.9
SMPR max	Nl/kgVS/d	78.32	75.59	62.00	76.37	51.63	41.67	36.24
% CH_4 in biogas (at day)	%	81.1±1	83.5±2	80.9±1	79.0±1	71.1±1	55.3±0.5	70.7±0.6
Conversion ratio substrate to CH_4*	%	100	90.5	87.6	79.6	80.8	81.5	76.4
*Amount of substrate converted into CH_4 (on a COD basis)								

If the final cumulative methane production is plotted against the added load (in VS), the slope of the line gives the average SMP, expressed as Nl_{CH4}/ g VS for the substrate used. Figure 17 shows the final methane volume in the reactors plotted against the VS substrate load. The result shows a linear relationship with a R^2 of 0.9885 and a SMP coefficient of 0.318 Nl CH_4 (STP)/ g VS added.

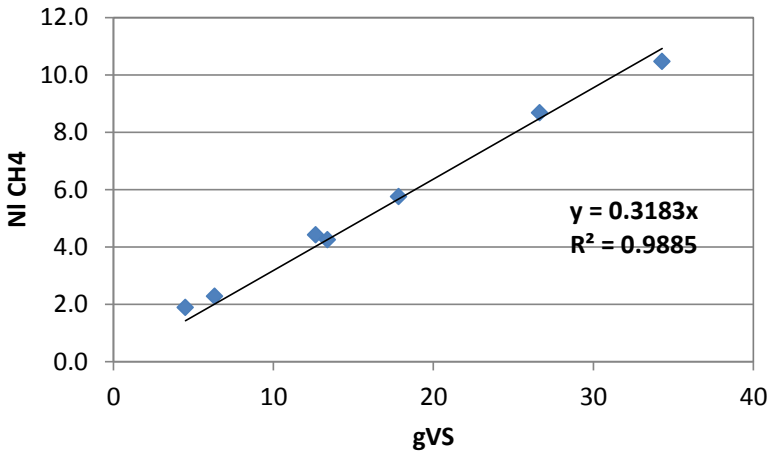

Figure 17: Final cumulative methane volume produced for each of the applied substrate loads

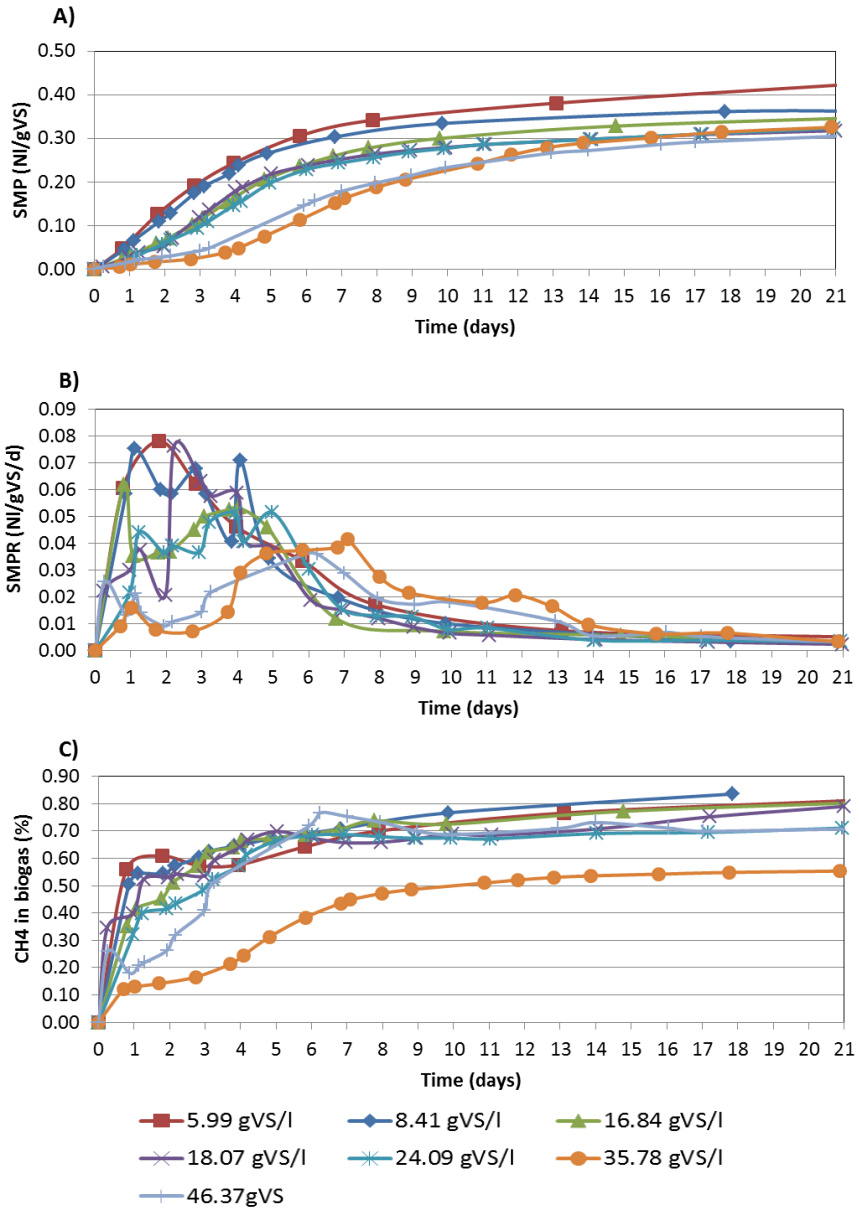

Figure 18: Variation of the SMP (A), SMPR (B), and CH_4 content in the biogas as a function of time

4.1.1.1.2 Changes in process parameters with digestion time and stability

The values for different monitored parameters, other than the biogas production and composition, are presented in Table 32. The VS removal decreased with increasing OL (and SIR), with the exception of the series with the OL of 35.78gVS/l (SIR of 1.83), as it happened with the biogas related parameters. As for the pH, the results showed that the higher the OL, the lower the minimum pH value. The minimum reached for the two highest OLs were of 6.52 and 6.65 respectively within the first two days, and then it increased to values comparable to those reached for other assays for the rest of the digestion period. As indicated in sub-chapter 2.2.4.3, methanogenic groups have an optimum operational pH range between 6.8 to 7.2. The decrease of the pH below 6.5 is critical because the enhanced acid production could result in further pH drop and affect CH_4 production. Therefore the assays with the two highest OLs

were at this critical limit, but the high buffering capacity in the reactors contributed to compensate for the important VFA concentrations measured.

Table 32: Process evolution parameters for GS 1 digestion at different OLs and SIRs

Parameter	Units	Experimental series						
OL	gVS/l	5.99	8.42	16.84	18.07	24.09	35.78	46.37
SIR		0.17	0.35	0.70	0.53	0.70	1.83	1.88
Final VS in digestate (day 21, calculated)	gVS	0	0.53	1.42	2.59	3.23	3.3	4.36
VS Removal ratio (by day 21, calculated)	%	100	92	89	81	82	83	77
Min. pH		7.84	7.51	7.46	7.56	7.57	6.52	6.65
Maximum HAc	mg HAc/l	643.12	982.02	1717.59	2313.87	3354.8	7693.85	8929.29
Maximum HPr	mg HPr/l	73.13	192.63	456.83	372.31	585.5	3468.24	3126.63
Max. Ratio HPr/HAc		0.11	0.2	0.27	0.2	0.23	7.02	7.37
Max Ratio TVFA/TIC (titration)		n.d.	0.21	0.45	0.34	0.42	n.d.	n.d.

*n.d. not determined

The evolutions of the TVFA (calculated as the sum of the concentrations of the different acids previously converted to COD using stoichiometric factors), HAc and HPr concentrations as well as the HPr/HAc ratio are presented in Figure 19 (A, B, C, and D respectively) for the different OLRs tested. The most dominant VFA were HAc and HPr, followed tightly by the n-HBu. The same pattern was observed for all individual VFAs amongst the different loadings tested: the higher the OL, the higher the peak values. The HVa concentrations were negligible for all tests (data therefore not shown). Figure 19.B shows that in the case of HAc, concentrations of 2 g/l were exceeded for the 4 assays with the highest OLs during the first 4 to 6 days of digestion. In the case of the two highest OLs, the HPr concentration went above 1.5 g/l from the first day of digestion until the 10th day, reaching a maximum of 3 gHPr/l, which was maintained from day 4 to day 9. This could have been related to an increase in the H_2 concentration in the liquid phase, with inhibitory effects on the HPr degraders. For the rest of the assays the concentration never went above 0.5 gHPr/l. The concentration of n-HBu was also considerably high for the two highest SIR with values above 1 g/l (with a maximum of 2.9 g/l on the second day of digestion) from the 1st until the 6th day of digestion (data not shown).

For the two assays with the highest OLs, the ratio HPr/HAc went above 1 between days 1 and 13 of the digestion, corresponding to elevated HPr concentrations (above 1g/l). The TVFA concentration exceeded 4 g/l. These values denote high probability of unstable digestion, resulting from acidification, as they are above critical values suggested in literature (see sub-chapter 2.2.4.2).

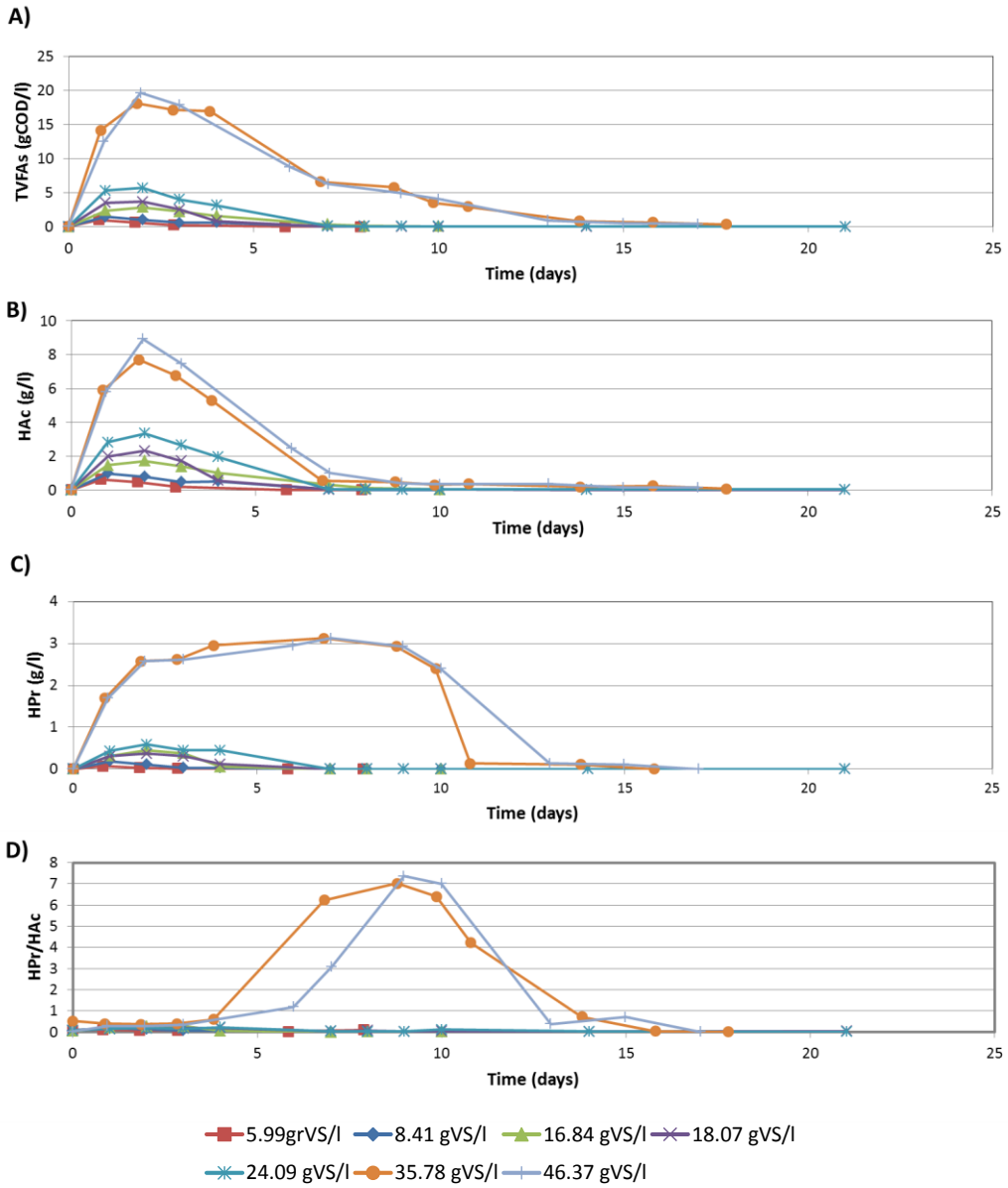

Figure 19: Concentration evolution of TVFA (expressed as gCOD/l) HAc, HPr, and the HPr/HAc ratio over time for the digestion assays for grass silage (GS 1) at different OLs

4.1.1.1.3 Changes in the process kinetics

Table 33 summarises the calculated first-order kinetic constants (k) for the 7 different loadings. A decrease was observed in the k values with increasing OL, thus suggesting an increasingly affected methane production. The drop in the k values is particularly significant for the two highest loadings, in relation with the observed increase in the concentration of the organic acids in the reactor, particularly HAc and HPr, and decrease in the pH below values considered as inhibitory for methanogens. Thus the kinetics in the methane production were clearly affected according to this parameter as a result of imbalanced methanogenesis and acetogenesis. The smaller amount of inoculum used to inoculate the reactors for the trial with the OL of 35.75 gVS/l (19.6g/reactor) resulted in a SIR very similar to the one of the trial with the OL of 46.37 gVS/l in spite of the difference of 23% in the OL, and a very similar behaviour for some parameters, including the first-order constant.

Table 33: Calibrated first-order rate constants (k) for the different OLs (fitted to the cumulative CH_4 production) during batch digestion of GS 1

OL (gVS/l)	SIR	k (d^{-1})	R^2
5.99	0.17	0.21	0.99
8.42	0.35	0.23	0.99
16.84	0.70	0.17	0.98
18.07	0.53	0.19	0.97
24.09	0.70	0.17	0.98
35.78	1.83	0.11	0.96
46.37	1.88	0.12	0.97

In spite of the detected process instability and impaired biogas production shown for the highest OLs by some indicators considered and presented in this sub-section, the system recovered after some times, and process failure was not observed. This highlights the good resilience of anaerobic systems in the case of well adapted biocenosis.

4.1.1.1.4 Correlation between the substrate to inoculum ratio, the organic loading and the different digestion parameters

The correlation of both the SIR and OL and different operational parameters was investigated in order to determine which one had the largest influence. It is important to highlight at this point that while the OL only considers the feed being added in the reactor, the SIR also considers the VS supplied by the inoculum (including the bacterial biomass). Each parameter considered was plotted against the different SIRs and OLs tested respectively. A possible linear correlation was assessed and R^2 determined to estimate the goodness of the fit. As an example, Figure 20 shows k versus the OL (left) and the SIR (right) tested. In this case the correlation was good in both cases (0.83 and 0.88 for the OL and SIR respectively). The results of this analysis are summarised in Figure 21. The goodness of the linear correlation was considered to be satisfactory for R^2 value above 0.8. Overall, it can be observed that:

- The correlation between most variables considered and the OL and SIR seemed to be linear (on the basis of the very good coefficient of determination).
- The correlation was not clear, or at least not explained by linear correlation, for variables related to the biogas performance, with the exception of the SMPR.
- Generally the correlations' goodness was better for the SIR than the OL, thus highlighting the relevance of this operational parameter to describe the feeding of the system and to explain certain disturbances, at least under batch conditions.

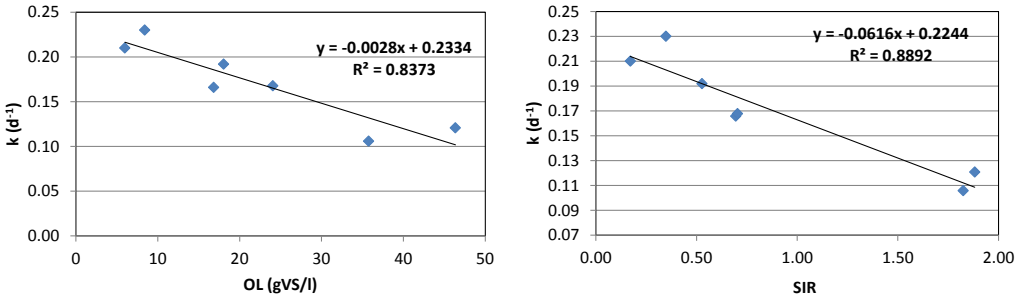

Figure 20: Variations in first-order rate constant (k) against the OLs (left) and the SIRs (right) tested

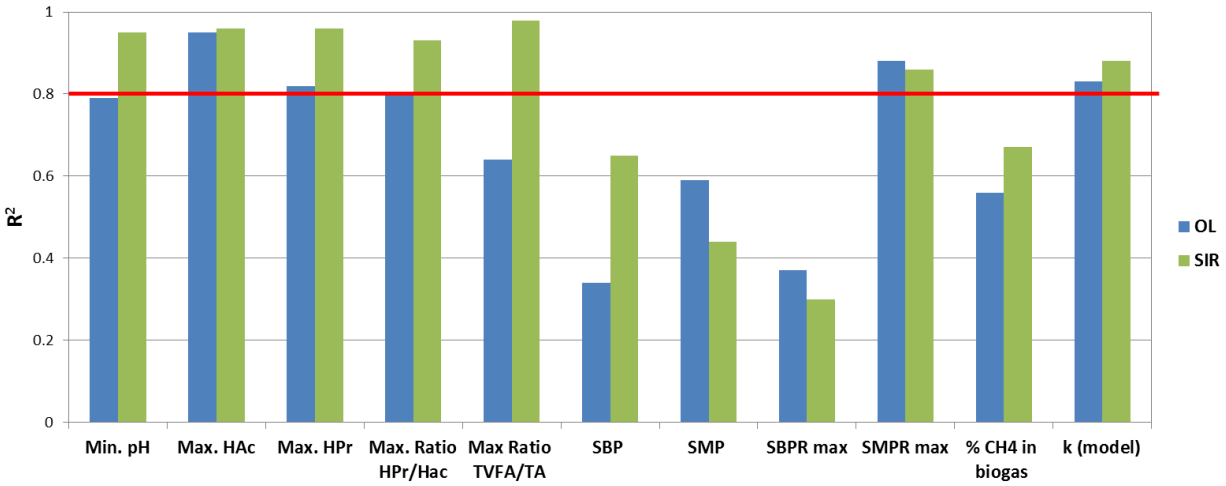

Figure 21: Goodness of the correlation between OL and SIR and different parameters considered. The red line represents the value at which a satisfactory fitting is considered ($R^2 \geq 0.80$)

4.1.1.2 Biodegradability of cellulose in a semi-continuously fed reactor at increasing organic loading rates

As indicated in Chapter 2, cellulose is an important component of plants and thus it is significantly present during the anaerobic digestion of energy crops and other lignocellulosic substrates.

The understanding of its degradation during fermentation is most relevant to optimise its application for biogas production. Different studies have analysed the influence of different factors on the anaerobic digestion of cellulose including the pH and particle size (Hu et al., 2004; Hu et al., 2005), the VFA concentration (Romsaiyud et al., 2009; Siegert and Banks, 2005) the pre-treatment and crystallisation (Hendriks and Zeeman, 2009; Jeihanipour et al., 2011), and the OL (Golkowska and Greger, 2010).

The influence of the inoculum source (e.g. rumen content, pure cultures or MSW leachate) on cellulose degradation and bacterial populations has also been investigated (Jensen et al., 2009; O'Sullivan et al., 2006; Song et al., 2005). There is a general agreement in the results that inoculum with rumen content presents faster hydrolysis rates compared to a MSW digester inoculum.

In spite of the importance of continuous operational conditions in waste management and renewable energy industries, most studies involving cellulose degradation analyse batch conditions, with the exception of few papers (Noike et al., 1985; Song and Clarke, 2009), which use MSW digester leachate and pure cultures (Desvaux et al., 2001) as inoculum. Moreover, to the knowledge of the author, there are currently no studies investigating the continuous digestion of cellulose using inoculum from agricultural biogas digester (i.e. containing rumen microorganism).

The objective of this experiment was to get a better insight into the degradation of cellulose in a semi-continuously fed reactor, and in particular the evolution of cellulose concentration, and to investigate the response of the system to increasing loadings, in terms of the impact on the SMP and biogas composition as well as on the process dynamics.

The degradation test was carried out in a double-jacket glass CSTR (described in sub-chapter 3.4.2) with a WV of 10 litres and fed with microcrystalline cellulose re-suspended in double distilled water at different OLRs (1 gVS/l/d and 1.5 gVS/l/d).

The experimental data (i.e. composition and quantity of biogas and VFA and the NH_4-N consumption) was used to calculate a mass balance of COD in the system. The mass balance for particulate cellulose in a continuous digester can be described by Eq. 57.

$$V \times \left(\frac{dS}{dt}\right) = q \times (S_o - S) + r_s \times V \qquad \text{Eq. 57}$$

where V is the liquid WV (l), q is the hydraulic flow rate (l/d), So and S are the influent and effluent cellulose concentrations respectively, expressed in terms of COD (g/l) and r_s is the rate of solubilisation expressed in units of COD (g/l/d). One method to determine r_s is by monitoring the formation of products, quantified in terms of COD, as expressed in Eq. 58.

$$r_s = r_{vfa} + r_{CH_4} + r_x \qquad \text{Eq. 58}$$

where r_{CH4} is the volumetric production rate of CH_4 in COD units (g/l/d), r_x is the volumetric production rate of bacterial biomass expressed in terms of COD (g/l/d), estimated by the uptake of N from the liquid phase and r_{vfa} is the volumetric production rate of VFA expressed in terms of COD (g/l/d), and estimated according to Eq. 59.

$$r_{vfa} = \frac{d[VFA]}{dt} - \frac{([VFA]_{in} - [VFA]_{out}) \times q}{V} \qquad \text{Eq. 59}$$

Bacterial biomass was determined indirectly by monitoring the accumulation or depletion of NH_4-N in the reactor and relating this to a biomass COD. This assumes that the extracellular polymeric substances do not contain any N. The NH_4-N uptake (r_N) can be estimated from the following Eq. 60.

$$r_N = \frac{d[NH_4^+ - N]}{dt} - \frac{([NH_4^+ - N]_{in} - [NH_4^+ - N]_{out}) \times q}{V} \qquad \text{Eq. 60}$$

r_x can be estimated from r_N with the following Eq. 61.

$$r_x = r_N \times Y_{x/N} \times COD_x \qquad \text{Eq. 61}$$

where $Y_{x/N}$ is the amount of biomass per unit mass of N (=9.36 g/g), based on the biomass stoichiometry of Mosey (1983), $C_5H_9O_3N$. CODx is the O_2 required to fully oxidize biomass (=1.221 g/g). The concentrations of VFA and NH_4-N were measured on a daily basis and used to estimate r_{vfa} and r_N.

It has been previously highlighted (O'Sullivan et al., 2006) that the volumetric solubilisation rates were not indicative of the true performance of digestion systems and that the normalised solubilisation rate (calculated by dividing r_s by the mass of cellulose in the reactor at each time step, and thus being expressed as $gCOD/g_{cellulose}/d$) should be used instead. The extent of cellulose solubilisation can then be expressed as the sum of the degradation products (CH_4, instantaneous VFA mass in the solution and biomass generation up to that point) divided by the initial COD in the system (in this case the COD from cellulose), by applying Eq. 62. The contribution from the H_2 was not taken into account.

$$D_s(\%) = \frac{COD_{CH_4} + COD_{vfa} + COD_{biomass}}{COD_{initial}} = \frac{r_s}{q \times So} \qquad \text{Eq. 62}$$

4.1.1.2.1 *Evolution of cellulose and intermediary products during digestion and solubilisation rate*

Figure 22 presents the evolution of the concentration of cellulose, the monosaccharides resulting from the hydrolysis of cellulose (i.e. glucose) and the sum of the individual VFA (resulting from the acetogenesis and acidogenesis steps) in the reactor (expressed in gCOD/l). It can be seen that the cellulose concentration increased (no degradation) during the initial lag phase of 48 hours with the initial loading of 1 gVS/l/d. Then, it declined significantly during the 3rd and 4th day and remained constant until day 35 of digestion, when the OLR was increased to 1.5gCOD/l/d. From that day onwards, an important accumulation of cellulose in the reactor was observed, along with an increase in the TVFA concentration.

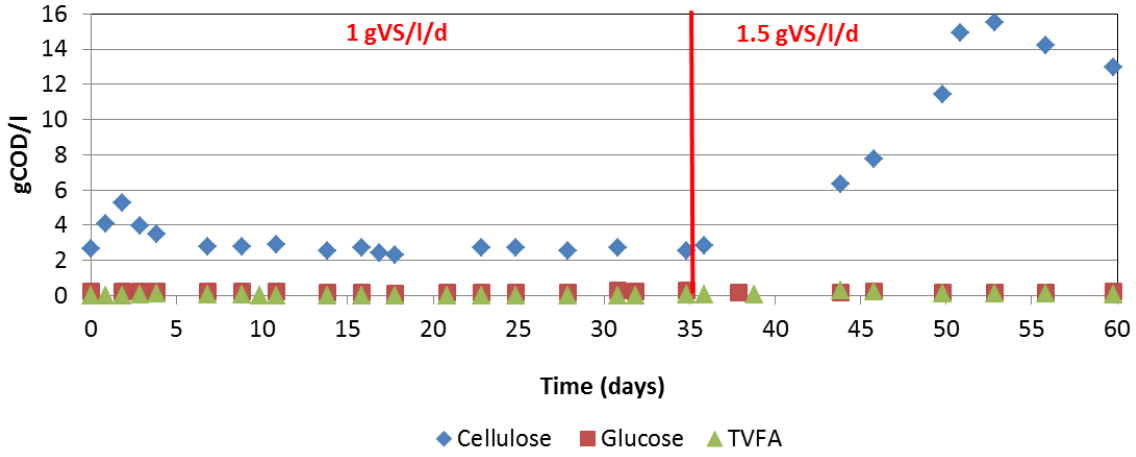

Figure 22: Evolution of the concentration of cellulose, glucose, and TVFA in the reactor during mesophilic semi-continuous digestion of microcrystalline cellulose

Under steady state conditions, the degree of solubilisation of cellulose was estimated to be of 84±7%, with an average mass normalised solubilisation rate (as proposed by O'Sullivan et al. (2006)) of 0.38 $gCOD_{formed}/gCOD_{cellulose}/d$. This value is lightly lower than the values estimated for inoculum with rumen content for batch digestion, ranging from 0.52 to 0.57 $gCOD_{formed}/gCOD_{cellulose}/d$ (Hu et al., 2004; O'Sullivan et al., 2006).

The first-order rate constant (k) was calculated to be 0.33 d^{-1} after applying Eq. 28 in sub-chapter 3.6.1.2 to the steady-state data. This value is in line with values reported for reactor inoculated with MSW leachate in the scarce papers addressing continuous digestion (e.g. Song and Clarke (2009)).

An increase in the OLR up to 1.5 gVS/l/d resulted in a decrease of the degree of solubilisation to 33% after 25 days and of the normalised solubilisation rate to 0.05 $gCOD_{formed}/gCOD_{cellulose}/d$. The observed decrease in the solubilisation rate related with an important accumulation of cellulose in the reactor, which can be observed in Figure 22.

The glucose concentration remained quite stable during the whole digestion period regardless of the OLR (Figure 22), reaching a steady value of 0.2 gCOD/l, which highlighted the fast kinetics of the acidogenesis step. The sCOD fluctuated in the beginning of the experiment (as a

result of hydrolysis) and decreased from the 5th day of digestion to a steady value of 2.5 gCOD/l (data not shown). After increasing the OLR, the sCOD increased by 30%, to decrease again afterwards. The evolution of the VFAs followed the same trend. Indeed, it was possible to observe an increase in the TVFA concentration in response to the increase in the OLR, reaching a maximum of 0.28 gCOD/l 8 days after increasing the OLR. There was a rapid increase of HAc after the increase in the OLR, reaching a maximum of 1.32 g/l (see Figure 23). This maximum seems to be related with the aforementioned accumulation of cellulose in the reactor after day 43. One likely explanation for this phenomenon could be the high acetate concentration, which could have impacted the enzymatic cellulose hydrolysis. Previous work in batch systems and using glucose and cellulose found that VFA can cause the inhibition of the cellulolytic activity at concentrations 2g/l (Siegert and Banks, 2005). A more recent study investigating the influence of pH and acetate concentration on the rates of enzymatic cellulose hydrolysis showed that acetate in the culture medium had an effect on cellulase production and, to a larger extent, on cellulose hydrolysis (Romsaiyud et al., 2009). In other words, the results suggested that acetate can inhibit the ability of cellulase for hydrolysing cellulose more strongly than inhibiting cells for cellulase production. The authors suggested a threshold of 30mmol/l (corresponding to 1.8 g/l) from which acetate accumulation could lead to a decrease of both cellulase production and cellulose uptake. The results presented here suggest that such inhibition could be initiated at lower acetate concentration values.

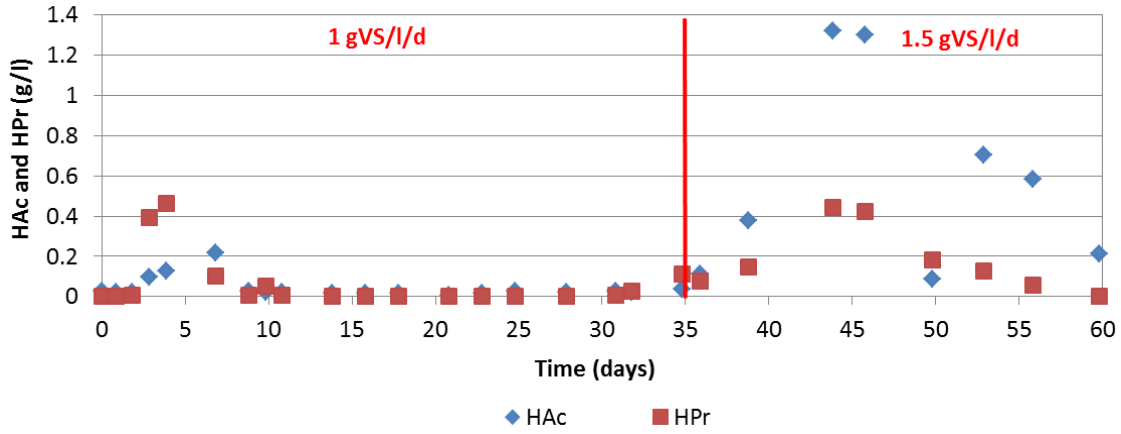

Figure 23: Evolution of the concentration of HAc and HPr during semi-continuous digestion of cellulose

4.1.1.2.2 Biogas production

The biogas and methane yields at the steady state conditions with a loading of 1 gVS/l/d were 0.604 Nl/gVS and 0.294 Nl/gVS respectively. Thus, the methane yield represented on average 96% of the BMP value (0.586 Nl/gVS) for this feeding regime, as it can be seen in Figure 24.

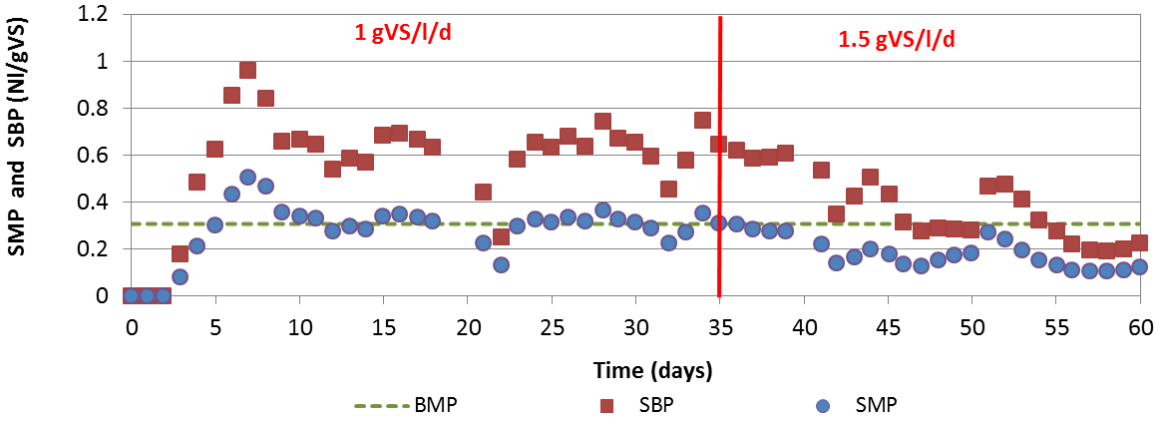

Figure 24: SMP and SBP during semi-continuous digestion of microcrystalline cellulose at different loadings. The SMP estimated through the BMP test is also displayed

As regards the composition of the biogas, while the methane content was of 50% on average for the loading of 1 gVS/l/d, it fluctuated during 25 days after increasing the loading, ranging from 39% to 65% (see Figure 25).

Thus, the accumulation of cellulose in the reactor after increasing the OLR to 1.5 gVS/l/d (see Figure 22) did not translate into critical values for any operational parameter (e.g. TVFA/TIC), but impacted the biogas production, i.e. the methane yield represented 52% of the potential value 25 days after changing the OLR to 1.5 gVS/l/d (Figure 24).

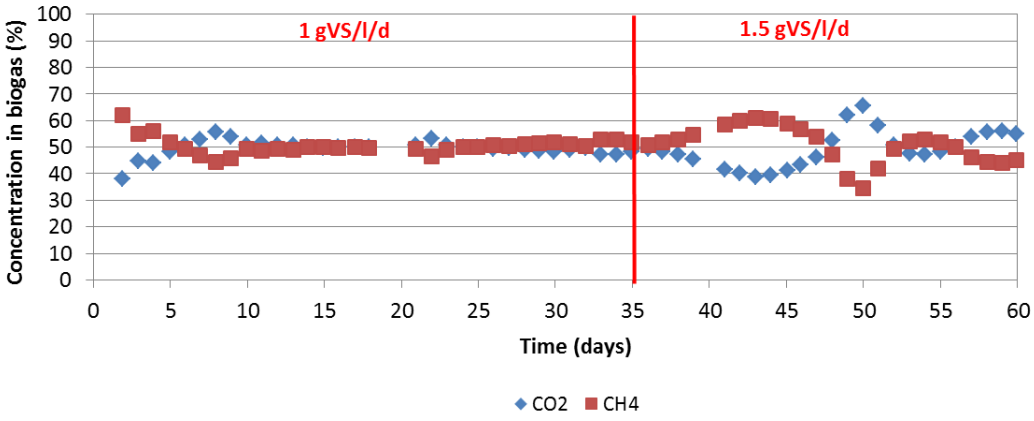

Figure 25: Evolution of the CO_2 and CH_4 content in biogas during semi-continuous digestion of microcrystalline cellulose at different loadings

4.1.1.2.3 COD, TS, and VS evolution and mass balance

Figure 26 (bottom) shows the evolution of the concentration of the VS, the TS, and the COD. It can be observed that the evolution of the concentrations for these three parameters over the digestion period showed the same trend, with an initial increase during the lag phase of 2 days followed by a decrease in these parameters to a steady value after 20 days of digestion with an OLR of 1 gVS/l/d. After the OLR was increased after day 35, the concentrations also increased, corresponding to the observed accumulation of cellulose. While Figure 22 presents the evolution of cellulose in the reactor only, this figure comprises the evolution of different organic fractions present in the reactor during digestion (including VFA, monomers, and accumulated inerts).

It is interesting to highlight that the correlation between the COD and the VS and TS changed respectively from day 35, when the OLR is increased. In Figure 26, the correlation between these parameters was estimated for data collected during the start-up phase and the steady state phase with the OLR of 1 gVS/l/d. The estimated COD equivalent of VS was of 1.39 gCOD/gVS, which is slightly lower than that estimated by Lübken et al. (2007) for the digestion of fodder for cows (1.56 gCOD/gVS) or by Wichern et al. (2009) for the digestion of grass silage (1.45 gCOD/gVS).

The mass balance of the system, in terms of gCOD, is shown in Figure 27 for 8 different days during the steady state phase for the OLR of 1 gVS/l/d, with the total sum of the products (CH_4, TVFA and the bacterial biomass). The recovery was satisfactory (when compared with the estimated available cellulose in the reactor on a daily basis). It can be seen in this figure that the proportion of each product considered remained constant during this period. The VFA yield ($gCOD_{vfas}/gCOD_{products}$) was 4% on average at steady state with the feeding of 1 gVS/l/d, which suggests a large utilization of the fermentation products by acetogenic and methanogenic organisms. After 30 days of digestion at the loading of 1 g/l/d, the bacterial biomass yield was of 3%.

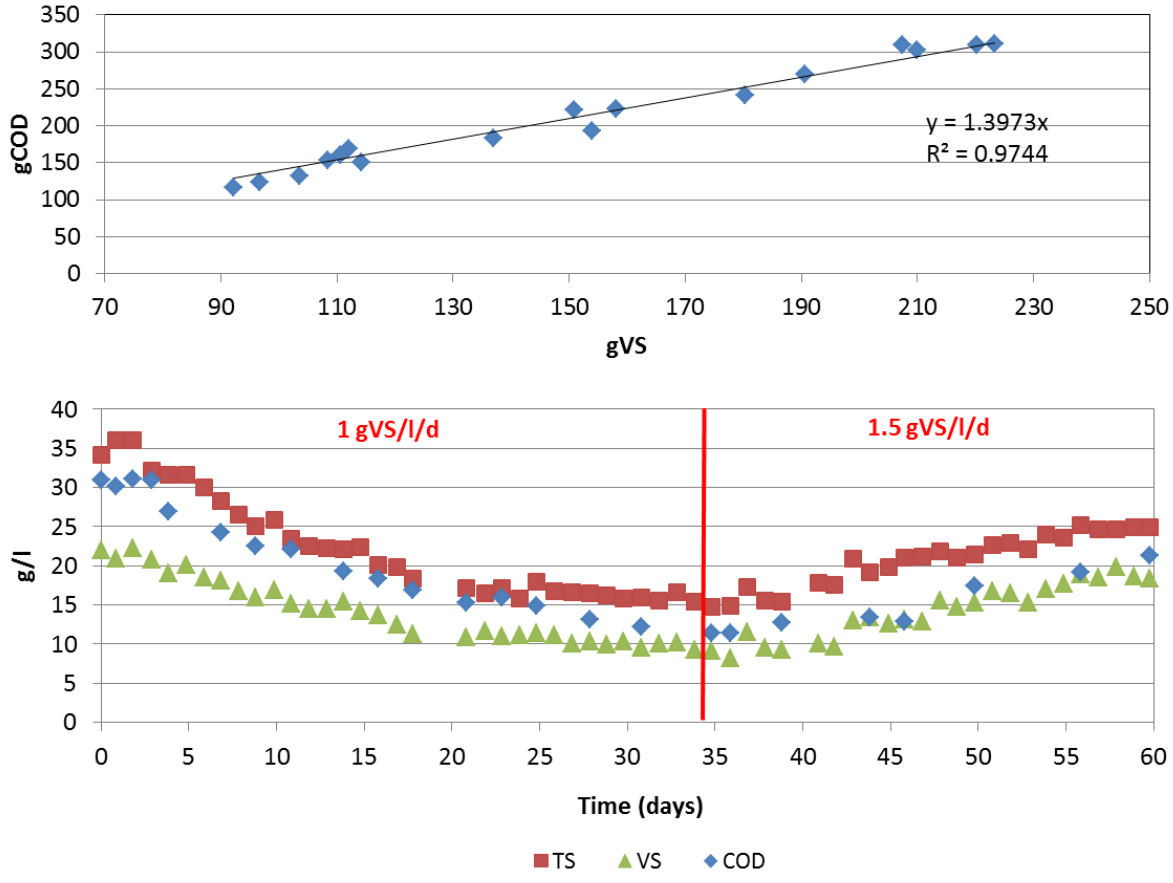

Figure 26: Evolution of the TS, VS, and COD concentrations (expressed in g/l, bottom) and the correlation between the measured COD and VS for the OLR of 1 gVS/l/d (top)

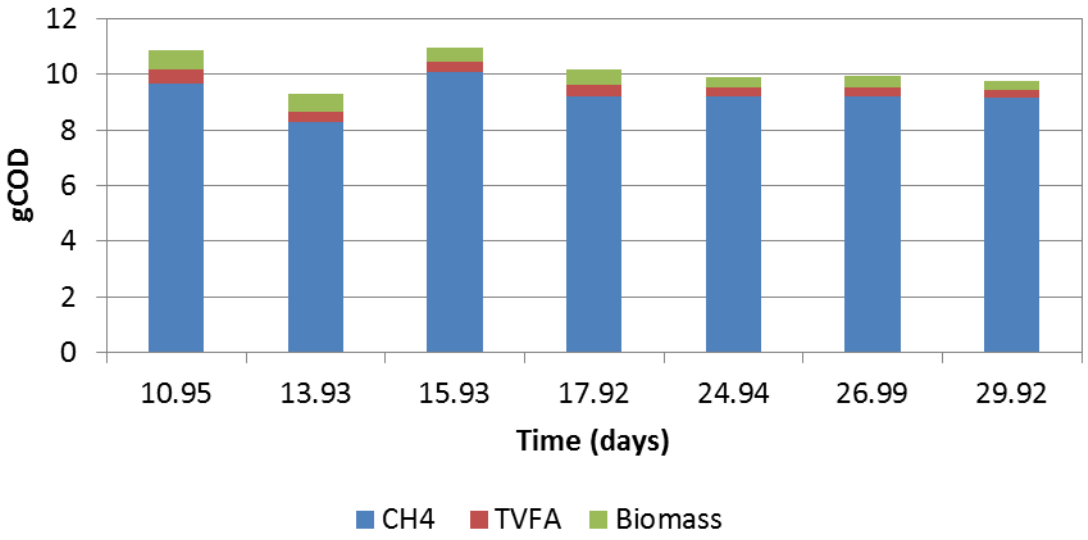

Figure 27: COD balance with the loading of 1 gVS/l/d during semi-continuous digestion of microcrystalline cellulose at different loadings

The results showed how a minor increase in the loading rate can have a large impact on the solubility of cellulose and on the methane production, and thus on the process efficiency. In particular, the results suggested that an acetate concentration above 1.3g/l, which was reached with a loading of 1.5g/l/d (Figure 23) could have an effect on cellulose hydrolysis, which had been already suggested in previous publications (Siegert and Banks, 2005; Romsaiyud et al., 2009), but for higher acetate concentrations.

Given the fact that most parameters fluctuated during the 25 days after increasing the loading (no steady-state was reached), and enough data was not available for steady-state conditions, correlation analysis and ANOVA were not applied for this experiment.

4.1.1.3 Digestion of grass silage in a semi-continuously fed reactor at increasing organic loading rates

Semi-continuous digestion of grass silage was investigated under increasing OLR, from 1.9 up to 4.7 gVS/l/d, in terms of system performance (biogas production and composition) and process stability and dynamics, with trace element addition. To this end, a one-stage semi-continuously fed CSTR without recirculation was used (described in sub-chapter 3.4.2.1) and fed with dried grass silage (DGS 3). Additional results to those presented in this sub-chapter are summarised in Annex K.

4.1.1.3.1 Methane production

For an OLR of 1.9 gVS/l/d, the average SMP achieved was of 0.24 Nl_{CH4}/gVS which represents 96% of the BMP value (0.25 Nl_{CH4}/gVS) determined for DGS 3. The average performance of the reactor for each feeding is presented in Table 34 and illustrated in Figure 28. The average VMPR was 0.46 $Nl_{CH4}/l_{reactor}$/d and the MPR of 5.34 Nl_{CH4}/d. These values are in line with those found in literature for mono-digestion of grass silage for similar OLRs. For example, Pakarinen et al. (2011) reported a CH_4 yield of 0.19–0.21 Nl/gVS for an OLR of 2 gVS/l/d and HRT of 30 days for a CSTR reactor, while Wichern et al. (2009) found a value of 0.33 Nl/gVS for an OLR of 2.5 gVS/l/d.

The increase of the OLR from 1.9 to 4.7 gVS/l/d impacted substantially the VMPR and the MPR ($p<0.05$) from an average of 0.32 Nl_{CH4}/l/d to 0.82 Nl_{CH4}/l/d and from 3.71 Nl_{CH4}/d to 9.42 Nl_{CH4}/d respectively (61% increase). This is illustrated in Figure 28 (right).

On the other hand, the increase of the OLR did not have a major impact on the SMP, with a decrease from 0.241 Nl_{CH4}/gVS to 0.208 Nl_{CH4}/gVS (representing a decrease of approximately 13%). This suggests that in the OLR range of 1.9–4.7 gVS/l/d, the overall specific efficiency of the mono-digestion of dried grass silage was affected but to a small degree, from a CH_4 yield point of view (difference not statistically significant, $p>0.05$). Annex J summarises the statistical analysis of the differences between means for the different OLRs. The CH_4 content in the produced biogas decreased with increasing loadings, but the difference was also minor and not statistically significant (Annex J). Similar trends were observed by Xie et al. (2012) who investigated the co-digestion of the solid fraction of separated pig manure with dried grass silage in CSTRs under mesophilic conditions at different mixing ratios and OLRs, although in this case, the impact of the loading was larger (i.e. 38% decrease in the SMP from an initial OLR of 1 to 3 gVS/l/d).

It is important to highlight that optimum OLR might be different for different configurations and reactor types. For example, Nizami et al. (2012) and Thamsiriroj et al. (2012) found a reduction in MPR up to 20% when increasing the OLR beyond 2 gVS/l/d in two-stages continuous CSTRs.

Table 34: Average performance during semi-continuous digestion of DGS 3 for different OLRs

	OLR (gVS/l/d)			
	1.9	2.7	3.3	4.7
SMP (Nl/KgVS)	240.99±9.60	219.02±4.13	215.44±9.08	208.46±17.04
VMPR ($NlCH_4$/l/d)	0.323±0.01	0.441±0.01	0.514±0.00	0.819±0.03
MPR (Nl_{CH4}/d)	3.71±0.74	5.07±0.11	5.91±0.09	9.42±0.39
CH_4 content (%)	57.72±0.45	56.87±0.77	56.75±0.17	56.91±0.29
% of BMP value (%)	96	88	86	83

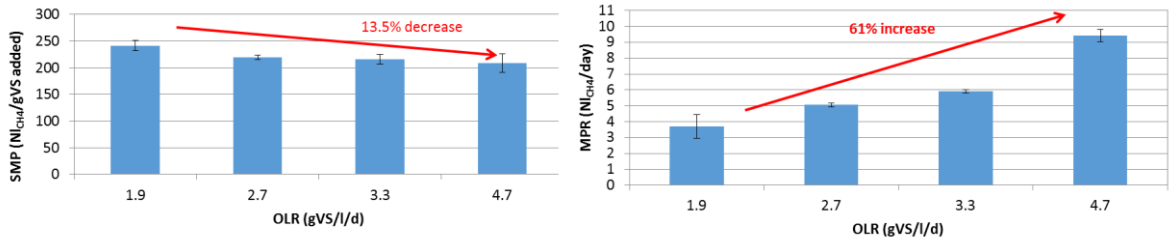

Figure 28: SMP (left) and MPR (right) during semi-continuous digestion of DGS 3 for different OLRs

4.1.1.3.2 Substrate removal and intermediary products evolution

The operational conditions of the reactor at the different OLRs investigated are summarised in Table 35. The concentration of TS and VS in the reactor effluent increased with increasing OLR, from 2.2% up to 4.3%, and from 1.5% to 3.1% respectively, thus suggesting a small accumulation in the reactor. On the other hand, the VS removal increased slightly with increasing OLR, and ranged between 54% and 62%. This could be explained by surface related hydrolysis kinetics. Regardless, the estimated values are in line with those found in literature

for the anaerobic digestion of grass silage, which can range from 34% to 67% depending on the operational conditions and reactor configuration (Lehtomäki, 2006; Cirne et al., 2007; Lehtomäki et al., 2008). The evolution of the TS, the VS, and the COD concentrations in the reactor can be seen in Figure 29 for DGS 3, with a clear correlation. The equivalence factor was determined to be 1.64 gCOD/gVS (R^2=0.95). Wichern et al. (2009) found for grass silage an equivalence of 1.45gCOD/gVS, while Schlattmann (2011) measured 1.5 gCOD/gVS, which highlights the influence of the specific feedstock composition and operational conditions. The formation of a crust layer in the upper part of the reactor was observed, particularly with the two highest loadings, which could have an impact if increasing the OLRs in the long term.

Table 35: Average operational conditions in CSTR reactor semi-continuously-fed with DGS 3

	OLR (gVS/l/d)			
	1.9	2.7	3.3	4.7
TS of digestate (%)	2.17±0.1	2.85±0.3	3.34±0.1	4.30±0.4
VS of digestate (%)	1.53±0.1	2.03±0.2	2.38±0.1	3.07±0.3
VS removal (%)	54.88	56.88	56.70	62.56
TVFA (mgHAc$_{eq}$/l)	18.24	58.63	80.55	32.9
NH_4^+-N (mg/l)	261.60±48	131.73±28	124.70±15	98.70±16
TN (mg/l)	917.70±60	977.00±42	1088.20±11	1274.60±71
sCOD (g/l)	1.60±0.1	1.64±0.1	1.99±0.0	2.31±0.1

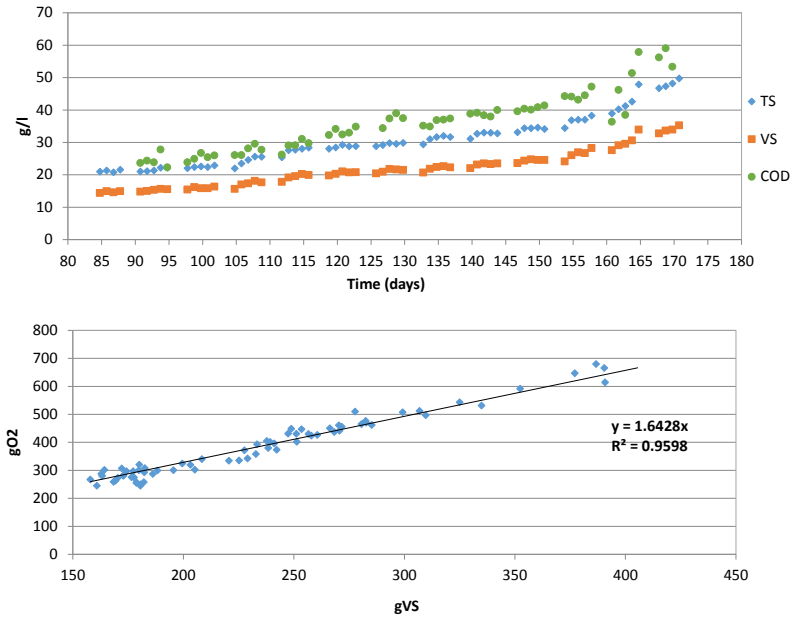

Figure 29: Evolution of TS, VS and COD during digestion of DGS 3 (top) and correlation between COD and VS (bottom)

The sCOD values ranged from 1.6 to 2.31 g/l and the VFA concentrations were low and not exceeding in any case concentrations above 0.3 gHAc/l. The VFA concentration systematically peaked slightly in the first days after changing the OLR. It is worth mentioning a small accumulation of VFA from the day 128th of digestion onwards with the feeding regime 2 (OLR of 2.7 gVS/l/d), which could be related to an increase of the lactate in the system, which can be observed during transient overload conditions. A peak of HPr was detected for several days after the 142nd day of digestion. This slight increase in the VFA inversely mirrored a decrease in the CH_4 content in the biogas (Figure 30). In any case, the gradual increase of the OLR

contributed to avoid any sharp accumulations of VFA. The fact that the amount of total organic matter and soluble organic matter (as indicated by VS and sCOD), increased in the digestate but not the VFA after increasing the OLR, suggests that VFA was rapidly consumed by the methanogens, thus pointing out hydrolysis as the limiting step. A similar observation was made by Lehtomäki et al. (2007) for the co-digestion of grass silage and cow manure.

The average ratio of TVFA to TIC (measured by titration) was below the critical limit of 0.4 until the end of the period with an OLR of 2.7 gVS/l/d (day 135), from when the ratio remained at that level until the end of the test (see Figure 31). The above mentioned likely presence of lactate in the grass silage fed could have contributed to this value, without having a remarkable correlation with other stability parameters.

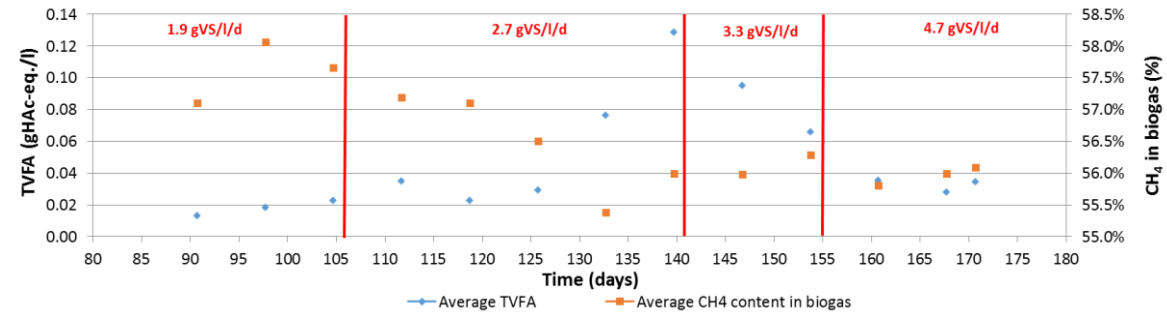

Figure 30: Evolution of the weekly averages for the TVFA (expressed as gHAc-eq./l) and the CH4 content in the biogas during semi-continuous digestion of DGS 3

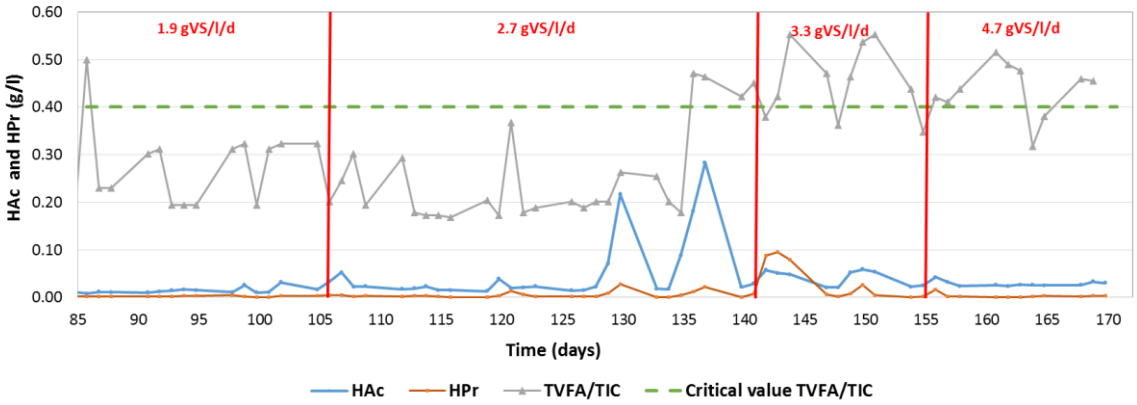

Figure 31: Evolution of the daily evolution of the HAc and HPr concentrations and the TVFA/TIC ratio during semi-continuous digestion of DGS 3

NH_4^+-N, which is the predominant form of ammoniacal nitrogen present in the reactor at the measured pH of 7, accounted on average 29% (0.261 g/l) of the TN in the digestate with the feeding regime 2, with a steady decrease overtime (see Figure 32). On average, this proportion decreased to 13%, 11% and 8% when increasing the OLRs to 2.7, 3.3, and 4.7 gVS/l/d and it never went above concentrations reported as inhibitory. For example, a decrease up to 50% in methane production have been found for total ammoniacal nitrogen concentrations between 1.7 g/l and 14 g/l, although the inhibitory effect can vary depending on the system (Chen et al., 2008). The observed decreasing trend differs from the one observed for the co-digestion of grass silage with manures, with increasing concentrations in the digestate for increasing loadings (Xie et al., 2012; Lehtomäki et al., 2007). The reasons for this difference might be the contribution of the manure fed as co-substrate to the total NH_4^+-N concentration (manure

represented up to 60% of the VS in the above mentioned studies, with a NH_4^+-N content almost 9 times higher than grass silage per gram of VS). Nizami et al. (2012) found that the total NH_3 content increased in a two stage CSTR system digesting grass silages with a HRT of 50 days with increasing OLR (up to 2.5 gVS/l/d), although never above inhibitory concentrations. The different pattern in the evolution presented in this research could be explained by the shorter HRT, which might have affected the degradation of certain fractions of the substrate including the proteins. Indeed, the TN, increased by 6%, 16% and 28% with increasing OLR from an initial average concentration of 917.7 mg/l for the 2 gVS/l/d loading (Table 35). This correlated with an increase of up to 52% of the protein concentration in the reactor from an OLR of 1.9 gVS/l/d to 4.7 gVS/l/d, as it can be seen in Figure 32.

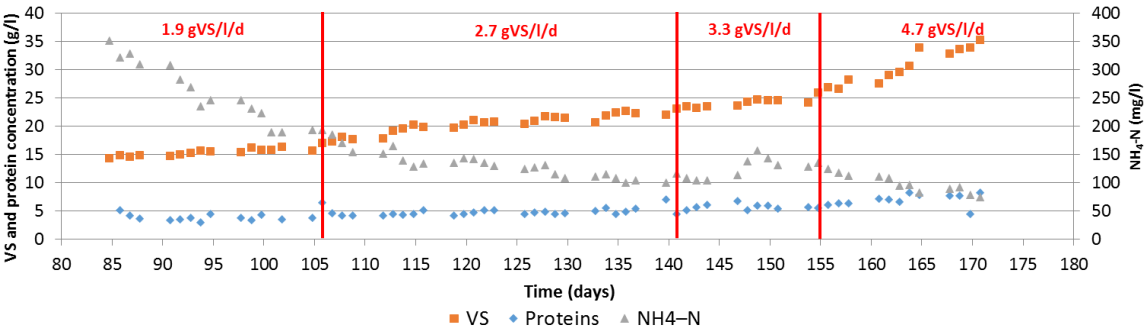

Figure 32: Evolution of the concentration of VS, proteins and NH_4^+-N in the reactor

4.1.1.3.3 Process kinetics during digestion of dried grass silage at increasing organic loading rates

In order to further investigate the influence of the OLR on the process dynamics, the first-order model (Eq. 28 in sub-chapter 3.6.1.2) was applied to the experimental data obtained for the 4 different loadings tested. The estimated equivalence factor ($i_{COD/VS}$) of 1.64 gCOD/gVS (see Figure 29) was used to convert from VS to COD units the concentration of the biodegradable material added daily and remaining in the reactor.

The calculated first-order rate constants (k) are presented in Table 36. A good fitting was found for all calibrations. The k values were similar for the 2 first loadings and slightly lower for the third loading of 3.3 gVS/l/d. In the case of the OLR of 4.7 gVS/l/d, the impact was clear ($p<0.05$), with the value decreased by 24%, thus indicating a slower degradation rate, which are in line with the accumulation of VS and proteins mentioned earlier. Indeed, the applied HRT of 17.7 days might not be sufficient to allow for the degradation of certain fractions of the feedstock, such as the proteins and the cellulose and hemicellulose. The estimated value of $0.59d^{-1}$ is almost identical to the value reported by Koch et al. of $0.6d^{-1}$ for the mono-digestion of grass silage in loop reactors (Koch et al., 2009). Moreover, the estimated first-order rate constant is approximately 3 times faster than the values estimated for the BMP test, using the methane production data and using the Microsoft Excel Solver tool. This could be explained by better adapted and balanced populations under continuous conditions in comparison with batch. This observation was also remarked by Song and Clarke (2009) for cellulose digestion under batch and continuous conditions.

Table 36: Calculated first-order rate constants for the different OLRs tested during semi-continuous digestion of DGS 3

OLR (gVS/l/d)	k (d^{-1})	R^2
1.9	0.59	0.94
2.7	0.59	0.96
3.3	0.57	0.99
4.7	0.45	0.81

4.1.1.3.4 Analysis of correlations

The Pearson correlation matrix for different parameters is presented in Table 37. It can be seen that the OLR seems to have a statistically significant correlation with the MPR, VS removal and the ratio TVFA/TIC ($p<0.01$). Amongst these three parameters, the strongest correlation was found for the MPR (the higher the OLR, the higher the MPR). The fact that a correlation was not found between the increasing OLR and the concentration of TVFA confirms previously presented statement that no accumulation (acidification) occurred for the OLR range tested with the addition of trace element solution. The correlation between the OLR and the CH_4 content is extremely weak, thus ruling out a negative impact for the operational conditions tested. On the other hand, the strong positive correlation of OLR with the ratio TVFA/TIC suggests that in spite of the fact that there is neither acidification nor accumulation of IN in the reactor, the increasing feeding leads to increasing acid concentrations. This supports the hypothesis that one or several acids not measured during digestion (e.g. lactate) could be accumulating in the reactor.

Table 37: Pearson matrix for the semi-continuous digestion of DGS 3 (Pearson correlation values for each pair of variables)

	OLR	MPR	VS removal	TVFA/TIC	TVFA	CH_4
OLR	1	.866**	.613**	.596**	.152	-.217
MPR		1	.434**	.473**	.104	-.266*
VS removal			1	.300**	.029	-.110
TVFA/TIC				1	.411**	-.234*
VMPR					.104	-.266*
TVFA					1	-.300**
CH_4						1

*. Correlation is significant at the 0.05 level (2-tailed).
**. Correlation is significant at the 0.01 level (2-tailed).

4.1.1.4 Effect of the organic loading rate on system performance and stability during semi-continuous digestion of maize silage

Lebuhn et al. (2008) found that in long-term operation of systems using maize as the sole substrate, process instability could rise due the deficiency of trace elements, even at low OLRs, with methanogens being the most affected bacterial group.

The objective of the experiment presented in this sub-chapter was to complement available knowledge by investigating if the process could be further optimised controlling the OLR (with addition of trace elements). To this end, the process stability (in terms of pH, VFA, TN and NH_4-N, sCOD and tCOD, and FOS/TAC) and system performance (in terms of volumetric biogas and methane production, the production rate, and the SMP) were investigated in a semi-continuously fed 1-stage CSTR digesting maize silage with trace element addition at increasing OLR (from 2 gVS/l/d to 10 gVS/l/d). The present sub-chapter covers thus the feeding regimes 1 to 5. The experimental set-up and monitoring plan and analytical methods are described in sub-chapter 3.4.2.2. Moreover, this experiment also contributed to investigate the possibility

of shifting a methanogenic process to H_2 production by changing the pH, and the efficiency of having a two-stage system with a hydrolytic and a methanogenic reactor running in series. The results of this second part (feeding regimes 6 and 7) are further described and discussed in the sub-chapter 4.1.4.

4.1.1.4.1 Biogas production and composition

Values related to the biogas performance (for feeding regimes 1 to 5) are presented in Table 38 as the average over the last weeks of each feeding regime, when reactor performance was considered to be adapted to the respective operational conditions. The change in the performance with increasing OLR is also illustrated in Figure 33.

At an OLR of 2 gVS/l/d, the average SMP achieved was of 0.325 Nl_{CH4}/gVS which represents 96% of the value determined with the BMP test (0.340 Nl_{CH4}/gVS). The observed BMP value is slightly lower than values reported in literature for maize silage. For example, Bruni et al. (2010) found values ranging from 0.37 to 0.41 Nl_{CH4}/gVS. But it is important to highlight that the MS used in this experiments was dried at 60°C, with the resulting loss of approximately 10% of the SMP value in comparison with fresh maize silage, as argued in Annex C.

Richards et al. (1991) investigated in thermophilic conditions the digestion of maize silage semi-continuously fed with recirculation and addition of trace elements for an OLR of 8.25 gVS/kg/d, with feed added and effluent removed 3 times per week. For these operational conditions, the authors found a SMP of 0.326 Nl/gVS, thus 20% higher than that found for the OLR of 6 gVS/l/d in the present research. These differences are most likely due to the very different operational and feeding conditions, including the fact that in the current experiment the maize has been dried.

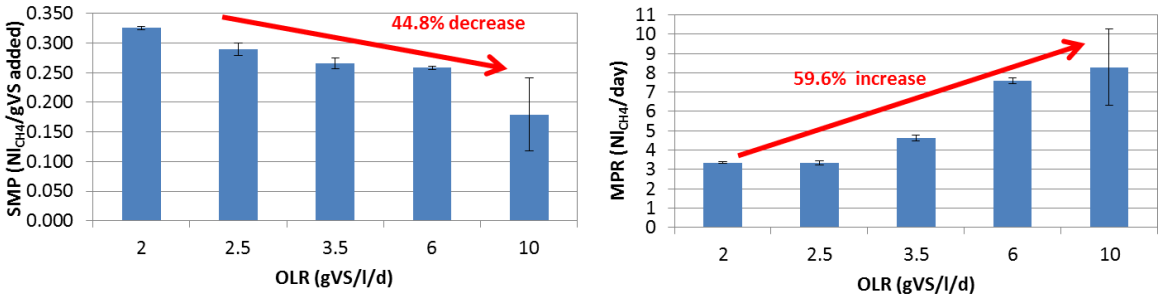

Figure 33: SMP (left) and MPR (right) for the different OLRs tested

The effect of increasing the OLR on the overall performance of the process, such as in the SMP, was significant ($p<0.05$ with ANOVA test) and more important than in the case of the dried grass silage (sub-chapter 4.1.1.3). Indeed, while in the case of dried grass silage an increase from 1.9 to 4.7 gVS/l/d resulted in a minor impact on the SMP (with a decrease of approximately 13%), in the case of dried maize silage, an increase from 2 to 3.5 gVS/l/d resulted in an 18.2% reduction in the SMP value. Such decrease amounted up to 44.8% when increasing the loading to 10 gVS/l/d. This increase also impacted the VMPR and the MPR but to a lower extent than in the case of grass silage, from an average of 0.501 $Nl_{CH4}/l_{reactor}$/d to 1.24 $Nl_{CH4}/l_{reactor}$/d and from 3.34 Nl_{CH4}/d to 8.28 Nl_{CH4}/d respectively (which is 59.6% increase). The explanation for this different effect of increasing loading (i.e. larger sensitivity in the case of maize silage) can lay in the composition of these two substrates, with more slowly

degradable material in the case of grass silage, which in turn can reduce the inhibitory effects resulting from overloading. Annex J summarises the statistical analysis for the differences between OLR means.

Table 38: Average performance in semi-continuously-fed CSTR reactor

	OLR (gVS/l/d)				
	2	2.5	3.5	6	10
SMP (Nl/kgVS added)	325.41±2.48	289.03±10.15	266.14±9.1	258.07±2.62	179.48±61.03
VMPR (Nl_{CH4}/l/d)	0.501±0.00	0.497±0.015	0.694±0.023	1.135±0.022	1.24±0.31
MPR (Nl_{CH4}/d)	3.34±0.04	3.32±0.10	4.63±0.15	7.58±0.14	8.28±2.12
CH_4 content (%)	53.9±0.31	53.8±0.45	52.7±0.05	53.2±0.41	40.07±2.35
% of BMP value (%)	96	85	78	76	53

The methane content in the produced biogas remained relatively stable at 53-52% for the OLRs of 2, 2.5, 3.5 and 6 gVS/l/d, as it can be seen in Figure 34, representing the daily off-line measurements of the CO_2 and CH_4 in the biogas (without considering H_2). With the OLR of 10 gVS/l/d, the CO_2 content in the biogas started to increase, with the resulting decrease in CH_4, and the first signs of instability were observed. Once the buffering capacity addition was removed (day 125th of the test), the pH dropped to values around 5, so it did the CH_4 content, thus inducing the shift into H_2 production. This is further described and discussed in the following sub-chapter 4.1.4.

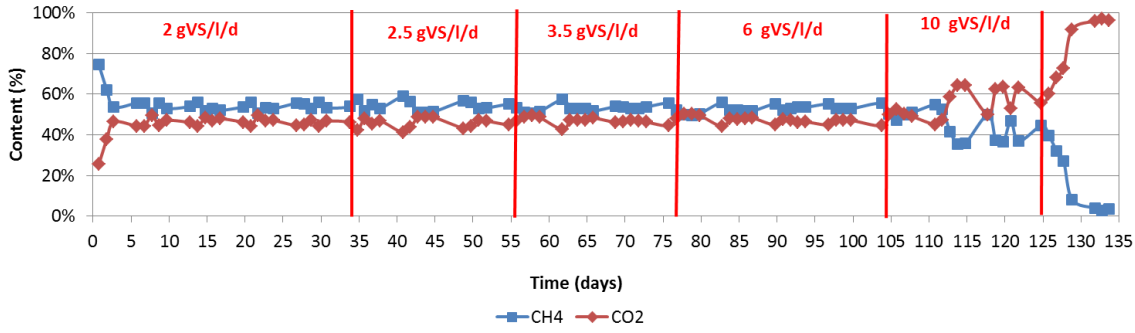

Figure 34: Evolution of the CH_4 and CO_2 in the biogas measured off-line. The red lines represent a change in the OLR

The composition of biogas measured off-line and on-line was almost identical, thus highlighting the reliability of the equipment used and the low variability of the measurements (as it can be seen in Annex L). The online measurements allowed to get a closer look into the response of the different gases measured to changes in the operational conditions, such as the feeding, the OLR, or the pH.

A clear pattern was observed in the H_2 content in the biogas, as it can be seen in Figure 35, with daily peaks after feeding. For feeding regimes 1 to 4 (2 to 6 gVS/l/d) the H_2 content never went above 0.5%. Figure 36 presents the evolution of H_2, CH_4 and CO_2 in the biogas for the whole duration of the experiment (for feeding regimes 1 to 5, with addition of trace element solution and buffering capacity) and the pH evolution. It can be observed that the CO_2 and CH_4 content also displayed a weekly pattern in response to the applied feeding (once a day, five times a week), although not very clear until feeding regime 4, with the OLR of 6 gVS/l/d. For this feeding regime, it was possible to observe the strong correlation between the pH and the CH_4 content, which followed identical evolution. After increasing the loading to 10 gVS/l/d, a

larger variability in the composition of these gases was observed in response to instability. The H_2 content peaked on a daily basis to values close to 5% (during feeding regime 5). This also correlated with rapid drops in the pH, in spite of the buffering capacity addition. The shift into H_2 production occurred after stopping the daily addition of buffering capacity, which resulted in a pH drop to values close to 5 on day 126. This is further discussed in sub-chapter 4.1.4.

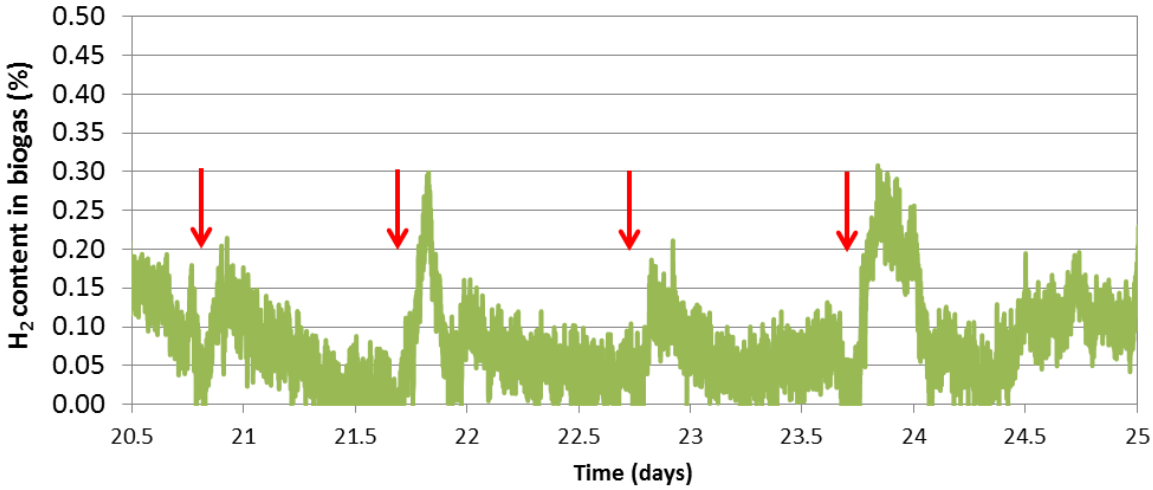

Figure 35: Evolution of the H_2 content in biogas, expressed as % during selected days for the feeding regime 1 (OLR of 2 gVS/l/d) during semi-continuous digestion of DMS 2. Red arrows represent the daily feedings

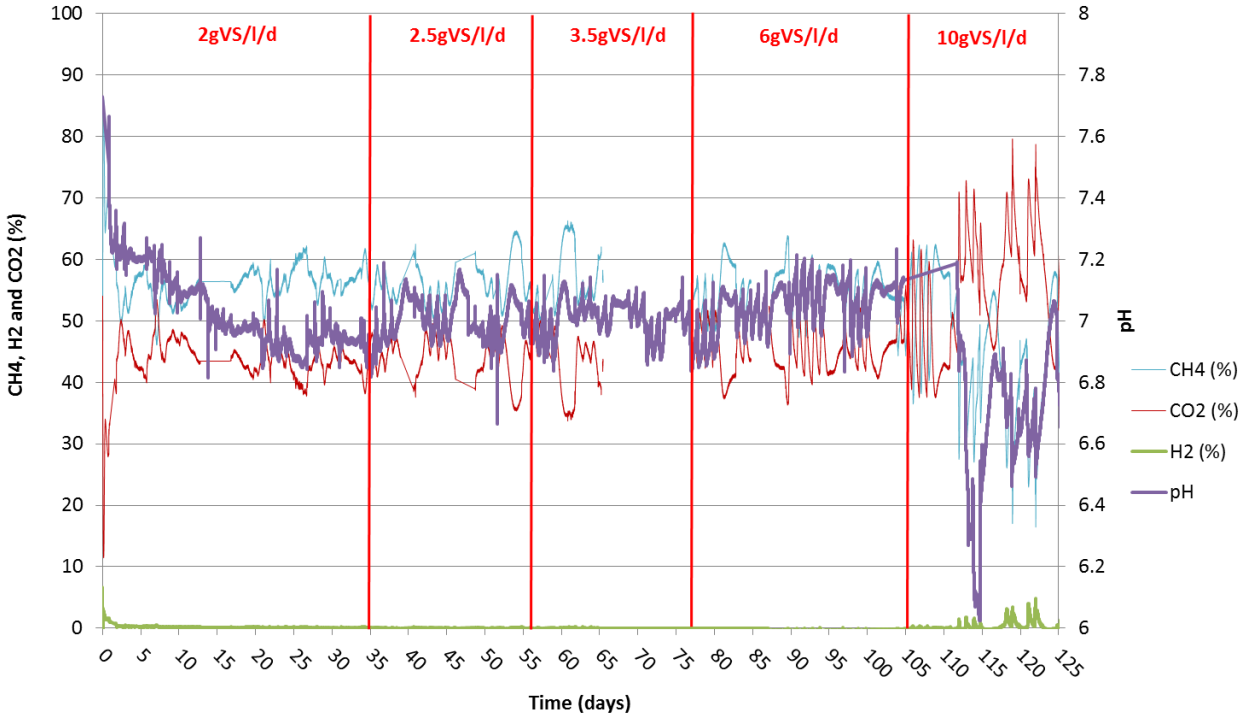

Figure 36: Evolution of the biogas content (measured online) and pH during semi-continuous digestion of DMS 2 at increasing OLR. The red lines represent the change in the feeding regime

4.1.1.4.2 Substrate removal and intermediary products evolution

The operational conditions of the reactor at the different OLRs investigated are summarised in Table 39. The results showed an increase of the concentrations of TS and VS in the reactor effluent with increasing OLR, from 1.94% up to 5.54%, and from 1.24% to 4.31% respectively, which suggested an accumulation of particulate material in the reactor. This started mainly with the feeding regime 4 (with the OLR of 6 gVS/l/d), and can be partially attributed to the short HRT of 16.69 days. The VS removal rate increased with increasing loading up to the OLR of 3.5 gVS/l/d and slowly decreased thereafter, and ranged between 60% and 83%. The comparison of the observed results is difficult as literature addressing continuous digestion of maize silage is scarce, and with a variety of operational conditions. The aforementioned study by Richards et al. (1991) reported a VS removal efficiency of 71.2% for an OLR of 8.25 gVS/l/d in a semi-continuous (3 times a week) reactor running under thermophilic conditions. The daily evolution of the TS, VS and tCOD and sCOD concentrations in the reactor can be seen in Figure 37. It is possible to observe for the higher loadings that the measured concentrations are more scattered that for the lower loadings, likely as a result of the higher particulate concentration in the digestate, which in turn can impact the representativity and homogeneity of the sampling method. In spite of this observation, TS, VS and COD followed a similar trend and strong linear correlation amongst them. Indeed, the equivalence factor ($i_{COD/VS}$) was determined to be 1.45 gCOD/gVS (R^2=0.88), which is the same value reported by Schlattmann (2011) also for maize silage.

It was possible to observe the formation of a crust layer in the upper part of the reactor, particularly with the two highest loadings. For the OLR of 10 gVS/l/d an important amount of foam was generated, likely as a result of the stripping of CO_2 with the high VFA production.

Table 39: Average operational conditions in semi-continuously-fed CSTR reactor digesting DMS 2

	OLR (gVS/l/d)				
	2	2.5	3.5	6	10
TVFA ($mgHAc_{eq}$/l)	12.46±8.8	163.63±107.1	342.03±16.6	384.81±210.1	5659.16±1804.7
TS of digestate(%)	1.94±0.1	1.77±0.0	1.73±0.1	2.77±0.2	5.54±0.2
VS of digestate (%)	1.24±0.1	1.15±0.0	1.18±0.1	2.14±0.2	4.31±0.1
sCOD (g/l)	2.61±0.37	2.01±0.02	2.63±0.04	3.30±0.23	16.71±5.2
VS removal (%)	60	73	83	81	74

The sCOD values ranged from 2.61 to 16.71 g/l from initial OLR of 2 gVS/l/d to 10 gVS/l/d, and almost doubled after the pH dropped to 5, due to the accumulation of VFA in the reactor. The most important accumulation of VFA was observed after changing the OLR to 10 gVS/l/d, with an average of 5.6 $g_{HAc\text{-}eq}$/l. The important increase in the VFA inversely mirrored a decrease in the CH_4 content in the biogas (as it can be seen in Figure 38). If looking at individual VFA concentration evolution (Figure 39), it is possible to observe that the acids that were more sensitive to OLR increases (for OLR of 3.5 gVS/l/d and higher) were the HPr and HBu. After increasing the OLR to 10 gVS/l/d, these acids accumulated up to a concentration of almost 5g/l in each case. This evolution is related to the peaks in H_2 content in the biogas mentioned above. Indeed, the appearance of HBu and HPr has been suggested to be the bacterial response to elevated H_2 concentrations (Mosey, 1983). As discussed in sub-chapter 2.2.4.2, it has been previously suggested to consider a HPr concentration of 1g/l, and a TVFA

concentration exceeding 4g/l as indicators of highly probable instable process. These two conditions were met 1 week after increasing the loading to OLR of 10 gVS/l/d.

The average ratio of TVFA to TIC (measured titrimetrically) was ranged from 0.1 up to 0.3 up to the loading of 6 gVS/l/d. This value started to increase when increasing the loading to 10 gVS/l/d, in response to the rapid and large increase in the concentration of different VFA. In spite of the buffering capacity addition, instabilities and signs of acidification were observed; with TVFA/TIC values peaking up to 1.78 in day 114.7 of digestion and never going below 1 (see Annex L). Lebuhn et al. (2008) suggested the TVFA/TIC ratio of 0.5 as indicative of process instability during semi-continuous digestion of maize and argued that HPr could not be used as the sole stability indicator, since low values could be obtained at severe process failure. The ratio obtained for the OLR of 10 gVS/l/d is above the value of 0.5 during the whole period, thus suggesting acidification. HPr concentration already started to peak for the OLR of 3.5 gVS/l/d to values close to 500 mg/l and to 700 mg/l for the OLR of 6 gVS/l, before the TVFA/TIC ratio went above 0.5. This highlights the role of the HPr concentration as an indicator of early process instabilities. The concentrations of HPr decreased considerably when the pH dropped to values close to 5 and the CH_4 production ceased. Therefore, while the HPr concentration seems to be a good indicator of pending instabilities, the TVFA/TIC ratio above 0.5 flags out ongoing acidification requiring correction. n-HBu concentration only peaked 10 days after the OLR was increased to 10 gVS/l/d, and thus does not seem to be an indicator of imminent instability but rather of ongoing acidification.

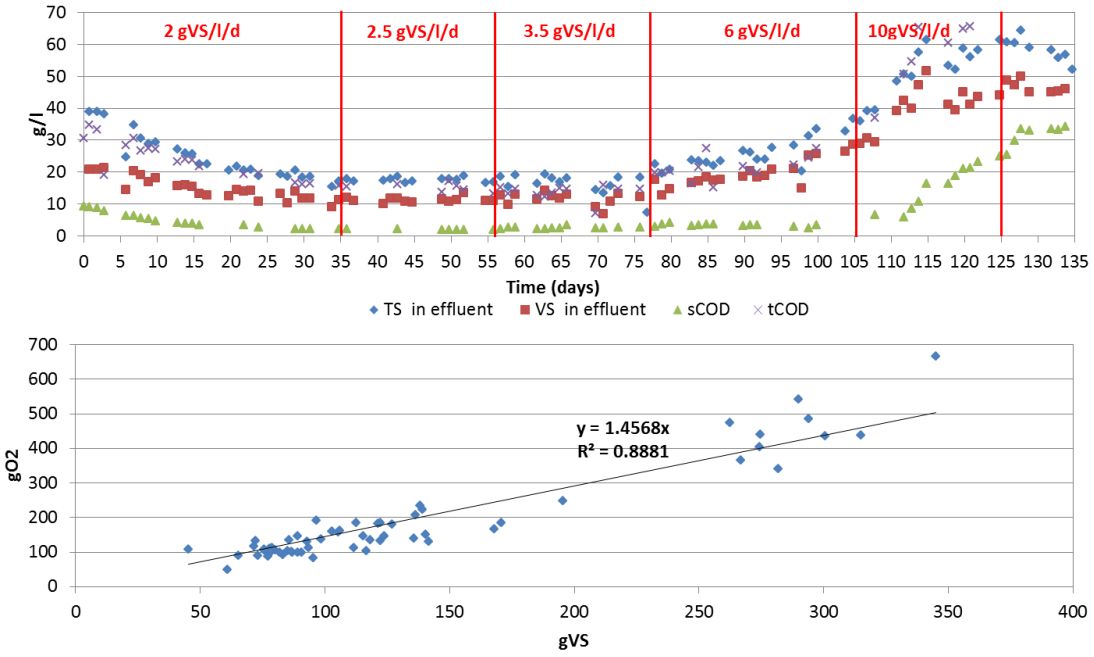

Figure 37: Evolution of TS, VS and COD during digestion of DMS 2 (top) and correlation between COD and VS (bottom)

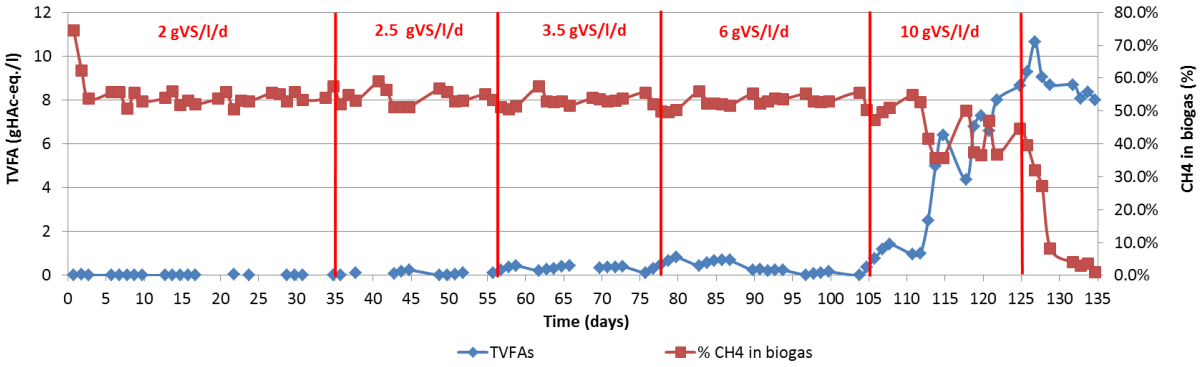

Figure 38: Evolution of TVFA (expressed as gHAc-eq./l) and the CH_4 content in the biogas during semi-continuous digestion of DMS 2 at increasing OLR

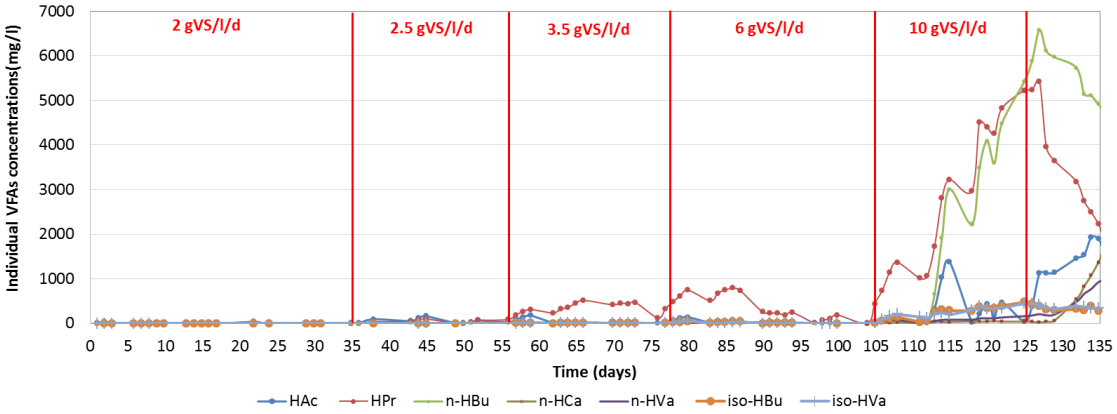

Figure 39: Evolution of the concentration of the individual VFA considered during semi-continuous digestion of DMS 2 at increasing OLR

NH_4^+-N, which is the predominant form of ammoniacal nitrogen in the reactor at the pH measured of 7, was always measured to be largely below levels reported as inhibitory (Chen et al., 2008).

4.1.1.4.3 Process kinetics during digestion of dried maize silage at increasing organic loading rates

In order to further investigate the influence of the OLR on the process dynamics, first-order kinetics (Eq. 27 in sub-chapter 3.6.1) were applied to describe the experimental data obtained for the 5 different loadings tested. As it was done for the semi-continuous digestion of grass silage, the equivalence factor ($i_{COD/VS}$) estimated for maize silage of 1.45 gCOD/gVS, was used to express in the same units (in gCOD/l) the daily added feedstock and the measured biodegradable material remaining in the reactor.

The calculated first-order rate constants for the different OLRs tested are presented in Table 40. An acceptable fitting between the experimental and calculated data was obtained for all calibrations. The k values calculated for the 2nd OLR was already half of that for the 1st OLR, which, for comparison, was 28% lower than for dried grass silage for the same OLR. The k constant values for the 3 last OLR were similar and almost half of that for the OLR of 2.5 gVS/l/d. This suggest that already a small increase in the OLR can have an important impact on the degradation rate for dried maize silage, and that even with the addition of buffering capacity and trace element solution, mono-digestion of dried maize silage in the long term can

be affected already at OLR below 2.5 gVS/l/d, in accordance with previous studies (e.g. Lebuhn et al., 2008). The estimated k values are in line with the calculated value by Richards et al. (1991) for mono-digestion of maize at an OLR of 8.25 gVS/l/d of 0.11d^{-1}, although the feeding and sampling conditions differ to those applied in the current research. Finally, the results also suggest a much higher impact of the overloading on the process kinetics for dried maize silage than for dried grass silage.

Table 40: Calculated first-order rate constants for the different OLRs tested during semi-continuous digestion of DMS 2

OLR (gVS/l/d)	k (d^{-1})	R^2
2	0.42	0.7
2.5	0.21	0.88
3.5	0.14	0.83
6	0.12	0.88
10	0.13	0.74

4.1.1.4.4 Analysis of correlations

The Pearson correlation matrix for different parameters is presented in Table 41. It can be seen that the OLR seems to have a statistically significant correlation ($p<0.01$) with all the variables considered, and that the linear relationship is particularly strong ($0.60<r<0.79$) with the BMP, the MPR, the CH_4 content, the sCOD concentration, the TVFA/TIC ratio, the total VFA concentration and the H_2S content. This detected correlation is negative in the case of the CH_4 content (i.e. it decreases with increasing OLR). This supports the previously stated observation that the maize silage seems to be more affected by the increase in the OLR than grass silage during semi-continuous digestion at the mesophilic range (see sub-chapter 4.1.1.3). Indeed, no linear correlation was identified for grass silage between the OLR and the SMP and CH_4 content for the tested range. The correlation is only moderate between the OLR and the VS removal.

A very strong linear correlation (>0.8) was detected between the CH_4 content and the TVFA/TIC ratio and the TVFA concentration (negative in both cases). The former highlights the relevance of the ratio TVFA/TIC to describe the performance of the process and the later the role that the VFA play in the stability and performance of the digester. Moreover, a very strong linear negative correlation was found ($p<0.01$) between the H_2S content and the CH_4 content in the biogas. Indeed, the H_2S content increased overtime with increasing OLR, in opposition to CH_4 content that decreased. As it has been explained in chapter 2, H_2S can have an inhibitory effect in the liquid phase. Moreover, the presence of sulphates can promote the growth of sulphate-reducing bacteria, which compete with methanogens for HAc and H_2, but also with the acetogenic bacteria for VFA. Indeed, a very strong linear correlation (and statistically significant with $p<0.01$) was found between TVFA and H_2S, which suggest that the high acid concentration could have promoted the growth of sulphate-reducing bacteria, which in turn could have contributed to the increase in the H_2S content both in the liquid and gas phases, thus disturbing the CH_4 production.

A strong correlation was also found between MPR and BPR, as it could be expected, and TVFA/TIC and TVFA concentration (given the fact that the alkalinity was kept relatively constant around 4g $CaCO_3$/l and the TVFA concentration increased with increasing OLR).

Table 41: Pearson matrix for the semi-continuous digestion of DMS 2 (Pearson correlation values for each pair of variables)

	OLR	BPR	MPR	CH_4	VS removal	sCOD	TVFA/TIC	TVFA	H_2S
OLR	1	.771**	.751**	-.660**	.407**	.786**	.721**	.730**	.712**
BPR		1	.961**	-.728**	.250	.425**	.569**	.479**	.510**
MPR			1	-.545**	.336*	.283	.373**	.303*	.339**
CH_4				1	-.014	-.799**	-.900**	-.856**	-.846**
VS removal					1	.025	-.052	.028	-.011
sCOD						1	.937**	.986**	.952**
TVFA/TIC							1	.960**	.973**
TVFA								1	.966**
H_2S									1

*. Correlation is significant at the 0.05 level (2-tailed).
**. Correlation is significant at the 0.01 level (2-tailed).

4.1.1.4.5 Diversity of methanogenic Archaea

In order to get a better insight into the evolution and prevalence of the different methanogenic Archaea during digestion at increasing OLR, samples were taken for feeding regimes 4 and 5 (OLR of 6 gVS/l/d and 10 gVS/l/d respectively) and examined by means of the real-time PCR technique by an external laboratory (Hochschule Offenburg, Germany). The polymerase chain reaction (PCR) is a technique to amplify DNA, using oligonucleotide primers and was further developed into real-time PCR (or q-PCR) to allow for quantifying DNA and RNA molecules. It can thus be applied to quantify the abundance of mayor Archaea groups, and has been applied, for example, by Nettmann et al. (2008) to analyse microbial diversity in commercial biogas plants.

Species-specific primers (see Annex U), were used to amplify the 16S rDNA gene of the archaeal micro-organisms. The primer sets used were for Archaea (ARC), Methanomicrobiales (MMB), Methanobacteriales (MBT), Methanosarcinaceae (Msc) and Methanosaetaceae (Mst). The results of the q-PCR analysis based of 16S rDNA primer is presented in Figure 40, in which the ordinate axis reflects the 16S rDNA copy number, which was detected in 1 ng of genomic DNA. The percentage calculations for the different taxonomic groups were carried out on basis of the detected copy number from Archaea.

An important shift can be observed in the methanogenic population considered for the OLR of 6 gVS/l/d. In the 91st day of digestion, the Methanosaetaceae, which are obligatory acetate degraders, were the dominant order (representing ca. 79% of the number of copies of Archaea). Methanomicrobiales was the second most abundant group. On the other hand, in day 97, the abundance of Methanosaetaceae decreased (to ca. 23%), while Methanosarcinaceae, which are facultative H_2 degraders at high acetate concentrations, and Methanomicrobiales, which are H_2 and CO_2 degraders, became the predominant orders (representing approximately 35% and 34% respectively). This is in line with recent observations by Nettmann et al. (2008) or Zhu et al. (2011). Given the fact that the acetate concentration was never high in the reactor for the OLR of 6 gVS/l/d, the aforementioned shift in Archaea population could be attributed to the presence of an inhibitory substance, such as H_2S. It is interesting to highlight that the abundance of Archaea decreased with increasing OLR, in relation with decreasing CH_4 content in biogas and SMP (see Table 38).

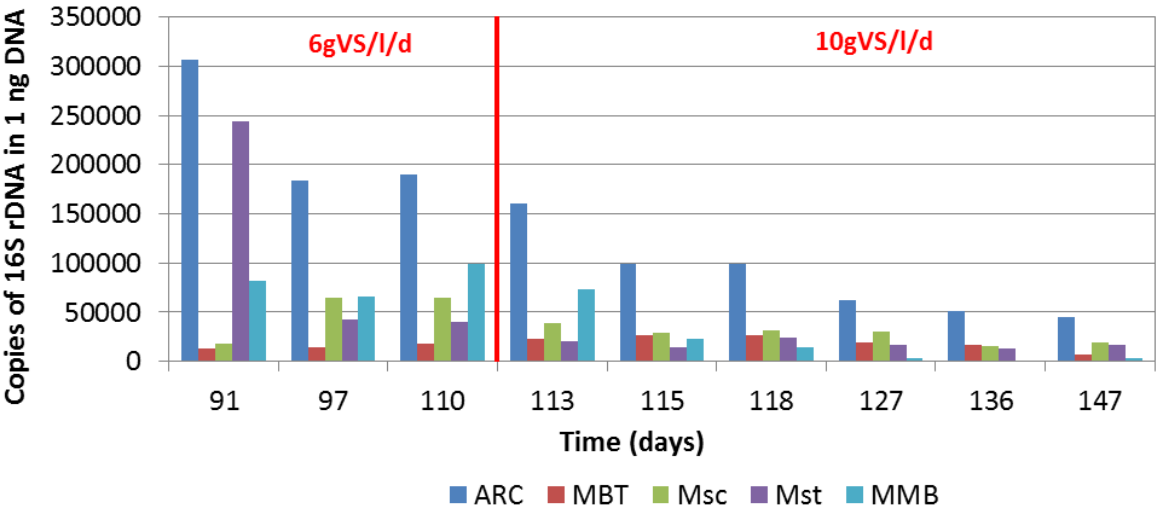

Figure 40: Results of the q-PCR for feeding regimes 4 (OLR of 6 gVS/l/d) and 5 (OLR of 10 gVS/l/d) during semi-continuous digestion of DMS 2

For comparison, the q-PCR technique was also applied to analyse the evolution of methanogenic groups during the batch degradation of grass silage (OL 6gVs/l). The results are presented in Figure 41. In this case it can be seen how the family Methanosaetaceae was the dominant order, representing ca. 74% of the Archaea in the beginning of the experiment, and 81% after 20 days of digestion. The second most abundant order was Methanomicrobiales, which abundance decreased during digestion. In any case, the concentration of acetate was never above 1g/l, nor inhibitory substances were detected. Therefore, it can be concluded that under the conditions of low acetate concentrations and lack of inhibitory substances, acetoclastic methanogens are the dominant group of Archaea.

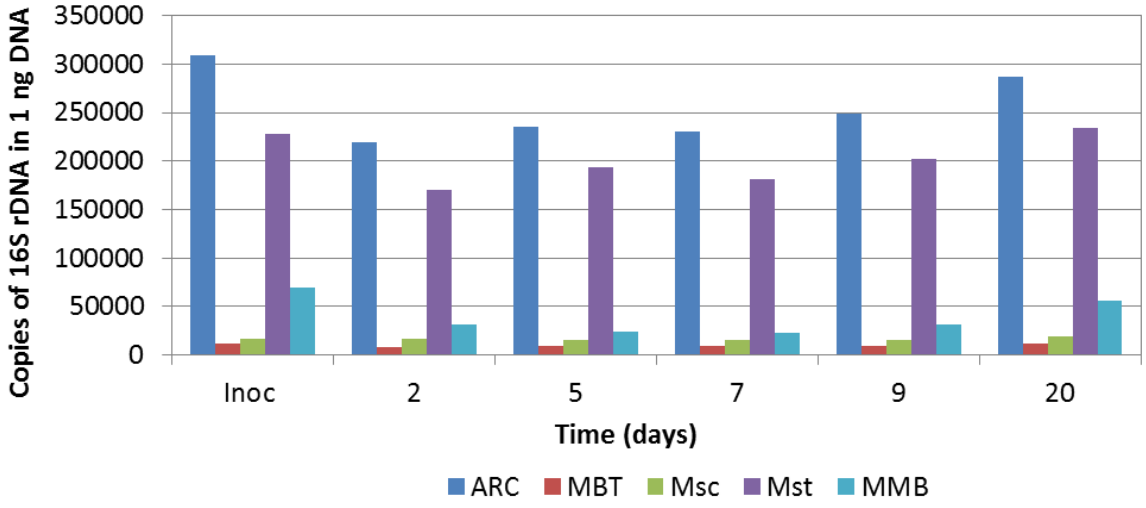

Figure 41: Results of the q-PCR analysis for a batch digestion of grass silage (GS 4) for an OL of 6gVS/l

IMPACT OF THE ORGANIC LOADING – MAIN RESULTS

*For batch digestion of grass silage, neither permanent inhibition nor cessation of the methane production was observed at any of the tested loadings (up to 46 gVS/l). Signs of instability were nevertheless detected for the two highest loadings (as denoted by the TVFA/TIC ratio or the HPr concentration), and also a worsen performance in terms of the methane yield (28% lower for the highest loading). The kinetics were also affected, with slower degradation.

*During semi-continuous digestion of cellulose, it was observed that a minor increase in the loading rate (from 1 to 1.5 gVS/l/d) could have a large impact on the solubility of cellulose and on the methane production, and thus on the process efficiency. In particular, the results suggest that an acetate concentration above 1.3g/l, which was reached with a loading of 1.5 g/l/d in the medium, could affect negatively cellulose hydrolysis.

*Results show that digestion of grass silage in one-stage CSTR was feasible and did not present any loading-induced inhibition up to an OLR of 4.7 gVS/l/d, with the addition of trace elements. While the volumetric methane production experienced an increase of 61%, the methane yield only decreased by 13% for the highest OLR. On the other hand, the estimated first-order rate constant decreased by 24% when increasing the loading from 1.9 to 4.7 gVS/l/d, which related with an accumulation of the organic material in the reactor.

*During semi-continuous digestion of maize silage, an increase from 2 to 3.5 gVS/l/d resulted in a 18.2% reduction in the methane yield. Signs of overloading-induced instabilities were observed at loadings of 6 gVS/l/d, which worsen for a loading of 10 gVS/l/d, with a consequent impact in the performance of the reactor. The effect of increasing loadings seemed to be larger for the semi-continuous digestion of maize silage than for grass.

*The acetotrophic methanogens seem to be predominant (representing up to 79% of the Archaea) during low acetate concentration and stable conditions both for batch and semi-continuous feeding conditions. Certain conditions (such as the accumulation of inhibitory substances) seem to trigger the shift to a hydrogenotrophic driven methanogenesis.

4.1.2 Impact of the feedstock characteristics

As discussed in chapter 2, the value of a substrate depends on its potential biogas yield and quality, i.e. methane content, which is determined by its composition in terms of the degradable fractions (both slowly and fast degradable fractions). The main objective of this part of the research was to investigate the influence of the feedstock characteristics, mainly in terms of the proteins, lipids, and carbohydrates content on the process performance and stability. To this end, the following aspects were addressed:

- The impacts of different mixtures of maize and grass silages (with different composition) during batch and semi-continuous experiments.
- The difference in the degradation dynamics for several carbohydrates that can be found during the anaerobic digestion of energy crops, both structural (i.e. cellulose), and non-structural carbohydrates (i.e. glucose and starch).

- For the same type of substrate (i.e. grass silage), how the differences in the composition, driven by different levels of maturity, can have an impact on the process performance during semi-continuous digestion.

Additionally, some experiments were carried out in order to get a better insight into the degradation of some intermediary products, to better determine their degradation kinetics (to be used for calibration and validation of the developed models). Experiments were implemented for sodium acetate and propionate for different loadings under batch feeding conditions. The results of these experiments are presented in Annex M.

4.1.2.1 Influence of the feedstock mixture on the process performance during co-digestion of maize and grass under batch and semi-continuous feeding conditions

Given that in most agricultural biogas plants the feedstock is generally a mixture of different substrates, data on optimal mixture ratios in terms of CH_4 yield is still necessary, as well as information on possible synergetic effects in co-digestion.

Some recent publications have reported on the co-digestion of manures and various agricultural by-products (Pagés Díaz et al., 2011; Cavinato et al., 2010; Fantozzi and Buratti, 2009). As regards energy crops, there are still very few studies examining different mixing ratios during co-digestion of energy crops (Bauer et al., 2009), and in most cases involve co-digestion with manures (Comino et al., 2010; Lehtomäki et al., 2007; Cuetos et al., 2011). Indeed, knowledge is limited regarding the process dynamics and stability during co-digestion in general and the co-digestion of maize and grass silages in particular.

The aim of this part of the research was to get a better insight into the influence of the feedstock mixture of maize and grass silages during co-digestion on the biogas yield and composition as well as on the process dynamics, both during batch and semi-continuous digestion.

Firstly, a BMP test was performed for all the mixtures considered and the grass and maize silages alone (GS 1 and MS 1) in an AMPTS system (Bioprocess Control AB, Sweden), as described in sub-chapter 3.3.2. The SIR was kept at 0.5 for all mixtures tested in this assay. Subsequently, batch experiments were implemented for some of the mixtures to monitor in detail some process parameters (see sub-chapter 3.4.1 for more detailed description of the set-up). Finally, a semi-continuous experiment was carried out for 90 days with dried (at 60°C) grass silage (DGS 4) and maize silage (DMS 2) in order to investigate possible effects for this feeding mode and the same OLR (see sub-chapter 3.4.2.4 for detailed description on the experimental set-up). Although the silages used were different for the batch and semi-continuous experiments, the difference between the two silages used each time were similar (in terms of the composition), and therefore the comparison remains valid in both cases.

4.1.2.1.1 Methane production

The SMP values after 27 days of digestion for the maize and grass silage (MS 1 and GS 1) and the 3 tested mixtures applied in the test are presented in Figure 42. The measured SMP for the mono-digestion trials are within the range reported in literature for maize and grass silages (Bauer et al., 2009; Weiland, 2010; Mähnert et al., 2005; Amon et al., 2007). Mono-digestion of grass silage presented the higher SMP (7% higher than for mono-digestion of maize). As

regards co-digestion, mixture 3 (30%MS1/70%GS1), with the higher proportion of grass in the feedstock, presented the best performance in comparison with mono-digestion of maize (SMP value 56% higher).

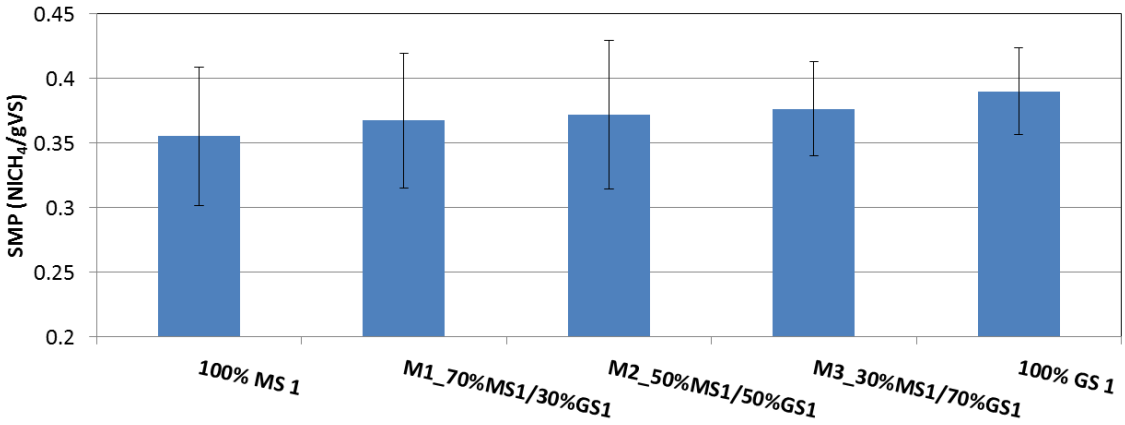

Figure 42: SMP for each feedstock tested (MS 1, GS 1 and 3 co-digestion mixtures) during batch digestion

The results suggest a positive linear correlation between the proportion of grass in the feedstock VS added and the SMP value. Figure 43 shows the final SMP for the individual silages and the 3 mixtures against VS concentration from grass silage in the feedstock. A strong linear relationship can be observed (R^2=0.98). This can be explained by the composition of each substrate used. The amount of proteins, with a higher CH_4 potential, is almost 2 times higher in the case of the grass silage in comparison to maize silage, which could explain the higher yields. The amount of carbohydrates (which represent the largest fractions of the total VS) is 1.12 times higher in the case of maize silage, while the proportion of lipids, with the higher CH_4 potential, is 3% in both cases.

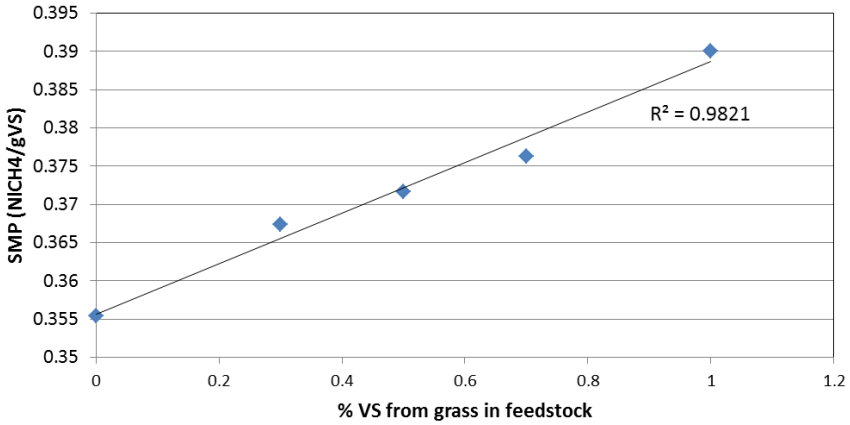

Figure 43: SMP for each feedstock tested vs the proportion of VS from grass for batch digestion

Regarding the batch experiments in 1 litre reactors, Figure 44 shows the cumulative SMP and the SMPR over time for maize silage and mixtures M1, M2, and M4. The values of cumulative methane after 17 days of digestion were, in increasing order, 0.34 Nl_{CH4}/gVS (MS 1), 0.35 Nl_{CH4}/gVS (M1_70%MS1/30%GS1), 0.35 Nl_{CH4}/gVS (M2_50%MS1/50%GS1), and 0.37 Nl_{CH4}/gVS (M4_40%MS1/60%GS1).

Although at this stage of the digestion (17 days) was not possible to observe any clear correlation between the SMP and the grass content in the feedstock for these experiments,

the evolution of the accumulated methane showed better yields for the co-digestion mixtures compared to mono-digestion of maize. On the other hand, it was observed that the co-digestion trials had lower SMPR than the maize silage alone, with values ranging from 77.80 $mlCH_4/gVS/d$ (mixture M1) to 86.77 $mlCH_4/gVS/d$ (M4), in comparison with 97.49 $mlCH_4/gVS/d$ for the mono-digestion of maize. A rapid increase in the daily methane yield (i.e. SMPR) at the beginning of each experimental trial was observed, reaching a maximum within the first 48 to 72h in the case of the co-digestion trials and during the first day for the maize trial. The measured SMPR also showed that while in the case of the mono-digestion trial with maize, after the peak the daily methane yield decreases rapidly, in the case of the co-digestion assays with the different mixtures this decline took place gradually. This can be explained by the fact that maize contains higher concentrations of easily biodegradable fractions, which are immediately assimilated by the bacteria. On the other hand, grass silage has generally higher slowly available fractions which are mostly gradually released after hydrolysis.

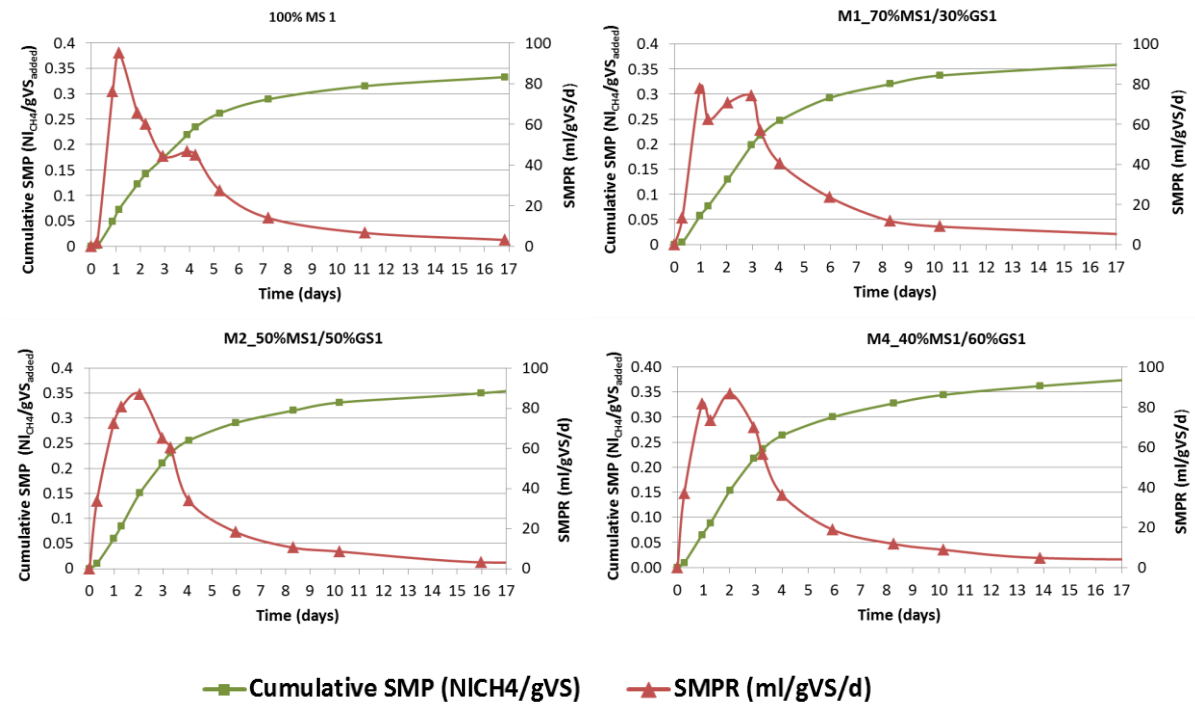

Figure 44: Cumulative SMP and SMPR for batch experiments in 1 litre reactors maize silage (MS 1) and co-digestion mixtures with grass silage (GS 1)

If considering semi-continuous digestion of grass and maize silage, it is possible to see certain deviation from what it could be expected if considering the observations made for the batch experiments (for GS 1 and MS 1 and their different mixtures).

The final SMP achieved after 30 days of digestion during the BMP test for the dried maize silage (DMS 2) and dried grass silage (DGS 4) used in the experiment were 0.34 Nl_{CH4}/gVS and 0.35 Nl_{CH4}/gVS respectively, thus 3.2% smaller for the dried maize silage (as it happened with GS 1 and MS 1). The average biogas performance for the different mixtures during semi-continuous digestion is presented in Table 42. It can be observed that the highest SMP values are for mono-digestion of dried maize silage (7.3% higher than for mono-digestion of dried grass silage), as it can be seen in Figure 45. The results obtained for the mono-digestion of dried maize silage at an OLR of 2 gVS/l/d (Table 42) are very similar to those obtained during

the experiment to analyse the impact of the OLR during semi-continuous digestion of dried maize silage for the same OLR (Table 38), for which the same maize was used (DMS 2). This highlights the good replicability of the results for the same operational conditions.

The SMP decreased with increasing proportion of dried grass silage in the feedstock. This trend seemed to be the opposite of that observed for batch trials. Only the CH_4 content increased with increasing proportion of dried grass silage ($p<0.05$). The trend for the MPR and BPR was not clear ($p>0.05$). Annex J summarises the statistical analysis for the differences between the means of the mixtures tested during semi-continuous digestion.

It is important to highlight that the values obtained for the feeding regime 3 (mixture 3: 30%DMS2/70%DGS4) seemed to be too low to fit the observed tendency (Table 42). A possible explanation could be the likely low concentration of trace elements after 73 days of digestion. At that point, a trace element solution was added and the average values of the biogas performance parameters for the final regime, such as the BPR, fit again well the trend (see Figure 45).

As it happened with silages used in the batch experiments for co-digestion, the dried grass silage used in the experiments (DGS 4) has double the amount of proteins, with a higher methane potential but slower degradation, and 23% more of cellulose. Therefore, although the potential was larger for grass silage, it was achieved later due to a higher content of slower degradable material. To achieve this potential might not have been possible under semi-continuous conditions, given the HRT of 16.69 days, likely too short.

Therefore, the satisfactory methane potential and content that can be attained when using grass silage as mono-substrate or as co-substrate might not be attainable in large agricultural biogas plants, which usually applied semi-continuous digestion. Additionally, other possible issues related to the use of grass silage in the long term previously highlighted, such as the formation of a scum layer, and its propensity to float have also to be taken into consideration, and be weighed against the advantages of using this type of substrate (such as the fact that it is a perennial crop widely available in certain climatic areas in Northern and Central Europe and it requires low input for growth).

Table 42: Average performance in semi-continuously-fed CSTR reactor with different grass to maize silage mixture ratios (for DGS 4 and DMS 2) for a constant OLR of 2 gVS/l/d and a HRT of 16.69 days

	100%DMS 2	M2 (50%DMS 2/50%DGS 4)	M3 (30%DMS 2/70%DGS 4)	100% DGS 4
SMP (Nl/kgVS added)	329.06±0.026	316.47±0.001	290.47±0.014	305.17±0.001
VMPR ($NlCH_4$/l/d)	0.49±0.039	0.50±0.003	0.43±0.008	0.55±0.061
MPR ($NlCH_4$/d)	3.24±0.26	3.34±0.06	2.87±0.06	3.66±0.41
CH_4 content (%)	53.31±0.02	54.16±0.35	55.41±0.04	63.24±0.08
% of BMP value (%)	96.78%	n.d.	n.d.	84.77%
n.d. not determined				

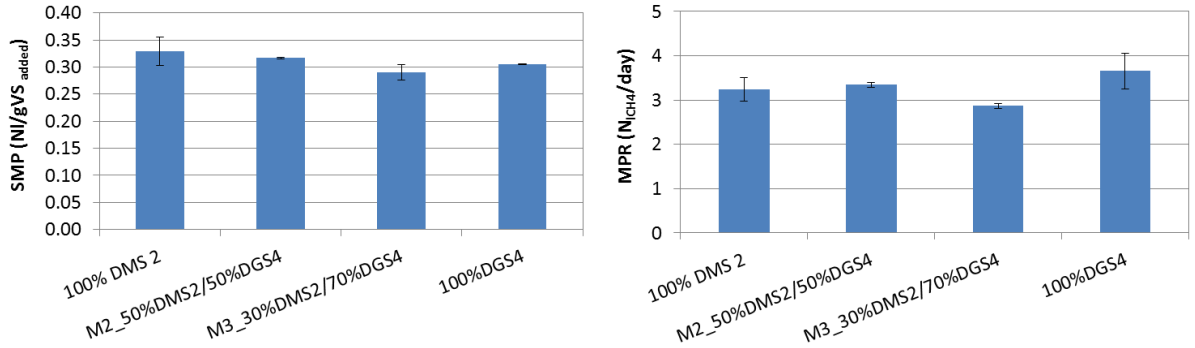

Figure 45: SMP for each feedstock tested (DMS 2, DGS and 2 co-digestion mixtures) during semi-continuous digestion (HRT of 16.69 days)

4.1.2.1.2 Control parameters evolution during co-digestion

Different control parameters were monitored over time for the batch trials (in 1 litre reactors) and the semi-continuous feeding experiment for selected mixtures to get a better insight into the co-digestion process under these feeding conditions.

The evolution of the TVFA (sum of C2 to C5 VFA) and sCOD, for batch mono-digestion of maize silage (MS 1) and co-digestion mixtures M2 (50%MS1/50%GS1), M3 (30%MS1/70%GS1), and M4 (40%MS1/60%GS1) can be found in Annex N. sCOD initially increased in the batch trials as a result of the solubilisation of the substrate and subsequent acidification and then decreased as digestion progressed. Such decrease was slower in the case of the mixture M3 (30%MS1/70%GS1), which could be explained by the higher protein content in this mixture. It can be observed that this parameter (sCOD) followed a similar trend to that of the TVFA during digestion, with maximums measured at the same time of digestion. At this time, the TVFA accounted for 41.2%, 58.3%, and 60.7% of the sCOD for the mixtures M3 (30%MS1/70%GS1), M2 (50%MS1/50%GS1), and M4 (40%MS1/60%GS1) respectively. The drops after the maximum concentration in VFA corresponded also to the times of the peaks in the SMPR.

The variation of pH over time for the different feedstock tested can also be found in Annex N. The pH values ranged from 7.85 to 7.3 during digestion. In spite of the rapid hydrolysis and VFA formation during the first two days of digestion, the appropriate buffering capacity in the reactors for all mixtures trials (from 8,750 to 13,950 mg$CaCO_3$/l) allowed maintaining the pH of the digester above 7.0 and within the optimal range for methanogenic bacteria. As regards the co-digestion stability, the TVFA/TIC ratio increased for all mixtures the first two days of digestion, but went above the 0.4 limit value only in the case of the mixtures M2 (50%MS1/50%GS1) and M4 (40%MS1/60%GS1), because of the lower initial buffering capacity in the inoculum.

For the co-digestion mixtures investigated under semi-continuous feeding conditions, the operational conditions of the reactor for the different feeding regimes are summarised in Table 43. The evolution of the TS, VS and COD concentrations in the reactor can be seen in Figure 46 (top figure). Accumulation was not observed in the reactor for any of the feeding regimes considered (with an OLR of 2 gVS/l/d). The VS removal rate increased, nevertheless, with increasing proportion of dried grass silage in the feedstock, and ranged between 46% and

64%. A strong linear correlation was found between COD and VS, as it can be seen in Figure 46 (bottom). The equivalence factor was determined to be 1.60 gCOD/gVS (R^2=0.88).

Table 43: Average operational conditions in semi-continuously-fed CSTR reactor for the different mixtures of DMS 2 and DGS 4 for an OLR of 2 gVS/l/d

	Mixture			
	100%DMS 2	M2 (50%DMS 2/50%DGS 4)	M3 (30%DMS 2/70%DGS 4)	100% DGS 4
TVFA (mgHAc$_{eq}$/l)	6.10±1.4	3.83±0.5	2.87±1.1	23.28±23.8
NH_4^+-N (mg/l)	1779.17±823.32	433.00±91.10	266.79±46.46	180.25±9.81
TN (mg/l)	1789.33±336.67	1262.78±103.83	807.5±18.50	797±21.18
TS of digestate (%)	3.23±0.8	1.83±0.2	1.76±0.0	1.80±0.1
VS of digestate (%)	2.20±0.47	1.32±0.10	1.24±0.01	1.20±0.04
sCOD (g/l)	4.49±0.98	2.15±0.03	2.62±0.26	2.98±0.05
Proteins	4.95±0.18	4.90±1.22	3.88±0.67	3.22±0.09
VS removal (%)	46.56±5.82	60.67±0.37	63.38±0.31	64.18±0.18

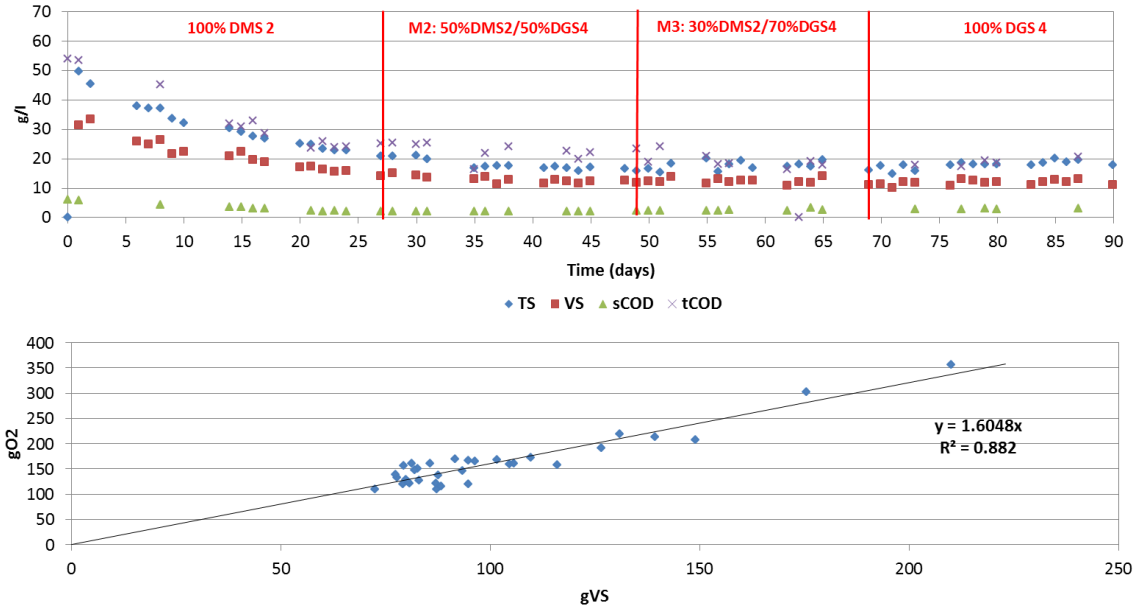

Figure 46: Evolution of TS, VS, tCOD and sCOD during semi-continuous digestion for the different mixtures of DMS 2 and DGS 4 (top) and correlation between COD and VS (bottom) for an OLR of 2 gVS/l/d

The average sCOD was 4.49 g/l for the mono-digestion of dried maize silage (DMS 2). The lower average sCOD was measured for the mixture 2 (50%DMS2/50%DGS4) (i.e. 2.15 gCOD/l), and increased with increasing content of dried grass silage up to an average value of 2.98 gCOD/l (for mono-digestion of DGS 4), thus suggesting a small increase of certain soluble materials. The VFA concentrations were low and not exceeding in any case concentrations above 0.05 gHAc-eq/l. It is worth mentioning a small peak (below 0.1g/l) of HPr and n-HBu detected for several days after the 80th day of digestion (for mono-digestion of dried grass silage), which is reflected in the high standard deviations estimated for that period. The average ratio of TVFA to TIC (measured titrimetrically) was below the critical limit of 0.4 for the 90 days of duration of the experiment. The TN did not increase with increasing share of grass in the feedstock as it could have been expected (because of higher protein content). Neither

the protein nor the NH_4^+-N concentrations increased. In fact, all N-containing components decreased overtime, suggesting a good degradation of the proteins in the substrate. The related and complementary summary of the experimental data for semi-continuous co-digestion of maize and grass silages can be found in Annex N.

4.1.2.1.3 Process kinetics during co-digestion of grass and maize silages

In order to further investigate the influence of the feedstock mixture ratio on the hydrolysis dynamics, first-order kinetics (Eq. 26 in sub-chapter 3.6.1.2) were applied to fit the experimental cumulative methane production obtained from the batch tests for grass and maize silages and mixtures M1 (70%MS1/30%GS1), M2 (50%MS1/50%GS1), and M3 (30%MS1/70%GS1). The first-order rate constant was also estimated for the semi-continuously fed reactor to the different mixtures applying Eq. 28 in sub-chapter 3.6.1.2. It is important to highlight that the grass and maize silages used in the batch and semi-continuous experiments were different (GS 1 and MS 1 and DGS 4 and DMS 2 respectively), but the differences amongst the mixtures used in each case are comparable.

The first-order rate constants thus calculated are presented in Table 44. The obtained values for the batch co-digestion trials showed that the higher the proportion of grass in the mixture (i.e. the higher the content of proteins, and structural fibrous carbohydrates), the slower the degradation, with the exception of mixture M3 (30%MS1/70%GS1). The same observation can be made for the first-order constants calculated for the semi-continuous experiments. These results support the analysis performed in the previous sub-chapters. A good fitting (R^2) between the experimental and calculated data was obtained for all calibrations.

Moreover, the obtained values of the first-order rate constants presented in this sub-chapter are very similar to those already presented for other experiments running with the same substrates and operational conditions. For example, the value obtained for the semi-continuous digestion for dried maize silage (DMS 2) with a loading of 2 gVS/l/d was 0.42 d^{-1}, which is the same to the value estimated for the experiment analysing the impact of the OLR during semi-continuous digestion of the same dried maize silage (DMS 2) and the same operational conditions, but with a different WVs. This highlights the good repeatability of the estimations presented here for the first-order constant. Finally, the goodness of the fit was better when using Eq. 26 and the CH_4 experimental data for calculation of the first-order rate constant.

Table 44: Calibrated first-order rate constants for the different mixtures of grass and maize silages for the batch (using Eq. 26) and semi-continuous (using Eq. 28) experiments

	Batch experiments (OL=12gVS/l)		Semi-continuous experiments (OLR=2gVS/l/d)	
Mixture	k (d^{-1})	R^2	k (d^{-1})	R^2
100% MS	0.22	0.98	0.41	0.96
M1_70%MS/30%GS	0.20	0.98	-	-
M2_50%MS/50%GS	0.19	0.98	0.32	0.86
M3_30%MS/70%GS	0.20	0.98	0.30	0.9
100% GS	0.17	0.97	0.29	0.89

4.1.2.1.4 Analysis of correlations

The Pearson correlation matrix for different parameters is presented in Table 45 for the experimental data of the semi-continuous experiment. It can be seen that the mixture (in terms of the share of grass in the total VS added with the feedstock, from 0 for mono-digestion of maize silage to 1 for the mono-digestion of grass silage) seems to have a statistically significant ($p<0.01$) strong positive linear correlation ($0.6<r<0.79$) with the VS removal and the CH_4 content in the biogas. In spite of the higher protein content in the grass silage than for the maize silage (double on average), the higher share of grass in the feedstock did not result in a higher concentration of proteins nor NH_4^+-N in the digestate with increasing grass share in the feedstock. This suggests that with the applied operational conditions (no recirculation and OLR of 2 gVS/l/d) and in spite of the increasing N content in the feedstock, the system is capable of solubilising and metabolise the N components, which decrease overtime, also as a result of dilution.

As it was observed for the semi-continuous experiments previously described, statistically significant ($p<0.01$) strong linear correlation ($r>0.8$) was found between BMP and MPR, as it was expected.

Not significant relation was found between the TVFA/TIC ratio and the TVFA concentration with other parameters, as in both cases, the measured values were always below critical values and no sign of instability was identified.

Table 45: Pearson matrix for the semi-continuous digestion of DMS 2 (Pearson correlation values for each pair of variables)

	BMP	MPR	CH_4	VS removal	sCOD	NH_4	TN	TVFA/TIC	TVFA	Mixture
BMP	1	.997**	-.393*	.022	-.212	-.104	-.168	-.036	-.060	.054
MPR		1	-.326*	.062	-.205	-.160	-.227	-.033	-.046	.115
CH_4			1	.495**	.162	-.607**	-.471	-.014	.197	.739**
VS removal				1	-.503*	-.956**	-.876**	.094	.164	.704**
sCOD					1	.466*	.081	-.256	.255	.105
NH_4						1	.968**	-.156	-.279	-.862**
TN							1	-.049	-.311	-.812**
TVFA/TIC								1	.006	-.027
TVFA									1	.342
Mixture										1

*. Correlation is significant at the 0.05 level (2-tailed).
**. Correlation is significant at the 0.01 level (2-tailed).

4.1.2.2 Kinetic analysis of the anaerobic digestion of different carbohydrates

The main objective of the experiments described in this sub-chapter was to investigate and compare the degradation kinetics of different carbohydrates that are present during anaerobic digestion of energy crops, namely the glucose (a monosaccharide), starch (a non-structural polysaccharide) and cellulose (a structural polysaccharide), under the same experimental and operational conditions. To this end, three sets of batch anaerobic experiments were carried out in parallel in 1 litre PET reactors, which ran at mesophilic condition, as described in sub-chapter 3.4.1. Each experimental series counted with 10 reactors with 750g of inoculum and the appropriate amount of substrate to achieve the same OL of 8 gVS/l. The characteristics of the three carbohydrates used as substrate for each experimental set are presented in Table 10, in sub-chapter 3.2.1.

4.1.2.2.1 Methane production

The final SMP values obtained for the glucose and corn starch were very similar (0.285 Nl_{CH4}/gVS and 0.280 Nl_{CH4}/gVS respectively), and approximately 15% smaller than that observed in the cellulose trial (0.329 Nl_{CH4}/gVS).

Taking into account the molecular formula of each saccharide considered, the ThSMP was calculated in each case, and compared with the experimental data (Table 46). The recovery rates (without considering the 10% losses during conversion) were overall satisfactory, particularly in the case of cellulose. Corn starch, with the same ThSMP than cellulose, was the saccharide showing the worst recovery.

Clear differences were observed for the evolution of the biogas and methane production for glucose, starch, and cellulose, resulting from their different bio-availability and kinetics. Indeed, while the added glucose was readily available for bacteria, and its degradation started without delay, in the case of starch and cellulose, degradation began after a lag time of 1 and 2 days respectively. These differences are illustrated in Figure 47, showing the evolution of the CH_4 content in the biogas, the SMP and the SMPR for the three saccharides. Glucose presented its maximum daily SMP (i.e. SMPR) within the first day (0.21 Nl_{CH4}/gVS/d), while in the case of starch and cellulose this peak was not observed until the 3rd day of digestion, with values of 0.091 Nl_{CH4}/gVS/d and 0.081 Nl_{CH4}/gVS/d respectively. It is also interesting to highlight that for the cellulose and glucose trials, two peaks were observed for the SMPR in days 3 and 4, and 1 and 2 respectively.

Table 46: Theoretical and experimental final SMP for glucose (7 days of digestion), corn starch (14 days of digestion), and cellulose (15.8 days of digestion) for an OL of 8 gVS/l

	$NlCH_4$/gVS		
	ThSMP	Experimental SMP	Recovery (%)
Glucose	0.373	0.285	76%
Starch	0.414	0.280	69%
Cellulose	0.414	0.329	79%

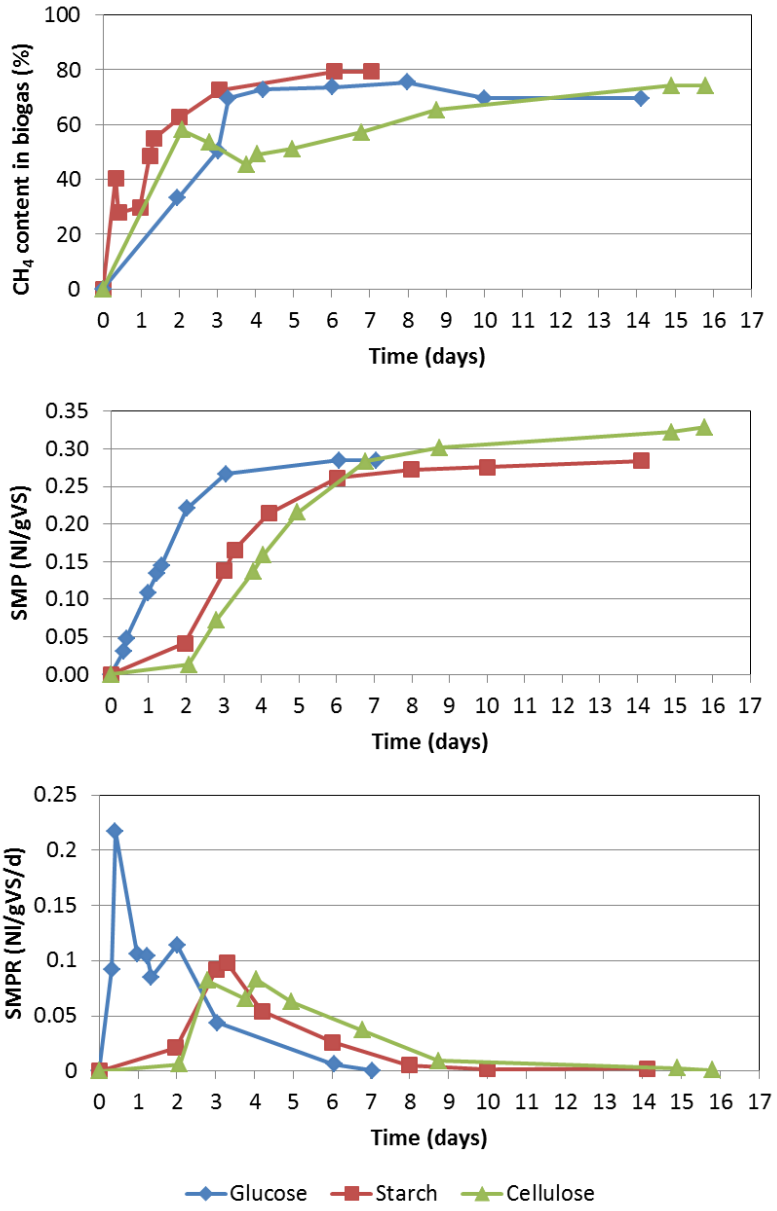

Figure 47: Evolution of the CH_4 content in the biogas (top), SMP (centre) and the SMPR (bottom) for the fermentation of glucose, corn starch, and cellulose (OL of 8 gVS/l)

4.1.2.2.2 Degradation of intermediary products and process stability

The monitored concentrations of VS and saccharides (as measured with the Anthrone method) allowed to closely investigate the evolution of the polysaccharides and the hydrolysis-resulting monosaccharides concentration during the digestion of the three saccharides. The evolution of these parameters is displayed in Figure 48.

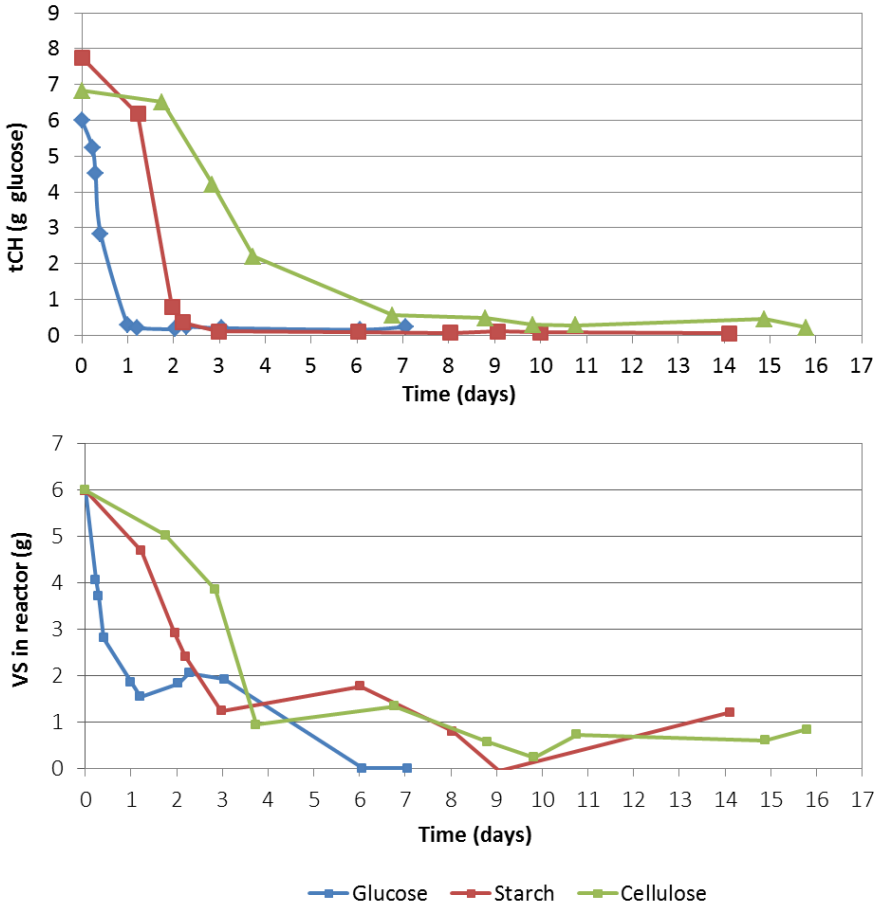

Figure 48: Evolution of the total mass of carbohydrates (expressed as g glucose) (top) and mass of VS (bottom) for the fermentation of glucose, corn starch and cellulose (OL of 8 gVS/l)

It can be seen in these figures that the uptake of glucose was quite fast, particularly within the first day of digestion, as it could be expected given its high bio-availability. Moreover, substrate uptake seemed to be faster for corn starch than for cellulose, with most of the degradation taking place between day 1 and 2 of digestion, while for cellulose was mainly from days 2 to 4. It is interesting to highlight some limitations of the monitoring plan. While in the case of glucose, and given the expected fast degradation, samples were taken every 2-3 hours during the first day and also quite regularly the second day, for starch the sampling was less regular, and turned out not to be sufficient to fully monitor the substrate uptake between days 1 and 2. It is worth mentioning also the absence of changes in the soluble monomers concentration (resulting from hydrolysis) for the starch and cellulose trials. Indeed, not major changes were observed overtime, thus suggesting that the monomers were quickly consumed once formed after hydrolysis. Sampling more regularly could have improved the monitoring of this parameter. Also, in opposition to what it could have been expected, a small decrease was observed in the concentration of monosaccharides during the first day after the lag phase. This same phenomenon was also observed in data reported by Noike at al. although no possible explanation is proposed (Noike et al., 1985). One possible explanation could be the formation and use of exopolysaccharides (EPS). Indeed, glucose is a carbon source for EPS production, which has been found to be stimulated by providing excess carbohydrates.

As regards the evolution of the NH_4^+-N, its concentration did not presented any significant change during the digestion of the three saccharides, with very similar values for the three trials.

The most abundant acids during the degradation of the 3 saccharides were HAc and HPr, while HBu and HVa were measured in very small concentrations. The peak concentrations for HAc and HPr for the glucose trial were high with values of 1.4g/l and 0.7g/l reached on days 1 and 2 respectively. In the case of the starch trial, HAc and HPr presented also high peaks but lower (0.74 g/l and 0.5 g/l respectively) on day 2. Finally, for the cellulose experiment, a peak seemed to be missing, as it should reach values similar to that of starch but in days 3 to 4 of digestion. The evolution of the VFA along with other monitored parameters is illustrated in Annex O.

4.1.2.2.3 Process kinetics

One of the main interests of the current set of experiments was the investigation of the degradation dynamics of different types of saccharides, which can be present during the anaerobic digestion of lignocellulosic material. The overall goal was to acquire experimental data to analyse the feasibility and the need of the definition of different hydrolysis rates for slowly and fast degradable carbohydrates. The first-order rate constant for each carbohydrate was calculated with Eq. 26 (sub-chapter 3.6.1.2) using nonlinear least-squares curve fitting with Microsoft Excel Solver. In Table 47, the values thus calculated are presented. The observed values are congruent with the results previously presented. They showed that the degradation of glucose was twice faster than starch degradation and more than 3 times faster than cellulose degradation. Therefore, using different hydrolysis values for the different carbohydrates could contribute to better fit experimental data.

Table 47: Calculated first-order rate constants for the different saccharides digested under batch conditions with an OL of 8 gVS/l

	k (d^{-1})	R^2
Glucose	0.58	0.98
Starch	0.26	0.92
Cellulose	0.17	0.91

4.1.2.3 Impact of the grass composition on the biogas performance during semi-continuous digestion

The impact of using as feedstock grass silages with a different composition on the process performance and dynamics was also analysed for semi-continuous digestion operation. Two different silages (dried at 60°C), DGS 2 and DGS 3, were used to this end (the main characteristics of these substrates are summarised in Table 10, in sub-chapter 3.2.1), keeping the OLR and HRT constant. The different grass composition was partly produced by different levels of maturity.

Values related to the system performance in terms of the biogas production (SMP, CH_4 content in the biogas, and MPR) are presented in Table 48. The evolution of the SMP for the two dried grass silages considered is shown in Figure 49. It is possible to observe in this figure the weekly variations, for both grass silage used, as a result of the feeding regime applied (daily feeding five times per week), with the lower values measured in the beginning of the week (on Mondays), after the 2 days without feeding.

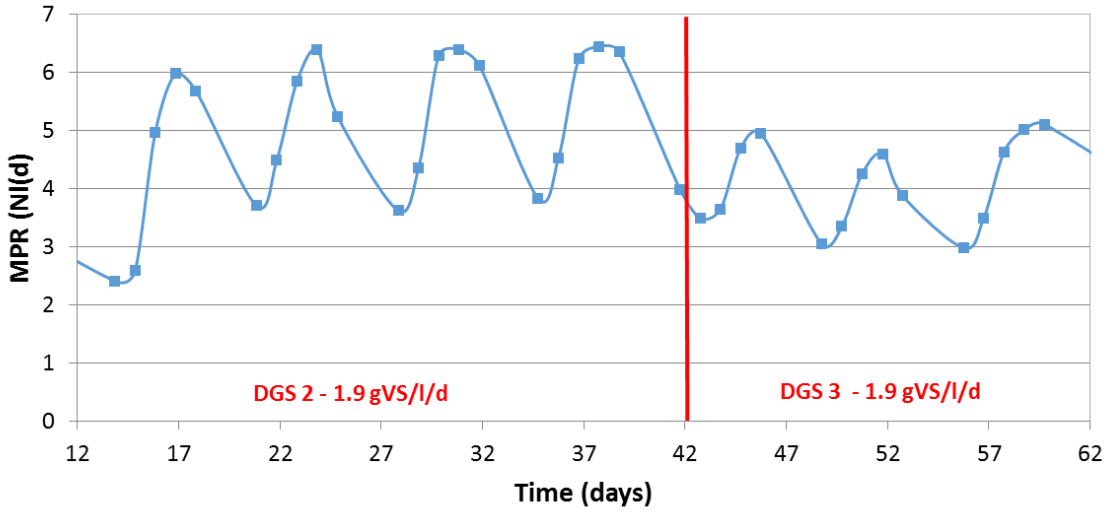

Figure 49: Evolution of the MPR for dried DGS 2 (until day 42 of digestion) and DGS 3 (from day 43 of digestion onwards)

The average values for these parameters showed a significant difference in the SMP, the MPR (Nl_{CH4}/d) and the methane composition in the biogas in response of the system to the characteristics of both dried grass silage used (with $p < 0.05$ with ANOVA test for CH_4 content and with Kruskal-Wallis test for SMP, SBP and MPR). Indeed, the SBP and SMP were 24% and 22% higher respectively in the case of DGS 2 in comparison to DGS 3. The same tendency was observed for the MPR (30.5% higher than for DGS 3). These variations were likely produced by the different characteristics of both grass silages. DGS 2, for example, had 26% more proteins per gram VS than DGS 3, with a slower degradation, but higher methane potential. Also, DGS 3 had 32% more fibrous carbohydrates than DGS 2, with 20% higher cellulose content and 40% higher lignin contents.

Table 48: Summarised biogas results in the semi-continuously fed reactor when using DGS 2 (day 0 to 42) and DGS 3 (from day 43 onwards) for an OLR of 1.9 gVS/l/d

Parameter	DGS 2	DGS 3
SBP (Nl/gVS)	556.55±19	425.41±78
SMP (Nl_{CH4}/gVS)	307.99±10.6	240.99±9.6
Methane in the biogas (%)	56.15±1.74	57.72±0.45
VMPR ($Nl_{CH4}/l_{reactor}/d$)	0.46±0.009	0.32±0.01
MPR (Nl_{CH4}/d)	5.34±1.04	3.71±0.74

IMPACT OF THE FEEDSTOCK CHARACTERISTICS – MAIN RESULTS

* The results showed a significant difference in the methane yield and production rate when changing the grass silage composition during semi-continuous digestion, thus highlighting the sensibility of the continuous systems to substrate characteristics.

* The influence of the mixture of maize and grass silages on process performance and dynamics was investigated during batch and semi-continuous digestion. In the case of semi-continuous digestion, the methane yield and production rates seemed to decrease with increasing proportion of grass silage in the feedstock. These observations are contradictory with the trend observed for batch conditions (i.e. increasing yield with increasing proportion of grass in the mixture). Grass silage had double the amount of proteins and 23% more of cellulose, with slower degradation, and so its larger methane production potential might not have been achieved under semi-continuous conditions with the given short HRT (i.e. 16.69 days) in the semi-continuous trial. Thus, when assessing the profitability of using grass silage in biogas plants, it is important to weigh the possible benefits (wide availability and low growing input requirements) against the potential shortcomings, including its possible impaired methane potential under semi-continuous digestion, particularly for HRT below 20 days.

*The adapted Anthrone method seemed to be reliable for measuring glucose and glucose-based polysaccharides during the digestion of lignocellulosic material. The concentrations thus measured for the batch digestion of glucose, cellulose, and corn starch were in accordance with the sCOD and VS values. The results showed that the uptake of glucose was quite fast, most of it taking place within the first day of digestion. Also, the substrate uptake seemed to be faster for corn starch than for cellulose, with most of the degradation taking place between day 1 and 2 of digestion, while for cellulose was mainly from days 2 to 4. This was also reflected in the calculated first-order rate constants.

4.1.3 Impact of the feeding mode

The aim of the experiments presented hereafter was to investigate the influence of the feeding mode (semi-continuous vs. batch) on the process dynamics.

To this end, two batch experiments were run with dried maize silage (DMS 2) and crystalline cellulose with the same reactor and operational conditions (e.g. volume, mixing conditions, etc.) as the ones applied to the corresponding semi-continuous experiments, which results have already been described and discussed in sub-chapters 4.1.1.2 for cellulose and 4.1.1.4 for maize silage. These experiments, which experimental set-up and operation is described in sub-chapter 3.4.1, ran in parallel to the semi-continuous experiments and with the same inoculum (i.e. starting conditions), and allowed to compare the degradation kinetics for these two modes.

First-order kinetics were applied to fit the experimental cumulative methane production obtained from the batch tests using Eq. 26 (in sub-chapter 3.6.1.2) using nonlinear least-squares curve fitting with Microsoft Excel Solver. The measured and predicted accumulated methane production for the batch experiments are presented in Figure 50 (top figure for the degradation of cellulose with an OL of 1g/l, and bottom figure for the degradation of DMS 2 for an OL of 2 g/l).

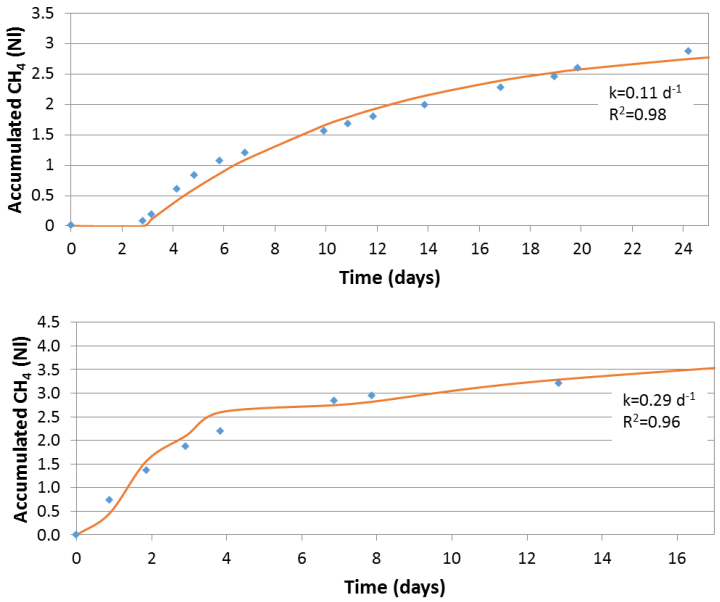

Figure 50: Evolution of the accumulated methane production for the batch digestion of cellulose with an OL of 1gVS/l (top) and maize silage (dried DMS 2) with an OL of 2 gVS/l (bottom)

The calculated first-order rate constants for the batch experiments were then compared with the constants estimated for semi-continuous feeding conditions (Eq. 28 in sub-chapter 3.6.1.2) for each substrate (see Table 49).

The collected data showed very different dynamics for the digestion of cellulose and dried maize silage under different feeding modes. Indeed, the k value estimated for the batch experiment for cellulose was of 0.11 d^{-1}, value that is similar to those previously reported for batch experiments for cellulose (O'Sullivan et al., 2006; Song et al., 2005) but 3 times lower than the value estimated for cellulose digestion in the semi-continuous reactor. This observation was also made by Song et al (2009) for cellulose. For the DMS 2 the value estimated for the batch experiment was 0.29 d^{-1}, which is 1.9 times lower than the value estimated in the semi-continuous reactor for the same WV (0.42 d^{-1}). This higher value (representing faster biogas production) can be attributed to more balanced conditions, better adapted bacterial population and lack of product inhibition.

This is in agreement with observations made by Golkowska et al. (2012) for the digestion of maize silage. In this paper, different kinetic constants were necessary to fit the experimental data of batch and semi-continuous digestion. Moreover, the first-order constants estimated for semi-continuous digestion conditions (once a day) were higher, thus suggesting higher digestion efficiency by more frequent feeding.

Table 49: Calibrated first-order rate constants for batch and semi-continuous digestion of cellulose and dried grass silage

Substrate	Feeding	Woking volume	Loading	k (d^{-1})	R^2
Cellulose	Semi-continuous	10 l	1 gVS/l/d	0.33	0.93
	Batch	9 l	1 gVS/l	0.11	0.95
DMS 2	Semi-continuous	6.7 l	2 gVS/l/d	0.42	0.70
	Batch	6.7 l	2 gVS/l	0.29	0.96

IMPACT OF THE FEEDING MODE – MAIN RESULTS

*When comparing feeding modes (batch vs. semi-continuous feeding conditions) for the same initial conditions and operation, the results showed that the degradation dynamics differed.

*Semi-continuous digestion presented faster degradation rates than batch digestion, on the basis of the calculated first-order rate constant, thus suggesting higher degradation efficiency.

*The first order-kinetic constant (to characterise the whole process assuming hydrolysis as the rate limiting step) estimated for a substrate on the basis of experimental data from batch experiments is a conservative estimate of the value that could be achieved under semi-continuous and continuous feeding conditions.

4.1.4 Impact of the system configuration and pH

The application of a two-stage system has been previously suggested for enhancing digestion performance. It is argued that the separation of the acidogenesis and methanogenesis phases can contribute to better meet the pH and environmental requirements of the bacterial groups involved (Boe and Angelidaki, 2009). On the other hand, the control of the two-phase system could also be more complicated as it requires adjusting the conditions of the effluent from the first-stage reactor to be used as fed in the second-stage reactor, in terms of pH and VFA, to avoid inhibitory effects.

One of the advantages of using this type of reactor configuration is that it could allow for the production of H_2 in the first reactor and CH_4 in the second, with a better optimisation of the production. For example Liu et al. (2006) showed a higher CH_4 production (21% higher) than in a one-stage configuration when digesting household solid waste.

In this sub-chapter, the feasibility of running a two-stage hydrogen-methane process for semi-continuous digestion of maize silage was investigated. Moreover, the shifting of the methanogenic process to H_2 production from the adjustment of the OLR and pH is described in detail with the help of online data for CO_2, H_2 and CH_4 content evolution. The detailed description of the experimental set-up and operation is given in sub-chapter 3.4.2.2.

4.1.4.1 Gas production and composition

When the daily addition of buffering capacity was removed with the feeding regime 5 (OLR of 10 gVS/l/d) in day 125th, the pH rapidly dropped to a value close to 5. Given the methanogens requirements in terms of the pH, this change triggered the shift into the production of H_2 in the reactor. From that moment onwards, until the day 185th of digestion, the biogas produced by the reactor consisted of a mixture of H_2 and CO_2, and only traces of CH_4 (below 0.7%).

The production of H_2 can be achieved by adjusting the process parameters to inhibit H_2-consuming bacteria (i.e. hydrogenotrophic methanogens). Most of the studies addressing the production of bio-H_2 are implemented under batch conditions and the production of H_2 is induced through heat treatment to inhibit methanogens (Davila-Vazquez et al., 2008). More recently, it has been proposed to induce H_2 production by changing the OLR and the HRT, without the need of heat shock or acid or base treatment (Wang et al., 2006). For example, Pakarinen et al. (2011) also reported a shift from methane to H_2 production in a one-stage CSTR semi-continuously fed with grass silage by increasing the OLR from 2 gVS/l/d to

10 gVS/l/d and shortening the HRT from 30 days down to 6 days. Research on H_2 production in continuous experiments is limited, particularly for energy crops and crop residues.

Two feeding regimes can be distinguished for this reactor during the H_2-producing phase: the first one, feeding regime 6, from day 126th to day 152nd of digestion with the reactor been fed with DMS 2 at an OLR of 5.87 gVS/l/d; and the second one, feeding regime 7, from day 153rd of digestion until day 185, with a very similar OLR (5.64 gVS/l/d) but with DMS 1 been used as feedstock. The characteristics of these two substrates were very similar (see Table 10 in sub-chapter 3.2.1), and no major impact of such change was expected. From day 135th of digestion, the CH_4-production CSTR reactor ran in series until the end of the experiment.

The biogas performance for the two reactors in the two-stage configuration is presented in Table 50 as the average over the last weeks of each feeding regime, when reactor performance was considered to be adapted to the respective operational conditions. Additionally, the performance measured for feeding regimes 4 (same OLR than the one applied in the two-stage process) and 5 (just before the shifting into the H_2-producing mode), are also displayed in this table for comparison purposes. Annex P presents additional data for this experiment not presented in this chapter.

Table 50: Average biogas performance of the two reactors composing the two-stage system semi-continuously fed with DMS (1 and 2), and the last two feeding regimes for the one-stage system

	One-stage System (HRT 16.69 days)		Two-stage system (HRT 33.38 days)		
	Feeding regime 4	Feeding regime 5	H_2-producing reactor		CH_4-producing reactor
			Feeding regime 6	Feeding regime 7	
Substrate	DMS 2	DMS 2	DMS 2	DMS 1	Outflow first-stage reactor
SMP ($NlCH_4$/kgVS added)	258.07±2.6	179.48±61.03	0.69±0.11	0.73±0.09	266.83±24.85
VMPR ($NlCH_4$/l/d)	1.13±0.02	1.24±0.32	0.00±0.00	0.00±0.00	1.10±0.03
MPR ($NlCH_4$/d)	7.58±0.14	8.28±2.12	0.02±0.01	0.02±0.00	7.34±0.21
CH_4 content (%)	53.2±0.41	40.07±2.35	0.71±0.41	0.63±0.12	63.88±1.76
SHP (NlH_2/kgVS added)	-	15.91±0.01	44.99±0.02	53.35±0.01	-
VHPR (NlH_2/l/d)	-	0.05±0.00	0.20±0.09	0.19±0.04	-
H_2 content (%)	-	4.04±2.50	31.56±6.39	38.28±4.52	-

An average SHP of 44.99±0.01 NlH_2/kgVS and 53.35±0.01 NlH_2/kgVS were obtained for feeding regimes 6 and 7 respectively. These values are in the range of values reported previously in literature (see Table 51) during semi-continuous digestion in CSTR reactors for different substrates, with the exception of the value reported for digestion of the organic fraction of MSW by Chu et al. (2008), which is more than 4 times higher. A possible explanation for such difference is the operational temperature (i.e. thermophilic for the experiment conducted by Chu et al. (2008)). Indeed, higher temperatures can thermodynamically enhance the conversion of sugars into H_2 (endothermic reaction) (Davila-Vazquez et al., 2008). For example, Valdez-Vazquez et al. (2005) evaluated the influence of the operation temperature during semi-continuous digestion of the organic fraction of MSW, and found that the H_2 yield of the thermophilic reactor was 54% higher than for the mesophilic reactor.

Table 51: SHP reported in literature for different substrates under semi-continuous feeding conditions

Substrate	SHP (Nl/kgVS)	OLR (KgVS/m^3/d)	Temperature (°C)	Source
Grass silage	42	10	35	Pakarinen et al. (2011)
Food waste	15-30	n.r.	37	Ohnishi et al. (2010)
Organic fraction of MSW	205	38.4	55	Chu et al. (2008)
Household solid waste	43	37.5	37	Liu et al. (2006)
Potato waste	30[a]	41[b]	35	Zhu et al. (2008)

n.r. not reported
[a] Nl/kgTS
[b] Unit L/kg TS

The SHP was slightly higher (by 16%) for the feeding regime 7 in comparison to feeding regime 6. The maximum H_2 content in biogas during regimes 6 and 7 was 43.62%, with an average of 31.56% and 38.28% respectively, thus also higher for regime 7. Pakarinen et al. (2011) found for grass silage semi-continuous digestion a maximum H_2 content of 24%. The evolution of the content of H_2 in the biogas (measured every minute for two months) can be observed in Figure 51. It is possible to see that the fluctuations were larger in the case of the feeding regime 6. A possible explanation might lay in the pH. For the feeding regime 6, the average pH was of 5.08±0.12, slightly lower than for the feeding regime 7, with an average value of 5.27±0.14. Previous studies have highlighted the important effect of pH on the H_2-production, and the need to control pH at values between 5 and 6 (Davila-Vazquez et al., 2008). More precisely, Liu et al. (2006) highlighted in one study that the optimum pH for H_2 production from household solid waste was in the range 5–5.5. Zhang et al. (2003) found that the maximum H_2 yield of 92 ml/g-starch, occurred at pH 6.0. The role of the pH effect on the H_2 production is partially explained by the inhibitory effect that lactate can have on H_2 production, effect that depends on pH and temperature (Chu et al., 2008; Escamilla-Alvarado et al., 2013). Lactate presence was not measured during the digestion in this experiment. This better H_2 yield at higher pH can also be related to the concentration of HAc and HBu, as it will be explained in sub-chapter 4.1.4.2, as the pH is going to regulate the H_2-production pathway.

As regards the CH_4-producing reactor, the average SMP over a period of two months was of 266.83±24.85 $Nl_{CH4}/kgVS_{added}$. In this research, the CH_4 yields are reported on the basis of VS added in the first reactor (and assuming that the whole volume extracted from the first reactor is fed into the second reactor), in order to be able to compare with reported data. The methane yield obtained in the two-stage CH_4-producing reactor was thus 3.3% higher than the value obtained in the one-stage configuration for the feeding regime 4 (258.07±2.6 $Nl_{CH4}/kgVS_{added}$), with an OLR of 6 gVS/l/d. While the MPR and the VMPR are very similar (see Table 50) for one-stage and two-stage process, the CH_4 content was almost 17% higher in the case of the two-stage process. Nevertheless, the HRT applied to the whole two-stage system was twice longer (33.38 days) than the HRT applied in the case of the one-stage system producing only methane (16.69 days), and therefore, it was not possible to properly compare both systems. Therefore, it was decided to use the developed model to perform a scenario analysis for a longer HRT. Indeed, the HRT for the one-stage system with an OLR of 6 gVS/l/d was increased to 33.38 days, and the modelled results used for analysing the possible differences from an energetic and degradability point of view between the two configurations with the same operational conditions. The scenario analysis and comparison is provided in 4.2.3.6.

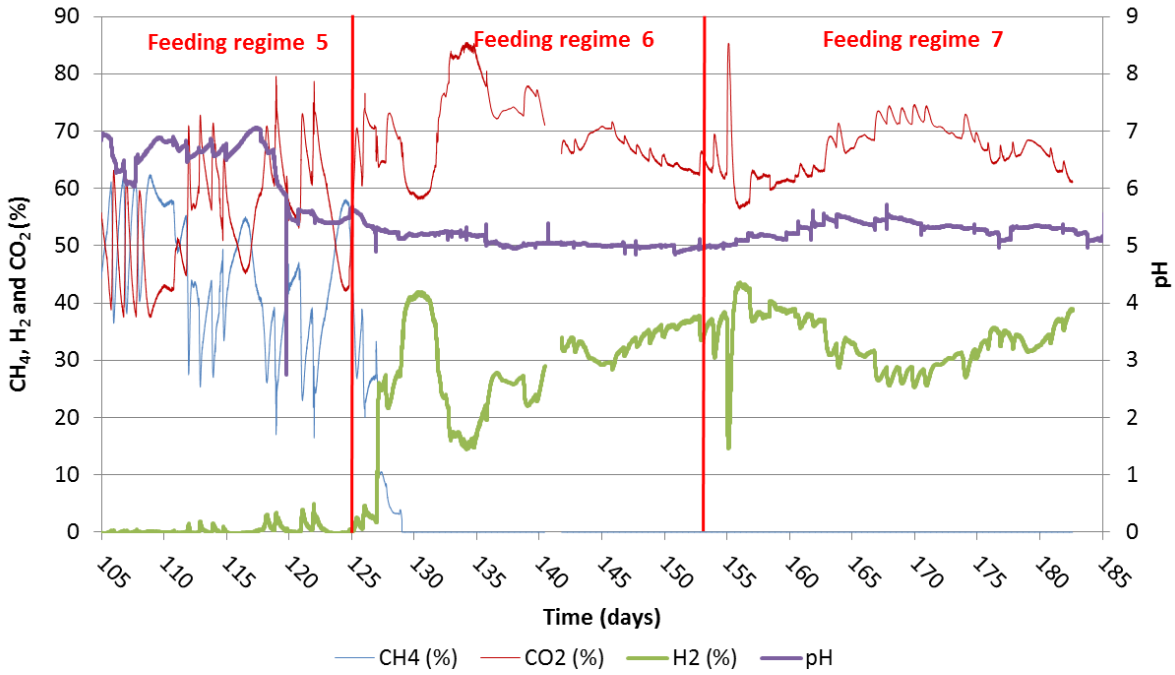

Figure 51: Evolution of the instantaneous H_2, CH_4 and CO_2 content in the biogas for regimes 6 and 7 in the H_2-producing reactor (in the two-stage system) after the drop of pH to 5 from day 125. The evolution of the biogas content in the biogas also shown for feeding regime 5 (one-stage operation) before drop in pH for comparison (days 105 to 124 of digestion)

Figure 52 presents the evolution of the HPR and the MPR (left axis) and the H_2 and CH_4 content in the biogas (right axis) for the H_2-producing reactor (top) and the CH_4-production reactor (bottom) respectively. In the second-stage (CH_4-producing reactor) the MPR evolution displayed a weekly pattern, in response to the weekly feeding (from Monday to Friday), while the CH_4 content in the biogas remained stable for the whole period of the experiment. On the other hand, in the first-stage reactor (H_2-producing reactor) the same pattern was not observed for the evolution of the HPR, and the H_2 content in the biogas fluctuated. Indeed, the stability in the CH_4-producing reactor was better (i.e. consistent pattern) than for the H_2-producing reactor. These variations in the first reactor could be related to the accumulation of particulate material.

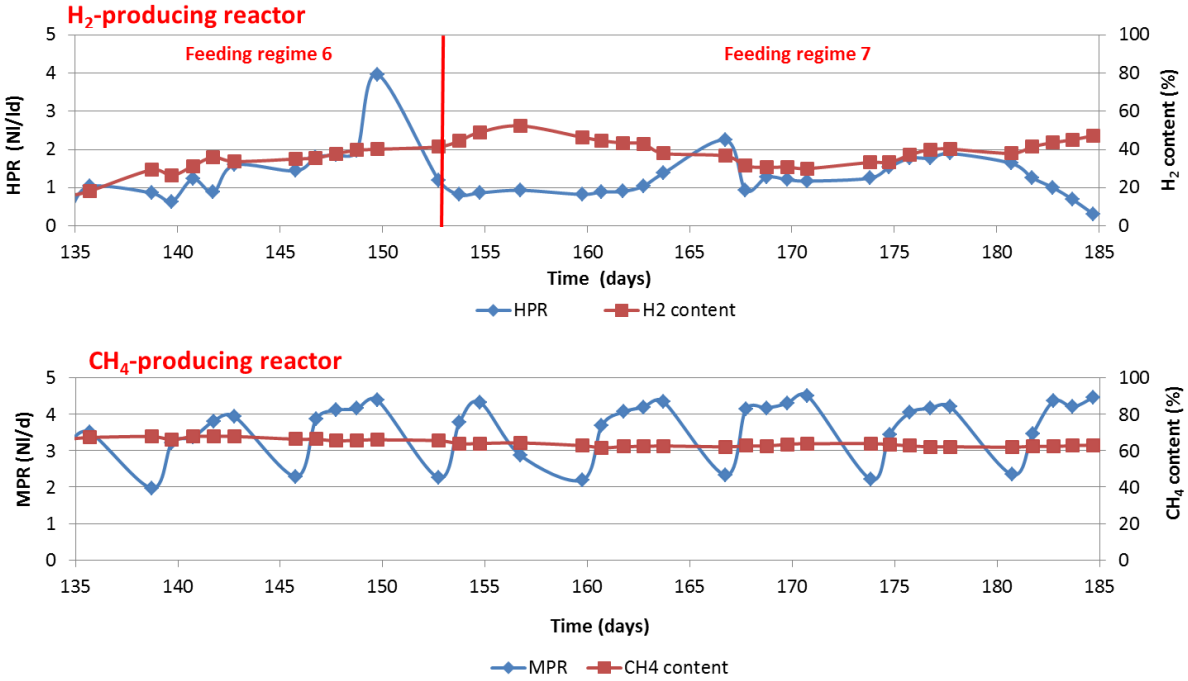

Figure 52: Daily evolution of the MPR and SHP (left axis) and the CH_4 and H_2 content in the biogas (daily accumulated) (right axis) for the H_2-producing reactor (top) and the CH4-producing reactor (bottom) respectively

4.1.4.2 Degradation of intermediary products

Different control parameters were monitored over time for semi-continuous digestion of maize silage in the two-stage process. The average values for several of these parameters are presented in Table 52 for the H_2-producing reactor (feeding regimes 6 and 7) and the CH_4-producing reactors in the two-stage system. For comparison purposes, the average values for the one-stage process equivalent methanogenic regime (feeding 4) are also included.

Table 52: Average operational conditions of the two reactors in the two-stage system semi-continuously fed with maize silage (DMS 1 and 2), and the last two feeding regimes for the one-stage system

	One-stage System (HRT 16.69 days)		Two-stage system (HRT 33.38 days)		
			H_2-producing reactor		CH_4-producing reactor
	Feeding regime 4	Feeding regime 5	Feeding regime 6	Feeding regime 7	
TVFA (mgHAc_{eq}/l)	384.81±210.1	5659.16±1804.7	6885.45±712.2	4552.46±521.9	97.38±144.3
TS of digestate(%)	2.77±0.2	5.54±0.2	5.37±0.1	6.62±0.3	1.67±0.1
VS of digestate (%)	2.14±0.2	4.31±0.1	4.52±0.2	5.80±0.2	0.99±0.1
sCOD (g/l)	3.30±0.23	16.71±5.17	36.51±1.07	37.33±1.18	2.08±0.27
VS removal (%)	81	74.46±0.01	57.43±5.53	41.16±1.50	82.63±2.76*
*Considering the VS concentration in the effluent from the first reactor fed into the second reactor.					

It is possible to observe that there was an accumulation of the VS (corresponding to the particulate fractions) over time with increasing OLR (in the one-stage process) and also with the two-stage configuration in the H_2-producing reactor. This accumulation could be explained by a possible inhibition of the enzymatic hydrolysis by some of the intermediaries, and could be related to the fluctuations observed in the HPR. Figure 53 presents the evolution in the concentration of monosaccharides, mainly glucose (as measured through the Anthrone

method) and the HPR. No clear correlation was found between these two parameters. On the other hand, the concentration of monosaccharides presented a fluctuating behaviour, particularly for feeding regime 7, which could suggest a possible inhibition of the enzymatic hydrolysis.

In Table 52 it can be seen that the TVFA accumulated progressively during the one-stage configuration for increasing OLR and again increased by 18% for feeding regime 6 in the H_2-producing reactor in the two-stage configuration. Finally the TVFA decreased again by 34% for feeding regime 7. The daily evolution can be seen in Figure 54 for the H_2-producing reactor and the CH_4-producing reactor. An overall daily decrease in the concentration of the TVFA can be observed for the first reactor. Indeed, the TVFA represented on average 63% of the measured sCOD in the reactor during the feeding regime 6, which decreased to 55% for feeding regime 7. This indicated a good efficiency of the acidogenic step. It has been previously suggested that high VHPR is associated with high HBu and HAc concentrations, while HPr accumulation is associated with impaired H_2 formation (Wang et al., 2006). It is possible to observe in Figure 54 that in the H_2-producing reactor, the concentration of HPr decreased steadily overtime after inducing the shift to H_2 production and stabilised to very low values, corresponding to higher average in the H_2 content in the biogas. The main VFAs were HBu and HAc. The concentration of n-HCa became also significant 5 days after shifting to H_2 production. A similar profile in the individual VFAs concentration was observed by Pakarinen et al. (2011) for grass silage.

Liu et al. (2006) argued that pH was the key factor regulating the fermentation pathway from glucose for H_2 production (with either HBu or HAc being produced as end-product with H_2). It was observed in that study that at higher pH, more glucose was converted into H_2 having acetate as end-product. Given the stoichiometric conversion of glucose into acetate and butyrate (see Table 1 in sub-chapter 2.2.1.2), having higher concentrations of acetate could result in higher H_2 production, as it was observed by Liu et al. (2006). In the H_2-producing reactor in the current research, HBu concentration remained very high (above 5g/l) during the whole period of digestion, while the concentration of HAc was generally below 1g/l. Thus, at the given operational pH of 5.17 (average pH for both feeding regimes 6 and 7), the butyrate pathway (i.e. H_2 production from glucose fermentation with production of butyrate) was the predominant one. Increasing the pH above 5.5 could increase the amount of acetate and reduce the butyrate concentration, thus resulting in better H_2 yields. Based on the results, it seems thus more advantageous to adjust the pH between 5.5 and 6.

When considering together the evolution of the different VFAs in the H_2-producing reactor and the glucose concentration (Figure 53) it was also possible to observe an opposite trend in the evolution of HBu and glucose. Indeed, the accumulations of glucose in the reactor were related to a decrease of the concentration of HBu (impaired fermentation of glucose).

In the case of the CH_4-producing reactor (second-stage reactor), the concentration of the TVFA was low (on average 97.38±144.3 $mgHAc_{eq}/l$) over the almost two months of digestion, but experienced a slight increase related to an increase in the HPr concentration, never above limits considered as inhibitory.

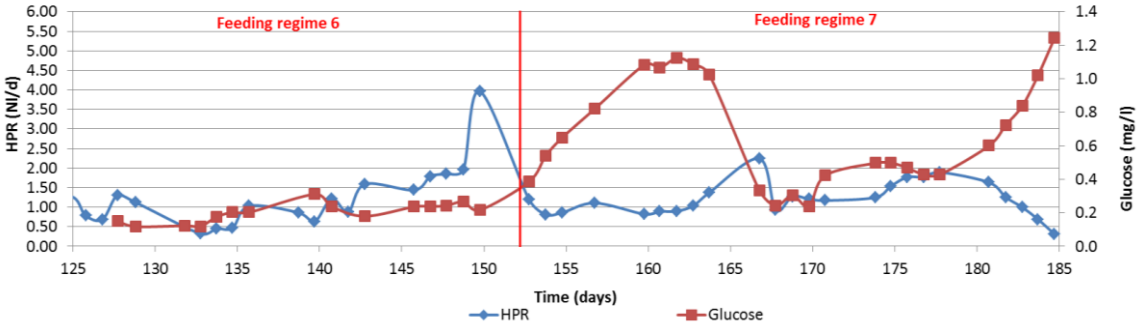

Figure 53: Evolution of the daily concentration of glucose (right axis) and HPR (left axis) in the H_2-producing reactor (first-stage reactor, OLR of 6 gVS/l/d, DMS 1 and DMS 2)

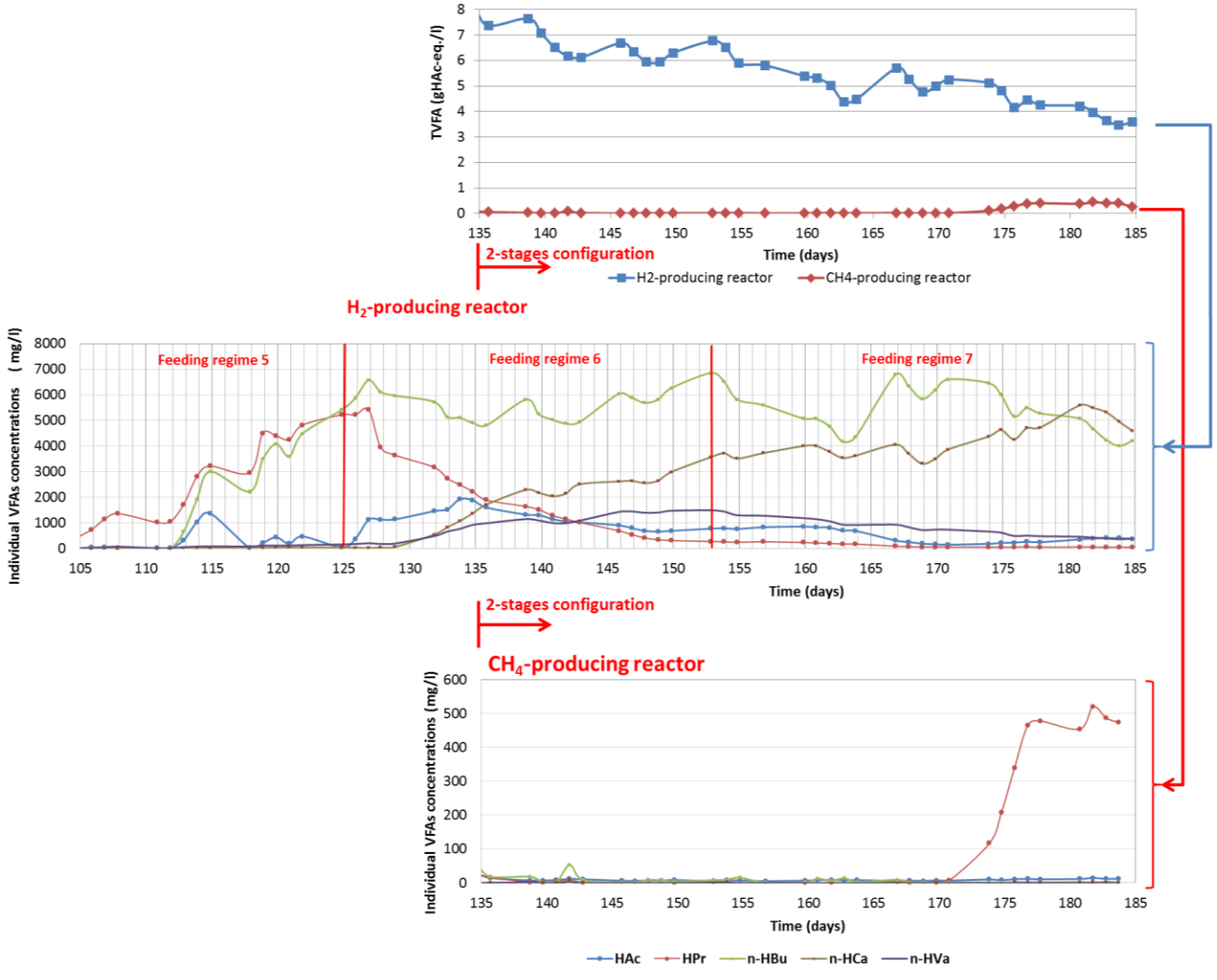

Figure 54: Evolution of the daily TVFA concentration (expressed as gHAc-eq./l) in the H_2-producing reactor and CH_4-producing reactor respectively (top), and detailed evolution of the concentration of individual VFAs in the CH_4-producing reactor (centre) and the H_2-producing reactor during two-stage process (bottom)

The sCOD was very high in the H_2-producing reactor for both regimes 6 and 7. More than half of it corresponded to the TVFA concentration. It has been estimated with the measured glucose concentration that monosaccharides represented a maximum of 4-5% of the sCOD in

the reactor during the peaks. The remaining degradation products were most probably alcohols (not measured) and/or lactic acid.

The diversity and abundance of methanogenic Archaea was investigated in the H_2-production reactor in the pH-driven two-stage system presented in this sub-chapter. As it could be expected, after shifting to a H_2-producing system, the methanogen concentration steadily decreased due to bacterial wash-out (inhibited growth due to low pH of 5.27).

IMPACT OF THE SYSTEM CONFIGURATION AND PH – MAIN RESULTS

*The advantages and feasibility of applying a pH-phased two-stage process in comparison to one-stage process was investigated for the semi-continuous digestion of maize silage.

*In the first reactor, CH_4 production was shifted into H_2 production by increasing the OLR (to 10 gVS/l/d) and removing the addition of buffering capacity. The pH was then kept between 5 and 5.5 in this reactor that became the hydrolytic reactor and a second methanogenic reactor was initiated to run in series.

*An average specific H_2 production of 49.17 NlH_2/kgVS was obtained in the first reactor, with an average H_2 content in the biogas of 35%.

*Accumulation of glucose in the reactor seemed to be associated with a decrease in the HBu concentration in the H_2-producing reactor. The butyrate pathway for the production of H_2 from glucose seemed to be the predominant fermentation pathway at the average operational pH of 5.17.

* The H_2 production and content in the biogas seemed to be positively related to the pH (i.e. 16% higher SHP was measured during the feeding regime with the highest pH, with an average of 5.3). Operation at higher pH could result in higher HAc and lower HBu concentrations in the reactor and thus higher H_2 production. A pH working range between 5.5 and 6 seems to be more advantageous for H_2 production.

4.1.5 Impact of the working volume - Scaling-up

As it was explained in chapter 3, a variety of WVs were applied in the experiments, ranging from 0.5 litres up to 11.5 litres. Unfortunately, the variety of operational conditions, including the type of mixing and reactors used, was large, which made it difficult for an adequate comparison and analysis of the impact of the WV on the process performance. A systematic analysis (for the same reactor type and mixing) was not performed, and therefore, conclusions could not be drawn in this regard. In any case, this parameter was not expected to have an influence in itself on the performance and dynamics, which could be rather affected by reactor type related aspects such as the mixing and configuration.

Figure 55 shows the accumulated methane yield for the batch digestion of fresh grass silage (GS 1) for WV of 0.75 litres and 10 litres. In spite of the different OL (8.54 gVS/l for the WV of 0.75 litres and 12 gVS/l for the OL of 10 litres) and mixing methods (continuous stirring vs. once a day manual mixing for the smaller WV), the evolution in the methane yield and value after 15 days of digestions is very similar (difference smaller than 5%). In spite of the fact that some of the operational parameters differed (e.g. mixing frequency and speed), and the OL (in any case not inhibitory), the methane performance was very similar, regardless of the WV, as it was expected.

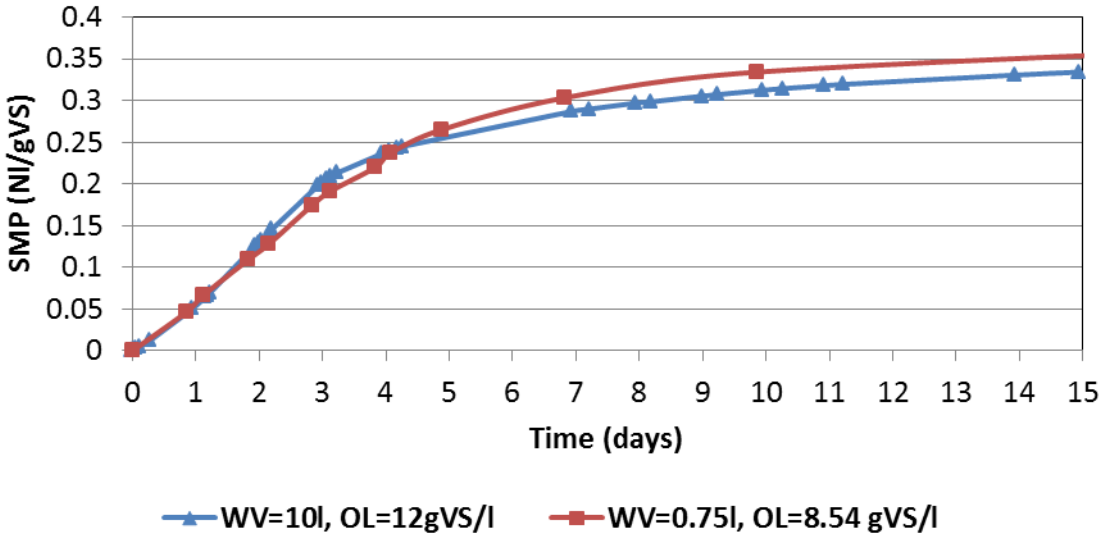

Figure 55: Evolution of the accumulated SMP (in Nl/gVS) for batch digestion of fresh grass silage (GS 1) for WV of 0.75l (1l PET reactor with OL of 8.54 gVS/l) and 10l (CSTR grass reactor, with OL of 12 gVS/l)

4.2 Modelling the digestion of lignocellulosic materials

4.2.1 Development of the models Lignogas and Lignogas-SIM

Two distinct models were developed in the context of the current work to describe the anaerobic digestion of lignocellulosic material, and in particular energy crops: the Lignogas model, and the lighter version, the Lignogas-SIM. Both models are based on the well-known and widely used ADM1 model. Nevertheless, the application of such complex model to the degradation of solid and heterogeneous substrates has been found to have limitations. The developed models address some of the previously highlighted limitations. Additionally, the Lignogas model tries to integrate current knowledge about microbial composition in biogas plants and explores alternative approaches to describe the hydrolysis of carbohydrates. The Lignogas and the Lignogas-SIM take into account specific substrate characteristics and are intended to be applicable in a wide variety of operational conditions, for different substrates, feeding modes (i.e. batch and continuous), different loadings and configurations (i.e. one and two-stages). The models are thus calibrated and validated with experimental data from experiments implemented with different operational conditions and presented in the sub-chapter 4.1. One of the novelties of the developed models is that they are tested and evaluated using experimental data from extreme loading or pH conditions, which helps to evaluate their strengths and limitations.

The Lignogas model is an extended version of the ADM1 model, which includes acetate oxidation to promote the hydrogenotrophic methanogenesis and a dedicated variable for the decayed biomass to close the C and N balance, and considers different hydrolysis rates for slowly and fast degradable carbohydrates. The Lignogas-SIM, on the other hand, is a simplified version of the ADM1 model, addressing some of its limitations, such as the use of feed characterisation data for the fractionation of the substrate, but also simplifies some processes, as it does not consider the HBu and HVa and all monomers produced during hydrolysis are lumped in one variable. The idea behind was to be able to compare both approaches and also with the original ADM1 in order to assess the most suitable development and limitations and possible future adaptations. The detailed description of the assumptions and structure of each model are presented in Chapter 3.6.

As it will be argued in this sub-chapter, the Lignogas model is the preferred model to predict the behaviour and performance of anaerobic digestion of lignocellulosic material. Indeed, in spite of its complexity, it did allow to model satisfactory a wide range of operational conditions, including extreme feeding conditions. The Lignogas-SIM model, on the other hand, was more sensible to certain inhibitory mechanisms, as a result of the simplifications made in this model. Therefore, the modelling performance worsened considerably for this model for certain operational conditions and substrates. In this sub-chapter, the main results related to the development and validation of the models and supporting the preference for the Lignogas model are summarised.

4.2.1.1 Impact of the different additions in the Lignogas model

Different additions to the original ADM1 mentioned earlier were introduced stepwise (resulting in versions 1 to 3) in order to build the final Lignogas model. The impact of

introducing each of these changes was analysed graphically and also in terms of the quality of the fit for each addition before calibration.

Figure 56 presents the measured BPR (a), the CH_4 content (b), the HAc concentration (c), and the HPr concentration for the batch digestion of fresh grass silage (GS 1), and the modelled evolution for the same variables using ADM 1 (with default values for the fractionation factors for the substrate), Lignogas 1 (the ADM1 with adapted values for the fractionation factors and a dedicated variable for the decayed biomass), Lignogas 2 (Lignogas 1 with different hydrolysis rates for the slowly and fast degradable carbohydrates fractions considered), and Lignogas 3 (the Lignogas 2 version with the acetate oxidation process). It is important to highlight that changes were nevertheless introduced in the ADM1 to close the N and C balances with the introduction of stoichiometric coefficients for the disintegration and decay of biomass processes, as suggested by Rosen et al. (2006) and explained in sub-chapter 3.7.2.2.

For this analysis, performed before the calibration task, the hydrolysis rates took the default values from the ADM1 (10 d^{-1}), and therefore, as it will be explained in sub-chapter 4.2.1.2, their influence on the model output was largely reduced. This is the reason why there was no difference between the versions Lignogas 1 and 2, which overlapped. The impact of considering the hydrolysis of different carbohydrates is further analysed in sub-chapter 4.2.1.4.

It is important to highlight that the ADM1 model version used presented already a good fitting with the measured values. The HPr concentration was notably satisfactory and better than with any modification introduced with the subsequent modifications of Lignogas (before calibration). The version Lignogas 3 seemed to fit better the measured data than any previous version (Figure 56) thus supporting its use for further modelling (hereafter referred simply as Lignogas). When looking at the quality of the fit, as described by means of the RMSE and summarised in Table 53 for different variables, the Lignogas 3 version (with the inclusion of the acetate oxidation) had better modelling performance than versions 1 and 2 of the model tested, and than the ADM1 model for all the variables except for the HPr concentration and the BPR (very similar for both models). The quality of the simulation additionally improved for the Lignogas model after calibration, as discussed in sub-chapter 4.2.1.3. The version 3 of the Lignogas model (the final version) was used then after and referred to simply as the Lignogas model.

Table 53: Quality of the fit, as measured by the RMSE, for the ADM1 model and the different versions of the Lignogas model before calibration applied to the mesophilic digestion of grass silage (GS 1) under batch conditions

	Performance of calibration (RMSE)			
	BPR (Nl/d)	MPR (Nl/d)	HAc (gCOD/l)	HPr (gCOD/l)
ADM1	0.102	0.065	0.396	0.016
Version Lignogas 1	0.117	0.071	0.964	0.071
Version Lignogas 2	0.117	0.071	0.960	0.071
Version Lignogas 3	0.106	0.047	0.347	0.080

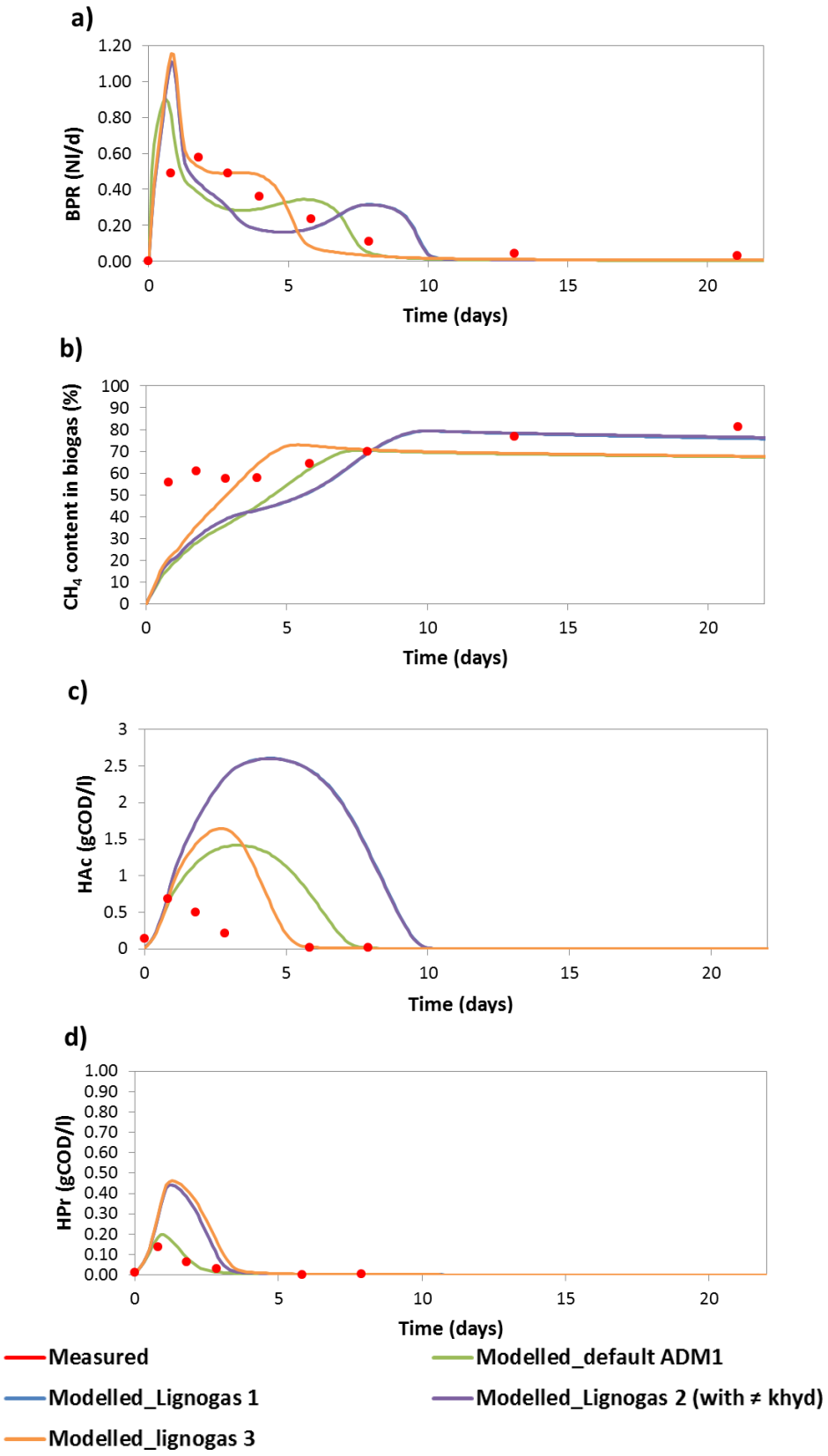

Figure 56: Measured and modelled BPR (a), CH_4 content in biogas (b), HAc concentration (c) and HPr concentration (d) evolution for the different models tested during batch digestion of GS 1. Lignogas 1 adds a dedicated variable for decayed biomass, Lignogas 2 adds to Lignogas 1 different hydrolysis rates for carbohydrates, and Lignogas 3 adds the acetate oxidation process to Lignogas 2

4.2.1.2 Sensitivity analysis and identifiability

In order to evaluate and characterise the changes in model results with changes in model parameters, a sensitivity analysis was performed. This analysis allowed to identify and prioritise the parameters undergoing parameter estimation. Moreover, the calculated sensitivity functions for the different variables and parameters also allowed analysing the identifiability of the parameters considered for optimisation.

The ranking of the averages of the absolute values of the absolute-relative sensitivity functions (Eq. 54) for all the state variables for the Lignogas-SIM and the Lignogas models are presented in Annex Q.1 and Q.3 respectively.

In the case of the Lignogas-SIM model, the parameters highlighted as having the largest impact on the model output were, in decreasing order, the disintegration constant (kdis), the maximum uptake rate for acetate degraders (km_ac), the yield from monomer degraders (Y_mo), the yield from acetate degraders (Y_ac), the maximum uptake rate for monomer degraders (km_mo), and the half-saturation concentration for acetate degraders (ks_ac). Of these 6 parameters, km_ac, kdis and ks_ac had also been identified as having significant sensitivity under steady-state conditions and critical under dynamic conditions for the ADM1 (Batstone et al., 2002).

Nevertheless, having a closer look into the time evolution of the sensitivity functions for different relevant variables (see Annex Q.2), it is possible to observe that the pairs km_ac and Yac, and Km_mo and Y_mo have sensitivity functions that are dependent linearly, thus highlighting an identifiability issue. This means that the impact of the changes in one parameter could be compensated by the appropriated changes in the other, and therefore, a large inaccuracy could result from considering these two parameters together in the parameter estimation. To solve this issue, Y_mo and Y_ac were not considered in the calibration.

In the case of the Lignogas model, and if considering default values for the parameters proposed in the ADM1 model (see Annex I), the parameters identified as most sensitive were the kdis, the maximum uptake rate for acetate oxidizing organisms (km_acetox), the maximum uptake rate for sugar degraders (km_su), km_ac, the half-saturation concentration for acetate oxidizing microorganisms (ks_acetox), inhibitory H_2 concentration for HBu and HVa degrading organisms (KI_h2_c4), and the maximum uptake rate for H_2 degrading organisms (km_h2). The ranking is presented in Annex Q.3. On the other hand, when considering the evolution of the sensitivity evolution (Annex Q.4), it is possible to see that the pair of parameters km_ac and km_acetox on the one hand and ks_ac and ks_acetox on the other hand have also collinear sensitivity functions, which make the parameters poorly identifiable. Therefore, it was decided to remove km_acetox and ks_acetox from the list of parameters to be optimised.

In the Lignogas model, the possibility of considering different hydrolysis constants for the fast degradable and slowly degradable carbohydrates fractions (namely khyd_ch_f and khyd_ch_s respectively) was evaluated. These fractions, resulting from the disintegration of the composite material, correspond to the starch (with the fractionation factor f_ch_xc_f) and the cellulose and hemicellulose (with the fractionation factor from composites f_ch_xc_s) present in the substrate, as defined on the basis of the Weende and Van Soest fractions (see 3.7.2.1). Nevertheless, these parameters were not identified as sensible in the analysis, when considering the default value of 10 d^{-1} proposed in the ADM1 model (see the ranking in Annex

Q.3). On the other hand, the kdis and hydrolysis rate constants (khyd_ch, khyd_pr, khyd_li) were identified as having the largest impact on the model output by Batstone et al. (2002) and in recent implementations for the anaerobic digestion of agricultural substrates (Wolfsberger, 2008; Biernacki et al., 2013). The proposed value for the hydrolysis rates in the ADM1 for the mesophilic digestion of solids is ten-fold larger than the hydrolysis constants estimated for different lignocellulosic substrates reported in literature (see Table 7 in sub-chapter 2.3.1.2), and presented in this study (see sub-chapter 4.1). Indeed, when the kdis is considerably lower than the hydrolysis constants of carbohydrates, proteins and lipids, the influence of hydrolysis is reduced (Feng et al., 2006). On this basis, another sensitivity analysis was performed for the Lignogas parameters but considering a lower starting value for the khyd_ch (both khyd_ch_s and khyd_ch_f). As a result, this parameter became part of the group of the most sensitive parameters, along with the kdis, km_ac, km_su, KI_h2_c4, and km_h2. This illustrates the fact that the sensitivity of the model results to the model parameters is dependent on the actual value of the parameters being considered. If analysing the evolution of the sensitive functions for these parameters (presented in Annex Q.5), it is possible to see that for some variables, such as the acetate and propionate concentrations, kdis and khyd_ch (in this case khyd_ch_s and khyd_ch_f), are linearly dependent, thus these two parameters cannot be identified uniquely from the available data.

Different approaches could be envisaged to address this issue. In recent publications authors have either focused the calibration on kdis, using default values from ADM1 for the hydrolysis constants (Wichern et al., 2009; Thamsiriroj and Murphy, 2010; Galí et al., 2009); or the other way around, they have calibrated khyd_ch and set kdis equal to 1 (Koch et al., 2010; Lübken et al., 2007). Both approaches were therefore tested for the calibration of the Lignogas model: focusing on the disintegration phase (option 1 of the Lignogas model) and focusing on the hydrolysis of the different fractions of carbohydrates (Option 2 of the Lignogas model).

To asses a possible change in the sensitivity of the model after calibration of the selected parameters, a sensitivity analysis was also performed *a posteriori* for both the Lignogas and the Lignogas-SIM models.

4.2.1.3 Parameter optimisation

4.2.1.3.1 Lignogas-SIM model

The experimental data obtained for the batch digestion of fresh grass silage (GS 1) under mesophilic conditions was used for the calibration of the selected parameters. The optimised values are presented in Table 54. The initial conditions for this experiment used in the simulations are presented in Table S.1 in Annex S. For the other parameters of the model, the default values from ADM1 were used (see Annex H). The performance of the calibration, as measured by the RMSE, considerably improved after the calibration for the BPR and the HAc and HPr concentrations.

The value estimated for the disintegration constant (0.20 d^{-1}, see Table 54) was very close to the value estimated for the first-order constant (k) based on the gas production (0.21 d^{-1}). Although the comparison with other proposed calibrated values found in literature is complicated given the difference in the assumptions and approach of the Lignogas-SIM model, it can be observed that the value determined for the disintegration constant was in line with values proposed in literature for this parameter. A summary of these values proposed for

different agricultural substrates and organic waste can be found in Annex R. For example Wichern et al. (2009) proposed a value of 0.26 d^{-1} for grass silage, while the calibrated values estimated by Wolfsberger (2008) varied from 0.3 to 0.41 d^{-1} depending on the version. Thamsiriroj and Murphy (2010) proposed a lower value for this parameter of 0.05 and 0.01d^{-1} for two reactors running in series digesting grass silage.

Table 54: Default ADM1 parameters and calibrated values for Lignogas-SIM under mesophilic condition for batch digestion of GS 1, with the quality of fit for BPR, HAc, and HPr concentrations

	Parameter	Description	ADM1 values	Calibrated values	Units	Performance of calibration (RMSE)		
						BPR (Nl/d)	HAc (gCOD/l)	HPr (gCOD/l)
Default values	-		-	-	-	0.083	0.499	0.120
Calibrated	kdis	Disintegration rate	0.5	0.20	d^{-1}	0.047	0.047	0.030
	km_mo	Maximum monomers uptake rate	30	34.98	gCOD/gCOD/d			
	km_ac	Maximum acetate uptake rate	8	11.97	gCOD/gCOD/d			
	ks_ac	Half-saturation concentration for acetate degraders	0.15	0.10	gCOD/l			

AQUASIM allows determining the uncertainty of the parameters that have been optimised by estimating the standard errors. Nevertheless, this can only be done if the parameters estimated are not closed to the defined lower or upper limits, which was the case for the Lignogas-SIM model for certain parameters. On the other hand, derivatives and standard deviations of uncorrelated parameters calculated during sensitivity analysis in AQUASIM allow estimating the uncertainty in any variable according to the linear error propagation formula. The calculation of the contribution of each parameter to the total uncertainty (error contribution) facilitates the identification of sources of uncertainty for the model outcome. To perform the uncertainty analysis, sensitivity analysis was performed after the parameter estimation. In Annex T.1, Figure T.2, the upper and lower error bounds generated by the uncertainty of the parameters on the model outcome are displayed for selected variables. This analysis showed that the main uncertainty in model results is observed in the first 5 days of digestion, and also that kdis is the parameter contributing the most to uncertainty for most variables considered. This sensitivity analysis highlighted the same parameters previously selected as having the largest impact on the model output, although the ranking changed slightly.

In this work km_ac was been calibrated to a value of 11.97 gCOD/gCOD/d, which is higher than the values of 2.5 gCOD/gCOD/d proposed by Koch et al. (2010) for digestion of grass silage or of 7.1 gCOD/gCOD/d proposed by Lübken et al. (2007) for digestion of a mixture of manure and fodder for cows, which are lower values than the initial default value of 8 gCOD/gCOD/d, proposed in the ADM1. Other authors have proposed, on the other hand, higher values than the ADM1 default ones, such as 12 gCOD/gCOD/d proposed by Ersahin et al. (2007) for corn processing wastewaters (high rate mesophilic digestion) or 9 gCOD/gCOD/d proposed by Blumensaat and Keller (2005) for sludge. Parameter calibration performed with experimental data for propionate and acetate degradation for batch conditions (see Annex M) also yielded higher values than the default in ADM1 proposed values, although the optimum (10.29 gCOD/gCOD/d) was not the same value than those estimated with experimental data from grass silage batch digestion and presented in Table 54. In this work, the experimental

data and resulted calibrated values for acetate related kinetic parameters suggested that the uptake of HAc is faster for the anaerobic digestion of lignocellulosic material under mesophilic conditions than originally considered by the ADM1.

The simulated biogas composition and production rate, and the acetate and propionate concentration evolution using calibrated parameters are presented in Figure 57. The goodness of the fit was overall satisfactory when using the calibrated values, with the model predicting well the evolution of the different variables. Nevertheless, the level of agreement between measured and modelled prediction changed for the different variables. For example, while the quality of the simulation is good for the BPR, the predicted CH_4 content in the biogas never reaches the measured values. Additionally, the validation of the model and calibrated values with independent data from other experimental sets with different substrates highlighted the need to optimise additional parameters, in particular when using certain simple substrates or under high loading conditions. This is further discussed in sub-chapter 4.2.2.

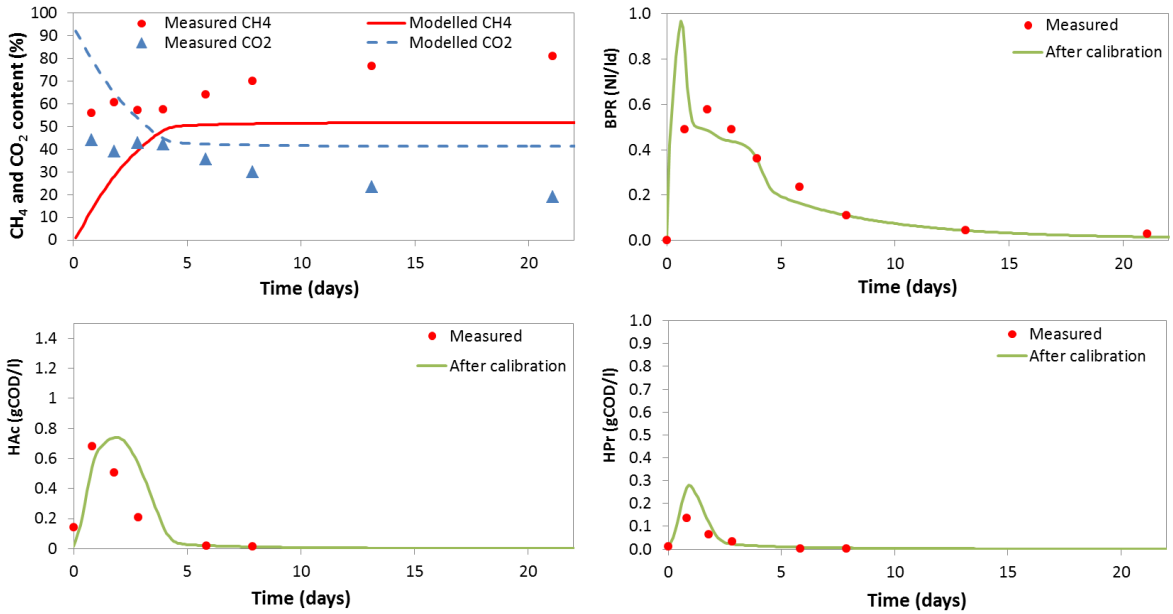

Figure 57: Simulation performed with calibrated parameters of the Lignogas-SIM model and measurement results for mesophilic digestion of fresh grass silage (GS 1): CH_4 and CO_2 gas composition [%] (top left), BPR [Nl/d] (top right), HAc concentration in effluent [gCOD/l] (bottom left), and HPr concentration in effluent [gCOD/l] (bottom right)

4.2.1.3.2 Lignogas model

Two different sets of parameters were calibrated, for options 1 and 2 respectively, corresponding to the two approaches tested, as explained earlier in sub-chapter 4.2.1.1. For the first option, the hydrolysis rate for carbohydrates had the same value as the default proposed by the ADM1 (10 d^{-1}), and only kdis was calibrated. For option 2, the influence of the hydrolysis rate was highlighted by reducing its value, and thus was identified as one of the parameters having most influence. For this second option, to avoid identifiability problems with the disintegration rate, it was decided to focus the calibration on khyd_ch and setting kdis equal to 1 d^{-1}. The results of the calibration for these two options using experimental data from the batch digestion of fresh grass silage (GS 1) are presented in Table 55.

It can be seen that for the first option, not considering the influence of hydrolysis of carbohydrates, the estimated disintegration value (0.20 d^{-1}) was very similar to that estimated

for the Lignogas-SIM model, and also close to the value calculated from experimental CH_4 production data (0.21 d^{-1}). The calibrated km_ac value increased by 25% in comparison to the default ADM1 value, indicating faster dynamics for the uptake of HAc, as it happened for the Lignogas-SIM. Thamsiriroj et al. (2012) proposed a value of 11.1 gCOD/gCOD/d for the first reactor of a two-stage system digesting grass silage with recirculation. The uptake value for sugars (km_su) was also 16% higher, thus suggesting higher uptake rates.

Table 55: Default ADM1 parameters and calibrated values for options 1 and 2 of the Lignogas model under mesophilic condition for GS 1

Parameter	Description	Default values	Calibrated values Option 1	Calibrated values Option 2	Units
kdis	Disintegration rate	0.5	0.2	1*	d^{-1}
khyd_ch_s	Slow hydrolysis carbohydrates rate	10	n.c.	0.26	d^{-1}
Km_su	Maximum sugars uptake rate	30	34.97	33.83	gCOD/gCOD/d
Km_ac	Maximum HAc uptake rate	8	10.06	8.62	gCOD/gCOD/d
km_h2	Maximum H_2 uptake rate	35	39.33	30.90	gCOD/gCOD/d
KI_h2_c4	H_2 inhibitory concentration for HBu and HVa degrading organisms	$1x10^{-5}$	$4.67x10^{-5}$	$6.57x10^{-8}$	gCOD/l
n.c. not calibrated. Default value taken from the ADM1 model. * Not calibrated, assumed to be 1 to avoid identifiability problems with kdis.					

As regards the option 2, considering the influence of the hydrolysis of carbohydrates, the optimized value was $0.26d^{-1}$ for the slowly degradable fractions (mainly cellulose). It is important to highlight that according to the measured Weende and Van Soest fractions, the grass silage used in the experiment (GS 1) had no starch, and thus this fraction of fast degradable carbohydrates was not considered. This value was more in line with values indicated for the first-order constant for carbohydrates (Garcia-Heras, 2003) or values proposed by Koch et al. (2010) for the semi-continuous digestion of grass silage (0.14-0.5 d^{-1}) or by Lübken et al. (2007) for the digestion of fodder for cows and slurry (0.31 d^{-1}). Another important difference in the estimated values for both options is that the H_2 maximum uptake rate (km_h2) increased for option 1 (by 12.37% in comparison to ADM1 default values), while in the case of option 2 it decreased (by 3.34%). The H_2 inhibitory concentration for HBu and HVa degrading organisms (KI_h2_c4) also decreased from the default value to $6.57x10^{-8}$ gCOD/l, similar value to the one used by Koch et al. (2010) of $5x10^{-8}$ gCOD/l or Wichern et al. (2009) of $5.4x10^{-8}$ gCOD/l for semi-continuous digestion of grass silage.

In the case of the Lignogas model, the sensitivity analysis after parameter estimation was performed for the Option 1. This analysis highlighted the same parameters previously selected as having the largest impact. It was observed that the parameter KI_h2_c4 was the main source of uncertainty for the model results. In Annex T.1, Figure T.3 displays the upper and lower error bounds generated by the uncertainty of the parameters (without considering the contribution from KI_h2_c4) for modelled selected variables (i.e. the BPR, HAc concentration, and HPr concentration). The uncertainty of the modelling results from Lignogas model (option 1) is overall smaller than that of the Lignogas-SIM model. Once more, kdis is the parameter contributing the most to uncertainty for most variables considered.

4.2.1.4 Impact of considering the influence of carbohydrates' hydrolysis at different rates for slowly and fast degradable fractions

The impact of considering the influence of the hydrolysis of carbohydrates for a fast and a slow degradable fraction (option 2) was investigated and compared with the approach of

considering default ADM1 values for the hydrolysis rate (option 1) in terms of the modelling performance after calibration of the selected parameters in each case. The graphical comparison can be found in Figure 58 while the summary of the quality of fit is presented in Table 56 in terms of the RMSE for the modelling of batch digestion of grass silage (GS 1) under batch conditions. Option 1 presented a better modelling performance after calibration for the MPR and the HAc concentration, while option 2 fitted better the BPR (see Table 56), albeit differences are minor. The modelling performance considerably improved after calibration for the options 1 and 2 in comparison to the ADM1 model (with default values for the fractionation factors) for all variables considered except to the HPr concentration.

Although the performance of both approaches implemented and analysed (option 1 and 2) for Lignogas were generally satisfactory after calibration, it was decided to select the option 1 for continuing the analysis and validation on the basis of the better modelling performance, particularly for the MPR and HAc concentration. On the other hand, it is worth mentioning that option 2 has the advantage of being more easily widely applicable as it does not require the systematic calibration or calculation of kdis for each substrate used, as long as the detailed substrate characteristics are known.

Table 56: Quality of the fit, as measured by the RMSE, for the ADM1 model and the two approaches for the Lignogas model after calibration applied to mesophilic batch digestion of GS 1

	Performance of modelling (RMSE)			
	BPR (Nl/d)	MPR (Nl/d)	HAc (gCOD/l)	HPr (gCOD/l)
ADM1	0.102	0.065	0.396	0.016
Lignogas_option 1	0.092	0.042	0.039	0.025
Lignogas_option 2	0.055	0.043	0.040	0.017

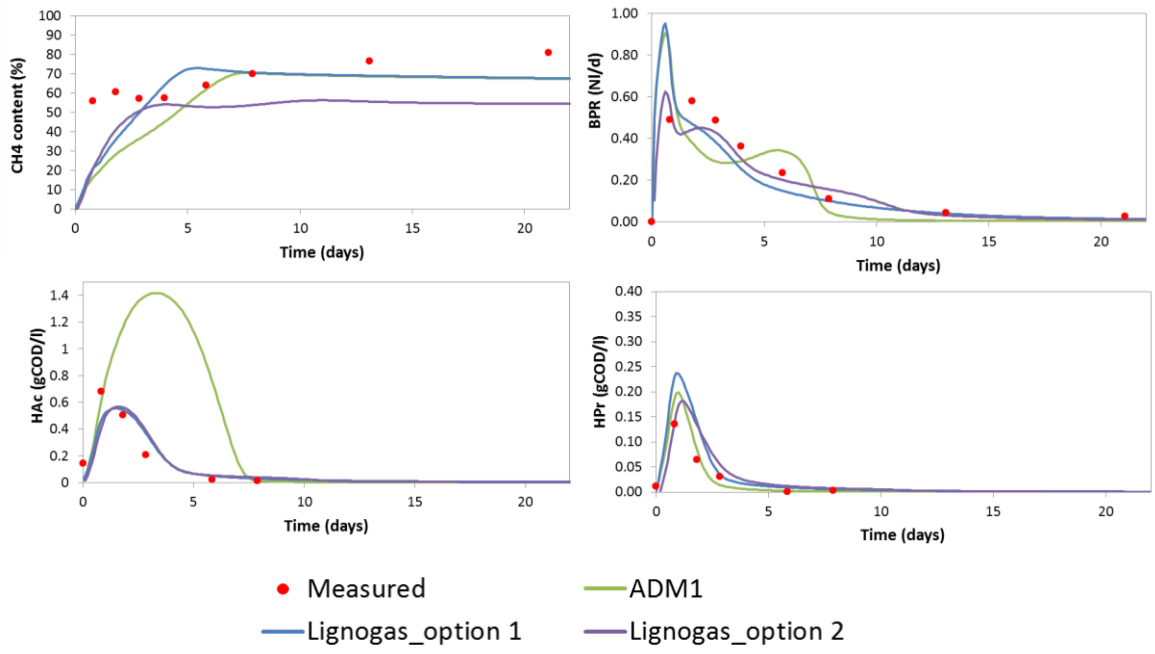

Figure 58: Measured and modelled CH_4 content [%] (top left), BPR [Nl/d] (top right), HAc concentration in effluent [gCOD/l] (bottom left), and HPr concentration in effluent [gCOD/l] (bottom right) performed with ADM1 and Lignogas (option 1 and 2) with calibrated parameters for mesophilic digestion of GS 1

DEVELOPMENT OF THE MODELS – SENSITIVITY ANALYSIS AND CALIBRATION

*The ADM1 model provided a very good modelling performance for batch digestion of grass silage after introducing the necessary stoichiometric coefficients for the disintegration and decay of biomass processes to close the N and C balances.

*Two different models were built and calibrated based on the ADM1, to be applied to describe the anaerobic digestion of lignocellulosic material: one extended version, the Lignogas model, and the lighter version, the Lignogas-SIM. The models addressed some previously highlighted limitations of ADM1. The Lignogas model additionally tried to integrate current knowledge about the microbial composition.

*After the sensitivity analysis and optimisation of selected parameters (kdis, km_ac, km_mo and Ks_ac) a very satisfactory modelling performance was achieved for the Lignogas-SIM model. The optimised values for these parameters were used in the validation with independent data.

*For the extended version, the Lignogas model, two sets of parameters were calibrated corresponding to two different options: the first one using default values for the hydrolysis rates from ADM1 thus diminishing the impact of this step on the model outcome, and the second option considering the influence of the hydrolysis of carbohydrates for a fast and a slow degradable fraction. Although the quality of the fit considerably improved in both cases after calibration and was satisfactory, the first option was selected for further application because it displayed a better modelling performance. Therefore, it was decided to use the default values proposed in the ADM1 for the hydrolysis constants.

4.2.2 Validation of the models

The adapted parameters and the modifications introduced for each model were validated using independent experimental data for different substrates and operational conditions. This analysis allowed to assess the applicability of the calibrated models and to identify possible limitations. The initial conditions (in inoculum and feed) applied for modelling each experimental set are presented in Annex S. In this sub-chapter, the validation for both models is presented with the different experimental sets, previously presented in sub-chapter 4.1. As proposed by Galí et al. (2009) for the digestion of agro-wastes, the value of the first-order rate constant (k) estimated from the experimental data for each experiment (according to the methods explained in sub-chapter 3.6.1.2) was used for the kdis. These values have been presented in sub-chapter 4.1 and are summarised in Table 57, as used for the validation of the models with the corresponding experimental data.

Table 57: Summary of the first-order constants calculated from the measured CH_4 production

Substrate	Treatment	Feeding mode	Kdis (d^{-1})
GS 1	None	Batch	0.21
MS 1	None	Batch	0.33
DGS 3	Dried at 60°	Batch	0.23
	Dried at 60°	Semi-continuous	0.59
DMS 2	Dried at 60°	Batch	0.29
	Dried at 60°	Semi-continuous	0.42

4.2.2.1 Batch digestion of propionate

The calibrated values for each model presented in sub-chapter 4.2.1.3 were applied to the experimental data for the batch digestion of 1g/l of propionate under mesophilic conditions (see Annex M). The simulated evolution of the acetate and propionate concentrations for this experiment using both models is presented in Figure 59. The initial conditions are presented in Annex S, Table S.2.

The quality of the fit was better for the Lignogas model than for the Lignogas-SIM, with a RMSE 8.5% lower for the acetate concentration simulation and 22.4% lower for the propionate concentration simulation respectively. These differences were partially due to the different values used for the maximum uptake rate for acetate and the half-saturation concentration for acetate degraders but also due to the complexity and structure of the model, as using the same values in the Lignogas model do not significantly change the modelling performance. The quality of the fitting for the BPR considerably improved when applying the Lignogas model (45.3% lower).

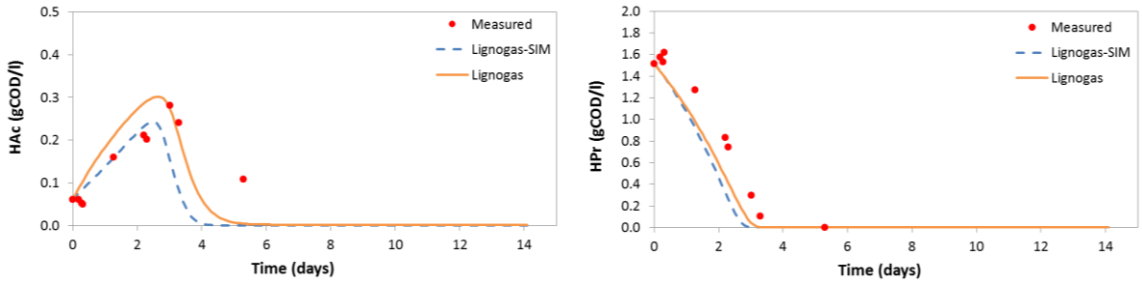

Figure 59: Measured and simulated acetate (left) and propionate (right) concentrations (expressed as gCOD/l) with the models Lignogas-SIM and Lignogas for the batch digestion of 1g/l of propionate

4.2.2.2 Batch and semi-continuous digestion of different carbohydrates

Experimental data from the batch experiment digesting glucose (OL of 7.99 gVS/l) was also used to validate the two developed models and assess their performance in describing the digestion of monosaccharides. The initial conditions used are summarised in Annex S, Table S.3. For this substrate, and in spite of the fact that the calibrated values for the maximum uptake of sugars (monomers in the case of Lignogas-SIM) were almost the same, the quality of the fit was better for the Lignogas-SIM model (see Figure 60). The reason for this may lay in the pH inhibition of acidogens, which is more significant in the case of the Lignogas model.

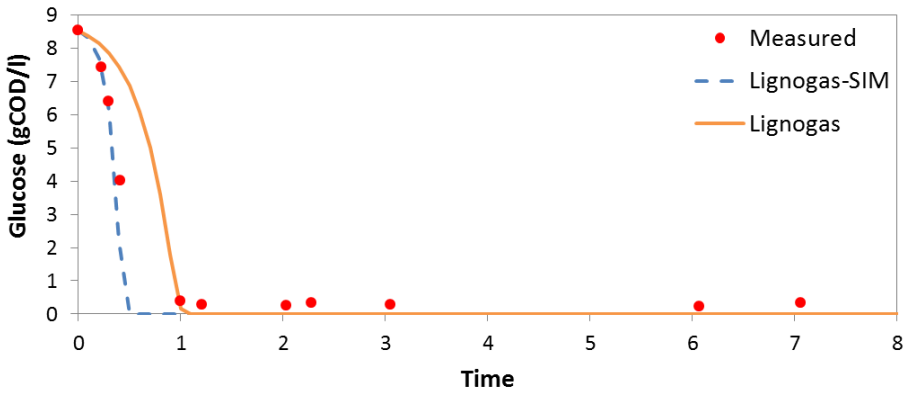

Figure 60: Measured and simulated glucose concentration (expressed as gCOD/l) with models Lignogas-SIM and Lignogas for the batch digestion of glucose (OL of 7.99 gVS/l)

Experimental data from the batch experiments with maize starch (OL of 7.99 gVS/l) and cellulose (OL of 8 gVS/l) was used to analyse the applicability of the calibrated models to properly describe the hydrolysis of the different polysaccharides commonly found in energy crops and other lignocellulosic material. In particular, specific experimental data on the concentration of these carbohydrates during digestion, measured through the Anthrone method, were used to further investigate the hydrolysis of carbohydrates. The initial conditions used for each of the experiments are presented in Annex S (Table S.4 and Table S.5 for starch and cellulose respectively).

It was clear from the initial analysis that, for both the Lignogas and the Lignogas-SIM models, the original value in the ADM1 for the hydrolysis of carbohydrates of 10 d^{-1} did not allow to properly fit the uptake of starch and cellulose. A recalibration was then performed to improve the modelling performance when using this type of carbohydrates as substrate, and compared with the default values used in the models. Given the fact that these polysaccharides do not undergo disintegration, kdis was set to 1 d^{-1} for this particular analysis, and a calibration was performed focused on the hydrolysis rate of carbohydrates (khyd_ch) for these two polysaccharides. As it can be seen in Table 58, regardless of the feeding mode (batch or semi-continuous) very similar hydrolysis rate constants were determined, thus suggesting that this operational parameter do not have an influence on the kinetic constant. Similar values were also estimated independently of the model applied.

Finally, a difference was found between the hydrolysis rate estimated for starch (0.67 d^{-1}), which is a non-structural carbohydrate, and for cellulose (0.21 d^{-1}) which is a structural carbohydrate known to have a slower degradation. These values could be used if considering the hydrolysis of different carbohydrates present in lignocellulosic material and applying first-order dynamics.

Table 58: Recalibrated carbohydrate hydrolysis rate constant (khyd_ch) for starch and cellulose for different feeding conditions, expressed in d^{-1}

Model	Default values	Cellulose		Starch
		Batch experiment	Semi-continuous experiment	Batch experiment
Lignogas	10	0.208	-	0.673
Lignogas-SIM	10	0.219	0.208	0.670

The simulations of the starch and cellulose concentrations using for the hydrolysis rate default values from the ADM1 model (10 d^{-1}) and calibrated values for the Lignogas and Lignogas-SIM models are presented in Figure 61. It shows that:

- The performance of the simulation was very poor when applying the ADM1 model with the original value (10 d^{-1}) for the hydrolysis of starch and cellulose.
- The simulation was the same (overlapping) for both models, given the same calibrated values for the hydrolysis rates (both models have the same approach for describing the hydrolysis of carbohydrates).
- The modelling performance considerably improved using calibrated values of the hydrolysis constants.
- As it has been highlighted in previous research (Golkowska, 2011; Ramirez et al., 2009), first-order dynamics did not explain satisfactory the hydrolysis of carbohydrates, as it

did not describe the initial lag phase observed for both starch (approximately 1 day) and cellulose (approximately 2 days).

- The limited simulation performance to describe the hydrolysis of polysaccharides using first-order dynamics could have an effect on the quality of the simulation of other variables. This effect was clearly shown when using directly starch and cellulose as substrate.

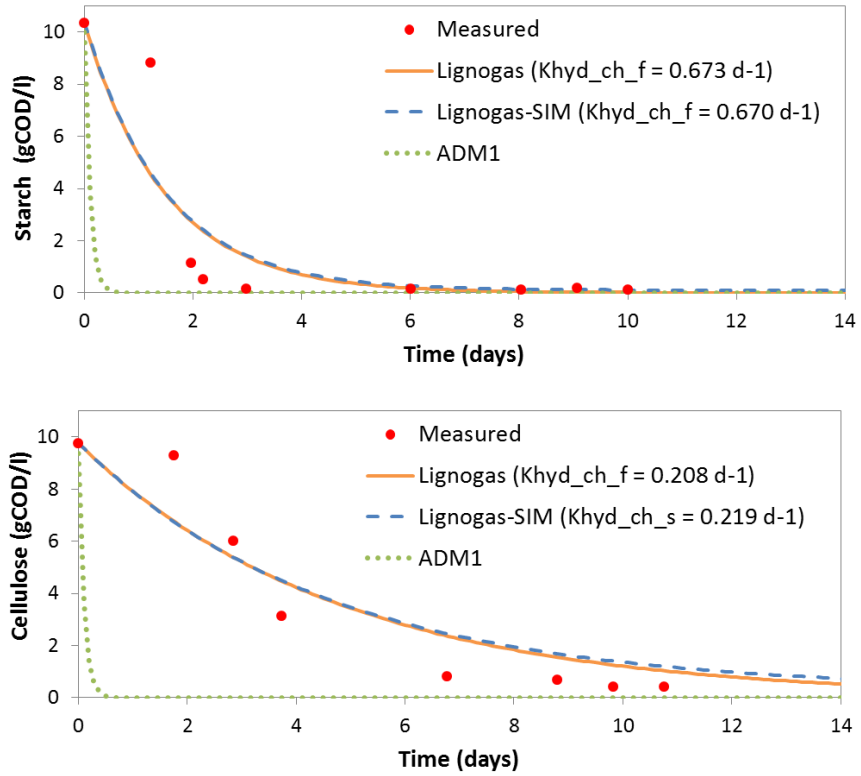

Figure 61: Measured and simulated starch (top) and cellulose (bottom) concentrations overtime using different models and thus carbohydrate hydrolysis rate constants (see Table 58) during batch digestion under mesophilic conditions. The initial conditions used are presented in Annex S (Table S.4 and Table S.5)

On the basis of these observations, both the Lignogas-SIM and the Lignogas models were applied to describe the semi-continuous digestion of cellulose under mesophilic conditions using the calibrated value of 0.21 d^{-1} for the hydrolysis rate. The experimental data used in the validation of the models were presented in sub-chapter 4.1.1.2. The initial conditions used for these simulations are summarised in Annex S, Table S.6. The simulation of 6 different variables with the two models is presented in Figure 62 for the semi-continuous digestion of cellulose at loadings of 1 gVS/l/d until the 35th day of digestion and 1.5 gVS/l/d from that day onwards.

Overall, the modelling performance was quite satisfactory for both models for the initial loading (until day 35) for all the variables considered. Some differences were nevertheless observable, particularly after the change in the loading to 1.5 gVS/l/d. For the first feeding, the Lignogas model presented a better fitting for the BPR and the evolution of the tCOD concentration. In the case of the gas composition, the quality of the fit was also better for this model after the 8th day of digestion. Both the HAc and the HPr concentration evolution were very similar for both models until the day 35 of digestion, although the uptake of acetate was slightly higher for the Lignogas-SIM model. As for the evolution of the N components, and in

particular NH_4^+-N, it is interesting to highlight that both models simulated well the steady decrease. This decrease results from the lack of N components in the feed, in spite of the occasional addition of trace elements. The minimum was nevertheless reached at different digestion times, after 40 days of digestion for the Lignogas-SIM and 50 days for the Lignogas model.

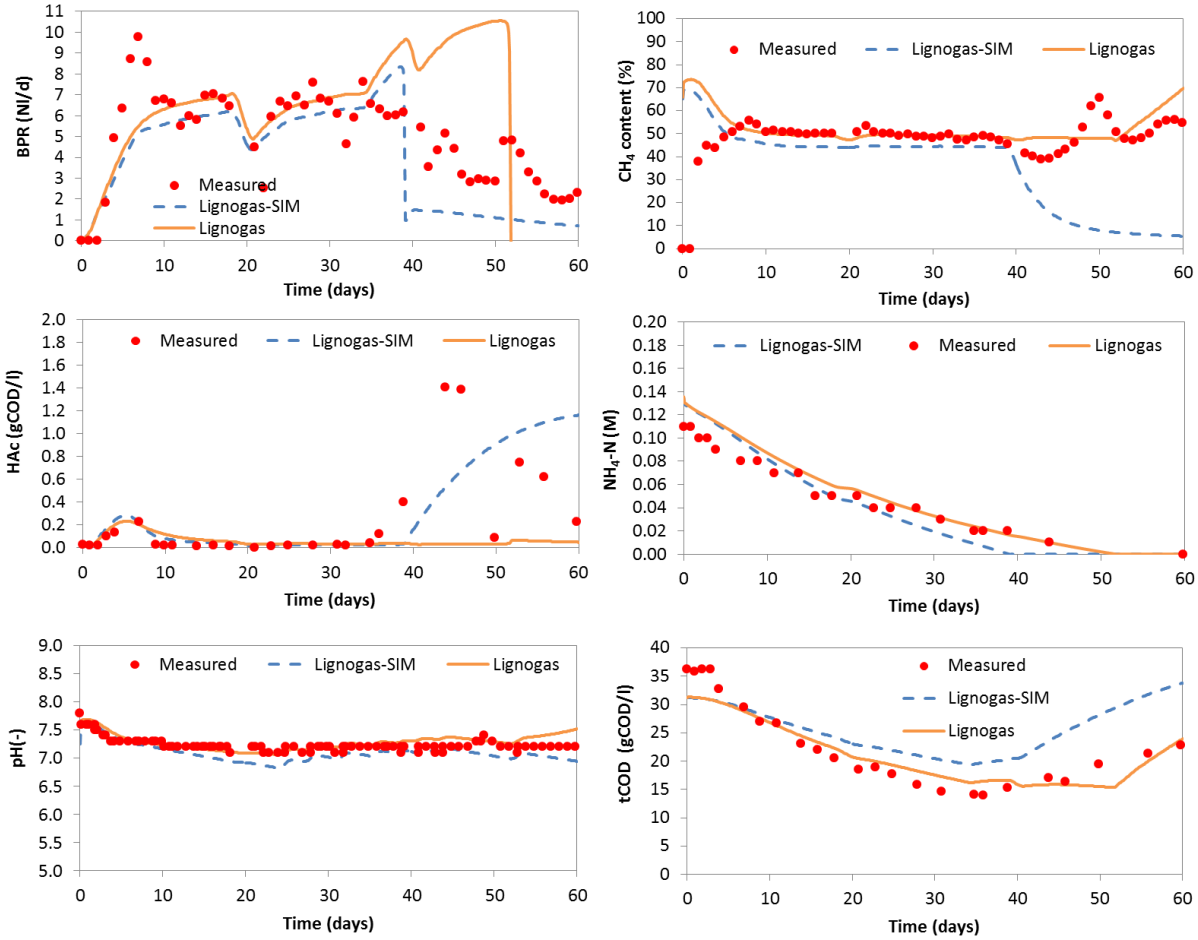

Figure 62: Measured and modelled BPR (Nl/d), CH_4 content (%), HAc concentration (gCOD/l), NH_4^+-N (moles N/l), pH and tCOD (gCOD/l) with the Lignogas-SIM (- - -) and Lignogas (___) for the semi-continuous digestion of cellulose at loadings of 1 gVS/l/d until the 35th day of digestion and 1.5 gVS/l/d from that day onwards. The initial conditions used are summarised in Annex S, Table S.6

One of the most interesting differences is nevertheless the behaviour of the two models after the day 35 of digestion. Neither of the models was capable of modelling accurately the evolution of the biogas production or its composition. It has been argued in sub-chapter 4.1.1.2 that the increase of the loading to 1.5 gVS/l/d triggered an increase in the acetate concentration to values (1.32g/l) that could have affected the enzymatic cellulose hydrolysis, thus resulting in an accumulation of cellulose concentration. On the other hand, both models correlated the changes in the gas production with the evolution of the concentration of IN (mainly NH_4^+-N), which reached almost null values after several weeks of digestion, thus triggering an important inhibition of the bacterial growth (see Annex T with the detailed simulation of the inhibition overtime for both models). In the case of the Lignogas model, this inhibition point was reached later (partially because of the recycling of the decayed biomass which disintegrates mainly as proteins) but was more intense, as it affected acidogens with a complete cessation of the biogas production. With the Lignogas-SIM, the lack of inorganic N

triggered the inhibition earlier and was accompanied with the production of H_2 and H_2 inhibition for propionate, thus resulting in its accumulation from the 40th day of digestion. This explained the important decrease in the CH_4 content in the biogas and the overall decrease in the biogas production. H_2 inhibition was not observed for the Lignogas model. Indeed, the Lignogas-SIM model seemed to be more sensible to changes and prone to process instability, partially as a result of the assumptions and simplifications that were made for its development.

4.2.2.3 Batch and semi-continuous digestion of grass silage at increasing loadings

The models, calibrated using the experimental data from the batch digestion of grass silage (GS 1, with an OL of 5.99 gVS/l), were validated with experimental data for a higher loading of 24gVS/l, experiment presented in sub-chapter 4.1.1.1. The simulation for 4 different variables with the two models is presented in Figure 63. The initial conditions used for these simulations are summarised in Annex S, Table S.7.

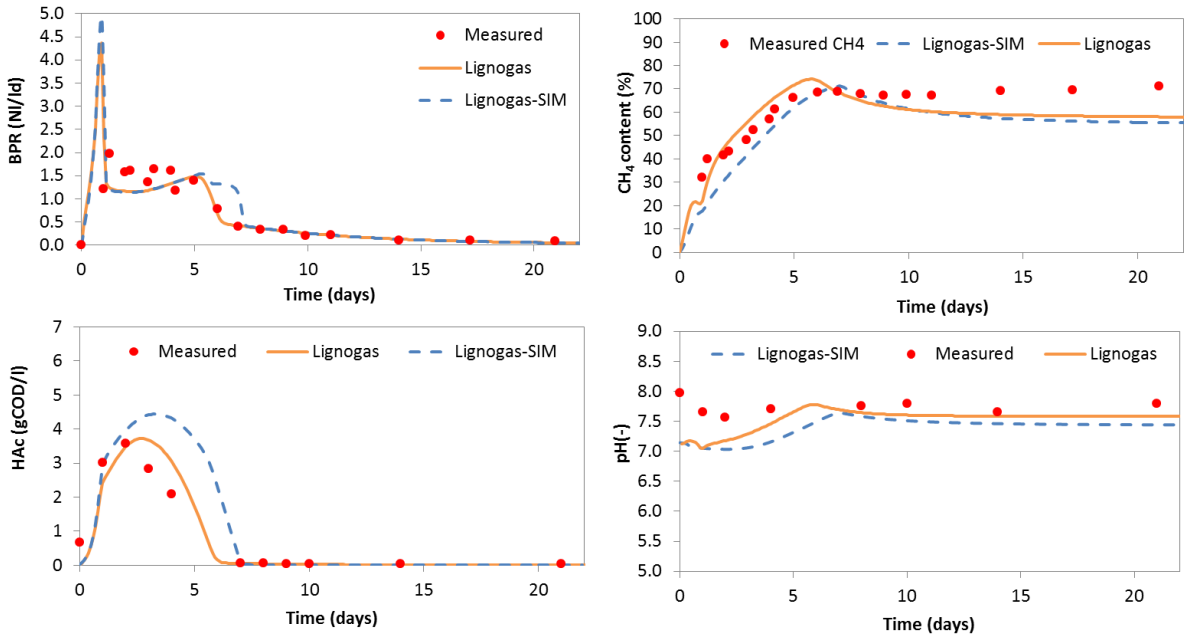

Figure 63: Simulation performed with calibrated parameters and experimental data for batch mesophilic digestion of grass silage at an OL of 24 gVS/l: BPR [Nl/d] (top left), CH_4 gas composition [%] (top right), HAc concentration in effluent [gCOD/l] (bottom left), and pH [-] (bottom right)

The simulations with calibrated parameters for both models allowed to see that while the modelling performance was satisfactory for certain variables such as the pH or the inorganic N evolution, for other important variables such as the BPR (lower values than measured) or the HAc concentration (two times higher values than measured) the fitting was not as good. It was observed that indeed, the NH_3 inhibition of acetoclastic methanogenesis was significant for both models particularly after the 5th day of digestion, with an increase of the NH_3 concentration in the reactor (related to a slight increase in the pH). It was therefore decided to calibrate the inhibitory free NH_3 concentration for acetate degrading organisms (KI_nh3_ac). The optimised value was estimated to be 0.0089M (from an original value of 0.0018 M). This new increased value allowed reducing the inhibition produced by NH_3 on acetogens and improving considerably the simulation for the BMP and the HAc concentration, as it can be seen in Figure 63. The optimisation of this parameter from default ADM1 value might became

particularly crucial in the case of substrates with high N release (i.e. with high protein content) or in the case of high loadings. This parameter was also calibrated by Wichern et al. (2009) to a value of 0.0084 M for the mono-fermentation of grass silage under mesophilic conditions.

Using this new calibrated value for KI_nh3_ac, a value of 0.59 d^{-1} for kdis (as estimated from experimental methane production data), and the fractionations values for composite material as determined for this grass silage (see Table 19 in sub-chapter 3.7.2.1), both models were further applied to simulate the semi-continuous digestion of dried grass silage (DGS 3), presented in sub-chapter 4.1.1.3. The initial conditions are summarized in Annex S (Table S.8), and the modelling results are presented for different variables considered in Annex T. Although the total duration of this experiment was of 171 days, only the latest period when using DGS 3 was considered in the modelling (from days 85 to 171, and therefore 86 days in total).

The simulation of 4 different variables with the two models is presented in Figure 64 for the semi-continuous digestion of DGS 3 at four different OLRs (1.9 gVS/l/d until day 20, 2.7 gVS/l/d until day 55, 3.3 gVS/l/d until day 69, and 4.7 gVS/l/d until day 86). It can be clearly seen that the simulation fitting was considerably better for the Lignogas model, particularly noticeable for the BPR and the HAc concentration. Indeed, overall, the performance of Lignogas was very satisfactory, except for the first 5 days, during which the model assumed transient, non-steady-state conditions due to adaptation, which was not in reality the case, as the system had been running for more than 80 days at that point. This model was therefore able to fit well the experimental data up to an OLR of 4.7 gVS/l/d in mono-digestion and without recirculation without the need of considering lactic acid in the model. This approach (i.e. addition of lactate) was undertaken by Thamsiriroj et al. (2012) to simulate 2-stage digester, loaded gradually with grass silage up to an OLR of 2.5 gVS/l/d, and with recirculation.

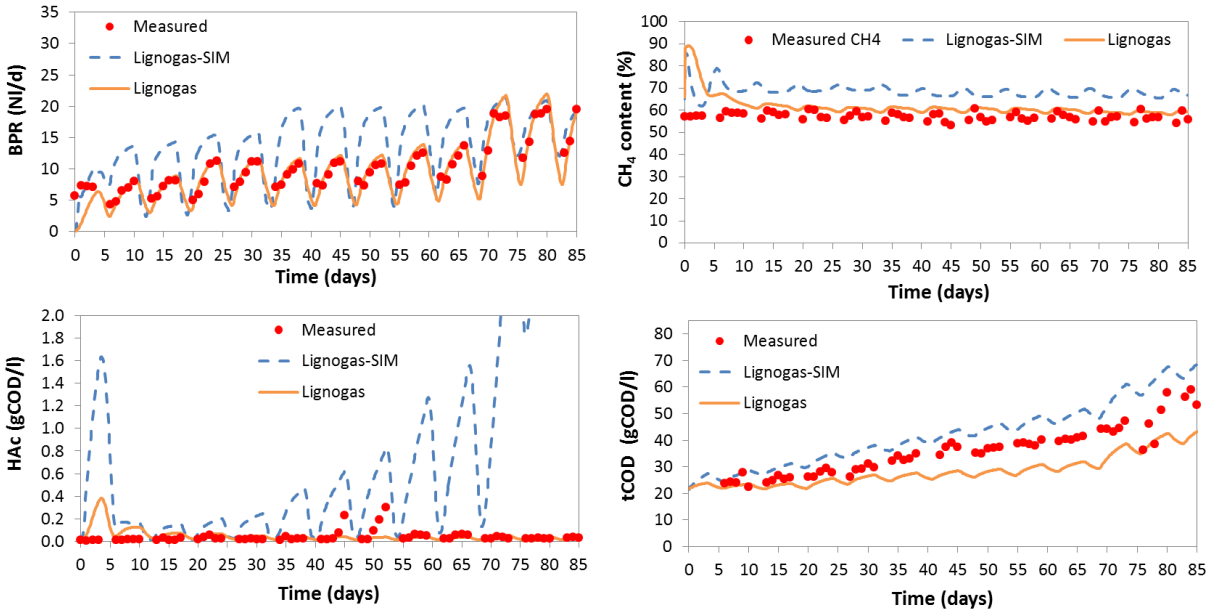

Figure 64: Measured and modelled BPR (Nl/d), CH_4 content (%), HAc concentration (gCOD/l), and tCOD (gCOD/l) with the Lignogas-SIM (- - -) and Lignogas (___) for the semi-continuous digestion of DGS 3 at different loadings (1.9 gVS/l/d until day 20, 2.7 gVS/l/d until day 55, 3.3 gVS/l/d until day 69, and 4.7 gVS/l/d until day 86)

The Lignogas-SIM, on the other hand, overestimated the daily biogas production but also the HAc concentration, as a result of the inhibition of acetate degrading organisms due to increasing free NH_3 concentration in the reactor. Indeed the model predicted an important increase of the inorganic N in the reactor that did not take place. With an estimated value of 11.97 gCOD/gCOD/l for km_ac and 0.1 gCOD/l for ks_ac, it would have been necessary to increase the value of KI_nh3_ac to 0.01 M to improve the modelling fitting for acetate concentration. The same observation was done by Wichern et al. (2009) for the mono-digestion of grass silage. Indeed, the value for this important inhibition constant will depend on the calibrated values for the acetate related uptake parameters.

4.2.2.4 Batch and semi-continuous digestion of maize silage at increasing loadings

The calibrated models were also tested to describe the digestion of different maize silages under batch and semi-continuous feeding conditions. The simulation for the BPR and the HAc concentration estimated with the two models for the digestion of fresh maize silage (MS 1) at a loading of 6gVS/l for batch feeding conditions is presented in Figure 65. A value of 0.33 d^{-1} was used for kdis (see Table 57) and the fractionation values determined for this type of maize were applied (see Table 19 in sub-chapter 3.7.2.1). The initial conditions used for these simulations are summarised in Annex S (Table S.9) and the simulation results for all the variables considered are presented in Annex T. It can be observed that overall, the quality of the fit was good for both models, with a better performance of Lignogas-SIM for the VFA and Lignogas for the BPR.

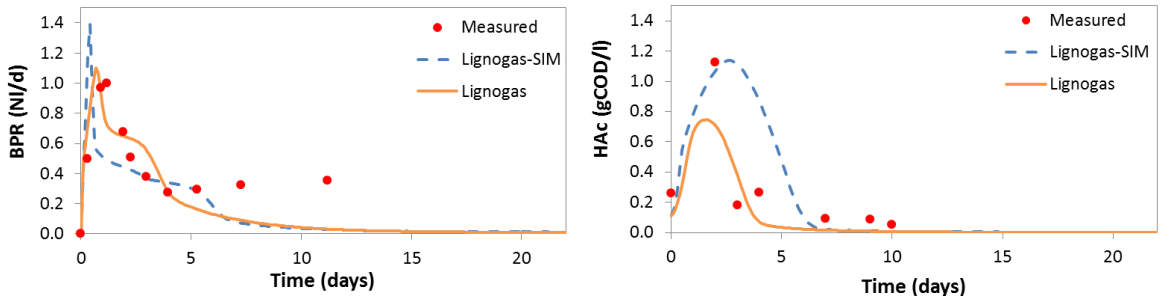

Figure 65: Simulation performed with calibrated parameters and experimental data for mesophilic batch digestion of MS 1 at an OL of 6 gVS/l: BPR [Nl/d] (left) and HAc concentration in effluent [gCOD/l] (right)

For the digestion of dried maize silage (DMS 2) under semi-continuous feeding conditions, a kdis value of 0.42 d^{-1} (see Table 57) and the fractionation values determined for this type of maize (see Table 19 in sub-chapter 3.7.2.1) were used. The initial conditions applied for these simulations are summarised in Annex S (Table S.10) and the simulation results for all the variables considered are presented in Annex T. The simulation of the BPR, the CH_4 content, the HAc concentration and the pH with the two models is presented in Figure 66 for 5 different OLRs (2 gVS/l/d until day 33, 2.5 gVS/l/d until day 54, 3.5 gVS/l/d until day 75, 6 gVS/l/d until day 103, and 10 gVS/l/d until day 125.

The quality of the fit for the BPR was satisfactory for Lignogas-SIM model for the first OLR tested (2 gVS/l/d) until the day 33 of digestion and worsened afterwards. The Lignogas model displayed a very good fitting for all the OLRs tested overall, although the performance was slightly decreased during the transient period for the first OLR and for the OLR of 10 gVS/l/d. For other parameters such as the VFA concentrations, the gas composition or the pH, the

Lignogas displayed a better modelling performance than the lighter version. Particularly poor was the simulation of the HAc concentration which was largely overestimated from the day 33 day of digestion onwards (after increasing the initial OLR to 2.5 gVS/l/d) for the Lignogas-SIM model. This was the main reason for the unsatisfactory simulation of the tCOD concentration in the reactor for the Lignogas-SIM model. This elevated concentration of HAc resulted from the inhibition of the acetogenic methanogenesis by the free NH_3 in the reactor (in spite of the calibrated value for this constant). Indeed, the inorganic N increased overtime for this model above the measured levels. This ultimately resulted in lower predictions in the biogas production, as can be observed in Figure 66.

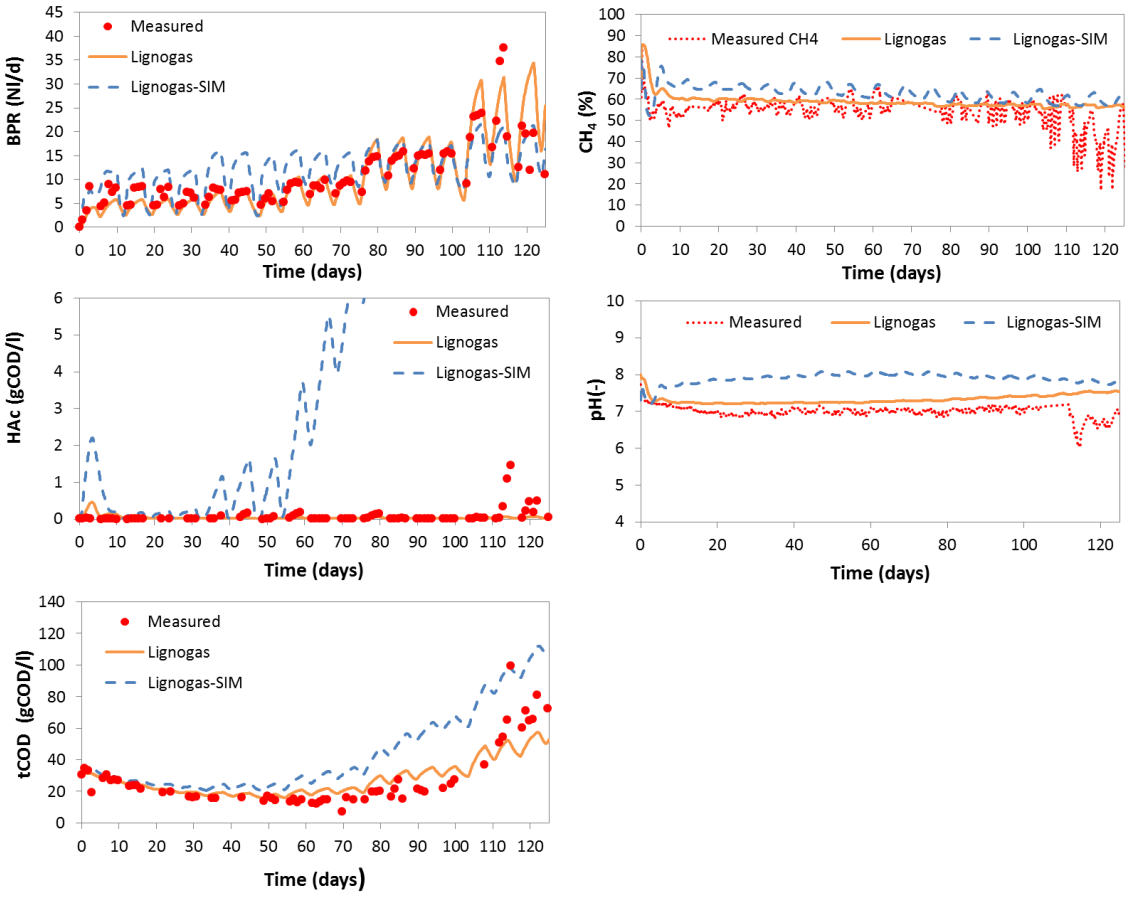

Figure 66: Measured and modelled BPR (Nl/d), CH_4 content (%), HAc concentration (gCOD/l), pH and tCOD (gCOD/l) with the Lignogas-SIM (- - -) and Lignogas (___) for the semi-continuous digestion of DMS 2 at different loadings (2 gVS/l/d until day 33, 2.5 gVS/l/d until day 54, 3.5 gVS/l/d until day 75, 6 gVS/l/d until day 103 and 10 gVS/l/d until day 125)

On the other hand, the Lignogas model did not seem to properly account for the inhibition of acidogens, which resulted in an accumulation of HPr and HBu in the reactor (especially after the shift to the highest OLR of 10 gVS/l/d at day 105 of digestion) (see Annex T with the simulation results). Consequently, the fitting for the tCOD worsened at this point. The instabilities in the CH_4 production for the last feeding of 10 gVS/l/d, and the peaks in the H_2 content in the biogas were not predicted, which in turn, could have additionally affected the HPr uptake. An increase in the concentration of lactic acid could be expected only for the last feeding (after day 110 of digestion), when peaks in the concentration of HAc were observed, followed by variations in the pH (average drop). Neither of the models was capable of predicting the fluctuations in the pH and the corresponding peaks in the HAc concentration.

Overall, the two models considered seemed to have more difficulties to properly simulate maize digestion for high OLRs, particularly the Lignogas-SIM model with its simpler structure. As it has been argued in sub-chapter 4.1, the mono-digestion of maize seems to be more sensible to inhibition with semi-continuous feeding, although the exact mechanisms are not fully understood.

For the Lignogas model, after manual calibration of some of the kinetic constants, in particular the inhibitory free NH_3 concentration for acetate degrading organisms (KI_nh3_ac) and the inhibitory H_2 concentration for propionate degrading organisms (KI_h2_pro), it was possible to better simulate the gas composition behaviour and promote the enrichment of H_2 in the gas phase. KI_nh3_ac was given its original value of 0.0018 M and KI_h2_pro was manually calibrated to a value of $3.5x10^{-8}$ gCOD/l. Figure 67 (top) shows the measured and simulated BPR with the Lignogas model with and without modification of the two mentioned inhibition constants, and the gas composition in terms of CH_4, CO_2 and H_2 with the adapted inhibition constants (bottom figure).

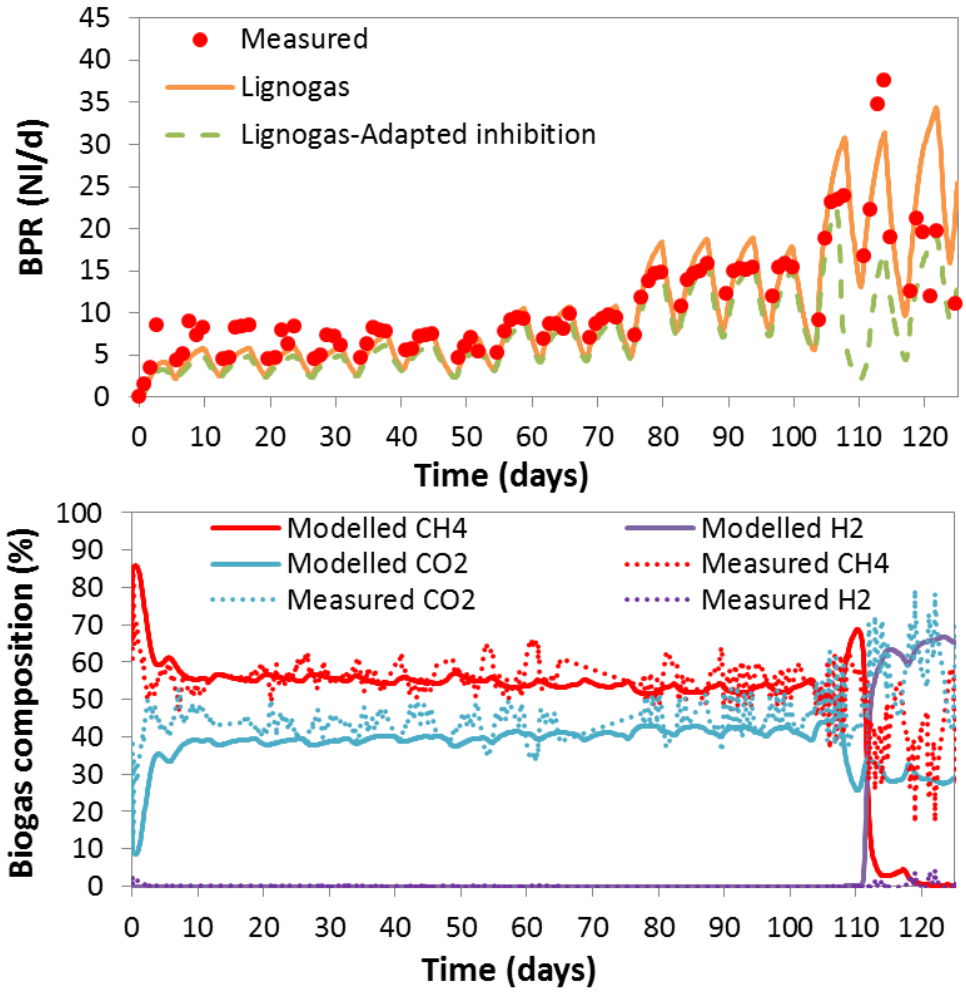

Figure 67: BPR (in Nl/d) (top) measured and modelled with Lignogas, with and without adapted inhibition factors and biogas compositions (in %) (bottom) measured and modelled with adapted inhibition factors, for the semi-continuous digestion of DMS 2 at different OLRs (2 gVS/l/d until day 33, 2.5 gVS/l/d until day 54, 3.5 gVS/l/d until day 75, 6 gVS/l/d until day 103, and 10 gVS/l/d until day 125)

It can be seen that with the adapted values for KI_nh3_ac and KI_h2_pro, the Lignogas model fitted better the evolution of the BPR and biogas composition. In particular, it is possible to see

how for the last OLR tested of 10 gVS/l/d the Lignogas model with the adapted inhibition factors was capable of simulating the drop in the CH_4 content and the increase of the H_2 content, and thus the instability associated with the high loading. But while the model predicted a complete shift into H_2 production and the cessation of CH_4 production, the measured data showed only peaks in the H_2 production related to the pH fluctuations.

Therefore, the model is still not accurate enough to properly model these rapid changes in the gas composition. The reasons that could explain this disagreement are manifold. The most likely explanation and triggering factor is the difficulty of the model to adequately predict the pH variations. Indeed, the Lignogas model with the adapted inhibition factors predicted a steady decrease in the pH starting on day 103 of digestion, resulting in a final pH of 4.4, which would have resulted in a complete cessation of the methanogenic activity, and thus an accumulation of the H_2. Moreover, the modelled evolution in the pH was related to a decreasing bicarbonate concentration, and also a modelled steady accumulation of propionate in the reactor, as a result of the new lower inhibitory hydrogen concentration for propionate degrading organisms. The predicted drop in the pH to a value below 4.5 was associated to a decrease in the methanogenic population.

Therefore, the results of this analysis highlighted the importance of the inhibitory concentration of hydrogen for propionate degrading organisms (KI_h2_pro) to properly model the degradation of high-carbohydrate-content substrates such as maize silage, particularly under extreme loading conditions. Additional optimisation of this kinetic parameter, in combination with other inhibitory factors, is necessary to properly describe transient conditions and the shift into H_2 producing systems.

Another important aspect was the regulation of the H_2 content in the biogas after the shift into H_2 production. As it can be seen in Figure 67 (bottom), the modelled content of H_2 in the biogas was of approximately 60%, while the experimental data displayed values ranging from 30 to 40% after the shift when the pH dropped to values close to 5 from the day 125 of digestion. Therefore, the current version of the Lignogas model seems to have a problem to predict the uptake and/or the production of H_2. As regards the uptake, sulphate reducing bacteria can compete with the methanogenic bacteria for HAc and H_2. Introducing this new bacterial group in the model could result in a higher consumption of H_2 and thus a lower concentration in the liquid and gas phase. The high concentration of H_2S measured in the biogas after changing to the highest OLR during semi-continuous digestion of maize silage supports the adequacy of introducing this change. As regards the inhibition of H_2 production, it has been suggested that an increase in the lactic acid concentration can negatively affect the production of H_2 (Escamilla-Alvarado et al., 2013) although the exact mechanism still requires further investigation. In any case, the model does not include lactic acid, which has a strong effect on pH values, given its relatively low pKa of 3.08. Finally, as it was discussed in sub-chapter 4.1.4.2, the pH is a key factor regulating the fermentation pathway for H_2 production, but its regulatory role in the conversion of glucose into H_2 and either HBu or HAc as end-products is not considered in the Lignogas model, nor in the ADM1 model (in both with fixed stoichiometric factors). The Lignogas model predicted an accumulation of acetate, and to a lesser extent also of butyrate in the reactor, triggered by the drop in the pH. Nevertheless, the experimental data showed that butyrate was the predominant acid at the operational average pH of 5.17, which could also explain the measured lower H_2 content in the biogas (the butyrate pathway results stoichiometrically in a lower production of H_2).

All this possibilities should be further explored in future work to better predict H_2 evolution and content.

VALIDATION OF THE MODELS – MAIN RESULTS

*The default value proposed in the ADM1 model for the hydrolysis constant of carbohydrates did not yield good modelling results when using cellulose or starch as substrate.

* Using the first-order rate constant (k) calculated from experimental data for each substrate (to characterise the overall kinetics of the process assuming hydrolysis as the rate limiting step) seems to be a good approach to determine kdis, without the need of calibration.

*Both models fitted satisfactory experimental data for the lower OLRs for a variety of substrates and feeding modes. In the case of the Lignogas-SIM, the quality of the simulations worsened for the highest OLR, often as a result of the simulated free NH_3 inhibition of acetogens.

*The Lignogas model simulated very satisfactorily the semi-continuous mono-digestion of grass silage up to a loading of 4.7 gVS/l/d (without recirculation) without the need of including lactate related process.

*Both models performed less satisfactorily in the case of maize semi-continuous digestion, which inhibition mechanisms due to the presence of faster degradable components might not be as well understood and described in the proposed models.

*The inhibition factors play a most relevant role in the simulation outcome of the models, and they have to be particularly considered in the case of high loadings. The importance of each inhibitory factor and the need to optimise the inhibition constants might depend on the substrate and operational conditions.

*Overall, the modelling performance of the Lignogas model was more satisfactory for most variables than that of its simpler version, the Lignogas-SIM model, for similar input data requirements. Indeed, the assumptions made for simplification purposes in the Lignogas-SIM model made the model more sensible to certain inhibitory mechanisms, and thus yielding erroneous predictions for certain extreme conditions. The Lignogas model is therefore propose for future testing and further development.

4.2.3 Discussion

On the basis of the different modelling results presented earlier, this sub-chapter analyses the impact of certain model and operational parameters on the modelling performance and some scenarios are explored.

4.2.3.1 Impact of the feeding mode on the model parameters determination

The wide variety of experimental data generated in this work to analyse the impact of different operational parameters allowed to further investigate the influence of some of them on the modelling outcome. Indeed, most model parameters found in literature are optimised for specific operational conditions and substrates and it is therefore interesting to analyse the effects that these might have on the proposed calibrated values to allow for comparison and analysis of applicability.

The available experimental data and modelling results presented in sub-chapter 4.2.2 shows that certain parameters might be independent of the feeding conditions, such as the hydrolysis constant for carbohydrates (khyd_ch). Indeed, Table 58 shows that this parameter is determined by the type of substrate rather than by the feeding mode, with almost identical values for semi-continuous and batch feeding for the same substrate, as calibrated for both the Lignogas and the Lignogas-SIM models.

Other parameters, on the other hand, seem to be largely determined by the type of substrate and also the feeding mode, such as the kdis, which describes the rate at which the composite material is converted into the different polymers. In this work, first-order kinetics were used to describe the disintegration of particulate organic matter, as in the ADM 1, and estimated on the basis of the experimental CH_4 production. Chapter 3 explains the methodology used for its calculation.

As it can be seen in Table 57, the calculated values differed for the same substrate under semi-continuous and batch feeding digestion for the same initial conditions. This is in line with the observations made by Golkowska et al. (2012) for the digestion of maize silage, finding higher values for semi-continuous digestion (once a day). This aspect is further discussed in sub-chapter 4.2.3 on the basis of the experimental results. The available simulation results allow the investigation of the impact of this parameter on the modelling outcome. Figure 68 presents the BPR measured for the semi-continuous digestion of DGS 3 at increasing loadings and the simulated evolution using different values of kdis: the values estimated for batch (0.23 d^{-1}) and semi-batch digestion (0.59 d^{-1}) as calculated from the methane production, and the values calibrated for Lignogas on the basis of the experimental BPR (0.43 d^{-1}). On the basis of the RMSE, the best quality of fit was obtained when using the kdis value estimated for semi-batch conditions (0.59 d^{-1}), and worsened (i.e. RMSE increased by 22%) when using the values estimated for batch conditions.

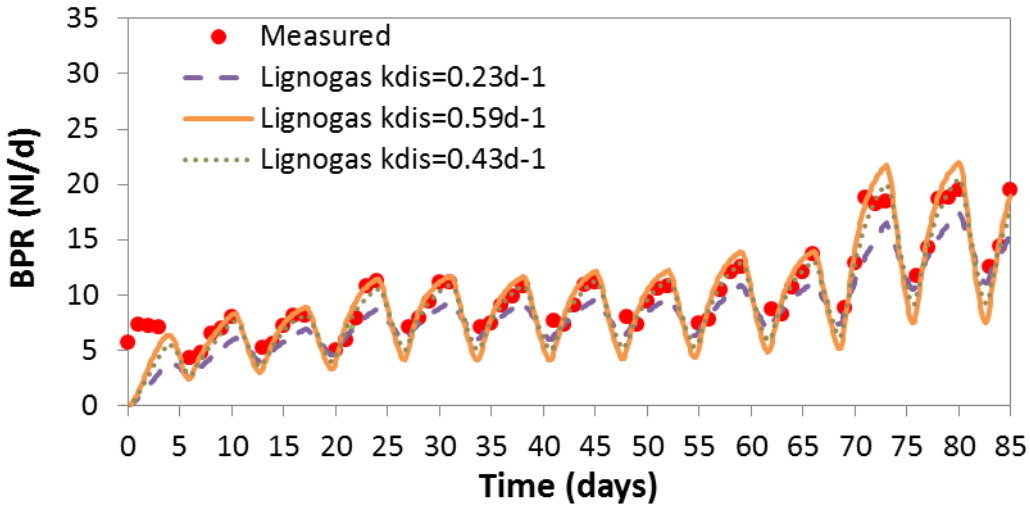

Figure 68: Simulated BPR (in Nl/d) with the Lignogas model for different disintegration values calculated for DGS 3 for different OLRs (1.9 gVS/l/d until day 20, 2.7 gVS/l/d until day 55, 3.3 gVS/l/d until day 69, and 4.7 gVS/l/d until day 86)

Figure 69 presents the evolution of the BPR measured and modelled with the Lignogas model using different kdis values (estimated for batch and semi-continuous conditions from CH_4 production data, and default value) for the semi-continuous (left) and batch (right) digestion of DMS 2 for the same initial conditions with a loading of 2 gVS/l/d for 30 days of digestion. The

impact of using the different values for the kdis can be clearly observed in both cases. For the semi-continuous digestion of DMS 2, the simulation performance was considerably better when using the value of 0.42 d^{-1}, and it worsened (RMSE increased by 61%) when using the value estimated for batch conditions. Correspondingly, the best fitting was obtained in the batch simulation when using the value of 0.29 d^{-1} and worsened (RMSE increased by 27%) when using the value estimated for semi-continuous digestion or the default value of 0.5 d^{-1} proposed originally in the ADM1 (RMSE increased by 45%). The impact of changing the kdis values seems to be more significant under semi-continuous conditions.

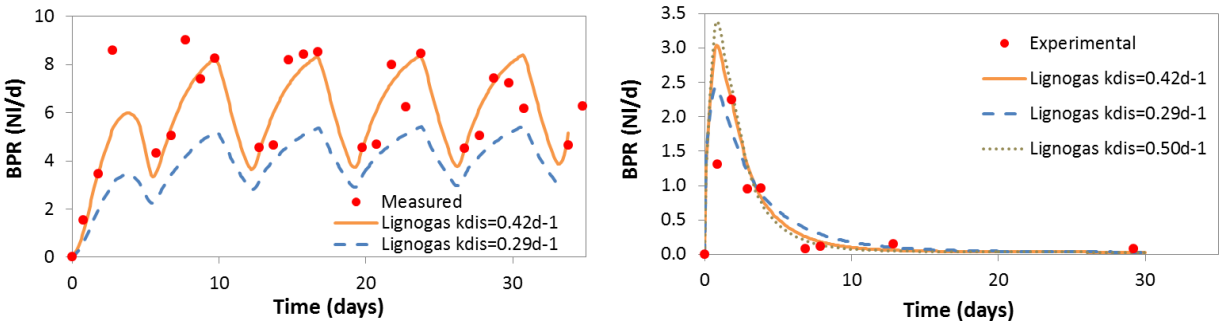

Figure 69: Simulated BPR (in Nl/d) with the Lignogas model for different disintegration values for the semi-continuous and batch digestion of DMS 2 with a loading of 2 gVS/l/d

4.2.3.2 Impact of the feedstock characteristics

Another important operational parameter analysed in this work was the feedstock characteristics and its impact on the process performance and stability. This aspect was further analysed in the light of the experimental data presented in sub-chapter 4.1.2.

The characteristics of a substrate in terms of the content in lipids, proteins, carbohydrates but also the inert fractions can be integrated in the ADM-based models by means of the fractionation factors. The method applied in this work to determine these fractions on the basis of the nutritional characteristics defined by the fodder analysis (Weende and Van Soest fractions) can be found in sub-chapter 3.7.2.1. The impact of changing the fractionation factors in the original ADM1 on the BPR and the HAc concentration during the batch digestion of grass silage (GS 1) is presented in Figure 70 for default and adapted values for the fractionation factors. It can be observed that the feedstock fractionation can have major impact on the simulation outcome, particularly for certain variables such as the VFAs concentration. The tCOD evolution can thus be largely affected, as it reflects the accumulation of intermediary products such as the VFAs, monomers and not digested composite material (i.e. accumulation of inerts).

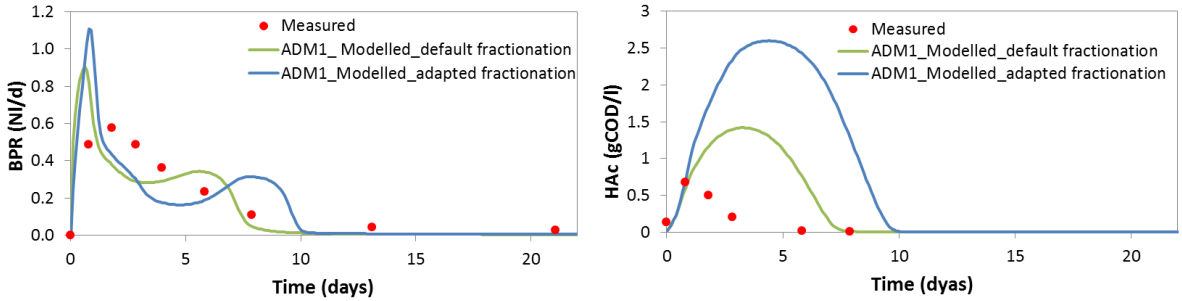

Figure 70: Simulated BPR (in Nl/d) (left) and HAc concentration (in gCOD/l) (right) for the batch digestion of GS 1 (fresh) with the ADM1 model at an OL of 5.99 gVS/l with default and adapted values for the fractionation factors

The impact of changing the feedstock characteristics during semi-continuous digestion of grass silage was analysed with the Lignogas model, investigating how the fractionation factors can contribute to better fit the BPR when changing from DGS 2 (until day 41) to DGS 3 (until day 60) for the same OLR of 1.9 gVS/l/d. The graphical representation of such analysis can be observed in Figure 71 (top).

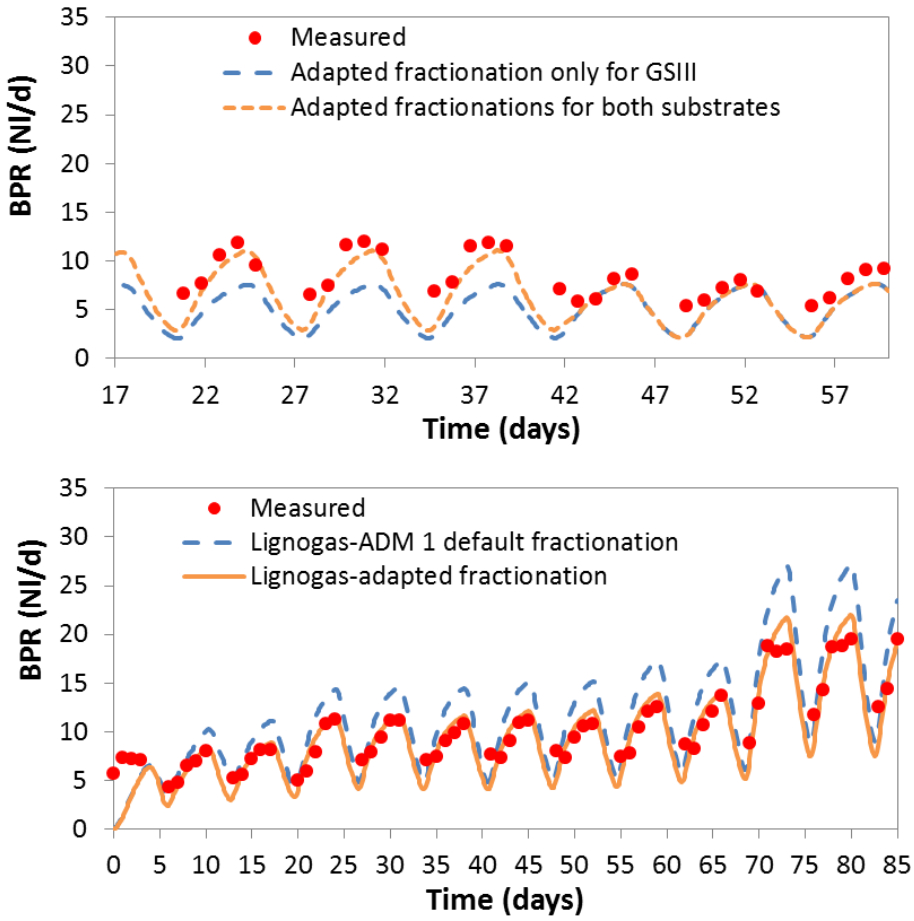

Figure 71: Simulated BPR (in Nl/d) with the Lignogas model for the semi-continuous digestion of DGS 2 (until day 41) and DGS 3 (until day 60) at an OLR of 1.9 gVS/l/d with different fractionation values (top) and for semi-continuous digestion of DGS 3 for different OLRs using default and adapted fractionation values from the substrate characterisation (bottom)

When using only the specific fractionation defined for DGS 3, the simulation was not satisfactory the first weeks when feeding DGS 2. If using the fractionation defined for each

grass used, Lignogas model simulated very satisfactory the daily biogas production for both silages used in the system.

The impact of using default and adapted fractionation factors during the mono-digestion of DGS 2 is analysed also in Figure 71 (bottom). It can be observed that the use of default values resulted in an over prediction of the daily biogas production, which translated into worse quality of the simulation (the RMSE increased by 26% for the whole period of 85 days considered and the four different OLRs tested).

4.2.3.3 Comparison of both models with ADM1

One of the main objectives of the current research was to develop a model, based on the ADM1 model, capable of describing accurately the digestion of lignocellulosic material under a wide range of operational conditions. To this end, limitations previously highlighted for the ADM1 were addressed and the Lignogas-SIM model and its extended version, the Lignogas model, were developed. Therefore, one important aspect of this work was the analysis of the impact of the changes introduced with respect to the original model, or in other words, the assessment of the added value and efficiency of the developed models.

The impact of the introduced changes to build the Lignogas model was discussed in sub-chapter 4.2.1.1. Figure 56 shows the impact of each of these changes on different variables in comparison with the ADM1 during the batch digestion of fresh grass silage (GS 1) for an OL of 5.99 gVS/l. Before calibration of the selected parameters for Lignogas, this extended version already allowed for an improvement of 7% for the BPR, 16% for the MPR, and 22% for the HAc concentration (on the basis of the RMSE), although it worsened for the HPr concentration.

This analysis was also performed for the semi-continuous digestion of dried grass silage (DGS 3), using the same initial conditions, as summarised in Table S.8, in Annex S. The simulations of the BPR produced by the original ADM1 and the Lignogas model (with the modifications specified in sub-chapter 4.2.1, and the adopted values for the different parameters summarised in Annex I) are presented in Figure 72. Overall, a better fitting to the measured data can be observed for the Lignogas model, with a decrease in the simulation performance of 36% when using the ADM1 model instead of the Lignogas model. Another important change introduced by the Lignogas model related to the microbial distribution and evolution, aspect that is further discussed in the next sub-chapter.

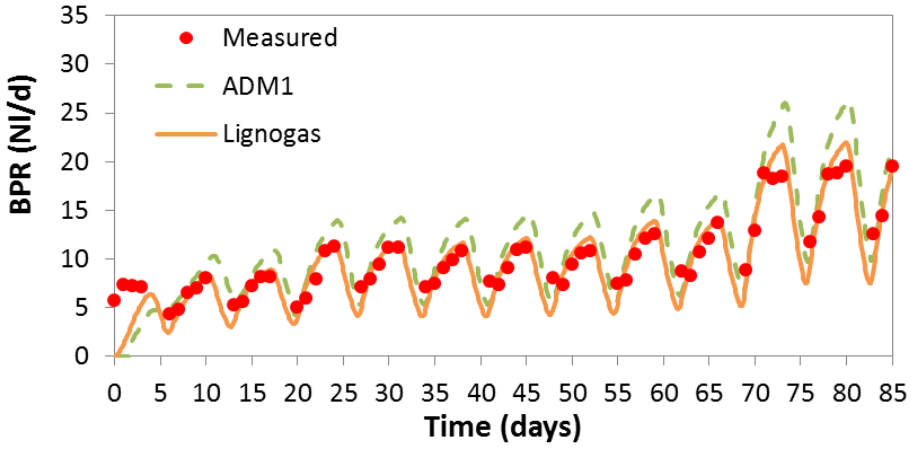

Figure 72: Measured and simulated BPR using the Lignogas (___) and the ADM1 (- - -) models for the semi-continuous digestion of DGS 3 at different OLRs

4.2.3.4 Microbial biomass evolution

As it was discussed in sub-chapter 2.2.1.4, recent investigations highlight the importance of hydrogenotrophic groups in the methanogenesis and suggest that the predominance of one or another pathway for the production of biogas depends largely on the presence of certain inhibitory substances and the concentration of VFAs. Although thermodynamically less favourable than the homoacetogenesis, the acetate oxidation process was introduced in the Lignogas model in order to promote the hydrogenotrophic biogas production. Figure 73 (left) shows the evolution of the different bacterial groups during the batch digestion of fresh grass silage (GS 1) at OL of 5.99 gVS/l. Table 59 summarises the concentration of each bacterial group.

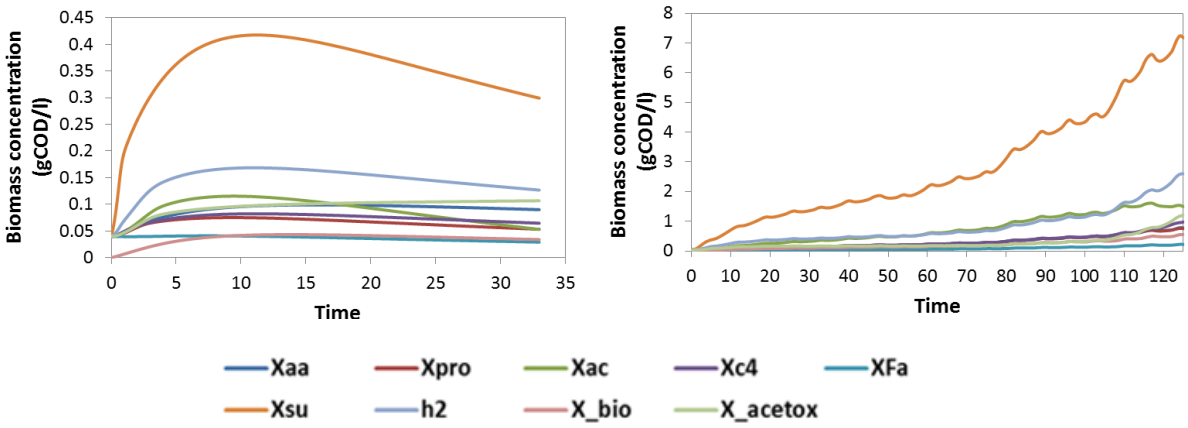

Figure 73: Evolution of the different bacterial groups during the batch digestion of GS 1 (fresh) at OL of 5.99 gVS/l (left) and semi-continuous digestion of DMS 2 at different OLRs (right) as simulated with the calibrated Lignogas model

Table 59: Final concentration (in gCOD/l) and content in the total bacterial biomass after 33 day of batch digestion of fresh grass silage (GS 1) at OL of 5.99 gVS/l as simulated with the calibrated Lignogas model. Bold letters highlight the methanogenic groups considered in both models

	Bacterial group	Final concentration (gCOD/l)		Biomass content (% total)	
		Original ADM1	Lignogas	Original ADM1	Lignogas
Xaa	Amino acid degrading organisms	0.07	0.09	13%	11%
Xpro	HPr degraders	0.04	0.05	7%	6%
Xac	**HAc degraders**	**0.12**	**0.05**	**21%**	**6%**
Xc4	HBu and HVa degrading organ-isms	0.05	0.06	8%	8%
Xfa	LCFA degrading organisms	0.08	0.03	14%	3%
Xsu	Monosaccharide degrading organisms	0.15	0.30	26%	35%
Xh2	**H_2 degrading organisms**	**0.07**	**0.13**	**12%**	**15%**
X_bio	Decayed organisms		0.03		4%
X_acetox	Acetate oxidizing		0.11		12%

The simulation results showed that for batch digestion of the grass silage considered (GS 1) the most important bacterial group was the sugar degraders one, representing 35% of the total bacterial biomass (against 26% when modelled with the original ADM1) after 33 days of digestion. One important difference was the share of LCFA degrading organisms, which decreased considerably in the Lignogas (given the small amount of lipids usually present in lignocellulosic material tested) in comparison to the ADM1 simulation (which assumes a

content of 25% in the composite material). In the Lignogas model, inactive biomass was estimated to represent 4% of the total biomass, which was to be further disintegrated and to enter the degradation process. The most important change is nevertheless the decrease of the concentration of acetate degraders (from 21% to 6% as simulated with Lignogas). Consequently, the acetate degraders passed from representing 63% to 29% of the total methanogens in the Lignogas model and H_2 degraders from 37% to 71%. As recent literature suggests, the presence of higher concentration of hydrogenotrophic methanogens can be related to the presence of high HAc concentration or high concentrations of NH_3 and H_2S (Demirel and Scherer, 2008), which was not the case for this batch experiment. PCR results obtained for the batch digestion of grass silage (GS 4) for an OL of 6 gVS/l (similar operational conditions) also showed the prevalence of acetoclastic methanogens (see sub-chapter 4.1.1.4.5, Figure 41).

Figure 73 also shows the evolution of the different bacterial groups during the semi-continuous digestion of DMS 2 at different OLRs tested (right). In this case, the evolution of the concentration of acetoclastic and hydrogenotrophic methanogens was quite similar until the day 110, in which peaks in the H_2 content in the biogas started to be noticeable (up to 5%). After 125 days of digestion and with the feeding regime of 10 gVS/l/d the hydrogenotrophic methanogens represented 64% of the total methanogens. PCR results suggest (see sub-chapter 4.1.1.4.5, Figure 40) that the concentration of Methanosaetaceae (strict acetate degraders) was important in the beginning of the feeding regime with the OLR of 6 gVS/l /d but decreased considerable at the end of this period, and during the feeding regime with the OLR of 10 gVS/l/d. This evolution is in agreement with the results found in literature.

Overall, the total biomass represented 18% of the tCOD in the reactor at the end of the feeding cycle with the OLR of 6 gVS/l/d, share that decreased to 14% at the end of the feeding cycle with the OLR of 10 gVS/l/d (with a final concentration of 15.76 gCOD/l after 125 days of semi-continuous digestion of dried maize silage). This decline in the concentration of biomass in the reactor predicted by the Lignogas model resulted mainly from the decrease in the concentration of methanogenic bacteria, which growth was gradually inhibited with the decreasing pH (see Figure 73). This evolution is in line with the results of the q-PCR analysis presented in sub-chapter 4.1.1.4.5 (Figure 40). The wash-out of methanogens increased after the shift to H_2 production in the reactor.

The results presented here suggest that mechanisms to better modulate the prevalence or one or the other group in the models require further modification so as to take into account the HAc concentration and presence of other inhibitory substances. New inhibitory factors might be modelled consequently.

4.2.3.5 Impact of N inhibition and H_2 inhibition on propionate uptake

The approach for the optimisation of the inhibition constants is different in the scarce literature found addressing the modelling of lignocellulosic material.

The inhibitory free NH_3 concentration for acetate degrading organisms (KI_nh3_ac) had to be changed to its original value to better fit for the biogas composition during mono-digestion of maize silage at different OLRs. Nevertheless, this parameter was originally changed to a value of 0.0089M to better fit the HAc concentration evolution during batch and semi-continuous digestion of grass silage, as explained in sub-chapter 4.2.2.3. The same optimisation had been

introduced by Wichern et al. (2009) to model semi-continuous digestion of grass silage. It is hypothesised that KI_nh3_ac might need to be evaluated and optimised depending on the specific substrates. Indeed, for those substrates with a higher protein content (such as grass silage), and thus with a higher IN release, microorganisms might be able to adapt better and thus tolerate higher concentrations (thus higher values for KI_nh3_ac). On the other hand, for other substrates with lower protein content (such as maize), the default KI_nh3_ac might be used.

As regards the inhibitory H_2 concentration for propionate degrading organisms (KI_h2_pro), Koch et al. (2010) or Wichern et al. (2009) changed the initial value of this constant to $4.8x10^{-8}$ gCOD/l and $4.6x10^{-8}$ gCOD/l for the digestion of grass silage, which is the same order of magnitude than the value used in this work ($3.5x10^{-8}$ gCOD/l) for improving the simulation performance for biogas composition during the semi-continuous digestion of dried maize silage (DMS 2), and two order of magnitude smaller than the values proposed in the ADM1 model. There is still scarce information about the inhibitory effect of H_2 during the mono-digestion of lignocellulosic material and H_2 inhibition constants are rarely discussed with the exception of the two mentioned studies. The current work contributes to the available knowledge in this regard.

4.2.3.6 Impact of increasing the HRT and comparison of one-stage and two-stage system

One scenario analysed with the help of the developed Lignogas model (with the adapted inhibition factors) for semi-continuous digestion of dried maize silage (DMS 2) was the increase of the HRT from 16.69 days to 33.34 days. This analysis also allowed to compare the one-stage and the two-stage configuration for the same operational conditions (OLR of 6 gVS/l/d, HRT of 33.34 days, and mesophilic temperature). Sub-chapter 4.1.4 presents and discusses the experimental results for a pH-driven two-stage configuration with H_2 production in the first hydrolytic reactor and CH_4 in the second reactor.

Table 60 summarises the methane performance of the one-stage system semi-continuously fed with dried maize silage (DMS 2) as measured and modelled with the Lignogas model for the one-stage configuration for the OLR of 6 gVS/l/d and HRT of 16.69 days. It also displays the modelled methane performance as modelled for a HRT of 33.34 days. The modelling performance for the Lignogas was very satisfactory (when compared with experimental values for a HRT of 16.69 days) even for extreme loading conditions. Indeed, the modelled SMP and MPR represented 92% and the CH_4 content in the biogas 98% of the measured values for these operational conditions.

Doubling the HRT resulted in an increase of 23% and 24% in the SMP and the MPR respectively. The modelling results also showed that the CH_4 content in the biogas only increased by 7% for the longer HRT. Additionally, Figure 74 shows the MPR evolution for the OLRs of 3.5 and 6 gVS/l/d as measured for a HRT of 16.69 days and modelled with the Lignogas model for HRTs of 16.69 and 33.34 days. Having longer HRT could have allowed to make use of the slowly degradable carbohydrates (i.e. cellulose) not used or accumulating for lower HRT, thus reaching higher degradability of the substrate. Indeed, the modelled SMP for a HRT of 33.34 days represented 90% of the BMP value, while if applying a HRT of 16.69 days, only 75% of the BMP value is reached (for the given operating conditions).

Table 60: Measured methane performance for the semi-continuous digestion of dried maize silage (DMS 2) for an OLR of 6 gVS/l/d, and modelled performance for a HRT of 16.69 days and 33.34 days with the Lignogas model

	1-stage system		
	HRT=16.69 d		HRT 33.34d (Modelled)
	Experimental	Modelled	
HRT (days)	16.69	16.69	33.34
OLR (gVS/l/d)	6.00	6.00	6.00
SMP (Nl/kgVS added)	258.07	238.56	310.89
Methane production rate (NlCH4/day)	7.58	6.95	9.13
CH_4 content (%)	0.53	0.52	0.56

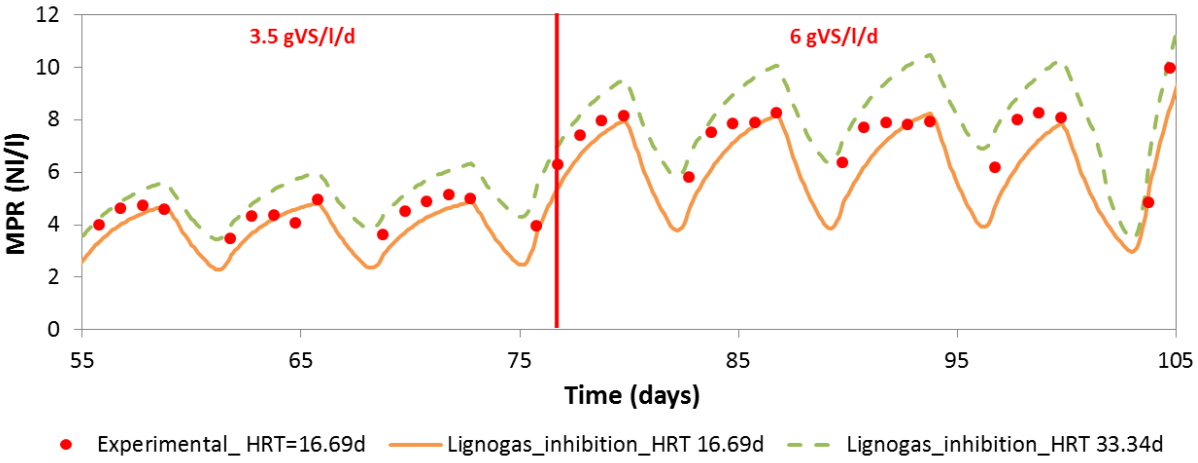

Figure 74: Measured daily MPR (in Nl/d) for semi-continuous digestion of dried maize silage (DMS 2) for a HRT of 16.69 days, and modelled MPR for a HRT of 16.69 days and 33.34 days with the HRT, for OLR of 3.5 and 6 gVS/l/d

Table 61 summarises the biogas performance for the one-stage CH_4-producing system (modelled) and the two-stage system producing H_2 and CH_4 (as measured for the feeding regime 6, see Table 15) for the same operational conditions. For the given configuration and operational conditions, the SMP for the one-stage system (310.89 Nl/kg VS) was 14% higher than for the two-stage system (267.52 Nl/kgVS in total). On the other hand, the CH_4 content in the biogas was 12% higher in the CH_4-producing reactor in the two-stage system (63% CH_4 content) than in the one-stage system (modelled 56% CH_4 content). This is explained by the fact that in the methanogenic reactor in the two-stage system, most of the degradable organic matter is fed in the form of VFAs, with higher CH_4 yields. Nevertheless, this higher CH_4 content is not enough to counteract the fact that in the one-stage system the longer HRT (of 33.34 days) allows achieving a higher SMP and MPR, as explained earlier. As commented above, the Lignogas model yields conservative estimates of the MPR and the SMP and thus, the difference between the two systems could be even slightly larger.

Table 61: Biogas performance for the semi-continuous digestion of dried maize silage (DMS 2) for an OLR of 6 gVS/l/d, as measured for a pH-driven two-stage system, and modelled (with the Lignogas model) for a one-stage system with a HRT of 33.34 days

	One-stage system (HRT 33.38 days)*	Two-stage system (HRT 33.38 days)**		
		H_2-producing reactor	CH_4-producing reactor	Total
OLR (gVS/l/d)	6	5.86		
SMP (Nl/kgVS added)	310.89	0.69	266.83	267.52
MPR ($NlCH_4$/d)	9.13	0.02	7.34	7.36
SHP (Nl/kgVS added)	-	44.99***	-	44.99
HPR (NlH2/d)	-	1.31	-	1.31
MJ/kgVS added	11.13	10.06		
MJ/d	0.33	0.28		

*Modelled with Lignogas model
**Experimental results
*** Average value for the feeding regime 6, with DMS 2 (see Table 50)

In this regard, Liu et al. (2006) conducted a comparison between a two-stage and one-stage process, using the organic fraction of MSW as substrate. The HRT was fixed at 2 days for the fermentative reactor and 15 days in the methanogenic step (thus 17 days in total). The estimated SHP was of 43 $Nl_{H2}/kgVS_{added}$ and the SMP of 500 $Nl_{CH4}/kgVS_{added}$ for the two stage process, which was 21% higher than the production of single stage anaerobic process (413 $Nl_{CH4}/kgVS_{added}$ with HRT of 15 days). Nevertheless, the comparison of the results of this study with the ones presented in this research is difficult given the different compositions of the substrates used and operational conditions. Indeed, the composition in lignocellulosic fractions in household waste is generally lower than in the case of energy crops and crop residues, and consequently the impact of the HRT is also smaller in the degradability of this type of substrate for semi-continuous feeding conditions.

On the basis of the total methane and hydrogen yields (i.e. SMP and SHP respectively) estimated for each configuration, the average energy yield was estimated per kg of VS added in the system, and tabulated in Table 61. To this end, the lower heating value (LHV), also known as net calorific value was used. The heating values of the hydrogen and methane used in this study were 10.8 MJ/m^3 and 35.8 MJ/m^3 respectively (Waldheim and Nilsson, 2001). The energy obtained from each kilogram of VS added (on average) was 11.13 MJ for the one-stage system and 10.06 MJ, thus 10 % lower for the two-stage system. Of the total energy produced per kg of VS added, only approximately 5% was from hydrogen production in the two-stage system. Therefore, increasing the hydrogen production efficiency in the hydrolytic reactor in the two-stage system, for example by setting the operating pH at 5.5, could contribute to increase the overall efficiency for this type of configuration and thus reduce the energetic difference between these two configurations.

For the comparison of the two configurations considered, the performance of the one-stage system was modelled with a longer HRT (to equal that of the two-stage system). An alternative option would have been to reduce the total HRT of the two-stage system to 16.69 days and to split the contribution from the hydrolytic and methanogenic reactors respectively. Unfortunately, the current version of the Lignogas model fails to predict accurately the H_2 content (see sub-chapter 4.2.2.4) and therefore this approach was not implemented in the analysis.

STRENGTHS AND WEAKNESSES OF THE DEVELOPED MODELS

*Overall, the ADM1 model described satisfactorily the mono-digestion of lignocellulosic material for normal loadings with only minor modifications, such as the adaptation of the fractionation factors to the substrate used and the optimisation of the inhibitory constants for standard operational conditions.

*The Lignogas model allowed nevertheless improving the quality of the simulation for the digestion of lignocellulosic material under different operational conditions, including partially extreme loading conditions. The positive benefit of using the Lignogas instead of the original ADM1 seems to be more significant under semi-continuous feeding conditions.

* The acetate oxidation process was introduced in the Lignogas model in order to take into account for this pathway for biogas production to integrate recent microbial knowledge. This addition contributed to increase the content of hydrogenotrophic methanogens but a mechanism should be included in the model to further regulate their presence.

*The disintegration constant rate is one of the most important parameters to consider, with a large impact on the process performance and simulation of different variables. It seems to be highly influenced by the feeding conditions and substrate type. Thus, when using the overall first-order rate constant value (k) estimated from experimental data for kdis, its value has to be determined for the specific feeding conditions to be applied (batch vs. semi-continuous).

*The fractionation of the feedstock is most relevant in order to ensure a satisfactory fitting of many different variables and particularly affecting the inhibition mechanisms. Its impact seems to be particularly significant in the case of semi-continuous digestion.

*Some of the inhibition constants, such as the KI_nh3_ac, seem to be substrate specific, and so it should be analysed in each case. Those substrates with a higher content of proteins seem to allow for higher values for this constant (adaptation to higher concentrations).

*Scenario analysis highlighted the relevance of the HRT during lignocellulosic material digestion and showed that doubling its value could result in an increase of the methane yield by 23%.

*Although from an energetic point of view the one-stage configuration seemed to be slightly more advantageous (10% higher energy production per kg of VS added) for the same HRT and OLR, the two-stage configuration provided a better operational stability and increased methane content in the methanogenic reactor.

5. Conclusions

Monitoring degradation during the digestion of lignocellulosic material

The results suggested that the applied method for measuring COD (with the adapted sample preparation method) can be appropriate for measuring the organic content of solid substrates commonly used in agricultural biogas plants. The COD thus measured was used with confidence as a substrate characterisation parameter and during digestion of different silages, either alone or as co-substrate, to monitor the solubilisation of the substrate.

The linear correlation between VS and COD during semi-continuous digestion was very strong for the different substrates tested, and the estimated equivalence factors ($i_{COD/VS}$) were in line with those found in the scarce literature that determine this parameter. This equivalence factors had to be determined for each new experiment as it was substrate-specific. It was also observed that with increased loading, the goodness of the correlation was less good, most probably due to sampling issues.

The proposed sample treatment for measuring the different nitrogen constituents in the substrate and during digestion seemed to be reliable and could be used with confidence. The maximum difference between the measured protein content and the measured values through NIRS was of a maximum of 5%. Values obtained for NH_4^+-N in the substrate and during digestion were in good accordance with those found in literature.

Moreover, the modelled values both for the tCOD and the NH_4^+-N are in good accordance with the measured values.

Impact of increasing the organic loading

The effects of increasing the OL during batch and semi-continuous digestion of lignocellulosic material on the process performance and stability were analysed. The results highlighted the resilience of the system to high loadings under batch conditions. For the batch digestion of grass silage, for example, signs of inhibition were observed for the two highest loadings, but the system recovered and process failure was not observed (up to an OL of 46 gVS/l). The CH_4 yield was nevertheless affected and decreased with increasing loading. The same behaviour was observed for the first-order constant (calculated on the basis of the methane production data), with lower rates (i.e. slower production) for increasing loadings.

For semi-continuous feeding, the performance of the process in terms of biogas production was affected to a different extent depending on the substrate. Thus the optimum OLR can only be determined considering the specific feedstock and operational conditions. Independently, ensuring that the necessary micro-nutrients were present in adequate quantity during digestion, allowed to increase the maximum OLR at which stable and inhibition-free operation was feasible for grass silage (3.7 gVS/l/d) and for maize silage (3.5 gVS/l/d).

In the case of the semi-continuous digestion of cellulose, a small increase in the loading (from 1 to 1.5 gVS/l/d) resulted in a large impact on the solubility of cellulose and CH_4 production. For the semi-continuous digestion of grass silage, an increase from 1.9 to 4.7 gVS/l/d, resulted in a minor impact on the CH_4 yield (with a decrease of approximately 13%), and no signs of inhibition observed, although certain fractions of the feedstock seemed to accumulate for the

two higher loadings, likely as a result of the short HRT applied. In the case of maize silage, an increase from 2 to 3.5 gVS/l/d resulted in a reduction of 18.2% in the methane yield. Signs of overloading-induced instabilities were observed at loadings of 6 gVS/l/d, which intensified for a loading of 10 gVS/l/d (with peaks in the H_2 content in the biogas or high HPr and n-HBu concentrations), with a consequent impact on the performance of the reactor. Thus, the effect of increasing loadings seemed to be larger for the semi-continuous digestion of maize silage, which could be explained partially by its lower content of slowly degradable components (such as proteins), which could reduce the inhibitory effects resulting from overloading.

In any case, the effects of increasing the loading seem to be more significant in the case of semi-continuous digestion, as the daily feeding does not allow the system to overcome or adapt to the effect of certain intermediary products that accumulate.

Impact of substrate characteristics

The impact of the feedstock characteristics, mainly in terms of the proteins, carbohydrates, lipids and inert content, on process dynamics and performance was investigated for a variety of operational conditions.

The analysis of the influence of the mixture ratios (on a VS basis) for grass and maize silage for batch trials showed that the higher the proportion of grass silage in the mixture (i.e. higher proteins content), the higher the CH_4 yield (proteins have a higher CH_4 potential). Under semi-continuous digestion, on the other hand, the CH_4 yield seemed to decrease with increasing proportion of grass silage in the feedstock, and only the CH_4 content increases. The explanation for this tendency for the CH_4 yield, contradictory to the one observed for the batch conditions, could lay in the fact that while the CH_4 potential is higher for grass silage given its higher protein content, it takes longer time to be achieved (higher content in slower degradable components such as grass silage and cellulose), and thus it might not be reached during-semi-continuous digestion, particularly in the case of short HRT (i.e. 17.7 days). For both the batch and semi-continuous trials, the higher the grass content, the slower the degradation, as indicated by the first-order rate constant.

Even using the same substrate, differences in its nutritional compositions, resulting, for example, from different levels of maturity, can have a significant impact on the performance of the process. Indeed, the results also showed a significant difference in the CH_4 yield and production rate when changing the grass silage composition during semi-continuous digestion, thus highlighting the sensibility of the continuous systems to substrate characteristics. The impact of the harvesting period or the grass species have been previously analysed but under batch conditions.

Another aspect investigated during the current research was the degradation dynamics for different types of saccharides, both polysaccharides and monosaccharides that can be present during the digestion of lignocellulosic material. In this regard, the adapted Anthrone method seemed to be reliable for measuring glucose and glucose-based polysaccharides during the digestion of lignocellulosic material. The results showed that the uptake of glucose was taking place immediately after feeding and was very fast (2 times faster than starch and 3 times faster than cellulose), while corn starch and cellulose presented a lag phase of 1.5 and 2 days respectively and a slower degradation. These results highlighted the interest of using different hydrolysis constants for both non-structural (i.e. starch) and structural (i.e. cellulose)

carbohydrates in the composite material. Weende and Van Soest fractions as measured through NIRS allowed introducing this distinction in the fractionation of carbohydrates between rapidly and slowly degradable carbohydrates.

Impact of the feeding mode

The influence of the feeding mode (semi-continuous vs. batch feeding) on the biogas performance and process dynamics were investigated for maize silage and cellulose. The results suggest that, while the final CH_4 and biogas yields are very similar independently of the feeding mode, the dynamics differ. Semi-continuous feeding seemed to present faster degradation rates than batch digestion, on the basis of the calculated first-order rate constant (for the same loading and HRT). For example, the degradation of maize silage was 1.5 faster for semi-continuous feeding, while in the case of microcrystalline cellulose the semi-continuous mode yielded rates 3 times faster than for batch conditions. This faster dynamics could be attributed to more efficient and better balanced bacterial population conditions and lack of product inhibition for the semi-continuous mode.

Inhibition mechanisms and indicators

Different types of inhibition have been observed during the increase of the OLR for the different substrates and operational conditions presented in this work.

For the batch digestion of grass silage, clear signs of instability due to acidification were observed for the two highest loadings (of 35.78 gVS/l and 46.37 gVS/l) as highlighted by the HPr/HAc and TVFA/TIC ratios, corresponding to very high concentration of HAc and HPr. This constituted a reversible inhibition as the system recovered once the HPr concentration decreased, after 10 days to 13 days of digestion.

Particularly interesting is the chain inhibition mechanisms observed for the semi-continuous digestion of cellulose, affecting different steps of the digestion. The increase in the OLR to 1.5 gVS/l/d, resulted after 5 days in a fluctuating biogas production and an impaired biogas yield, related to an accumulation in the HAc concentration above 1.3 g/l (inhibited methanogenesis), which in turn could have affected the mechanisms of cellulose enzymatic hydrolysis, thus reducing its solubilisation and resulting in accumulation in the reactor. Given that the pH remained above 7 for the duration of the experiment, inhibitions of methanogens due to low pH is not likely. The inhibition of microorganisms and in particular methanogens could have been induced by the very low concentration of IN, registered in the reactor after 40 days of digestion, which in turn could have triggered the accumulation of HAc. 25 days after changing the loading, the system still presented important fluctuations.

The results showed that anaerobic digestion of grass silage in CSTRs could be stable and feasible and do not present any overloading-induced instability in the tested range, from 1.9 gVS/l/d up to 4.7 gVS/l/d (with the addition of trace element solutions). Nevertheless, an accumulation of certain fractions of the feedstock and a lower first-order constant were observed for the highest loading, which could suggest that the system is surpassing its optimum for the applied short HRT of 17.7 days. The IN, mainly NH_4^+-N, steadily decreased overtime and never went above concentrations reported as inhibitory. The average ratio of TVFA to TIC was above the critical limit of 0.4 after increasing the OLR to 3.7gVS/l, possibly in relation to an increase in the concentration of lactate in the reactor, without having a noticeable correlation with other stability parameters.

As for the semi-continuous digestion of maize silage, the increasing OLR was translated into an increase of the HPr concentrations. With the daily additions of buffering capacity, these high concentrations did not impact the pH. But for the highest OLR of 10 gVS/l/d, it became more difficult to control the pH. The pH started to fluctuate, which would have affected the activity of the methanogens, resulting in H_2 accumulation (observed peaks in the biogas), and in turn, increased the n-HBu and additionally the HPr concentrations. HPr concentration already started to peak for the OLRs of 3.5 gVS/l/d and of 6 gVS/l/d above concentrations considered as problematic, thus earlier than the TVFA/TIC ratio increased above 0.5 for the OLR of 10 gVS/l/d. This highlights the role of the HPr concentration as an important indicator of early process instabilities, while TVFA/TIC ratio above 0.5 flags out ongoing acidification requiring correction. The n-HBu concentration did not seem to be an indicator of imminent instability but rather of ongoing acidification. Contrary to what happened for the batch digestion of grass, the HPr concentration only decreased when the pH dropped to values close to 5, but the CH_4 production had already ceased, thus the inhibition was not reversible.

The calculated first-order rate constant seems to reflect well ongoing changes in degradation process, particularly when estimated from the experimental VS or COD concentration in the reactor, as it can point out possible accumulation of composite material, and therefore problems in the solubility of the feedstock, which might be particularly important in the case of lignocellulosic material (with slowly degradable fractions) under semi-continuous and continuous feeding conditions, as it can impact the efficiency of the process.

Hydrogen production from maize silage

During semi-continuous digestion of maize silage, CH_4 production was shifted towards H_2 production by increasing the OLR (to 10 gVS/l/d) and removing the addition of buffering capacity. Given that the VFA had increased previously with increasing loadings (particularly n-HBu and HPr), this resulted in a decrease of the pH value to 5, which in turn, inhibited acetate degrading organisms, and thus the CH_4 content in the biogas decreased to values below 1%. At this point the loading was decreased again to 6 gVS/l/d and pH kept between 5 and 5.5 in this reactor that became the hydrolytic reactor and a second methanogenic reactor was initiated to run in series. The feasibility and performance of applying a two-stage configuration was analysed. An average specific H_2 production of 49.17 NlH_2/kgVS was obtained, which is in the range with values reported previously in literature during semi-continuous digestion in CSTR reactors for different substrates. The average H_2 content under these conditions was 35%. The results highlighted the important role that the operating pH can have in the H_2 yield, in particular through the regulation of the production pathway. At the average operational pH of 5.17 in the H_2-producing reactor, the butyrate pathway (i.e. H_2 production from glucose fermentation with production of butyrate) was the predominant one. Increasing the pH to values between 5.5 and 6 could promote the acetate pathway and thus increase the H_2 yield. Of the estimated total energy produced per kg of VS added in the two-stage system, only approximately 5% was from hydrogen production. Therefore, increasing the hydrogen production efficiency in the hydrolytic reactor could contribute to increase the overall energetic efficiency for two-stage configuration, which for the analysed operational conditions and substrate, seemed to be less advantageous than for the one-stage configuration (modelled for the same HRT and OLR).

The work presented in this dissertation shows the feasibility of shifting the methanogenic process into a H_2 production process by adjusting the OLR and regulating the pH during semi-continuous digestion of maize silage. This work provides new insight into the production of bio-H_2 from lignocellulosic material, which until now had only been shown for grass silage.

Modelling of lignocellulosic material

Two different models were built and calibrated based on the ADM1, to be applied to describe the anaerobic digestion of lignocellulosic material: one extended version, the Lignogas model, and the lighter version, the Lignogas-SIM. The models address some previously highlighted limitations of ADM1 and try to integrate current knowledge about the microbial composition in biogas plants.

Overall, the ADM1 model provides a very good modelling performance for the batch and semi-continuous digestion of different lignocellulosic material after introducing the necessary stoichiometric coefficients for the disintegration and decay of biomass processes to close the N and C balances. Nevertheless, the results suggested that the proposed models, and in particular the Lignogas model, allowed further improving the quality of the simulation. Both developed models fitted satisfactory experimental data for the lower standard OLRs for a variety of substrates and feeding modes. kdis was identified in both models as one of the most important parameters to consider, with a large impact on the process performance and simulation of different variables. Using detailed feedstock characterisation data, the proposed model can be used to explore different scenarios and better design future experiments.

One of the novelties of the developed models is that they were tested and evaluated using experimental data from extreme loading or pH conditions, which helped to evaluate their strengths and weaknesses. In the case of the Lignogas-SIM, the quality of the simulations worsened for the highest OLR, often as a result of the simulated free NH_3 inhibition of acetogens. As for the Lignogas model, its application for the simulation of the semi-continuous digestion of maize silage highlighted some limitations. After adapting some of the inhibition factors, the model was capable of simulating the drop in the CH_4 content and the increase of the H_2 content, and thus the instability associated with the high loading, but it was not capable of modulating the shift (too high estimated H_2 content in the biogas), resulting from difficulties at simulating the measured fluctuations in the pH (i.e. the model predicts a sharp drop), the pH dependence of the glucose fermentation pathway for H_2 production, and probably the uptake of H_2.

The feedstock characteristics determine the release of certain intermediary products which, under specific conditions, can become inhibitory for some processes, thus affecting the overall performance. Therefore, the feedstock fractionation factors can have a most relevant impact on some inhibition functions under certain conditions, particularly at high loadings. The importance of each inhibitory factor and the need to optimise the inhibition constants might depend on the substrate and operational conditions.

In this regards, there is still scarce information about the inhibitory effect of H_2 during the mono-digestion of lignocellulosic material and H_2 inhibition constants are rarely discussed. The current work contributes to the available knowledge in this regard.

The addition of the acetate oxidation process in the Lignogas model contributed to increase the content of hydrogenotrophic methanogens but a mechanism should be included in the model to further regulate their presence, to better fit experimental observations.

6. Outlook

Much research has been done to date for analysing the impact of different agronomic parameters on the biogas performance during the anaerobic digestion of maize and grass silage, two of the most popular energy crops in central and northern Europe. The current research provides further insight into the impact of different operational parameters, including the organic feeding rate or the feedstock characteristics. Moreover, the limits of stable operation have been explored for different substrates. Results can be used to enhance the performance of biogas plants using this type of substrate. Efforts are being put in recent years on the analysis of the performance and economic feasibility of new energy crops such as miscanthus, switch grass, festuca, or hemp. Additional analysis about their long-term digestion, under different operational conditions, as pointed out in the present work, should also be conducted in order to optimise its digestion and detect potential problems. It would be useful to get a better insight into the stability and process performance of substrates used in biogas plants more rich in proteins and lipids (that can be found, for example, in MSW) during long-term operation and at different operational conditions). This line of research is currently being addressed in the University of Luxembourg.

For the long-term semi-continuous experiments presented in this dissertation, trace elements addition was necessary to avoid the possible impact of low or insufficient concentration on the biogas performance. Although some studies have analysed the effect of the lack of micronutrients, there is still no standard procedure regarding the amount to be added and frequency required. This aspect shall be further analysed and determined in the future given its influence on the stability and also to allow for better comparison of the results.

The possibility of applying the Van Soest method (chemical analysis) to monitor the degradation of structural carbohydrates was analysed. Preliminary results showed unsatisfactory results. Due to time constraints, it was not possible to define the modifications that were required, in the method or the sample preparation. It could be interesting that future research investigate the required changes to allow for the assessment of the degradability of slowly degradable fractions during digestion.

The present work shows the feasibility of producing H_2 from semi-continuous digestion of maize silage. Given the interest in bio-H_2 and the scarce information in this regard in the field of lignocellulosic material digestion, it could be interesting to further investigate the optimisation of this process, in terms, for example, of the pH regulatory role for the fermentation pathway from glucose to H_2 production and the operating temperature. Work in this regard is being carried out currently in the University of Luxembourg (i.e. H_2-producing reactor under thermophilic conditions). Moreover, the use and application of the obtained biogas mainly constituted by H_2 and CO_2 should be explored more in detail. One possibility could be to re-inject this gas into a methanogenic reactor, to enhance the CH_4 production (application as substrate).

As regards the modelling of lignocellulosic material digestion, two distinct approaches for modelling have been tested and compared with the ADM1 model. Some limitations have been highlighted when validating the models with extreme feeding conditions. It was observed that the model had difficulties to regulate the H_2 concentration (overestimation), which can result

from a problem with the uptake and/or the production of H_2 and the prediction of the pH evolution in current models. An important modification that could be envisaged to address this issue relates to the regulation of the fermentation of glucose for H_2 production through the butyrate or the acetate pathways with the pH. Additionally, the effect of introducing simultaneously sulphate reducing bacteria (which would result in a higher consumption of H_2 and thus a lower concentration in the liquid and gas phase) and the production and uptake of lactic acid (which has been suggested to have an inhibitory effect on H_2 production and strongly affects pH evolution) could also be explored to investigate the mechanisms of H_2 production, including inhibition, and the different trade-offs, which are not well understood.

The modelling results also suggest that a mechanism to better modulate the prevalence of hydrogenotrophic and acetoclastic methanogens taking into account the HAc concentration and presence of other inhibitory substances needs to be introduced to better reflect the latest knowledge about methanogenic population in biogas plants

Process models, such as the ones presented in this work, are a good possibility to gain more insight into the biogas process. The Lignogas model could be used to perform scenario analysis for different substrates and their mixtures at different loadings. This knowledge can be used to optimise the operation of biogas plants (i.e. scale up) and to better define and implement effective control tools. Work addressing control strategies and energy management of biogas plants is being carried out in the University of Luxembourg, using data presented in this dissertation.

REFERENCES

AEBIOM. (2009). A Biogas Road Map for Europe. *World Review*. Brussels - Belgium. Retrieved from www.aebiom.org

Amon, T., Amon, B., Kryvoruchko, V., Machmu, A., Hopfner-sixt, K., Bodiroza, V., and Hrbek, R. (2007). Methane production through anaerobic digestion of various energy crops grown in sustainable crop rotations. *Bioresource Technology*, *98*, 3204–3212. doi:10.1016/j.biortech.2006.07.007

Amon, T., Amon, B., Kryvoruchko, V., Zollitsch, W., Mayer, K., and Gruber, L. (2007). Biogas production from maize and dairy cattle manure—Influence of biomass composition on the methane yield. *Agriculture, Ecosystems and Environment*, *118*(1-4), 173–182. doi:10.1016/j.agee.2006.05.007

Angelidaki, I. and Ahring, B. K. (1994). Anaerobic thermophilic digestion of manure at different ammonia loads: Effect of temperature. *Water Research*, *28*(3), 727–731. doi:10.1016/0043-1354(94)90153-8

Angelidaki, I., Alves, M., Bolzonella, D., Borzacconi, L., Campos, J.L., Guwy, A. J., Kalyuzhnyi, S., Jenicek, P., and van Lier, J.B. (2009). Defining the biomethane potential (BMP) of solid organic wastes and energy crops: a proposed protocol for batch assays. *Water Science and Technology : A Journal of the International Association on Water Pollution Research*, *59*(5), 927–34. doi:10.2166/wst.2009.040

Angelidaki, I., Ellegaard, L., and Ahring, B. (1999). A comprehensive model of anaerobic bioconversion of complex substrates to biogas. *Biotechnology and Bioengineering*, *63*(3), 363–72. Retrieved from http://www.ncbi.nlm.nih.gov/pubmed/10099616

Antonopoulou, G., Gavala, H. N., Skiadas, I. V., and Lyberatos, G. (2012). Modeling of fermentative hydrogen production from sweet sorghum extract based on modified ADM1. *International Journal of Hydrogen Energy*, *37*(1), 191–208. doi:10.1016/j.ijhydene.2011.09.081

APHA–AWWA–WPC. (1998). *Standard methods for the examination of water and wastewater* (20th ed.). Washington, DC.

Batstone, D. J., Keller, J., Angelidaki, I., Kalyuzhnyi, S. V., Pavlostathis, S. G., Rozzi, A., Sanders, W.T.M., Siegrist, H., and Vavilin, V. A. (2002). *Anaerobic Digestion Model No.1 (ADM1) Scientific and Technical Report No. 13*. (J. Hammett, Ed.). London - United Kingdom: IWA Publishing.

Bauer, A., Leonhartsberger, C., Bösch, P., Amon, B., Friedl, A., and Amon, T. (2009). Analysis of methane yields from energy crops and agricultural by-products and estimation of energy potential from sustainable crop rotation systems in EU-27. *Clean Technologies and Environmental Policy*, *12*(2), 153–161. doi:10.1007/s10098-009-0236-1

Benito, P. C., Greger, M., and Sibisi-Beierlein, N. N. (2012). Optimisation of the co-digestion of maize and grass silage: Influence of the substrate mixture on the biogas yield. In *Fourth International Symposium on Energy from Biomass and Waste* (pp. 90–95). Venice.

Biermayr, P., Cremer, C., Faber, T., Kranzl, L., Ragwitz, M., Resch, G., and Toro, F. (2007). *Bestimmung der Potenziale und Ausarbeitung von Strategien zur verstärkten Nutzung von erneuer baren Energien in Luxemburg*. Retrieved from https://www.gouvernement.lu/4608317/endbericht.pdf

Biernacki, P., Steinigeweg, S., Borchert, A., and Uhlenhut, F. (2013a). Application of Anaerobic Digestion Model No. 1 for describing anaerobic digestion of grass, maize, green weed silage, and industrial glycerine. *Bioresource Technology*, *127*(1), 188–94. doi:10.1016/j.biortech.2012.09.128

Biernacki, P., Steinigeweg, S., Borchert, A., and Uhlenhut, F. (2013b). Bioresource Technology Application of Anaerobic Digestion Model No . 1 for describing anaerobic digestion of grass , maize , green weed silage , and industrial glycerine. *Bioresource Technology*, *127*(1), 188–194. doi:10.1016/j.biortech.2012.09.128

Blumensaat, F. and Keller, J. (2005). Modelling of two-stage anaerobic digestion using the IWA Anaerobic Digestion Model No. 1 (ADM1). *Water Research*, *39*(1), 171–83. doi:10.1016/j.watres.2004.07.024

Boe, K. (2006). *Online monitoring and control of the biogas process*. *Dissertation*. Technical University of Denmark.

Boe, K. and Angelidaki, I. (2009). Serial CSTR digester configuration for improving biogas production from manure. *Water Research*, *43*(1), 166–72. doi:10.1016/j.watres.2008.09.041

Boe, K., Batstone, D., Steyer, J.-P., and Angelidaki, I. (2010). State indicators for monitoring the anaerobic digestion process. *Water Research*, *44*(20), 5973–5980. doi:10.1016/j.watres.2010.07.043

Boyle, W. C. (1977). Energy Recovery from Sanitary Landfills. In A. G. Schlegel and J. Barnea (Eds.), *Microbial Energy Conversion* (pp. 119–138). Gottingen: Pergamon Press.

Braun, R., Weiland, P., and Wellinger, A. (2010). *Biogas from energy crop digestion*. *International Energy Agency Bioenergy-Task 37*. Retrieved from http://www.iea-biogas.net/files/daten-redaktion/download/energycrop_def_Low_Res.pdf

Bruni, E., Jensen, A. P., Pedersen, E. S., and Angelidaki, I. (2010). Anaerobic digestion of maize focusing on variety, harvest time and pretreatment. *Applied Energy*, *87*(7), 2212–2217. doi:10.1016/j.apenergy.2010.01.004

Buswell, A. M., and Mueller, H. F. . (1952). Mechanism of methane fermentation. *Ind Eng Chem*, *44*, 550–552.

Cavinato, C., Fatone, F., Bolzonella, D., and Pavan, P. (2010). Thermophilic anaerobic co-digestion of cattle manure with agro-wastes and energy crops: comparison of pilot and full scale experiences. *Bioresource Technology*, *101*(2), 545–50. doi:10.1016/j.biortech.2009.08.043

Cecchi, F., Traverso, P., Pavan, P., Bolzonella, D., and Innocenti, L. (2003). Characteristics of the OFMSW and behaviour of the anaerobic digestion process. In J. Mata-Alvarez (Ed.), *Biomethanization of the organic fraction of municipal solid wastes.* (pp. 141–179). London: IWA Publishing.

Chen, Y., Cheng, J. J., and Creamer, K. S. (2008). Inhibition of anaerobic digestion process: a review. *Bioresource Technology*, *99*(10), 4044–64. doi:10.1016/j.biortech.2007.01.057

Chen, Y. and Hashimoto, A. (1978). Kinetics of methane fermentation. In *Proceedings of Biotechnology and Bioengineering Symposium* (pp. 269– 282).

Chen, Y. R. and Hashimoto, A. G. (1980). Substrate utilization kinetic model for biological treatment process. Biotechnol. *Biotechnology and Bioengineering*, *12*, 2081–2095.

Chu, C. F., Li, Y. Y., Xu, K. Q., Ebie, Y., Inamori, Y., and Kong, H. N. (2008). A pH- and temperature-phased two-stage process for hydrogen and methane production from food waste. *International Journal of Hydrogen Energy*, *33*, 4739–4746. doi:10.1016/j.ijhydene.2008.06.060

Chynoweth, D. P., Turick, C. E., Owens, J. M., Jerger, D. E., and Peck, M. W. (1993). Biochemical methane potential of biomass and waste feedstocks. *Biomass Bioenergy*, *5*(1), 95–111.

Cirne, D. G., Lehtomäki, A., Bjornsson, L., and Blackall, L. L. (2007). Hydrolysis and microbial community analyses in two-stage anaerobic digestion of energy crops. *Journal of Applied Microbiology*, *103*(2007), 516–527. doi:10.1111/j.1365-2672.2006.03270.x

Comino, E., Rosso, M., and Riggio, V. (2010). Investigation of increasing organic loading rate in the co-digestion of energy crops and cow manure mix. *Bioresource Technology*, *101*(9), 3013–9. doi:10.1016/j.biortech.2009.12.025

Contois, D. E. (1959). Kinetics of bacterial growth: relationship between population density and specific growth rate of continuous cultures. *Journal of General Microbiology*, *21*, 40–50.

Cuetos, M. J., Fernández, C., Gómez, X., and Morán, A. (2011). Anaerobic co-digestion of swine manure with energy crop residues. *Biotechnology and Bioprocess Engineering*, *16*(5), 1044–1052. doi:10.1007/s12257-011-0117-4

Davila-Vazquez, G., Arriaga, S., Alatriste-Mondragón, F., De León-Rodríguez, A., Rosales-Colunga, L. M., and Razo-Flores, E. (2008). Fermentative biohydrogen production: Trends and perspectives. *Reviews in Environmental Science and Biotechnology*, *7*, 27–45. doi:10.1007/s11157-007-9122-7

De Pauw, D. (2005). *Optimal experimental design for calibration of bioprocess models: A validated software toolbox*. *Dissertation*. Ghent University.

Demirel, B. and Scherer, P. (2008). The roles of acetotrophic and hydrogenotrophic methanogens during anaerobic conversion of biomass to methane: a review. *Reviews in Environmental Science and Bio/Technology*, *7*(2), 173–190. doi:10.1007/s11157-008-9131-1

Desvaux, L., Guedon, E., Petitdemange, H., Scientifique, D., Grignard, V., and Poincare, H. (2001). Carbon flux distribution and kinetics of cellulose fermentation in steady-state

continuous cultures of clostridium cellulolyticum on a chemically defined medium. *Journal of Bactereology*, *183*(1), 119–130. doi:10.1128/JB.183.1.119

Deublein, D. and Steinhauser, A. (2011). *Biogas from waste and renewable resources-An introduction*. Weinheim: Wiley-VCH.

Donoso-Bravo, A., Mailier, J., Martin, C., Rodríguez, J., Aceves-Lara, C. A., and Wouwer, A. Vande. (2011). Model selection, identification and validation in anaerobic digestion: A review. *Water Research*, *45*(17), 5347–5364. doi:10.1016/j.watres.2011.08.059

Drosg, B. (2013). *Process monitoring in biogas plants*. International Energy Agency Bioenergy. Retrieved from http://www.iea-biogas.net/files/daten-redaktion/download/Technical Brochures/Technical Brochure process_montoring.pdf

Eastman, J. A. and Ferguson, J. F. (1981). Solubilization of particulate organic carbon during the acid phase of anaerobic digestion. *J WPCF*, *53*(3), 352–366.

Ecofys and Golder Associates. (2009). Benchmark of bioenergy permitting procedures in the European Union. DG TREN. Retrieved from https://ec.europa.eu/energy/sites/ener/files/ecofys_final_report_benchmark_bioenergy.pdf

El-Mashad, H. M., Zeeman, G., van Loon, W. K. P., Bot, G. P. a, and Lettinga, G. (2004). Effect of temperature and temperature fluctuation on thermophilic anaerobic digestion of cattle manure. *Bioresource Technology*, *95*(2), 191–201. doi:10.1016/j.biortech.2003.07.013

Ersahin, M. E., Insel, G., Dereli, R. K., Ozturk, I., and Kinaci, C. (2007). Model Based Evaluation for the Anaerobic Treatment of Corn Processing Wastewaters. *CLEAN – Soil, Air, Water*, *35*(6), 576–581. doi:10.1002/clen.200700105

Escamilla-Alvarado, C., Ponce-Noyola, T., Ríos-Leal, E., and Poggi-Varaldo, H. M. (2013). A multivariable evaluation of biohydrogen production by solid substrate fermentation of organic municipal wastes in semi-continuous and batch operation. *International Journal of Hydrogen Energy*, *38*, 12527–12538. doi:10.1016/j.ijhydene.2013.02.124

Eskicioglu, C. and Ghorbani, M. (2011). Effect of inoculum/substrate ratio on mesophilic anaerobic digestion of bioethanol plant whole stillage in batch mode. *Process Biochemistry*, *46*(8), 1682–1687. doi:10.1016/j.procbio.2011.04.013

EurObserv'ER. (2013). 13th EurObserv'ER report: The state of renewable energies in Europe. Paris. Retrieved from http://www.energies-renouvelables.org/observ-er/stat_baro/barobilan/barobilan13-gb.pdf

EurObserv'ER. (2014). *Biogas Barometer*. Retrieved from http://www.energies-renouvelables.org/observ-er/stat_baro/observ/baro224_Biogas_en.pdf

European Commission. (2005). *Communication from the Commission - Biomass action plan* (No. COM(2005) 628 final). Brussels - Belgium.

European Commission. Communication from the European Commission to the european Council and the European Parliament "An energy Policy for europe". (2007). Brussels - Belgium.

European Commission. Directive 2009/28/EC of the European Parliament and the Council of 23 April 2009 on the promotion of the use of energy from renewable sources and amending and subsequently repealing Directives 2001/77/EC and 2003/30/EC (2009). Strasbourg - France.

European Commission. (2010). *Report from the Commission to the Council and the European Parliament on on sustainability requirements for the use of solid and gaseous*. Brussels - Belgium.

European Environment Agency. (2006). *How much bioenergy can Europe produce without harming the environment? EEA Report No 7/2006*. Copenhagen - Denmark. Retrieved from http://www.eea.europa.eu/publications/eea_report_2006_7

European Environment Agency. (2013). *EU bioenergy potential from a resource-efficiency perspective. Report No 6/2013*. Copenhagen - Denmark. Retrieved from http://www.eea.europa.eu/publications/eu-bioenergy-potential

European Environment Agency. (2014). *Renewable energy in gross inland energy consumption (CSI 030/ENER 029)*. Retrieved January 19, 2015, from http://www.eea.europa.eu/data-and-maps/indicators/renewable-primary-energy-consumption-3/assessment

European Environment Agency. (2015). *Total Gross Inland Consumption by Fuel (CSI 029/ENER 026)*. Retrieved from http://www.eea.europa.eu/data-and-maps/indicators/primary-energy-consumption-by-fuel-5/assessment

Fachagentur Nachwachsende Rohstoffe (FNR). (2013). *Biogas - an introduction. N°. 329.* Gülzow - Germany. Retrieved from http://mediathek.fnr.de/media/downloadable/files/samples/b/r/brosch.biogas-2013-en-web-pdf.pdf

Fantozzi, F. and Buratti, C. (2009). Biogas production from different substrates in an experimental Continuously Stirred Tank Reactor anaerobic digester. *Bioresource Technology*, *100*(23), 5783–9. doi:10.1016/j.biortech.2009.06.013

Feitkenhauer, H., Von Sachs, J., and Meyer, U. (2002). On-line titration of volatile fatty acids for the process control of anaerobic digestion plants. *Water Research*, *36*(1), 212–8. Retrieved from http://www.ncbi.nlm.nih.gov/pubmed/11766797

Feng, Y., Behrendt, J., Wendland, C., and Otterpohl, R. (2006). Parameter analysis of the IWA Anaerobic Digestion Model No.1 for the anaerobic digestion of blackwater with kitchen refuse. *Water Science and Technology*, *54*(4), 139–147.

Fezzani, B. and Cheikh, R. Ben. (2008). Implementation of IWA anaerobic digestion model No. 1 (ADM1) for simulating the thermophilic anaerobic co-digestion of olive mill wastewater with olive mill solid waste in a semi-continuous tubular digester. *Chemical Engineering Journal*, *141*(1-3), 75–88. doi:10.1016/j.cej.2007.10.024

Frigon, J.-C., Roy, C., and Guiot, S. R. (2012). Anaerobic co-digestion of dairy manure with mulched switchgrass for improvement of the methane yield. *Bioprocess and Biosystems Engineering*, *35*(3), 341–9. doi:10.1007/s00449-011-0572-5

Galí, A., Benabdallah, T., Astals, S., and Mata-Alvarez, J. (2009). Modified version of ADM1 model for agro-waste application. *Bioresource Technology*, *100*(11), 2783–90. doi:10.1016/j.biortech.2008.12.052

Garcia-Heras, J. L. (2003). Reactor sizing, process kinetics and modelling of anaerobic digestion of complex substrates. In J. Mata-Alvarez (Ed.), *Biomethanization of the organic fraction of municipal solid wastes.* (pp. 21–62). IWA Publishing.

Gerardi, M. H. (2003). *The microbiology of anaerobic digesters.* (M. H. Gerardi, Ed.). Hoboken, New Jersey.: Wiley-Interscience.John Wiley and Sons, Inc.

Gerber, M. and Span, R. (2008). An Analysis of Available Mathematical Models for Anaerobic Digestion of Organic Substances for Production of Biogas. In *International Gas Union Research Conference.* (p. 30). Paris.

Gerin, P. A., Vliegen, F., and Jossart, J.-M. (2008). Energy and CO2 balance of maize and grass as energy crops for anaerobic digestion. *Bioresource Technology*, *99*(7), 2620–7. doi:10.1016/j.biortech.2007.04.049

Golkowska, K. (2011). *Anaerobic mono-digestion of maize and cellulose at different temperatures and operating modes*. *Dissertation*. University of Luxembourg.

Golkowska, K. and Greger, M. (2010). Thermophilic digestion of cellulose at high-organic loading rates. *Engineering in Life Sciences*, *10*(6), 600–606. doi:10.1002/elsc.201000105

Golkowska, K., Sibisi-Beierlein, N., and Greger, M. (2012). Kinetic Considerations on Thermophilic Digestion of Maize Silage at Different Feeding Modes. *Chemie Ingenieur Technik*, *84*(9), 1551–1558. doi:10.1002/cite.201100242

González-Fernández, C. and García-Encina, P. A. (2009). Impact of substrate to inoculum ratio in anaerobic digestion of swine slurry. *Biomass and Bioenergy*, *33*, 1065–1069. doi:10.1016/j.biombioe.2009.03.008

Hashimoto, A. G. (1989). Effect of inoculum/substrate ratio on methane yield and production rate from straw. *Biological Wastes*, *28*, 247–255.

Hauduc, H., Neumann, M. B., Muschalla, D., Gamerith, V., Gillot, S., and Vanrolleghem, P. A. (2011). Towards quantitative quality criteria to evaluate simulation results in wastewater treatment – A critical review. In *8th IWA Symposium on Systems Analysis and Integrated Assesment. Watermatex* (pp. 36–49).

Hendriks, A. T. W. M. and Zeeman, G. (2009). Pretreatments to enhance the digestibility of lignocellulosic biomass. *Bioresource Technology*, *100*(1), 10–8. doi:10.1016/j.biortech.2008.05.027

Hill, D. (1983). Simplified monod kinetics of methane fermentation of animal wastes. *Agricultural Wastes*, *5*(1), 1–16. doi:10.1016/0141-4607(83)90009-4

Hill, D. and Holmberg, R. D. (1988). Long chain volatile fatty acid relationships in anaerobic digestion of swine waste. *Biological Wastes*, *23*(3), 195–214. doi:10.1016/0269-7483(88)90034-1

Hu, Z.-H., Wang, G., and Yu, H.-Q. (2004). Anaerobic degradation of cellulose by rumen microorganisms at various pH values. *Biochemical Engineering Journal*, *21*(1), 59–62. doi:10.1016/j.bej.2004.05.004

Hu, Z.-H., Yu, H.-Q., and Zhu, R.-F. (2005). Influence of particle size and pH on anaerobic degradation of cellulose by ruminal microbes. *International Biodeterioration and Biodegradation*, *55*(3), 233–238. doi:10.1016/j.ibiod.2005.02.002

Institut Luxembourgeois de Régulation. (2008). Règlement grand-ducal du 8 février 2008 relatif à la production d'électricité basée sur les sources d'énergie renouvelable. Au Mémorial A n° 16 du 12.02.2008. Retrieved from http://www.legilux.public.lu/leg/a/archives/2008/0016/2008A0260A.html

IPCC. (2014). *Climate change 2014 : Synthesis report - (Fifth assessment report of the Intergovernmental Panel on Climate Change)*. Cambridge University Press, Cambridge. Retrieved from www.ipcc.ch/pdf/assessment-report/ar4/

Jeihanipour, A., Niklasson, C., and Taherzadeh, M. J. (2011). Enhancement of solubilization rate of cellulose in anaerobic digestion and its drawbacks. *Process Biochemistry*, *46*(7), 1509–1514. doi:10.1016/j.procbio.2011.04.003

Jensen, P. D., Hardin, M. T., and Clarke, W. P. (2009). Effect of biomass concentration and inoculum source on the rate of anaerobic cellulose solubilization. *Bioresource Technology*, *100*(21), 5219–25. doi:10.1016/j.biortech.2009.05.018

Klass, D. L. (1984). Methane from Anaerobic Fermentation. *Science*, *223*(4640), 1021–1028.

Kleerebezem, R. and van Loosdrecht, M. C. M. (2006). Waste characterization for implementation in ADM1. *Water Science and Technology*, *54*(4), 167–174.

Koch, K., Helmreich, B., and Drewes, J. E. (2015). Co-digestion of food waste in municipal wastewater treatment plants : Effect of different mixtures on methane yield and hydrolysis rate constant. *Applied Energy*, *137*, 250–255. doi:10.1016/j.apenergy.2014.10.025

Koch, K., Lübken, M., Gehring, T., Wichern, M., and Horn, H. (2010). Biogas from grass silage - Measurements and modeling with ADM1. *Bioresource Technology*, *101*(21), 8158–65. doi:10.1016/j.biortech.2010.06.009

Koch, K., Wichern, M., Lübken, M., and Horn, H. (2009). Mono fermentation of grass silage by means of loop reactors. *Bioresource Technology*, *100*(23), 5934–5940. doi:10.1016/j.biortech.2009.06.020

Koster, I. W., and Koomen, E. (1988). Applied Microbiology Biotechnology Ammonia inhibition of the maximum growth rate (Jim) of hydrogenotrophic methanogens at various pH-levels and temperatures. *Applied Biochemistry and Biotechnology*, *28*, 500–505.

Lebuhn, M., Liu, F., Heuwinkel, H., and Gronauer, A. (2008). Biogas production from mono-digestion of maize silage-long-term process stability and requirements. *Water Science and Technology : A Journal of the International Association on Water Pollution Research*, *58*(8), 1645–51. doi:10.2166/wst.2008.495

Lehtomäki, A. (2006). *Biogas production from energy crops and crop residues*. *Dissertation*. University of Jyväskylä.

Lehtomäki, A., Huttunen, S., Lehtinen, T. M., and Rintala, J. A. (2008). Anaerobic digestion of grass silage in batch leach bed processes for methane production. *Bioresource Technology*, *99*(8), 3267–78. doi:10.1016/j.biortech.2007.04.072

Lehtomäki, A., Huttunen, S., and Rintala, J. A. (2007). Laboratory investigations on co-digestion of energy crops and crop residues with cow manure for methane production: Effect of crop to manure ratio. *Resources, Conservation and Recycling*, *51*(3), 591–609. doi:10.1016/j.resconrec.2006.11.004

Liu, D., Liu, D., Zeng, R. J., and Angelidaki, I. (2006). Hydrogen and methane production from household solid waste in the two-stage fermentation process. *Water Research*, *40*, 2230–2236. doi:10.1016/j.watres.2006.03.029

Liu, G., Zhang, R., El-Mashad, H. M., and Dong, R. (2009). Effect of feed to inoculum ratios on biogas yields of food and green wastes. *Bioresource Technology*, *100*(21), 5103–8. doi:10.1016/j.biortech.2009.03.081

Lübken, M., Gehring, T., and Wichern, M. (2010). Microbiological fermentation of lignocellulosic biomass: current state and prospects of mathematical modeling. *Applied Microbiology and Biotechnology*, *85*(6), 1643–52. doi:10.1007/s00253-009-2365-1

Lübken, M., Wichern, M., Schlattmann, M., Gronauer, A., and Horn, H. (2007). Modelling the energy balance of an anaerobic digester fed with cattle manure and renewable energy crops. *Water Research*, *41*(18), 4085–96. doi:10.1016/j.watres.2007.05.061

Lyberatos, G. and Skiadas, I. V. (1999). Modelling of anaerobic digestion - A review. *Global Nest: The International Journal*, *1*(2), 63–76.

Mähnert, P., Heiermann, M., and Linke, B. (2005). Batch- and semi-continuous biogas production from different grass species. *Agricultural Engineering International: The CIGR Ejournal.*, *VII*(Manuscript EE 05 010), 1–11.

Malherbe, S. and Cloete, T. E. (2002). Lignocellulose biodegradation : Fundamentals and applications. *Views in Environmental Science and Bio/Technology*, *1*, 105–114.

Marchaim, U. and Krause, C. (1993). Propionic to acetic acid ratios in overloaded anaerobic digestion. *Bioresource Technology*, *43*(3), 195–203. doi:10.1016/0960-8524(93)90031-6

Mata-Alvarez, J. (2002). *Biomethanization of the organic fraction of municipal solid wastes*. IWA Publishing Company.

McEniry, J. and O'Kiely, P. (2013). Anaerobic methane production from five common grassland species at sequential stages of maturity. *Bioresource Technology*, *127*, 143–50. doi:10.1016/j.biortech.2012.09.084

McMahon, K. D., Stroot, P. G., Mackie, R. I., and Raskin, L. (2001). Anaerobic codigestion of municipal solid waste and biosolids under various mixing conditions--II: Microbial population dynamics. *Water Research*, *35*(7), 1817–27. Retrieved from http://www.ncbi.nlm.nih.gov/pubmed/11329684

Ministère du Développement durable et des Infrastructures - Département de l'Environnement. Plan général de gestion des déchets (2010). Luxembourg. Retrieved from http://www.environnement.public.lu/dechets/dossiers/pggd/pggd_plan_general.pdf

Mosey, F. E. (1983). Mathematical modelling of the anaerobic digestion process: regulatory mechanisms for the formation of short-chain volatile acids from glucose. *Water Science Technology*, *15*, 209–232.

Mshandete, A., Bjornsson, L., Kivaisi, A., Rubindamayugi, M., and Mattiasson, B. (2006). Effect of particle size on biogas yield from sisal fibre waste. *Renewable Energy*, *31*(14), 2385–2392. doi:10.1016/j.renene.2005.10.015

Muller, A. (2008). Sustainable agriculture and the production of biomass for energy use. *Climatic Change*, *94*(3-4), 319–331. doi:10.1007/s10584-008-9501-2

Munk, B., Bauer, C., Gronauer, A., and Lebuhn, M. (2010). Population dynamics of methanogens during acidification of biogas fermenters fed with maize silage. *Engineering in Life Sciences*, *10*(6), 496–508. doi:10.1002/elsc.201000056

Murphy, J., Bochmann, G., Weiland, P., and Wellinger, A. (2011). Biogas from Crop Digestion. *IEA Bioenergy - Task 37*, 24. Retrieved from http://www.iea-biogas.net/files/daten-redaktion/download/publi-task37/Update_Energy_crop_2011.pdf

Myint, M., Nirmalakhandan, N., and Speece, R. E. (2007). Anaerobic fermentation of cattle manure: Modeling of hydrolysis and acidogenesis. *Water Research*, *41*, 323–332. doi:10.1016/j.watres.2006.10.026

Nettmann, E., Bergmann, I., Mundt, K., Linke, B., and Klocke, M. (2008). Archaea diversity within a commercial biogas plant utilizing herbal biomass determined by 16S rDNA and mcrA analysis. *Journal of Applied Microbiology*, *105*(6), 1835–50. doi:10.1111/j.1365-2672.2008.03949.x

Nielsen, H. B., Uellendahl, H., and Ahring, B. K. (2007). Regulation and optimization of the biogas process : Propionate as a key parameter. *Bioma*, *31*, 820–830. doi:10.1016/j.biombioe.2007.04.004

Nizami, a. S., Orozco, a., Groom, E., Dieterich, B., and Murphy, J. D. (2012). How much gas can we get from grass? *Applied Energy*, *92*, 783–790. doi:10.1016/j.apenergy.2011.08.033

Nizami, A.-S. and Murphy, J. D. (2010). What type of digester configurations should be employed to produce biomethane from grass silage? *Renewable and Sustainable Energy Reviews*, *14*(6), 1558–1568. doi:10.1016/j.rser.2010.02.006

Noike, T., Endo, G., Chang, J. E., Yaguchi, J. I., and Matsumoto, J. . (1985). Characteristics of carbohydrate degradation and the rate- limiting step in anaerobic digestion. *Biotechnology and Bioengineering Neering*, *27*, 1482–1489.

Nordmann, W. (1977). Die Überwachung der Schlammfaulung. Eine einfache Methode zur Bestimmung der organischen Säuren und der Kalkreserve im Faulwasser. In *Beilage zur Korrespondenz Abwasser, informationen für das Betriebspersonal von Abwasseranlagen* (pp. 3–4).

O'Sullivan, C. A., Burrell, P. C., Clarke, W. P., and Blackall, L. L. (2006). Comparison of cellulose solubilisation rates in rumen and landfill leachate inoculated reactors. *Bioresource Technology*, *97*(18), 2356–63. doi:10.1016/j.biortech.2005.10.021

Ohnishi, A., Bando, Y., Fujimoto, N., and Suzuki, M. (2010). Development of a simple bio-hydrogen production system through dark fermentation by using unique microflora. *International Journal of Hydrogen Energy*, *35*(16), 8544–8553. doi:10.1016/j.ijhydene.2010.05.113

Pagés Díaz, J., Pereda Reyes, I., Lundin, M., and Sárvári Horváth, I. (2011). Co-digestion of different waste mixtures from agro-industrial activities: kinetic evaluation and synergetic effects. *Bioresource Technology*, *102*(23), 10834–40. doi:10.1016/j.biortech.2011.09.031

Pagés Díaz, J., Pereda Reyes, I., Lundin, M., and Sárvári Horváth, I. (2011). Co-digestion of different waste mixtures from agro-industrial activities: kinetic evaluation and synergetic effects. *Bioresource Technology*, *102*(23), 10834–40. doi:10.1016/j.biortech.2011.09.031

Pakarinen, O., Kaparaju, P., and Rintala, J. (2011). The effect of organic loading rate and retention time on hydrogen production from a methanogenic CSTR. *Bioresource Technology*, *102*(19), 8952–7. doi:10.1016/j.biortech.2011.07.020

Pakarinen, O., Lehtomäki, A., Rissanen, S., and Rintala, J. (2008). Storing energy crops for methane production: effects of solids content and biological additive. *Bioresource Technology*, *99*(15), 7074–82. doi:10.1016/j.biortech.2008.01.007

Palatsi, J., Illa, J., Prenafeta-Boldú, F. X., Laureni, M., Fernandez, B., Angelidaki, I., and Flotats, X. (2010). Long-chain fatty acids inhibition and adaptation process in anaerobic thermophilic digestion: batch tests, microbial community structure and mathematical modelling. *Bioresource Technology*, *101*(7), 2243–51. doi:10.1016/j.biortech.2009.11.069

Parawira, W., Murto, M., Read, J. S., and Mattiasson, B. (2005). Profile of hydrolases and biogas production during two-stage mesophilic anaerobic digestion of solid potato waste. *Process Biochemistry*, *40*(9), 2945–2952. doi:10.1016/j.procbio.2005.01.010

Pavlostathis, S. G. and Giraldo-Gomez, E. (1991). Kinetics of anaerobic treatment: A critical rewiev. *Critical Reviews in Environmental Control*, *21*(5-6), 411–490.

Pfeffer, J. T. (1974). Temperature Effects on Anaerobic Fermentation of Domestic Refuse. *Biotechnology and Bioengineering*, *16*, 771 – 787.

Pind, P. F., Angelidaki, I., and Ahring, B. K. (2003). Dynamics of the anaerobic process: Effects of volatile fatty acids. *Biotechnology and Bioengineering*, *82*(1383), 791–801. doi:10.1002/bit.10628

Pind, P. F., Angelidaki, I., Ahring, B. K., Stamatelatou, K. and Lyberatos, G. (2003). Monitoring and control of anaerobic reactors. In *Biomethanation II.* (pp. 135–182). Berlin: Springer.

Poeschl, M., Ward, S., and Owende, P. (2010). Prospects for expanded utilization of biogas in Germany. *Renewable and Sustainable Energy Reviews*, *14*(7), 1782–1797. doi:10.1016/j.rser.2010.04.010

Pöschl, M., Ward, S., and Owende, P. (2010). Evaluation of energy efficiency of various biogas production and utilization pathways. *Applied Energy*, *87*(11), 3305–3321. doi:10.1016/j.apenergy.2010.05.011

Ramirez, I., Mottet, A., Carrère, H., Déléris, S., Vedrenne, F., and Steyer, J.-P. (2009). Modified ADM1 disintegration/hydrolysis structures for modeling batch thermophilic anaerobic digestion of thermally pretreated waste activated sludge. *Water Research*, *43*(14), 3479–92. doi:10.1016/j.watres.2009.05.023

Ramirez, I., Volcke, E. I. P., Rajinikanth, R., and Steyer, J.-P. (2009). Modeling microbial diversity in anaerobic digestion through an extended ADM1 model. *Water Research*, *43*(11), 2787–800. doi:10.1016/j.watres.2009.03.034

Ramos Suarez, J. L. (2014). *Produccion de biogas a partir de biomasa de la microalaga scenedesmus sp. procedente de diferente procesos*. *Dissertation*. Universidad politécnica de Madrid.

Raposo, F., Banks, C., Siegert, I., Heaven, S., and Borja, R. (2006). Influence of inoculum to substrate ratio on the biochemical methane potential of maize in batch tests. *Process Biochemistry*, *41*(6), 1444–1450. doi:10.1016/j.procbio.2006.01.012

Raposo, F., Borja, R., Martín, M. A., Martín, A., de la Rubia, M. A., and Rincón, B. (2009). Influence of inoculum–substrate ratio on the anaerobic digestion of sunflower oil cake in batch mode: Process stability and kinetic evaluation. *Chemical Engineering Journal*, *149*(1-3), 70–77. doi:10.1016/j.cej.2008.10.001

Reichert, P. (1998). AQUASIM 2.0 - User manual. Computer program for the identication and simulation of aquatic systems. Dübendorf: Swiss Federal Institute for Environmental Science and Technology (EAWAG).

Resch C., Braun, R., and Kirchmayr, R. (2008). The influence of energy crop substrates on the mass-flow analysis and the residual methane potential at a rural anaerobic digestion plant. *Water Science and Technology : A Journal of the International Association on Water Pollution Research*, *57*(73-81). doi:10.2166/wst.2008.733

Richards, B. K., Cummings, R. J., and Jewell, W. J. (1991). High rate low solids methane fermentation of sorghum, corn and cellulose. *Biomass and Bioenergy*, *1*(5), 249–260.

Rojas, C., Fang, S., Uhlenhut, F., Borchert, A., Stein, I., and Schlaak, M. (2010). Stirring and biomass starter influences the anaerobic digestion of different substrates for biogas production. *Engineering in Life Sciences*, *10*(4), 339–347. doi:10.1002/elsc.200900107

Romsaiyud, A., Songkasiri, W., Nopharatana, A., and Chaiprasert, P. (2009). Combination effect of pH and acetate on enzymatic cellulose hydrolysis. *Journal of Environmental Sciences*, *21*(7), 965–970. doi:10.1016/S1001-0742(08)62369-4

Rosen, C. and Jeppsson, U. (2006). *Aspects on ADM1 Implementation within the BSM2 Framework*. *Technical report. Lund University*.

Rosen, C., Vrecko, D., Gernaey, K. V., Pons, M. N., and Jeppsson, U. (2006). Implementing ADM1 for plant-wide benchmark simulations in Matlab/Simulink. *Water Science and Technology*, *54*(4), 11. doi:10.2166/wst.2006.521

Schink, B. (1997). Energetics of syntrophic cooperation in methanogenic degradation. *Microbiology and Molecular Biology Reviws*, *61*(2), 262–280.

Schlattmann, M. (2011). *Weiterentwicklung des „ Anaerobic Digestion Model (ADM1)“ zur Anwendung auf landwirtschaftliche Substrate*. *Dissertation*. Technischen Universität München.

Schoen, M. A., Sperl, D., Gadermaier, M., Goberna, M., Franke-Whittle, I., Insam, H., Ablinger, J., Wett, B. (2009). Population dynamics at digester overload conditions. *Bioresource Technology*, *100*(23), 5648–55. doi:10.1016/j.biortech.2009.06.033

Schön, M. (2009). *Numerical modelling of anaerobic digestion processes in agricultural biogas plants*. *Dissertation*. Universität Innsbruck.

Siegert, I. and Banks, C. (2005). The effect of volatile fatty acid additions on the anaerobic digestion of cellulose and glucose in batch reactors. *Process Biochemistry*, *40*(11), 3412–3418. doi:10.1016/j.procbio.2005.01.025

Song, H. and Clarke, W. P. (2009). Cellulose hydrolysis by a methanogenic culture enriched from landfill waste in a semi-continuous reactor. *Bioresource Technology*, *100*(3), 1268–73. doi:10.1016/j.biortech.2008.08.029

Song, H., Clarke, W. P., and Blackall, L. L. (2005). Concurrent microscopic observations and activity measurements of cellulose hydrolyzing and methanogenic populations during the batch anaerobic digestion of crystalline cellulose. *Biotechnology and Bioengineering*, *91*(3), 369–78. doi:10.1002/bit.20517

Strigul, N., Dette, H., and Melas, V. B. (2009). A practical guide for optimal designs of experiments in the Monod model. *Environmental Modelling and Software*, *24*(9), 1019–1026. doi:10.1016/j.envsoft.2009.02.006

Thamsiriroj, T. and Murphy, J. D. (2010). Modelling mono-digestion of grass silage in a 2-stage CSTR anaerobic digester using ADM1. *Bioresource Technology*. doi:10.1016/j.biortech.2010.09.051

Thamsiriroj, T., Nizami, a. S., and Murphy, J. D. (2012). Why does mono-digestion of grass silage fail in long term operation? *Applied Energy*, *95*, 64–76. doi:10.1016/j.apenergy.2012.02.008

Thauer, R. K., Jungermann, K., and Decker, K. (1977). Energy conservation in chemotrophic anaerobic bcteria. *Bacteriological Reviews*, *41*(1), 100–180.

Tomei, M., Braguglia, C., Cento, G., and Mininni, G. (2009). Modeling of anaerobic digestion of sludge. *Critical Reviews in Environmental Science and Technology*, *39*(12), 1003–1051. doi:10.1080/10643380801977818

Valdez-Vazquez, I., Ríos-Leal, E., Esparza-García, F., Cecchi, F., and Poggi-Varaldo, H. M. (2005). Semi-continuous solid substrate anaerobic reactors for H2 production from organic waste: Mesophilic versus thermophilic regime. *International Journal of Hydrogen Energy*, *30*, 1383–1391. doi:10.1016/j.ijhydene.2004.09.016

Van Soest, P. J. and Wine, R. H. (1967). Use of detergent in the analysis of fibrous feeds. IV. Determination of plant cell wall constituents. *Journal of Association of Official Analytical Chemists*, *50*(1), 50–55.

Vavilin, V. A. and Angelidaki, I. (2005). Anaerobic degradation of solid material: importance of initiation centers for methanogenesis, mixing intensity, and 2D distributed model. *Biotechnology and Bioengineering*, *89*(1), 113–22. doi:10.1002/bit.20323

Vavilin, V. A., Fernandez, B., Palatsi, J., and Flotats, X. (2008). Hydrolysis kinetics in anaerobic degradation of particulate organic material: an overview. *Waste Management (New York, N.Y.)*, *28*(6), 939–51. doi:10.1016/j.wasman.2007.03.028

Vavilin, V. A., Rytov, S. V., and Lokshina, L. Y. (1996). A description of hydrolysis kinetics in anarobic degradation of particulate organic matter. *Bioresource Technology*, *56*, 229–237.

Verein Deutscher Ingenieure. (2004). Guideline VDI 4630: Fermentation of organic materials - Characterisation of the substrate, sampling, collection of material data, fermentation tests (VDI-Handbu., p. 96). Düsseldorf: Beuth Verlag GmbH.

Waldheim, L. and Nilsson, T. (2001). *Heating value of gases from biomass gasification. Report prepared for the IEA Bioenergy Agreement , Task 20-thermal gasification of biomass.* Retrieved from http://www.ieatask33.org/app/webroot/files/file/publications/HeatingValue.pdf

Wall, D. M., Allen, E., Straccialini, B., O'Kiely, P., and Murphy, J. D. (2014). The effect of trace element addition to mono-digestion of grass silage at high organic loading rates. *Bioresource Technology*, *172*, 349–55. doi:10.1016/j.biortech.2014.09.066

Wang, L., Zhou, Q., and Li, F. T. (2006). Avoiding propionic acid accumulation in the anaerobic process for biohydrogen production. *Biomass and Bioenergy*, *30*, 177–182. doi:10.1016/j.biombioe.2005.11.010

Weiland, P. (2010). Biogas production: current state and perspectives. *Applied Microbiology and Biotechnology*, *85*(4), 849–60. doi:10.1007/s00253-009-2246-7

Weiβbach F. and Strubelt C. (2008). Die Korrektur des Trockensubstanzgehaltes von Maissilagen als Substrat für Biogasanlagen. *Landtechnik*, *63*(2), 82–83.

Weiβbach, F. and Strubelt, C. (2008). Die Korrektur des Trockensubstanzgehaltes von Grassilagen als Substrat für Biogasanlagen. *Landtechnik*, (4), 210–211.

Wellinger, A. (1999). *Process design of agricultural digesters*. *Nova Energie GmbH*. Ettenhausen.

Wellinger, A. (2005). *Biogas production and utilisation*. *International Energy Agency Bioenergy-Task 37*. Retrieved from www.iea-biogas.net/publicationspublic.htm

Wichern, M., Gehring, T., Fischer, K., Andrade, D., Lübken, M., Koch, K., … Horn, H. (2009). Monofermentation of grass silage under mesophilic conditions: measurements and mathematical modeling with ADM 1. *Bioresource Technology*, *100*(4), 1675–81. doi:10.1016/j.biortech.2008.09.030

Wolfsberger, A. (2008). *Modelling and Control of the Anaerobic Digestion of Energy Crops*. *Dissertation*. Universität für Bodenkultur Wien.

Xie, S., Wu, G., Lawlor, P. G., Frost, J. P., and Zhan, X. (2012). Methane production from anaerobic co-digestion of the separated solid fraction of pig manure with dried grass silage. *Bioresource Technology*, *104*, 289–97. doi:10.1016/j.biortech.2011.11.076

Zaher, U., Li, R., Jeppsson, U., Steyer, J.-P., and Chen, S. (2009). GISCOD: general integrated solid waste co-digestion model. *Water Research*, *43*(10), 2717–27. doi:10.1016/j.watres.2009.03.018

Zeeman, G., Wiegant, W. M., Koster-Treffers, M. E., and Lettinga, G. (1985). The influence of the total ammonia concentration on the thermophilic digestion of cow manure. *Agricultural Wastes*, *14*, 19–35.

Zhang, T., Liu, H., and Fang, H. H. P. (2003a). Biohydrogen production from starch in wastewater under thermophilic condition. *Journal of Environmental Management*, *69*(2), 149–156. doi:10.1016/S0301-4797(03)00141-5

Zhang, T., Liu, H., and Fang, H. H. P. (2003b). Biohydrogen production from starch in wastewater under thermophilic condition. *Journal of Environmental Management*, *69*, 149–156. doi:10.1016/S0301-4797(03)00141-5

Zhu, C., Zhang, J., Tang, Y., Zhengkai, X., and Song, R. (2011). Diversity of methanogenic archaea in a biogas reactor fed with swine feces as the mono-substrate by mcrA analysis. *Microbiological Research*, *166*(1), 27–35. doi:10.1016/j.micres.2010.01.004

Zhu, H., Stadnyk, A., Béland, M., and Seto, P. (2008). Co-production of hydrogen and methane from potato waste using a two-stage anaerobic digestion process. *Bioresource Technology*, *99*, 5078–5084. doi:10.1016/j.biortech.2007.08.083

ANNEXES

Annex A: Examples of feed-in tariffs in Germany and Luxembourg[7]

	Germany	Luxembourg
Feed-in tariff	Biogas from biomass*: €ct 5.85 – 27.73 per kWh (according to plant size and fuel) (§§ 44-46 EEG 2014) minus €ct 0.2 per kWh (§ 37 par. 3 no. 1 EEG 2014)	€ct 19.2 per kWh for biogas plants with a nominal electric capacity > 500 kW and ≤ 2,500 kW
	Landfill gas*: €ct 5.83 – 8.42 per kWh (§ 41 EEG) minus €ct 0.2 per kWh (§ 37 par. 3 no. 1 EEG 2014)	€ct 18.1 per kWh for biogas plants with a nominal electric capacity > 300 kW and ≤ 500 kW
	Sewage gas*: €ct 5.83 – 6.69 per kWh (§ 42 EEG) minus €ct 0.2 per kWh (§ 37 par. 3 no. 1 EEG 2014).	€ct 17.1 per kWh for biogas plants with a nominal electric capacity > 150 kW and ≤ 300 kW
		€ct 15.3 per kWh for biogas plants with a nominal electric capacity ≤ 150 kW (Art. 19 RGD du 1 août 2014)
Conditions	For most technologies, the tariff levels will decrease in regular periods of time to provide an incentive to reduce costs through technological innovation	The tariff for new plants depends on the source of energy and the year of commissioning and decreases according to a percentage set by law (Art. 16-23 RGD du 1 août 2014). The tariff in force in the year of commissioning is applicable during the entire eligibility period.
Guarantee years	20	15
Notes	* Applicable to plants put into operation after 01.01.2014	

[7] Source: http://www.res-legal.eu. Date last accessed : 9th of June 2015

Annex B: The ADM1 model

Table B.1: Stoichiometric coefficients and process rates for biochemical reactions in the ADM1 model for soluble components (Batstone et al., 2002)

Component → i		1	2	3	4	5	6	7	8	9	10	11	12	***Rate (ρj)***
j	Process ↓	Ssu	Saa	Sfa	Sva	Sbu	Spro	Sac	Sh2	Sch4	S_{IC}	S_{IN}	S_I	
1	Disintegration												f_{xi_xc}	$k_{dis}*X_c$
2	Hydrolysis Carb.	1												$K_{hyd\_ch}*X_{ch}$
3	Hydrolysis Proteins		1											$K_{hyd\_pr}*X_{pr}$
4	Hydrolyis Lipids	1-fa_li		fa_li										$K_{hyd\_li}*X_{li}$
5	Uptake sugars	-1				$(1-Y_{su})*f_{fbu\_su}$	$(1-Y_{su})*f_{pro\_su}$	$(1-Y_{su})*f_{ac\_su}$	$(1-Y_{su})*f_{h2\_su}$		$-\sum_{i=1-9,11-24} C_i\nu_{i,5}$	$-(Y_{su}*N_{bac})$		$K_{m\_su}\times\frac{S_{su}}{K_{s\_su}+S_{su}}\times X_{su}\times I_1$
6	Uptake amino acids		-1		$(1-Y_{aa})*f_{va\_aa}$	$(1-Y_{aa})*f_{bu\_aa}$	$(1-Y_{aa})*f_{pro\_aa}$	$(1-Y_{aa})*f_{ac\_aa}$	$(1-Y_{aa})*f_{h2\_aa}$		$-\sum_{i=1-9,11-24} C_i\nu_{i,6}$	$N_{aa}-Y_{aa}*N_{bac}$		$K_{m\_aa}\times\frac{S_{aa}}{K_{s\_aa}+S_{aa}}\times X_{aa}\times I_1$
7	Uptake LCFA			-1				$(1-Y_{fa})*0.7$	$(1-Y_{fa})*0.3$			$-(Y_{fa}*N_{bac})$		$K_{m\_fa}\times\frac{S_{fa}}{K_{s\_fa}+S_{fa}}\times X_{fa}\times I_2$
8	Uptake of HVa				-1		$(1-Y_{c4})*0.54$	$(1-Y_{c4})*0.31$	$(1-Y_{c4})*0.15$			$-(Y_{c4}*N_{bac})$		$K_{m\_c4}\times\frac{S_{va}}{K_{s\_c4}+S_{va}}\times X_{va}\times\frac{1}{1+S_{bu}/S_{va}}\times I_2$
9	Uptake HBu					-1		$(1-Y_{c4})*0.8$	$(1-Y_{c4})*0.2$			$-(Y_{c4}*N_{bac})$		$K_{m\_c4}\times\frac{S_{bu}}{K_{s\_c4}+S_{bu}}\times X_{va}\times\frac{1}{1+S_{va}/S_{bu}}\times I_2$
10	Uptake HPr						-1	$(1-Y_{pro})*0.57$	$(1-Y_{pro})*0.43$		$-\sum_{i=1-9,11-24} C_i\nu_{i,10}$	$-(Y_{pro}*N_{bac})$		$K_{m\_pro}\times\frac{S_{pro}}{K_{s\_pro}+S_{pro}}\times X_{pro}\times I_2$
11	Uptake HAc							-1		$(1-Y_{ac})$	$-\sum_{i=1-9,11-24} C_i\nu_{i,11}$	$-(Y_{ac}*N_{bac})$		$K_{m\_ac}\times\frac{S_{ac}}{K_{s\_ac}+S_{ac}}\times X_{ac}\times I_3$
12	Uptake H_2								-1	$(1-Y_{h2})$	$-\sum_{i=1-9,11-24} C_i\nu_{i,12}$	$-(Y_{h2}*N_{bac})$		$K_{m\_h2}\times\frac{S_{ac}}{K_{s\_h2}+S_{h2}}\times X_{h2}\times I_2$
13	Decay of Xsu													$K_{dec,\ Xsu}*X_{su}$
14	Decay of Xaa													$K_{dec,\ Xaa}*X_{aa}$
15	Decay of Xfa													$K_{dec,\ Xfa}*X_{fa}$
16	Decay of Xc4													$K_{dec,\ Xx4}*X_{x4}$
17	Decay of Xpro													$K_{dec,\ Xpro}*X_{pro}$
18	Decay of Xac													$K_{dec,\ Xac}*X_{ac}$
19	Decay of Xh2													$K_{dec,\ Xh2}*X_{h2}$
		Mono sacharides	Amono adcids	LCFA	Total Valerate	Tptal Propionate	Total Butyrate	Total Acetate	Hydrogen	Methane	Inorganic Carbon	Inorganic Nitrogen	Soluble Inerts	Inhibition factors: $I_1=I_{ph}I_{N,lim}$ $I_2=I_{ph}I_{N,lim}I_{h2}$ $I_3I_{ph}I_{N,lim}I_{nh3,Xac}$

Table B.2: Stoichiometric coefficients and process rates for reactions assumed in the ADM1 model for particulate components (Batstone et al., 2002)

Component → i		13	14	15	16	17	18	19	20	21	22	23	24	
j	Process ↓	Xc	Xch	Xpr	Xli	Xsu	Xaa	Xfa	Xc4	Xpro	Xac	Xh2	Xi	***Rate (ρj)***
1	Disintegration	-1	fch_xc	fpr_xc	fli_xc								fxi_xc	$k_{dis}*X_c$
2	Hydrolysis Carb.		-1											$K_{hyd\_ch}*X_{ch}$
3	Hydrolysis Proteins			-1										$K_{hyd\_pr}*X_{pr}$
4	Hydrolyis Lipids				-1									$K_{hyd\_li}*X_{li}$
5	Uptake sugars					Ysu								$K_{m\_su} \times \frac{S_{su}}{K_{s\_su}+S_{su}} \times X_{su} \times I_1$
6	Uptake amino acids						Yaa							$K_{m\_aa} \times \frac{S_{aa}}{K_{s\_aa}+S_{aa}} \times X_{aa} \times I_1$
7	Uptake LCFA							Yfa						$K_{m\_fa} \times \frac{S_{fa}}{K_{s\_fa}+S_{fa}} \times X_{fa} \times I_2$
8	Uptake of HVa								Yc4					$K_{m\_c4} \times \frac{S_{va}}{K_{s\_c4}+S_{va}} \times X_{va} \times \frac{1}{1+S_{bu}/S_{va}} \times I_2$
9	Uptake HBu								Yc4					$K_{m\_c4} \times \frac{S_{bu}}{K_{s\_c4}+S_{bu}} \times X_{va} \times \frac{1}{1+S_{va}/S_{bu}} \times I_2$
10	Uptake HPr									Ypro				$K_{m\_pro} \times \frac{S_{pro}}{K_{s\_pro}+S_{pro}} \times X_{pro} \times I_2$
11	Uptake HAc										Yac			$K_{m\_ac} \times \frac{S_{ac}}{K_{s\_ac}+S_{ac}} \times X_{ac} \times I_3$
12	Uptake H_2											Yh2		$K_{m\_h2} \times \frac{S_{ac}}{K_{s\_h2}+S_{h2}} \times X_{h2} \times I_2$
13	Decay of Xsu	1				-1								$K_{dec,\ Xsu}*X_{su}$
14	Decay of Xaa	1					-1							$K_{dec,\ Xaa}*X_{aa}$
15	Decay of Xfa	1						-1						$K_{dec,\ Xfa}*X_{fa}$
16	Decay of Xc4	1							-1					$K_{dec,\ Xx4}*X_{x4}$
17	Decay of Xpro	1								-1				$K_{dec,\ Xpro}*X_{pro}$
18	Decay of Xac	1									-1			$K_{dec,\ Xac}*X_{ac}$
19	Decay of Xh2	1										-1		$K_{dec,\ Xh2}*X_{h2}$
		Composites	Carbohydrates	Proteins	Lipids	Sugar degraders	Amoni acid degraders	LCFA degradeers	Valerate and butyrate degraders	Propionate degraders	Acetate degraders	Hydrogen degraders	Particulate inerts	Inhibition factors: $I_1=I_{ph}I_{N,lim}$ $I_2=I_{ph}I_{N,lim}I_{h2}$ $I_3I_{ph}I_{N,lim}I_{nh3,Xac}$

Table B.3: Stoichiometric coefficients and mass transfer rates assumed in the ADM1 model (Batstone et al., 2002)

Component →		i	8	9	10	***Rate (ρj) (gCOD/l/d)***
j	Process ↓		Sh2	Sch4	Sco2	
T8	H_2 mass transfer		-1			$k_L a \times (S_{liq,H2} - 16 \times K_{H\_h2} \times p_{gas,H2})$
T9	CH_4 mass transfer			-1		$k_L a \times (S_{liq,ch4} - 64 \times K_{H\_ch4} \times p_{gas,ch4})$
T10	CO_2 mass transfer				-1	$k_L a \times (S_{liq,ch4} - K_{H\_co2} \times p_{gas,co2})$

Table B.4: Inhibition terms of the ADM1 model (Batstone et al., 2002)

	Equation	Inhibition	Inhibited process
Non-competitive inhibition	$I_{h2/NH3,Xac} = \frac{1}{1+\frac{Si}{Ki}}$	Free ammonia, hydrogen	LCFA, valeric, butyric, propionic and acetic acid consumption
Empiric model (upper and lower form)	$I_{pH} = \frac{1+2.10^{0.5(pH_{LL}-pH_{UL})}}{1+10^{(pH-pH_{UL})}+10^{(pH_{LL}-pH)}}$	pH*	Hydrogen, sugars, aminoacids, LCFA, valeric, butyric, propionic and acetic acid consumption
Empiric model (only lower **form)**	$I_{pH} = \exp\left[-3\left(\frac{pH-pH_{UL}}{pH_{UL}-pH_{LL}}\right)^2\right]$ for $pH<pH_{UL}$ I=1 for $pH>pH_{UL}$	pH†	Hydrogen, sugars, aminoacids, LCFA, valeric, butyric, propionic and acetic acid consumption
Competitive **inhibition**	$I = \frac{1}{1+\frac{Si}{S}}$	HBu inhibits the con-sumption of HVa and vice versa	HBu and HVa consumption
Limiting **substrate**	$I_{IN,\lim} = \frac{1}{1+\frac{Ki}{Si}}$	IN	Hydrogen, sugars, aminoacids, LCFA, valeric, butyric, propionic and acetic acid consumption for low concentration of IN

∗pHUL and pHLL are respectively the upper and lower pH limit causing 50% inhibition.
†pHUL is the pH value of no–inhibition, while pHLL is instead the pH value giving complete inhibition.

Table B.5: Components in the liquid phase and C (Ci) and N (Ni) content originally used in the ADM1

Component (i)	Symbol	Description	Canbon content (Ci) (mole C /gCOD)	Nitrogen content (Ni) (mole N /gCOD)
1	Ssu	Monoshaccaride	6/192	0
2	Saa	Amino acids	0.03	0.007
3	Sfa	LCFA	0.0217	0
4	Sva	Total valerate	5/208	0
5	Sbu	Total butyrate	4/160	0
6	Spro	Total propionate	3/112	0
7	Sac	Total acetate	2/64	0
8	Sh2	Hydrogen	0	0
9	Sch4	Methane	1/64	0
10	SIC	Inorganic carbon	-	0
11	SIN	Inorganic nitrogen	0	1
12	SI	Soluble inerts	0.03	0.002
13	Xc	Composites	0.03	0.002
14	Xch	Carbohydrates	6/192	0
15	Xpr	Proteins	0.03	0.007
16	Xli	Lipids	0.022	0
17-23	Xsu –Xh2	Biomass	5/160	0.00625
24	Xi	Particulate inerts	0.03	0.002

Table B.6: Kinetic parameters in the ADM1 model

Parameter	Name	Units	ADM1 default value
Hydrolisis rates			
Khyd_ch	Hydrolysis rate carbohydrates	d^{-1}	10
Khyd_pr	Hydrolysis rate proteins	d^{-1}	10
Khyd_li	Hydrolysis rate lipids	d^{-1}	10
kdis	Disintegration constant	d^{-1}	0.5
Maximum uptake rate			
Km_su	Sugar degradation	gCOD/gCOD/d	30
Km_aa	Amino acids degradation	gCOD/gCOD/d	50
Km_fa	LCFA degradation	gCOD/gCOD/d	6
Km_c4	valerate and butyrate degradation	gCOD/gCOD/d	20
Km_pr	Propionate degradation	gCOD/gCOD/d	13
Km_ac	Acetate degradation	gCOD/gCOD/d	8
Km_h2	Hydrogen degradation	gCOD/gCOD/d	35
Half saturation constants			
Ks_su	Sugar degradation	gCOD/l	0.5
Ks_aa	Amino acids degradation	gCOD/l	0.3
Ks_fa	LCFA degradation	gCOD/l	0.4
Ks_c4	valerate and butyrate degradation	gCOD/l	0.2
Ks_pr	Propionate degradation	gCOD/l	0.1
Ks_ac	Acetate degradation	gCOD/l	0.15
Ks_h2	Hydrogen degradation	gCOD/l	7×10^{-6}
Logarithmic constant pKa (at 298K)			
pKa_co2	- log10ka CO2		6.35
pKa_ac	- log10ka HAc		4.76
pKa_pro	- log10ka HPr		4.88
pKa_bu	- log10ka HBu		4.84
pKa_va	- log10ka HVa		4.80
pKa_nh3	- log10ka NH3		9.25
pKa_h2o	- log10ka H2O		14
Mass rate coefficients			
Kla_h2	Mass transfer coefficient for hydrogen	d^{-1}	200
Kla_ch4	Mass transfer coefficient for methane	d^{-1}	200
Kla_co2	Mass transfer coefficient for CO_2	d^{-1}	200
KH_h2	Henry's law coefficient for hydrogen	k mole COD/ m^3bar	0.00078
KH_co2	Henry's law coefficient for CO2	k mole COD/ m^3bar	0.035

Parameter	Name	Units	ADM1 default value
kp	pipe resistance coefficient	l/bar.d	-
KH_ch4	Henry's law coefficient for methane	k mole COD/ m^3bar	0.0014
Decay rates			
Kdec	Decay rate for biomass	d^{-1}	0.02
Biomass yileds			
Ysu	Yield in for sugar degraders	gCOD/gCOD	0.1
Yaa	Yield for amino acid degraders	gCOD/gCOD	0.08
Yfa	Yield for LCFA degraders	gCOD/gCOD	0.06
Yc4	Yield for valerate and buterate degraders	gCOD/gCOD	0.06
Ypro	Yield for propionate degraders	gCOD/gCOD	0.04
Yac	Yield in acetate degraders	gCOD/gCOD	0.05
Yh2	Yield in hydrogen degraders	gCOD/gCOD	0.06
Inhibition factors			
KI_h2_pro	Inhibitory hydrogen concentration during HPr uptake	gCOD/l	$3.5x10^{-6}$
Ks_IN	IN concentration at which growth ceases	M	0.0001
KI_h2_fa	hydrogen inhibitory concentration for LCFA degrading organisms	gCOD/l	$5x10^{-6}$
KI_h2_c4	hydrogen inhibitory concentration for C4 degrading organisms	gCOD/l	$1 x10^{-5}$
KI_nh3_ac	inhibitory NH3 concentration for acetate degrading organisms	M	0.0018
pHUL_aa	pH upper limit for acidogens and aceto-gens	-	5.5
pHLL_aa	pH lower limit for acidogens and aceto-gens	-	4
pHUL_ac	pH upper limit for acetate degraders	-	7
pHLL_ac	pH lower limit for acetate degraders	-	6
pHUL_h2	pH upper limit for h2 degraders	-	6
pHLL_h2	pH lower limit for h2 degraders	-	5

Table B.7: Stoichiometric parameters in the ADM1 model

Parameter	Unit	Description	ADM1 default values
fpr_Xc	-	Proteins from Xc	0.20
fli_Xc	-	Lipids from Xc	0.25
fch_Xc	-	Carbohydrates from Xc	0.20
fxi_Xc	-	Particular inerts from Xc	0.25
fsi_xc	-	Soluble inerts from Xc	0.10
ffa_li	-	LCFA from lipids	0.95
fh2_mo	-	Hydrogen from sugars	0.19
fbu_su		butyrate from sugars	0.13
fpro_su		Propionate from sugars	0.27
fac_su	-	Acetate from sugars	0.41
fh2_aa		hydrogen from amino acids	0.06
fva_aa		valerate from amino acids	0.23
fbu_aa		butyrate from amino acids	0.26
fpro_aa		propionate from amino acids	0.05
fac_aa		acetate from amino acids	0.40

Annex C: Influence of the drying temperature on biogas production

One litre batch PET reactors were used to compare the CH_4 production from the digestion of fresh grass silage from May 2013 (GS 3) and the same silage dried (DGS 3) at different temperature (60° and 105°) under the same operational conditions. The OL was of 12 gVS/l and the reactors were kept at 38°C and run against a control of inoculum without substrate ("blank"). Each series was run in duplicate. The stability and progress of the reaction were monitored for 21 days by measuring gas production and composition on a daily basis.

The biogas final values are summarised in Table C.1. It is possible to see that the final SBP after 21 days of digestion was 8% and 20% lower for the grass silage dried at 60° and 105° respectively in comparison with the values for the fresh silage. These values were 9% and 18% lower respectively in the case of the SMP. This lower value could correspond to the organic acids that are available in the fresh silage but are removed during the drying process.

Table C.1: Summarised biogas results after 21 days of digestion

	GS 3 (fresh)	DGS 3 (dried at 60°C)	DGS 3 (dried at 105°C)
Accumulated biogas (Nl)	4.38	3.99	2.93
Accumulated CH_4 (Nl)	2.69	2.43	1.84
SBP (Nl/gVS)	0.49	0.45	0.39
SMP (Nl/gVS	0.30	0.27	0.25
Methane in the biogas (%)	62%	61%	63%
Max SBPR (Nl/gVS/d)	0.078	0.056	0.055
Max SMPR (Nl/gVS/d)	0.041	0.029	0.032

Figure C.1. shows the evolution of the biogas quantity and quality during digestion. The two dried silages (at 60°C and 105°C respectively) had a similar evolution in terms of the SMP and SBP during the first 6 days and it was only after that the differences were more appreciable. The SBPR and SMPR were very similar for both dried silages. The fresh silage also followed the same evolution with the exception of the period from day 1 to 4 during which the yield was higher due to the digestion of the organic acids. The results suggest that drying at a temperature between 40°C and 60°C will ensure differences in the biogas composition below 10% in comparison to the fresh silage. While the CH_4 content in the biogas evolved similarly for the fresh and the silage dried at 60°, the silage dried at 105° showed the particularity of reaching within 2 days a constant value of 63%.

Moreover, the loss of in the VFA during drying was also examined into more detail for two of the substrates (GS 2 and GS 3). As it can be seen in Table C.2, a loss of the total VFA content (in mass) of 46.3% and 52% was observed during the drying from 60°C to 105°C for GS 2 and GS 3 respectively. The short-chained HAc was more prompt to removal by drying than the other acids.

Table C.2: Changes in the VFA composition during the drying

Substrate	Drying temperature	HAc (mg/l)	HPr (mg/l)	HBu (mg/l)	HVa (mg/l)	Sum (mg/gTS)
GS 2	105°C	7.3	0.7	2.6	0.6	2.8
	60°C	8.2	0.6	2.3	5.6	5.3
GS 3	105°C	13.1	4.7	27.9	5.4	13.9
	60°C	38.2	6.9	47.5	6.5	29.4

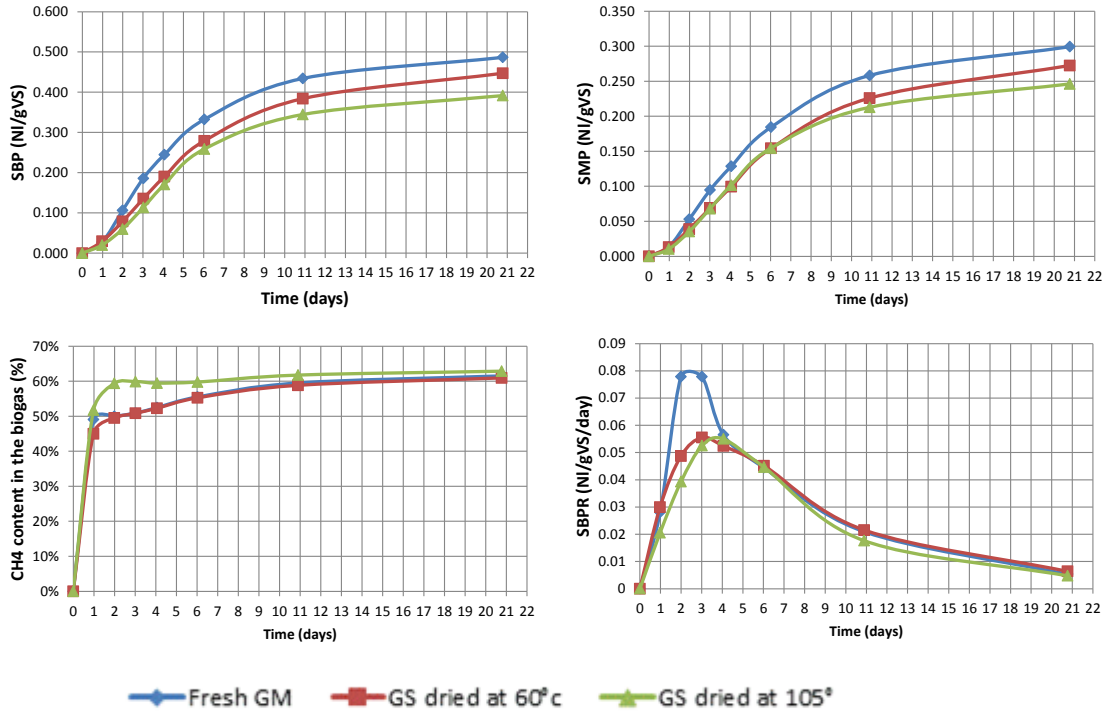

Figure C.1: Comparison of the SMP, SMP, CH_4 content in biogas, and SBPR for fresh grass silage (GS 3), and grass silage dried (DGS 3) at 105° and 60°.

Annex D: Influence of the inoculum characteristics and conditioning on the biogas production

Two parallel batch anaerobic experiments were carried out in 1 litre PET reactors running at mesophilic conditions and under the same operational conditions for 15 days. Both of the inoculums came from Beckerich agricultural biogas plant in Luxembourg. The only difference was the conditioning history of the inoculum that was used in each case, which are summarised in Table D.1. One inoculum (which will be called 1) was acclimated with two consecutive feedings with grass silage and cellulose. The second one (which will be called 2) came from a continuous reactor fed with cellulose (the effluent that was collected every day). Each experimental series counted with 3 reactors with 750g of inoculum and the appropriate amount of cellulose to achieve the same OL, of 5.99 gVS/l. The VS and TS content of both inoculums are also indicated in Table D.1. For these experiments the $r_{S/I}$ ratio was 0.3 and 0.47 for the inoculums 1 and 2. One control ("blank") reactor without substrate addition was set up to run in parallel to monitor the background biogas production. Biogas production and composition were monitored over time for both series. VFA and pH were monitored also for the inoculum 1.

Table D.1: History of the inoculums used in the experiment

Inoculum	Origin	Conditioning substrates	Number of feedings before experiment	TS (%FM)	VS (%FM)
1	Stored in the lab	Grass and cellulose	2	3.36	2.08
2	From previous continuous experiment with cellulose	Grass and cellulose	At least 20 times	2.02	1.28

The SBP and the SMP after 14 days of digestion were 0.568 Nl/gVS and 0.307 Nl/gVS for inoculum 1 and 0.606 Nl/gVS and 0.308 Nl/gVS for inoculum 2, thus with a difference of 6% and 0.3% respectively. The results of this experiment are summarized in Table D.2 for inocula 1 and 2. Regardless of the inoculum history, the final values for most parameters were similar for the two experiments. This highlights the good reproducibility of the experimental results in batch mode when applying the same operational conditions.

Table D.2: Comparison of main digestion parameters for 3 inocula with different conditioning history

Parameter	Unit	Inoculum 1	Inoculum 2
OL	gVS/l	5.99	5.99
rS/I	-	0.3	0.47
Temperature range	°C	39	39
Final SBP	Nl/gVS	0.586	0.606
SBPR	Nl/gVS/d	0.191 (day 4)	0.2 (day 4.82)
Final CH_4 content in biogas	%	76.49	73.81
Max HAc	mg/l	540	-
Max. HPr	mg/l	80.4	-
Initial pH		7.89	-
Min. pH		7.15	-

Figure D.1 illustrates the main difference in the biogas evolution for the two inocula tested. In spite of the fact that the final values were very similar, the evolution in the BPR and MPR showed some differences in the bacterial populations. Inoculum 2 seemed to be less active as

its response was “delayed” by one day for all the parameters there presented. Besides this delay, the evolution observed for the different parameters was very similar.

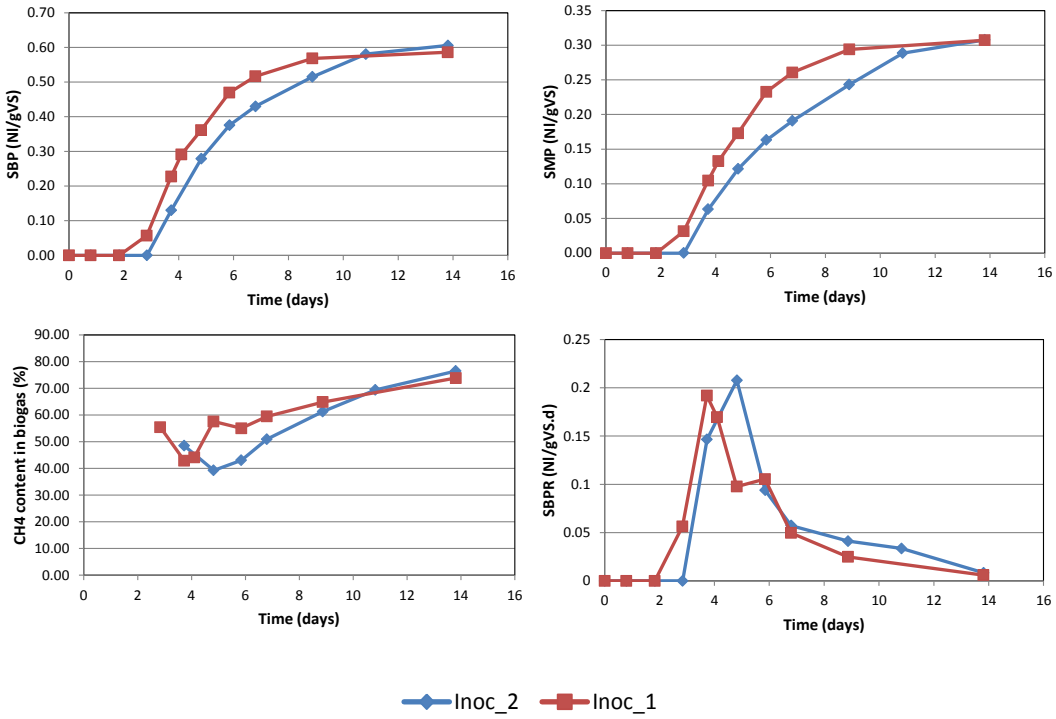

Figure D.1: Comparison of the SMP, SMP, CH_4 content in biogas, and SBPR for the two inocula considered

Annex E: Main characteristics of the inocula used in the tests

Start	End	Substrate	Feeding mode	TS (%FM)	VS (%FM)	pH	TIC (gCaCO3/l)
5/30/2011	6/27/2011	MS 1	Batch	4.88	3.05	7.85	14.50
5/30/2011	6/27/2011	MS 1	Batch	4.88	3.05	7.85	14.50
7/4/2011	7/27/2011	GS 1	Batch	3.90	2.37	7.72	14.12
7/4/2011	7/27/2011	GS 1	Batch	3.90	2.37	7.72	14.12
1/10/2012	2/3/2012	Co-digestion MS 1 + GS 1 (30/70)	Batch	6.00	3.65	7.96	19.06
1/10/2012	2/3/2012	Co-digestion MS 1 + GS 1 (70/30)	Batch	6.00	3.65	7.96	19.06
3/5/2012	4/2/2012	Co-digestion MS 1 + GS 1 (50/50)	Batch	4.63	2.66	7.96	8.75
5/15/2012	6/5/2012	Co-digestion MS 1 + GS 1 (40/60)	Batch	4.63	2.66	7.96	8.75
7/9/2012	7/24/2012	Co-digestion MS 1 + GS 1	Batch	3.30	2.17	N.D.	N.D.
5/15/2012	6/5/2012	GS 1	Batch	3.58	2.01	7.70	12.81
7/19/2012	7/23/2012	HAc	Batch	3.74	2.20	7.97	N.D.
7/23/2012	7/26/2012	HAc	Batch	3.74	2.20	7.95	N.D.
7/26/2012	7/30/2012	HPr	Batch	3.74	2.20	7.95	N.D.
7/16/2012	8/6/2012	GS 1	Batch	5.57	3.41	7.98	16.38
7/16/2012	8/6/2012	GS 1	Batch	5.57	3.41	7.98	16.38
7/25/2012	8/17/2012	MS 1	Batch	5.46	3.44	7.70	16.56
7/31/2012	9/3/2012	GS 1	Batch	5.43	3.47	7.97	17.93
8/21/2012	9/11/2012	GS 1	Batch	3.89	2.21	N.D.	N.D.
1/7/2013	3/8/2013	Cellulose	Semi-cont.	3.47	2.19	7.80	14.56
1/7/2013	2/4/2013	GS 1	Batch	3.44	1.94	8.00	N.D.
2/25/2013	3/11/2013	Cellulose	Batch	3.36	2.02	7.73	12.18
2/5/2013	3/27/2013	GS 1	Batch	4.22	2.43	7.77	12.43
9/20/2013	10/17/2013	Cellulose	Batch	3.60	2.20	7.70	12.50
10/21/2013	4/11/2014	DGS 2 and DGS 3 (dried 60°C)	Semi-cont.	3.82	2.15	N.D.	12.80
4/23/2014	5/23/2014	DGS 3 – BMP test	Semi-cont.	3.15	1.75	7.71	8.81
12/16/2013	1/6/2014	GS 3 (Fresh, dried at 105° and 60°)	Batch	N.D.	N.D.	N.D.	N.D.
03/03/2014	04/02/2014	Sodium acetate	Batch	3.32	2.05	7.71	11.18
04/03/2014	05/05/2014	Sodium Propionate	Batch	3.51	1.81	7.72	9.46
5/6/2014	10/13/2014	DMS 2 (dried at 60°C)	Semi-cont.	3.93	2.15	7.73	9.68
5/6/2014	6/5/2014	DMS 2 (dried at 60°C) – BMP test	Batch	3.93	2.15	7.73	9.68
05/26/2014	06/11/2014	Glucose	Batch	5.36	3.27	8.04	15.31
05/26/2014	06/11/2014	Starch	Batch	5.36	3.27	8.04	15.31
05/26/2014	06/11/2014	Cellulose	Batch	5.36	3.27	8.04	15.31
07/21/2014	08/11/2014	Gluten	Batch	5.21	3.15	7.54	14.56
06/09/2014	09/08/2014	Co-digestion DMS 2 and DGS 4	Semi-cont.	5.06	3.13	N.D.	13.18
7/14/2014	8/13/2014	DGS 4 dried at 60°C – BMP test	Batch	4.07	2.52	N.D.	10.72
5/6/2014	6/5/2014	DMS 2 (dried at 60°C)	Batch	3.93	2.15	7.80	9.68
08/28/2014	09/27/2014	GS 4	Batch	5.00	2.96	8.10	7.25

Annex F: Logging of the experiments and summary of the operational conditions

Start	End	Substrate	WV (l)	Running time (days)	Temp. (°C)	Feeding mode	OL – OLR (gVS/l-gVS/l/d)
5/30/2011	6/27/2011	MS 1	0.75	28	39	Batch	6
5/30/2011	6/27/2011	MS 1	0.75	28	39	Batch	12
7/4/2011	7/27/2011	GS 1	0.75	23	39	Batch	8.42
7/4/2011	7/27/2011	GS 1	0.75	23	39	Batch	16.84
1/10/2012	2/3/2012	Co-digestion MS 1 + GS 1 (30/70)	0.75	24	39	Batch	12
1/10/2012	2/3/2012	Co-digestion MS 1 + GS 1 (70/30)	0.75	24	39	Batch	12
3/5/2012	4/2/2012	Co-digestion MS 1 + GS 1 (50/50)	0.75	22	39	Batch	12
5/15/2012	6/5/2012	Co-digestion MS 1 + GS 1 (40/60)	0.75	22	39	Batch	12
7/9/2012	7/24/2012	Co-digestion MS 1 + GS 1	0.4	28	39	Batch	12
5/15/2012	6/5/2012	GS 1	10	15	39	Batch	12
7/19/2012	7/23/2012	Acetic acid	0.75	4	39	Batch	1g/l
7/23/2012	7/26/2012	Acetic acid	0.75	3	39	Batch	3g/l
7/26/2012	7/30/2012	HPr	0.75	4	39	Batch	0.5g/l
7/16/2012	8/6/2012	GS 1	0.75	21	39	Batch	18.07
7/16/2012	8/6/2012	GS 1	0.75	21	39	Batch	24.09
7/25/2012	8/17/2012	MS 1	10	23	39	Batch	12
7/31/2012	9/3/2012	GS 1	0.75	33	39	Batch	5.99
8/21/2012	9/11/2012	GS 1	0.75	21	39	Batch	7, 14, 18, 24
1/7/2013	3/8/2013	Cellulose	10	60	39	Semi-continuous	1, 1.5
1/7/2013	2/4/2013	GS 1	0.75	28	39	Batch	35.78
2/25/2013	3/11/2013	Cellulose	0.75	14	39	Batch	5.99
2/5/2013	3/27/2013	GS 1	0.75	50.	39	Batch	46.37
9/20/2013	10/17/2013	Cellulose	9	26	39	Batch	1
10/21/2013	4/11/2014	DGS 2 and DGS 3 (dried 60°C)	11.5	172	39	Semi-continuous	1.9
4/23/2014	5/23/2014	DGS 3 – BMP test	0.75	30	39	Batch	6
12/16/2013	1/6/2014	GS 3 (Fresh, dried at 105° and 60°)	0.75	21	39	Batch	9

Start	End	Substrate	WV (l)	Running time (days)	Temp. (°C)	Feeding mode	OL – OLR (gVS/l-gVS/l/d)
03/03/2014	04/02/2014	Sodium acetate (from stock solution)	0.75	30	39	Batch	0.5, 1, 2 and 4 g/l
04/03/2014	05/05/2014	Sodium Propionate (from stock solution)	0.75	32	39	Batch	0.5, 1, and 2 g/l
5/6/2014	10/13/2014	DMS 2 (dried at 60°C)	6.675	185	39	Semi-conti	2, 2.5, 3.5, 6 and 10
5/6/2014	6/5/2014	DMS 2 (dried at 60°C) – BMP test	0.75	30	39	Batch	6
05/26/2014	06/11/2014	Glucose	0.75	17	39	Batch	6
05/26/2014	06/11/2014	Starch	0.75	17	39	Batch	6
05/26/2014	06/11/2014	Cellulose	0.75	17	39	Batch	6
07/21/2014	08/11/2014	Gluten	0.75	21	39	batch	6
06/09/2014	09/08/2014	Co-digestion DMS 2 and DGS 4	0.75	90	39	Semi-continuous	2
7/14/2014	8/13/2014	DGS 4 dried at 60°C – BMP test	0.75	30	39	Batch	6
5/6/2014	6/5/2014	DMS 2 (dried at 60°C)	6.675	30	39	Batch	2
08/28/2014	09/27/2014	GS 4	0.75	30	39	Batch	6

Annex G: Composition of the trace element solution

Trace elements solution as described in Mata-Alvarez (2002)

Component	Concentration
$FeCl_2.4H_2O$	2000mg/l
H_3BO_3	50mg/l
$ZnCl_2$	50mg/l
$CuCl_2.2H_2O$	38mg/l
MnCl2.4H2O	500mg/l
$(NH_4)6Mo_7O_{24}.4H_2O$	50mg/l
$AlCl_3.6H_2O$	90mg/l
$CoCl_2.6H_2O$	2000mg/l

Annex H: Lignogas-SIM model

The variables considered in the Lignogas-SIM model are presented in Table H.1. The Kinetic and stoichiometric parameters are presented in tables H.2 and H.3 respectively. The reaction rates ρ_i are presented in the Petersen matrix form in Table H.4 for the liquid phase. The reactions rates $\rho_{T,i}$ for the gas phase are the same than for the ADM1, and are presented in the Petersen matrix shown in Table B.3. The inhibition terms considered in the model are the same than for the ADM1 (for the considered variables) and are summarised in Table B.4.

Table H.1: Components in the liquid phase and C (Ci) and N (Ni) used in the Lignogas-SIM

Component (i)	Symbol	Description	Ci	Ci used (mole C /gCOD)	Ni	Ni used (mole N /gCOD)
1	Smo	Monomers	C_{mo}	6/192	N_{mo}	0.007
2	Spro	Total propionate	C_{pro}	3/112	N_{pro}	0
3	Sac	Total acetate	C_{ac}	2/64	N_{ac}	0
4	Sh2	Hydrogen	C_{h2}	0	N_{h2}	0
5	Sch4	Methane	C_{ch4}	1/64	N_{ch4}	0
6	SIC	Inorganic carbon	C_{IC}	1	N_{IC}	0
7	SIN	Inorganic nitrogen	C_{IN}	0	N_{IN}	1
8	Xci	Composite substrate i	C_{xc}	0.0279*	N_{xc}	0.002
9	Xch	Carbohydrates	C_{ch}	6/192	N_{ch}	0
10	Xpr	Proteins	C_{pr}	0.03	N_{pr}	0.007
11	Xli	Lipids	C_{li}	0.022	N_{li}	0
12-15	Xsu –Xh2	Biomass	C_{bio}	5/160	N_{bio}	0.08/14*
16	Xi	Particulate inerts	C_i	0.03	N_i	0.06/14*

*From Rosen and Jeppsson (2006)

Table H.2: Kinetic parameters in the ADM1 model and used in Lignogas-SIM

Parameter	Name	Units	ADM1 default value	Used values
Hydrolisis rates				
Khyd_ch	Hydrolysis rate carbohydrates	d^{-1}	10	10
Khyd_pr	Hydrolysis rate proteins	d^{-1}	10	10
Khyd_li	Hydrolysis rate lipids	d^{-1}	10	10
kdis	Disintegration constant	d^{-1}	0.5	**Variable**
Maximum uptake rate				
Km_mo	Monomers degradation	gCOD/gCOD/d	30	**34.98**
Km_pr	Propionate degradation	gCOD/gCOD/d	13	13
Km_ac	Acetate degradation	gCOD/gCOD/d	8	**11.97**
Km_h2	Hydrogen degradation	gCOD/gCOD/d	35	
Half saturation constants				
Ks_mo	Monomers degradation	gCOD/l	0.5	0.5
Ks_pr	Propionate degradation	gCOD/l	0.1	0.1
Ks_ac	Acetate degradation	gCOD/l	0.15	**0.1**
Ks_h2	Hydrogen degradation	gCOD/l	$7x10^{-6}$	$7x10^{-6}$
Logarithmic constant pKa (at 298K)				
pKa_co2	- log10ka CO2		6.35	6.35
pKa_ac	- log10ka HAc		4.76	4.76
pKa_pro	- log10ka HPr		4.88	4.88
pKa_nh3	- log10ka NH3		9.25	9.25
Mass rate coefficients				
Kla_h2	Mass transfer coefficient for hydrogen	d^{-1}	200	200
Kla_ch4	Mass transfer coefficient for methane	d^{-1}	200	200
Kla_co2	Mass transfer coefficient for CO_2	d^{-1}	200	200
KH_h2	Henry's law coefficient for hydrogen	k mole COD/ m^3bar	0.00078	0.00078
KH_co2	Henry's law coefficient for CO2	k mole COD/ m^3bar	0.035	0.035
KH_ch4	Henry's law coefficient for methane	k mole COD/ m^3bar	0.0014	0.0014
kp	pipe resistance coefficient	l/bar.d	-	**50000***
Decay rates				
Kdec	Decay rate for biomass	d^{-1}	0.02	0.02
Biomass yileds				
Ymo	Yield in for monomer degraders	gCOD/gCOD	0.1	0.1

Parameter	Name	Units	ADM1 default value	Used values
Ypro	Yield for propionate degraders	gCOD/gCOD	0.04	0.04
Yac	Yield in acetate degraders	gCOD/gCOD	0.05	0.05
Yh2	Yield in hydrogen degraders	gCOD/gCOD	0.06	0.06
Inhibition factors				
KI_h2_pro	Inhibitory hydrogen concentration during HPr uptake	gCOD/l	3.5×10^{-6}	3.5×10^{-6}
Ks_IN	IN concentration at which growth ceases	M	0.0001	0.0001
KI_nh3_ac	inhibitory NH3 concentration for acetate degrading organisms	M	0.0018	**0.089-0.01****
pHUL_aa	pH upper limit for acidogens and aceto-gens	-	5.5	5.5
pHLL_aa	pH lower limit for acidogens and aceto-gens	-	4	4
pHUL_ac	pH upper limit for acetate degraders	-	7	7
pHLL_ac	pH lower limit for acetate degraders	-	6	6
pHUL_h2	pH upper limit for h2 degraders	-	6	6
pHLL_h2	pH lower limit for h2 degraders	-	5	5

*From Rosen and Jeppsson (2006)
**Values depending on the optimised values for km_ac and ks_ac

Table H.3: Stoichiometric parameters in the Lignogas-SIM

Parameter	Unit	Description	ADM1 default values	
fpr_Xc	-	Proteins from Xc	0.20	**Variable***
fli_Xc	-	Lipids from Xc	0.25	**Variable***
fch_Xc	-	Carbohydrates from Xc	0.20	**Variable***
fxi_Xc	-	Particular inerts from Xc	0.25	**Variable***
fsi_xc	-	Soluble inerts from Xc	0.10	**0**
fh2_mo	-	Hydrogen from sugars	0.19	**0.1945****
fbu_mo		butyrate from sugars	0.13	**0**
fpro_mo		Propionate from sugars	0.27	**0.3204****
fac_mo	-	Acetate from sugars	0.41	**0.4852****

*See Table 19.
**See Table 24 in sub-chapter 3.7.2.3.

Table H.4: Petersen matrix for both soluble and particulate components for the Lignogas-SIM model

Component → i		1	2	3	4	5	6	7	8	9	10	11	12	13	14	15	16	***Rate (ρj)***
j	Process ↓	Smo	Spro	Sac	Sh2	Sch4	S_{IC}	S_{IN}	Xc	Xch	Xpr	Xli	Xmo	Xpro	Xac	Xh2	Xi	
1	Disintegration i						$-\sum_{i=1-5,7-16} C_i \nu_{i,1}$	$-\sum_{i=1-6,8-16} N_i \nu_{i,1}$	-1	f_{ch_xci}	f_{ch_xci}	f_{li_xc}					f_{i_xc}	$k_{dis}*X_{ci}$
2	Hydrolysis Carb.	1								-1								$K_{hyd\_ch}*X_{ch}$
3	Hydrolysis Proteins	1					$-\sum_{i=1-5,7-16} C_i \nu_{i,3}$				-1							$K_{hyd\_pr}*X_{pr}$
4	Hydrolysis Lipids	1					$-\sum_{i=1-5,7-16} C_i \nu_{i,4}$					-1						$K_{hyd\_li}*X_{li}$
5	Uptake monomers	-1	$(1-Y_{mo})*f_{pro\_mo}$	$(1-Y_{mo})*f_{ac\_mo}$	$(1-Y_{mo})*f_{h2\_mo}$		$-\sum_{i=1-5,7-16} C_i \nu_{i,5}$	$-\sum_{i=1-6,8-16} N_i \nu_{i,5}$					Y_{mo}					$K_{m\_mo} \times \frac{S_{su}}{K_{s\_mo}+S_{mo}} \times X_{mo} \times I_1$
6	Uptake HPr		-1	$(1-Y_{pro})*0.57$	$(1-Y_{pro})*0.43$		$-\sum_{i=1-5,7-16} C_i \nu_{i,6}$	$-\sum_{i=1-6,8-16} N_i \nu_{i,6}$						Y_{pro}				$K_{m\_pro} \times \frac{S_{pro}}{K_{s\_pro}+S_{pro}} \times X_{pro} \times I_2$
7	Uptake HAc			-1		$(1-Y_{ac})$	$-\sum_{i=1-5,7-16} C_i \nu_{i,7}$	$-\sum_{i=1-6,8-16} N_i \nu_{i,7}$							Y_{ac}			$K_{m\_ac} \times \frac{S_{ac}}{K_{s\_ac}+S_{ac}} \times X_{ac} \times I_3$
8	Uptake H_2				-1	$(1-Y_{h2})$	$-\sum_{i=1-5,7-16} C_i \nu_{i,8}$	$-\sum_{i=1-6,8-16} N_i \nu_{i,8}$								Y_{h2}		$K_{m\_h2} \times \frac{S_{ac}}{K_{s\_h2}+S_{h2}} \times X_{h2} \times I_2$
9	Decay of Xsu						$-\sum_{i=1-5,7-16} C_i \nu_{i,9}$	$-\sum_{i=1-6,8-16} N_i \nu_{i,9}$	1									$K_{dec,\,Xmo}*X_{su}$
10	Decay of Xpro						$-\sum_{i=1-5,7-16} C_i \nu_{i,10}$	$-\sum_{i=1-6,8-16} N_i \nu_{i,10}$	1									$K_{dec,\,Xpro}*X_{pro}$
11	Decay of Xac						$-\sum_{i=1-5,7-16} C_i \nu_{i,11}$	$-\sum_{i=1-6,8-16} N_i \nu_{i,11}$	1									$K_{dec,\,Xac}*X_{ac}$
12	Decay of Xh2						$-\sum_{i=1-5,7-16} C_i \nu_{i,12}$	$-\sum_{i=1-6,8-16} N_i \nu_{i,12}$	1									$K_{dec,\,Xh2}*X_{h2}$
		Monomers	Total propionate	Total acetate	Hydrogen	Methane	Inorganic carbon	Inorganic nitrogen	Composite	Carbohydrates	Proteins	Lioids	Monomers degraders	Propionate degraders	Acetate degraders	H2 degraders	Inerts	Inhibition factors: $I_1=I_{ph}I_{N,lim}$ $I_2=I_{ph}I_{N,lim}I_{h2}$ $I_3I_{ph}I_{N,lim}I_{nh3,Xac}$

Annex I: Lignogas model

The variables considered in the Lignogas-SIM model are presented in Table I.1. The Kinetic and stoichiometric parameters are presented in tables I.2 and I.3 respectively. The reaction rates ρ_i are presented in the Petersen matrix form in Table I.4 (soluble components) and Table I.5 (particulate components) for the liquid phase. The reactions rates $\rho_{T,i}$ for the gas phase are the same than for the ADM1, and are presented in the Petersen matrix shown in Table B.3. The inhibition terms considered in the model are the same than for the ADM1 (for the considered variables) and are summarised in Table B.4.

Table I.1: Components in the liquid phase and C (Ci) and N (Ni) content used in the Lignogas (Option 1)

Component (i)	Symbol	Description	Ci	Ci used (mole C /gCOD)	Ni	Ni used (mole N /gCOD)
1	Ssu	Monoshaccaride	C_{su}	6/192	N_{su}	0
2	Saa	Amino acids	C_{aa}	0.03	N_{aa}	0.007
3	Sfa	LCFA	C_{fa}	0.0217	N_{fa}	0
4	Sva	Total valerate	C_{va}	5/208	N_{va}	0
5	Sbu	Total butyrate	C_{bu}	4/160	N_{bu}	0
6	Spro	Total propionate	C_{pro}	3/112	N_{pro}	0
7	Sac	Total acetate	C_{ac}	2/64	N_{ac}	0
8	Sh2	Hydrogen	C_{h2}	0	N_{h2}	0
9	Sch4	Methane	C_{ch4}	1/64	N_{ch4}	0
10	SIC	Inorganic carbon	C_{IC}	-	N_{IC}	0
11	SIN	Inorganic nitrogen	C_{IN}	0	N_{IN}	1
12	SI	Soluble inerts	C_i	0.03	N_i	0.002
13	Xc	Composites	C_{xc}	0.0279*	N_{xc}	0.0027*
14	Xch	Carbohydrates	C_{ch}	6/192	N_{ch}	0
15	Xpr	Proteins	C_{pr}	0.03	N_{pr}	0.007
16	Xli	Lipids	C_{li}	0.022	N_{li}	0
17-23	X_{su} –X_{h2}	Biomass	C_{bio}	5/160	N_{bio}	0.08/14*
24	Xi	Particulate inerts	C_i	0.03	N_i	0.06/14*
25	X_{bio}	Decayed biomass	C_{xbio}	0.0293**	N_{xbio}	0.0055**
26	X_{acetox}	Acetate oxidizing bacteria	C_{bio}	5/160	N_{bio}	0.08/14*

*From Rosen and Jeppsson (2006)
** C_{ch}*f_{ch_xb}+C_{pr}* f_{pr_xb}+ C_{li}* f_{li_xb} (see Table I.3)

Table I.2: Kinetic parameters in the ADM1 and Lignogas (option 1) models

Parameter	Name	Units	ADM1 default value	Used in Lignogas-Option 1
Hydrolisis rates				
Khyd_ch	Hydrolysis rate carbohydrates	d^{-1}	10	10
Khyd_pr	Hydrolysis rate proteins	d^{-1}	10	10
Khyd_li	Hydrolysis rate lipids	d^{-1}	10	10
kdis	Disintegration constant	d^{-1}	0.5	**Variable**
Kdis_bio	**Disintegration for decayed biomass**	**d^{-1}**	-	**0.5**
Maximum uptake rate				
Km_su	Sugar degradation	gCOD/gCOD/d	30	**34.97**
Km_aa	Amino acids degradation	gCOD/gCOD/d	50	50
Km_fa	LCFA degradation	gCOD/gCOD/d	6	6
Km_c4	valerate and butyrate degradation	gCOD/gCOD/d	20	20
Km_pr	Propionate degradation	gCOD/gCOD/d	13	13
Km_ac	Acetate degradation	gCOD/gCOD/d	8	**10.06**
Km_acetox	**Acetate oxidation**	**gCOD/gCOD/d**	-	**10**
Km_h2	Hydrogen degradation	gCOD/gCOD/d	35	**39.33**
Half saturation constants				
Ks_su	Sugar degradation	gCOD/l	0.5	0.5
Ks_aa	Amino acids degradation	gCOD/l	0.3	0.3
Ks_fa	LCFA degradation	gCOD/l	0.4	0.4
Ks_c4	valerate and butyrate degradation	gCOD/l	0.2	0.2

Parameter	Name	Units	ADM1 default value	Used in Lignogas-Option 1
Ks_pr	Propionate degradation	gCOD/l	0.1	0.1
Ks_ac	Acetate degradation	gCOD/l	0.15	0.15
Ks_acetox	Acetate oxidation	gCOD/l	-	0.5*
Ks_h2	Hydrogen degradation	gCOD/l	7 x10^{-6}	7 x10^{-6}
Logarithmic constant pKa (at 298K)				
pKa_co2	- log10ka CO2		6.35	6.35
pKa_ac	- log10ka HAc		4.76	4.76
pKa_pro	- log10ka HPr		4.88	4.88
pKa_bu	- log10ka HBu		4.84	4.84
pKa_va	- log10ka HVa		4.80	4.80
pKa_nh3	- log10ka NH3		9.25	9.25
pKa_h2o	- log10ka H2O		14	14
Mass rate coefficients				
Kla_h2	Mass transfer coefficient for hydrogen	d^{-1}	200	200
Kla_ch4	Mass transfer coefficient for methane	d^{-1}	200	200
Kla_co2	Mass transfer coefficient for CO_2	d^{-1}	200	200
KH_h2	Henry's law coefficient for hydrogen	k mole COD/ m^3bar	0.00078	0.00078
KH_co2	Henry's law coefficient for CO2	k mole COD/ m^3bar	0.035	0.035
kp	pipe resistance coefficient	l/bar.d	-	50000*
KH_ch4	Henry's law coefficient for methane	k mole COD/ m^3bar	0.0014	0.0014
Decay rates				
Kdec	Decay rate for biomass	d^{-1}	0.02	0.02
Biomass yileds				
Ysu	Yield in for sugar degraders	gCOD/gCOD	0.1	0.1
Yaa	Yield for amino acid degraders	gCOD/gCOD	0.08	0.08
Yfa	Yield for LCFA degraders	gCOD/gCOD	0.06	0.06
Yc4	Yield for valerate and buterate degraders	gCOD/gCOD	0.06	0.06
Ypro	Yield for propionate degraders	gCOD/gCOD	0.04	0.04
Yac	Yield for acetate degraders	gCOD/gCOD	0.05	0.05
Yh2	Yield for hydrogen degraders	gCOD/gCOD	0.06	0.06
Yacetox	**Yield for acetate oxidation**	**gCOD/gCOD**	-	**0.05**
Inhibition factors				
KI_h2_pro	Inhibitory hydrogen concentration during HPr uptake	gCOD/l	3.5 x10^{-6}	**3.5 x10^{-8}****
Ks_IN	IN concentration at which growth ceases	M	0.0001	0.0001
KI_h2_fa	hydrogen inhibitory concentration for LCFA degrading organisms	gCOD/l	5E-E06	5E-E06
KI_h2_c4	hydrogen inhibitory concentration for C4 degrading organisms	gCOD/l	1E-E05	**4.67x10^{-5}**
KI_nh3_ac	inhibitory NH3 concentration for acetate degrading organisms	M	0.0018	**0.0018-0.01****
pHUL_aa	pH upper limit for acidogens and aceto-gens	-	5.5	5.5
pHLL_aa	pH lower limit for acidogens and aceto-gens	-	4	4
pHUL_ac	pH upper limit for acetate degraders	-	7	7
pHLL_ac	pH lower limit for acetate degraders	-	6	6
pHUL_h2	pH upper limit for h2 degraders	-	6	6
pHLL_h2	pH lower limit for h2 degraders	-	5	5

*From Schlattmann (2011)

** Need for optimisation and value depending on the type of substrate and loading

Table I.3: Stoichiometric parameters in the ADM1 model (option 1)

Parameter	Unit	Description	ADM1 default values	Used in Lignogas
fpr_Xc	-	Proteins from Xc	0.20	**Variable***
fli_Xc	-	Lipids from Xc	0.25	**Variable***
fch_Xc	-	Carbohydrates from Xc	0.20	**Variable***
fxi_Xc	-	Particular inerts from Xc	0.25	**Variable***
fsi_xc	-	Soluble inerts from Xc	0.10	$1- f_{pr\_Xc}- f_{li\_Xc}- f_{xi\_Xc}- f_{ch\_Xc}$
ffa_li	-	LCFA from lipids	0.95	0.95
fh2_su	-	Hydrogen from sugars	0.19	0.19
fbu_su	-	butyrate from sugars	0.13	0.13
fpro_su	-	Propionate from sugars	0.27	0.27
fac_su	-	Acetate from sugars	0.41	0.41
fh2_aa	-	hydrogen from amino acids	0.06	0.06
fva_aa	-	valerate from amino acids	0.23	0.23
fbu_aa	-	butyrate from amino acids	0.26	0.26
fpro_aa	-	propionate from amino acids	0.05	0.05
fac_aa	-	acetate from amino acids	0.40	0.40
fpr_Xb	-	Proteins from decayed biomass	-	0.783**
fli_Xb	-	Lipids from decayed biomass	-	0.102**
fch_Xb	-	Carbohydrates from decayed biomass	-	0.115**

*See Table 19.
**See Table 23.

Table I.4: Stoichiometric coefficients and process rates for biochemical reactions in the Lignogas model for soluble components (extension of the ADM1 model)

Component → i		1	2	3	4	5	6	7	8	9	10	11	12	***Rate (ρj)***
j	Process ↓	Ssu	Saa	Sfa	Sva	Sbu	Spro	Sac	Sh2	Sch4	S_{IC}	S_{IN}	S_I	
1o	**Dis. biomass**													$k_{dis\text{-}bio}*X_{bio}$
1	Disintegration										$-\sum_{i=1-9,11-26} C_i\nu_{i,1}$	$-\sum_{i=1-10,12-26} N_i\nu_{i,1}$	f_{xi_xc}	$k_{dis}*X_c$
2	Hydrolysis Carb.	1												$K_{hyd\_ch}*X_{ch}$
3	Hydrolysis Proteins		1											$K_{hyd\_pr}*X_{pr}$
4	Hydrolyis Lipids	1-fa_li		fa_li							$-\sum_{i=1-9,11-26} C_i\nu_{i,4}$			$K_{hyd\_li}*X_{li}$
5	Uptake sugars	-1				$(1\text{-}Y_{su})*f_{bu\_su}$	$(1\text{-}Y_{su})*f_{pro\_su}$	$(1\text{-}Y_{su})*f_{ac\_su}$	$(1\text{-}Y_{su})*f_{h2\_su}$		$-\sum_{i=1-9,11-26} C_i\nu_{i,5}$	$-\sum_{i=1-10,12-26} N_i\nu_{i,5}$		$K_{m\_su}\times\frac{S_{su}}{K_{s\_su}+S_{su}}\times X_{su}\times I_1$
6	Uptake amino acids		-1		$(1\text{-}Y_{aa})*f_{va\_aa}$	$(1\text{-}Y_{aa})*f_{bu\_aa}$	$(1\text{-}Y_{aa})*f_{pro\_aa}$	$(1\text{-}Y_{aa})*f_{ac\_aa}$	$(1\text{-}Y_{aa})*f_{h2\_aa}$		$-\sum_{i=1-9,11-26} C_i\nu_{i,6}$	$-\sum_{i=1-10,12-26} N_i\nu_{i,6}$		$K_{m\_aa}\times\frac{S_{aa}}{K_{s\_aa}+S_{aa}}\times X_{aa}\times I_1$
7	Uptake LCFA			-1				$(1\text{-}Y_{fa})*0.7$	$(1\text{-}Y_{fa})*0.3$		$-\sum_{i=1-9,11-26} C_i\nu_{i,7}$	$-\sum_{i=1-10,12-26} N_i\nu_{i,7}$		$K_{m\_fa}\times\frac{S_{fa}}{K_{s\_fa}+S_{fa}}\times X_{fa}\times I_2$
8	Uptake of HVa				-1		$(1\text{-}Y_{c4})*0.54$	$(1\text{-}Y_{c4})*0.31$	$(1\text{-}Y_{c4})*0.15$		$-\sum_{i=1-9,11-26} C_i\nu_{i,8}$	$-\sum_{i=1-10,12-26} N_i\nu_{i,8}$		$K_{m\_c4}\times\frac{S_{va}}{K_{s\_c4}+S_{va}}\times X_{va}\times\frac{1}{1+S_{bu}/S_{va}}\times I_2$
9	Uptake HBu					-1		$(1\text{-}Y_{c4})*0.8$	$(1\text{-}Y_{c4})*0.2$		$-\sum_{i=1-9,11-26} C_i\nu_{i,9}$	$-\sum_{i=1-10,12-26} N_i\nu_{i,9}$		$K_{m\_c4}\times\frac{S_{bu}}{K_{s\_c4}+S_{bu}}\times X_{va}\times\frac{1}{1+S_{va}/S_{bu}}\times I_2$
10	Uptake HPr						-1	$(1\text{-}Y_{pro})*0.57$	$(1\text{-}Y_{pro})*0.43$		$-\sum_{i=1-9,11-26} C_i\nu_{i,10}$	$-\sum_{i=1-10,12-26} N_i\nu_{i,10}$		$K_{m\_pro}\times\frac{S_{pro}}{K_{s\_pro}+S_{pro}}\times X_{pro}\times I_2$
11	Uptake HAc							-1		$(1\text{-}Y_{ac})$	$-\sum_{i=1-9,11-26} C_i\nu_{i,11}$	$-\sum_{i=1-10,12-26} N_i\nu_{i,11}$		$K_{m\_ac}\times\frac{S_{ac}}{K_{s\_ac}+S_{ac}}\times X_{ac}\times I_3$
12	**Oxidation of acetate**							-1	$(1\text{-}Y_{acetox})$		$-\sum_{i=1-9,11-26} C_i\nu_{i,12}$	$-\sum_{i=1-10,12-26} N_i\nu_{i,12}$		$K_{m\_acetox}\times\frac{S_{acetox}}{K_{s\_acetox}+S_{acetox}}\times X_{acetox}\times I_2$
13	Uptake H_2								-1	$(1\text{-}Y_{h2})$	$-\sum_{i=1-9,11-26} C_i\nu_{i,13}$	$-\sum_{i=1-10,12-26} N_i\nu_{i,13}$		$K_{m\_h2}\times\frac{S_{ac}}{K_{s\_h2}+S_{h2}}\times X_{h2}\times I_2$
14	Decay of Xsu										$-\sum_{i=1-9,11-26} C_i\nu_{i,14}$	$-\sum_{i=1-10,12-26} N_i\nu_{i,14}$		$K_{dec,\ Xsu}*X_{su}$
15	Decay of Xaa										$-\sum_{i=1-9,11-26} C_i\nu_{i,15}$	$-\sum_{i=1-10,12-26} N_i\nu_{i,15}$		$K_{dec,\ Xaa}*X_{aa}$
16	Decay of Xfa										$-\sum_{i=1-9,11-26} C_i\nu_{i,16}$	$-\sum_{i=1-10,12-26} N_i\nu_{i,16}$		$K_{dec,\ Xfa}*X_{fa}$
17	Decay of Xc4										$-\sum_{i=1-9,11-26} C_i\nu_{i,17}$	$-\sum_{i=1-10,12-26} N_i\nu_{i,17}$		$K_{dec,\ Xx4}*X_{x4}$
18	Decay of Xpro										$-\sum_{i=1-9,11-26} C_i\nu_{i,18}$	$-\sum_{i=1-10,12-26} N_i\nu_{i,18}$		$K_{dec,\ Xpro}*X_{pro}$
19	Decay of Xac										$-\sum_{i=1-9,11-26} C_i\nu_{i,19}$	$-\sum_{i=1-10,12-26} N_i\nu_{i,19}$		$K_{dec,\ Xac}*X_{ac}$
20	Decay of Xh2										$-\sum_{i=1-9,11-26} C_i\nu_{i,20}$	$-\sum_{i=1-10,12-26} N_i\nu_{i,20}$		$K_{dec,\ Xh2}*X_{h2}$
21	Decay of X_{acetox}										$-\sum_{i=1-9,11-26} C_i\nu_{i,21}$	$-\sum_{i=1-10,12-26} N_i\nu_{i,21}$		$K_{dec,\ Xacetox}*X_{acetox}$
		Mono sacharides	Amono adcids	LCFA	Total Valerate	Total Propio-nate	Total Butyrate	Total Acetate	H2	CH4	IC	IN	Soluble Inerts	Inhibition factors: $I_1=I_{ph}I_{N,lim}$ $I_2=I_{ph}I_{N,lim}I_{h2}$ $I_3I_{ph}I_{N,lim}I_{nh3,Xac}$

Table I.5: Stoichiometric coefficients and process rates for reactions assumed in the Lignogas model for particulate components (extension of the ADM1 model)

Component → i		13	14	15	16	17	18	19	20	21	22	23	24	25	26	Rate (ρj)
j	Process ↓	Xc	Xch	Xpr	Xli	Xsu	Xaa	Xfa	Xc4	Xpro	Xac	Xh2	Xi	Xbio	Xacetox	
1o	Dis. biomass		fch_xb	fpr_xb	fli_xb									-1		$k_{dis\text{-}bio}*X_{bio}$
1	Disintegration	-1	fch_xc	fpr_xc	fli_xc								fxi_xc			$k_{dis}*X_c$
2	Hydrolysis Carb.		-1													$K_{hyd\_ch}*X_{ch}$
3	Hydrolysis Proteins			-1												$K_{hyd\_pr}*X_{pr}$
4	Hydrolyis Lipids				-1											$K_{hyd\_li}*X_{li}$
5	Uptake sugars					Ysu										$K_{m\_su}\times\frac{S_{su}}{K_{s\_su}+S_{su}}\times X_{su}\times I_1$
6	Uptake amino acids						Yaa									$K_{m\_aa}\times\frac{S_{aa}}{K_{s\_aa}+S_{aa}}\times X_{aa}\times I_1$
7	Uptake LCFA							Yfa								$K_{m\_fa}\times\frac{S_{fa}}{K_{s\_fa}+S_{fa}}\times X_{fa}\times I_2$
8	Uptake of HVa								Yc4							$K_{m\_c4}\times\frac{S_{va}}{K_{s\_c4}+S_{va}}\times X_{va}\times\frac{1}{1+S_{bu}/S_{va}}\times I_2$
9	Uptake HBu								Yc4							$K_{m\_c4}\times\frac{S_{bu}}{K_{s\_c4}+S_{bu}}\times X_{va}\times\frac{1}{1+S_{va}/S_{bu}}\times I_2$
10	Uptake HPr									Ypro						$K_{m\_pro}\times\frac{S_{pro}}{K_{s\_pro}+S_{pro}}\times X_{pro}\times I_2$
11	Uptake HAc										Yac					$K_{m\_ac}\times\frac{S_{ac}}{K_{s\_ac}+S_{ac}}\times X_{ac}\times I_3$
12	Oxidation HAc														Yacetox	$K_{m\_acetox}\times\frac{S_{acetox}}{K_{s\_acetox}+S_{acetox}}\times X_{acetox}\times I_2$
13	Uptake H_2											Yh2				$K_{m\_h2}\times\frac{S_{ac}}{K_{s\_h2}+S_{h2}}\times X_{h2}\times I_2$
14	Decay of Xsu					-1								1		$K_{dec,\,Xsu}*X_{su}$
15	Decay of Xaa						-1							1		$K_{dec,\,Xaa}*X_{aa}$
16	Decay of Xfa							-1						1		$K_{dec,\,Xfa}*X_{fa}$
17	Decay of Xc4								-1					1		$K_{dec,\,Xx4}*X_{x4}$
18	Decay of Xpro									-1				1		$K_{dec,\,Xpro}*X_{pro}$
19	Decay of Xac										-1			1		$K_{dec,\,Xac}*X_{ac}$
20	Decay of Xh2											-1		1		$K_{dec,\,Xh2}*X_{h2}$
21	Decay of Xacetox													1	-1	$K_{dec,\,Xacetox}*X_{acetox}$
		Composites	Carbohydrates	Proteins	Lipids	Sugar degraders	Amoni acid degraders	LCFA degradeers	Valerate and butyrate degraders	Propionate degraders	Acetate degraders	Hydrogen degraders	Particulate inerts			Inhibition factors: $I_1=I_{ph}I_{N,lim}$ $I_2=I_{ph}I_{N,lim}I_{h2}$ $I_3I_{ph}I_{N,lim}I_{nh3,Xac}$

Annex J: Results of the statistical analysis for mean comparison

Annex J.1: Semi-continuous digestion of grass silage (type DGS 3)

Normal distribution assessment

Parameter	OLR	Kolmogorov-Smirnova			Shapiro-Wilk		
		Statistic	df	Sig.	Statistic	df	Sig.
MPR	1.90	.132	20	.200*	.961	20	.564
	2.70	.168	20	.140	.894	20	.032
	3.30	.171	8	.200*	.929	8	.510
	4.70	.346	11	.001	.765	11	.003
SMP	1.90	.209	20	.022	.919	20	.094
	2.70	.188	20	.061	.907	20	.055
	3.30	.171	8	.200*	.929	8	.510
	4.70	.346	11	.001	.765	11	.003
CH4	1.90	.129	20	.200*	.968	20	.718
	2.70	.130	20	.200*	.972	20	.795
	3.30	.220	8	.200*	.931	8	.529
	4.70	.243	11	.068	.879	11	.102

*. This is a lower bound of the true significance.
a. Lilliefors Significance Correction

A non-significant result (Sig value of more than 0.05) indicates normality. In this case, the results from the Shapiro-Wilk test are considered as the number of samples is below 50 for each OLR. The significance value (p) is above 0.05 in all cases except for the parameters MPR for OLR 2.7 gVS/l/d and 4. 7 gVS/l/d and SMP for OLR 4.7 gVS/l/d. If taking into consideration the Q-Q plots for these cases (in Figure J.1) we could assume that normality is probably a good approximation.

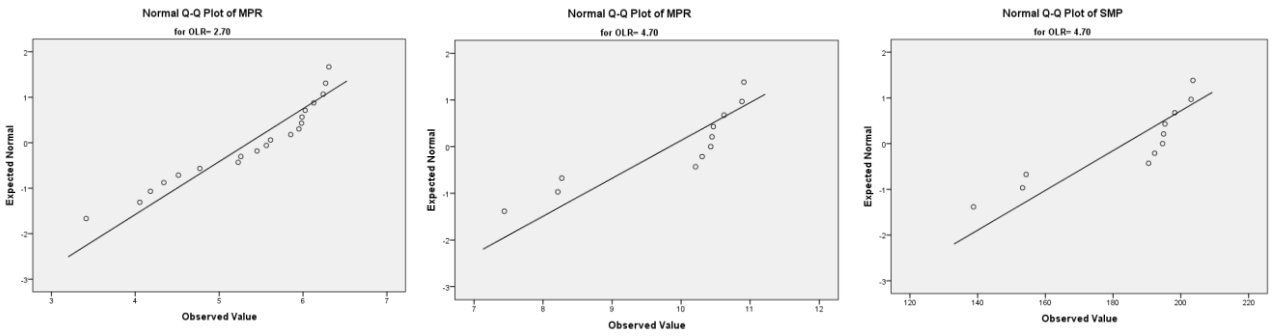

Figure J.1: Q-Q plot for MPR for OLR 2.7 and 4.7 (left and centre) and SMP for OLR 4.7 gVS/l/d (right)

Homogeneity of the variance

Parameter	Levene Statistic	df1	df2	Sig.
MPR	2.739	3	55	.052
SMP	.358	3	55	.783
CH_4	1.646	3	55	.189

The homogeneity test shows that for all variables considered the significance value is ≥0.05, and therefore the null hypothesis can be accepted, thus the variances of the data are homogenous.

⇨ SMP

The p-value is >0.05 for the variable SMP, which means that there were no statistically significant differences between group means as determined by one-way ANOVA ($F(3,58) = 0.557$, $p = .645$). Post hoc tests were not carried out in this case.

ANOVA

	Sum of Squares	df	Mean Square	F	Sig.
Between Groups	1347.634	3	449.211	.557	.645
Within Groups	44322.749	55	805.868		
Total	45670.383	58			

⇨ CH_4 content

p-value is >0.05 for the variable CH_4 content, and therefore no statistically significant differences between group means are detected by one-way ANOVA ($\boldsymbol{F}(3,58) = 0.919$, $\boldsymbol{p} = .438$). Post hoc tests were not carried out in this case.

ANOVA

	Sum of Squares	df	Mean Square	F	Sig.
Between Groups	7.293	3	2.431	.919	.438
Within Groups	145.555	55	2.646		
Total	152.848	58			

⇨ MPR

As the p-value for the MPR is <0.05, the null hypothesis can be rejected, thus there is a statistically significant difference between groups. The Tukey post hoc test was performed in order to identify the means that were significantly different from each other. The mean of the OLR 1.9 gVS/l/d is statistically different from that of all the other OLR. This is also applicable to OLR 4.7 gVS/l/d. The mean of OLR 2.7 gVS/l/d differs from that of OLR 1.9 gVS/l/d and 4.7 gVS/l/d but not of the OLR of 3.3 gVS/l/d. Correspondingly, the mean of OLR 3.3 gVS/l/d differs from that of OLR 1.9 gVS/l/d and 4.7 gVS/l/d but not of OLR 2.7 gVS/l/d.

ANOVA

	Sum of Squares	df	Mean Square	F	Sig.
Between Groups	242.113	3	80.704	97.343	.000
Within Groups	45.599	55	.829		
Total	287.712	58			

Tukey HSD

Dependent Variable	(I) OLR	(J) OLR	Mean Difference (I-J)	Std. Error	Sig.	95% Confidence Interval	
						Lower Bound	Upper Bound
MPR	1.90	2.70	-1.26344*	.28794	.000	-2.0263	-.5006
		3.30	-2.08057*	.38090	.000	-3.0897	-1.0714
		4.70	-5.74216*	.34180	.000	-6.6477	-4.8366
	2.70	1.90	1.26344*	.28794	.000	.5006	2.0263
		3.30	-.81714	.38090	.152	-1.8263	.1920
		4.70	-4.47872*	.34180	.000	-5.3843	-3.5732
	3.30	1.90	2.08057*	.38090	.000	1.0714	3.0897
		2.70	.81714	.38090	.152	-.1920	1.8263
		4.70	-3.66159*	.42309	.000	-4.7825	-2.5407
	4.70	1.90	5.74216*	.34180	.000	4.8366	6.6477
		2.70	4.47872*	.34180	.000	3.5732	5.3843
		3.30	3.66159*	.42309	.000	2.5407	4.7825

*. The mean difference is significant at the 0.05 level.

Annex J.2: Semi-continuous digestion of dried grass silage (DGS 2 and DGS 3, OLR of 1.9 gVS/l/d)

Normal distribution assessment

Parameter	GS	Kolmogorov-Smirnov[a]			Shapiro-Wilk		
		Statistic	df	Sig.	Statistic	df	Sig.
MPR	DGS 2	.266	12	.019	.777	12	.005
	DGS 3	.132	20	.200*	.961	20	.564
SBP	DGS 2	.249	12	.038	.799	12	.009
	DGS 3	.173	20	.119	.949	20	.353
SMP	DGS 2	.273	12	.014	.814	12	.014
	DGS 3	.209	20	.022	.919	20	.094
CH_4	DGS 2	.186	12	.200*	.927	12	.345
	DGS 3	.129	20	.200*	.968	20	.718

*. This is a lower bound of the true significance.
a. Lilliefors Significance Correction

The results from the Shapiro-Wilk test (number of samples below 50) show that the significance value is above 0.05 for all parameters only for DGS 3, and for DGS 2 only for the CH_4 content. Therefore, it was decided to perform the homogeneity test and ANOVA for the CH4 content to compare both groups, and to perform the non-parametric Kruskal-Wallis H Test for the other variables (i.e. MPR, SBP, and SMP), which does not require the assumption of normality.

⇨ CH_4 content

Homogeneity of the variance

Parameter	Levene Statistic	df1	df2	Sig.
CH_4	3.151	1	30	.086

The homogeneity test shows that for the CH_4 content the significance value is ≥0.05, and therefore the null hypothesis can be accepted, thus the variances of the data are homogenous. The ANOVA test was therefore performed, which resulted in a p-value <0.05. Therefore, a statistically significant difference between both tested grass silages was detected. The Tukey post hoc test was not performed because there are fewer than three groups

ANOVA

	Sum of Squares	df	Mean Square	F	Sig.
Between Groups	33.105	1	33.105	16.639	.000
Within Groups	59.688	30	1.990		
Total	92.793	31			

⇨ MPR, SBP and SMP

The Kruskal-Wallis H test performed for the variables MPR, SBP and SMP showed that there was a statistically significant difference for the two grass silages considered for these three variables, with $\chi^2(2) = 14.85$, $p = 0.000$, $\chi^2(2) = 13.38$, $p = 0.000$, and $\chi^2(2) = 15.45$, $p = 0.000$ respectively.

Test Statistics[a,b]

	MPR	SBP	SMP
Chi-Square	14.850	13.388	15.456
df	1	1	1
Asymp. Sig.	.000	.000	.000
a. Kruskal Wallis Test b. Grouping Variable: GS_type			

Annex J.3: Semi-continuous digestion of dried maize silage (DMS 2)

Normal distribution assessment

Parameter		Kolmogorov-Smirnova			Shapiro-Wilk		
		Statistic	df	Sig.	Statistic	df	Sig.
BPR	2.00	.161	9	.200*	.930	9	.480
	2.50	.231	9	.181	.873	9	.132
	3.50	.244	10	.093	.848	10	.055
	6.00	.302	14	.001	.691	14	.000
	10.00	.206	10	.200*	.881	10	.135
MPR	2.00	.197	9	.200*	.920	9	.396
	2.50	.224	9	.200*	.888	9	.189
	3.50	.237	10	.117	.836	10	.040
	6.00	.266	14	.008	.694	14	.000
	10.00	.249	10	.080	.851	10	.060
CH4	2.00	.191	9	.200*	.888	9	.189
	2.50	.185	9	.200*	.882	9	.165
	3.50	.182	10	.200*	.941	10	.559
	6.00	.231	14	.041	.875	14	.049
	10.00	.205	10	.200*	.907	10	.260

*. This is a lower bound of the true significance.
a. Lilliefors Significance Correction

The results from the Shapiro-Wilk test are considered as the number of samples is below 50 for each OLR. The p-value is above 0.05 in all cases except for the parameters BPR for OLR 6, MPR for OLR 3.5 gVS/l/d and 6 gVS/l/d, and CH_4 content for OLR 6 gVS/l/d. If taking into consideration the Q-Q plots for these cases (in Figure J.2) we could assume that normality is probably a good approximation.

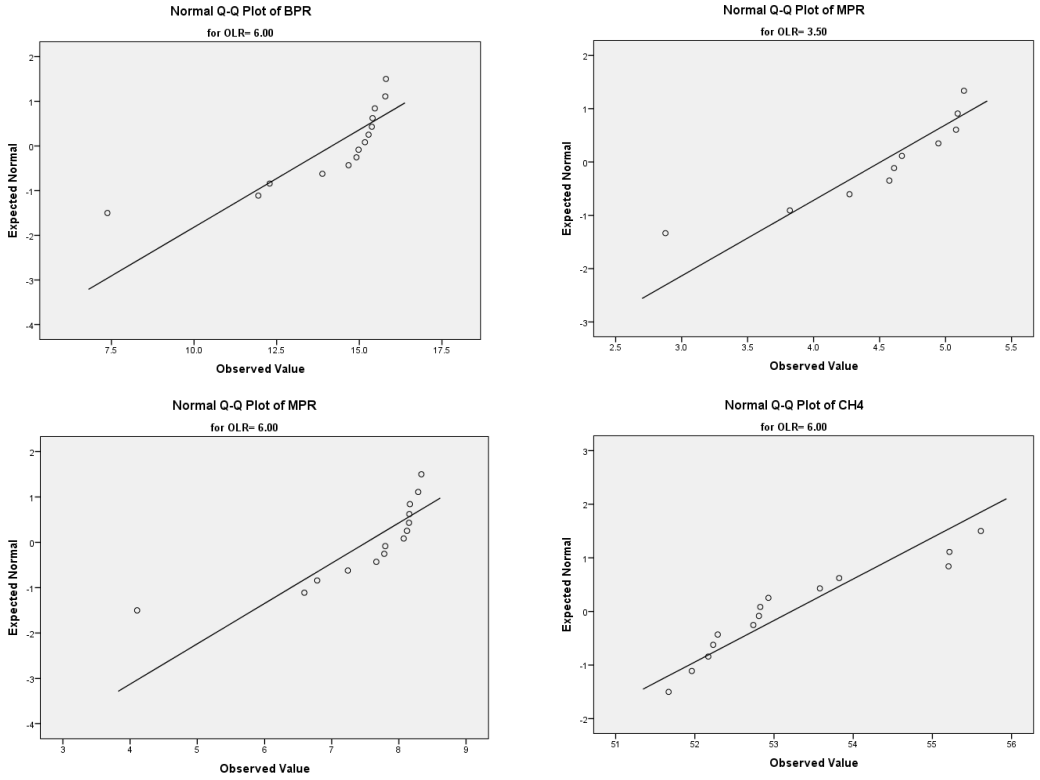

Figure J.2: Q-Q plot for BPR for OLR 6 gVS/l/d (top left), MPR for 3.5 gVS/l/d (top right) and 4.7 gVS/l/d (bottom left) and CH_4 for OLR 6 gVS/l/d (bottom right)

Homogeneity of the variance

Parameter	Levene Statistic	df1	df2	Sig.
MPR	8.884	4	47	.000
SMP	12.934	4	47	.000
CH4	19.810	4	47	.000

The homogeneity test shows that for all variables considered the significance value is <0.05, and therefore the null hypothesis has to be rejected, thus the variances of the data are not homogenous. Consequently, the Welch test was performed to test for the equality of group means, followed by the Games-Howell test.

Welch test for analyzing equality of means

Parameter	Statistic[a]	df1	df2	Sig.
BPR	34.805	4	22.702	.000
MPR	40.681	4	22.671	.000
CH4	4.168	4	20.970	.012
a. Asymptotically F distributed.				

The Welch test shows p-values<0.05 for all parameters considered, and therefore there is a statistically significant difference between groups. On the basis of the results of the Games-Howell test is possible to conclude that for BPR, the mean values for OLR 2 gVS/l/d and 2.5 gVS/l/d on the one hand, and for 6 gVS/l/d and 10 gVS/l/d on the other do not differ significantly. The same observation can be applied to the MPR. As for the CH4 content, the mean value for the OLR 10 gVS/l/d significantly differs from that of the other OLR.

Games-Howell test

Dependent Variable	(I) OLR	(J) OLR	Mean Difference (I-J)	Std. Error	Sig.	95% Confidence Interval	
						Lower Bound	Upper Bound
BPR	2.00	2.50	.24088	.61585	.995	-1.6585	2.1403
		3.50	-2.06812*	.65850	.042	-4.0761	-.0602
		6.00	-7.75354*	.78113	.000	-10.0806	-5.4265
		10.00	-13.58951*	3.11475	.011	-23.9574	-3.2217
	2.50	2.00	-.24088	.61585	.995	-2.1403	1.6585
		3.50	-2.30900*	.58603	.008	-4.0940	-.5240
		6.00	-7.99442*	.72109	.000	-10.1512	-5.8376
		10.00	-13.83039*	3.10024	.010	-24.1890	-3.4718
	3.50	2.00	2.06812*	.65850	.042	.0602	4.0761
		2.50	2.30900*	.58603	.008	.5240	4.0940
		6.00	-5.68542*	.75784	.000	-7.9370	-3.4338
		10.00	-11.52139*	3.10899	.029	-21.8853	-1.1575
	6.00	2.00	7.75354*	.78113	.000	5.4265	10.0806
		2.50	7.99442*	.72109	.000	5.8376	10.1512
		3.50	5.68542*	.75784	.000	3.4338	7.9370
		10.00	-5.83597	3.13726	.396	-16.2191	4.5471
	10.00	2.00	13.58951*	3.11475	.011	3.2217	23.9574
		2.50	13.83039*	3.10024	.010	3.4718	24.1890
		3.50	11.52139*	3.10899	.029	1.1575	21.8853
		6.00	5.83597	3.13726	.396	-4.5471	16.2191
MPR	2.00	2.50	.14878	.29095	.985	-.7536	1.0512
		3.50	-1.06802*	.32529	.031	-2.0592	-.0768
		6.00	-4.07871*	.38258	.000	-5.2184	-2.9390
		10.00	-4.94520*	1.13390	.010	-8.6906	-1.1998
	2.50	2.00	-.14878	.29095	.985	-1.0512	.7536
		3.50	-1.21680*	.28025	.004	-2.0737	-.3599
		6.00	-4.22750*	.34509	.000	-5.2632	-3.1918
		10.00	-5.09399*	1.12181	.008	-8.8302	-1.3578
	3.50	2.00	1.06802*	.32529	.031	.0768	2.0592
		2.50	1.21680*	.28025	.004	.3599	2.0737
		6.00	-3.01070*	.37450	.000	-4.1230	-1.8984

Dependent Variable	(I) OLR	(J) OLR	Mean Difference (I-J)	Std. Error	Sig.	95% Confidence Interval	
						Lower Bound	Upper Bound
		10.00	-3.87719*	1.13120	.042	-7.6202	-.1342
	6.00	2.00	4.07871*	.38258	.000	2.9390	5.2184
		2.50	4.22750*	.34509	.000	3.1918	5.2632
		3.50	3.01070*	.37450	.000	1.8984	4.1230
		10.00	-.86649	1.14898	.938	-4.6245	2.8915
	10.00	2.00	4.94520*	1.13390	.010	1.1998	8.6906
		2.50	5.09399*	1.12181	.008	1.3578	8.8302
		3.50	3.87719*	1.13120	.042	.1342	7.6202
		6.00	.86649	1.14898	.938	-2.8915	4.6245
CH4	2.00	2.50	.28558	.96503	.998	-2.6876	3.2588
		3.50	.63396	.66484	.870	-1.5052	2.7732
		6.00	.66531	.69523	.869	-1.5182	2.8489
		10.00	10.14231*	2.38779	.011	2.3159	17.9688
	2.50	2.00	-.28558	.96503	.998	-3.2588	2.6876
		3.50	.34838	.80322	.991	-2.2861	2.9829
		6.00	.37973	.82855	.990	-2.2832	3.0426
		10.00	9.85673*	2.42996	.013	1.9826	17.7309
	3.50	2.00	-.63396	.66484	.870	-2.7732	1.5052
		2.50	-.34838	.80322	.991	-2.9829	2.2861
		6.00	.03135	.44411	1.000	-1.2864	1.3491
		10.00	9.50835*	2.32711	.017	1.7309	17.2858
	6.00	2.00	-.66531	.69523	.869	-2.8489	1.5182
		2.50	-.37973	.82855	.990	-3.0426	2.2832
		3.50	-.03135	.44411	1.000	-1.3491	1.2864
		10.00	9.47700*	2.33597	.017	1.6943	17.2597
	10.00	2.00	-10.14231*	2.38779	.011	-17.9688	-2.3159
		2.50	-9.85673*	2.42996	.013	-17.7309	-1.9826
		3.50	-9.50835*	2.32711	.017	-17.2858	-1.7309
		6.00	-9.47700*	2.33597	.017	-17.2597	-1.6943

Annex J.4: Semi-continuous co-digestion of dried maize and grass silage (DMS 2 and DGS 4)

Normal distribution assessment

Parameters	Mixture	Kolmogorov-Smirnova			Shapiro-Wilk		
		Statistic	df	Sig.	Statistic	df	Sig.
BMP	DMS 2	.271	10	.036	.850	10	.058
	Mixture 2	.303	10	.010	.816	10	.023
	Mixture 3	.171	9	.200*	.929	9	.475
	DGS 4	.259	10	.056	.869	10	.098
MPR	DMS 2	.275	10	.031	.851	10	.059
	Mixture 2	.291	10	.016	.817	10	.024
	Mixture 3	.164	9	.200*	.933	9	.510
	DGS 4	.284	10	.022	.862	10	.082
CH4	DMS 2	.278	10	.027	.884	10	.147
	Mixture 2	.161	10	.200*	.923	10	.380
	Mixture 3	.175	9	.200*	.933	9	.513
	DGS 4	.109	10	.200*	.950	10	.667

*. This is a lower bound of the true significance.
a. Lilliefors Significance Correction

The results from the Shapiro-Wilk test are considered as the number of samples is below 50 for each feedstock mixture considered. The p-value is above 0.05 in all cases except for the parameters BPR and MPR for mixture 2. If taking into consideration the Q-Q plots for these cases (in Figure J.3) we could assume that normality is probably a good approximation.

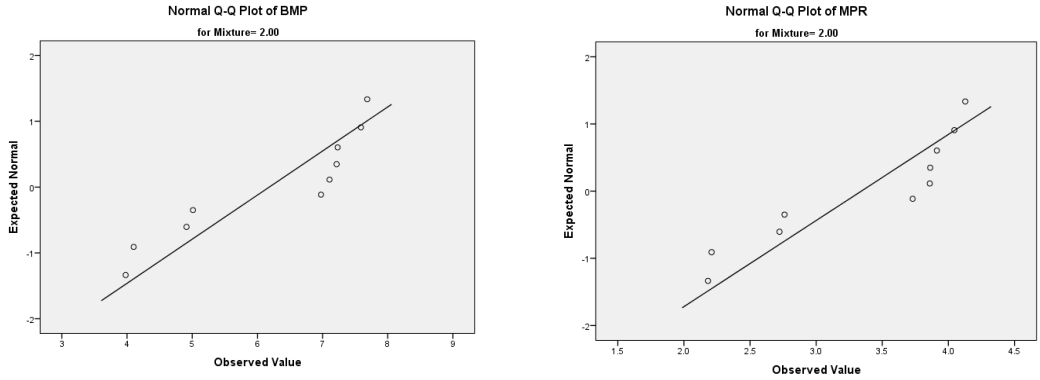

Figure J.3: Q-Q plot for BPR and MPR for mixture 2 (left and right respectively)

Homogeneity of the variance

Parameter	Levene Statistic	df1	df2	Sig.
MPR	1.084	3	35	.369
SMP	.831	3	35	.486
CH4	.073	3	35	.974

The homogeneity test shows that for all variables considered the significance value is >0.05, and therefore the null hypothesis can be accepted, thus criteria of the homogeneity of the variance is met. The ANOVA test was therefore performed, which resulted in a p-value >0.05 for BPR and MPR, which indicates that there are no statistically significant differences between group means for these variables ($F(3,35) = 0.820$, $p = .492$ and $F(3,35) = 0.913$, $p = .444$). Post hoc tests were not carried out in this case. For the CH4 content, on the other hand, p<0.05, which meant that ANOVA test detected statistically significant difference between mixtures for this variable.

ANOVA

		Sum of Squares	df	Mean Square	F	Sig.
BMP	Between Groups	9.288	3	3.096	.820	.492
	Within Groups	132.134	35	3.775		
	Total	141.423	38			
MPR	Between Groups	2.929	3	.976	.913	.444
	Within Groups	37.413	35	1.069		
	Total	40.342	38			
CH4	Between Groups	36.931	3	12.310	17.583	.000
	Within Groups	24.505	35	.700		
	Total	61.436	38			

The results of the Tukey post hoc test showed that the mean of CH_4 content for the maize silage (DMS 2) and the mixture 2 (50%DMS 2 2/50%DGS 4) are not statistically different, neither are the means of dried grass silage (DGS 4) and the mixture 3 (30%DMS 2/70%DGS 4).

Tukey HSD

(I) Mixture	(J) Mixture	Mean Difference (I-J)	Std. Error	Sig.	95% Confidence Interval	
					Lower Bound	Upper Bound
DMS 2	2.00	-.84800	.37420	.126	-1.8572	.1612
	3.00	-2.10378*	.38446	.000	-3.1406	-1.0669
	5.00	-2.40400*	.37420	.000	-3.4132	-1.3948
Mixture 2	.00	.84800	.37420	.126	-.1612	1.8572
	3.00	-1.25578*	.38446	.012	-2.2926	-.2189
	5.00	-1.55600*	.37420	.001	-2.5652	-.5468
Mixture 3	.00	2.10378*	.38446	.000	1.0669	3.1406
	2.00	1.25578*	.38446	.012	.2189	2.2926
	5.00	-.30022	.38446	.863	-1.3371	.7366
DGS 4	.00	2.40400*	.37420	.000	1.3948	3.4132

(I) Mixture	(J) Mixture	Mean Difference (I-J)	Std. Error	Sig.	95% Confidence Interval	
					Lower Bound	Upper Bound
	2.00	1.55600*	.37420	.001	.5468	2.5652
	3.00	.30022	.38446	.863	-.7366	1.3371
*. The mean difference is significant at the 0.05 level.						

Annex K: Results for the semi-continuous digestion of DGS 3 at increasing organic loading rate

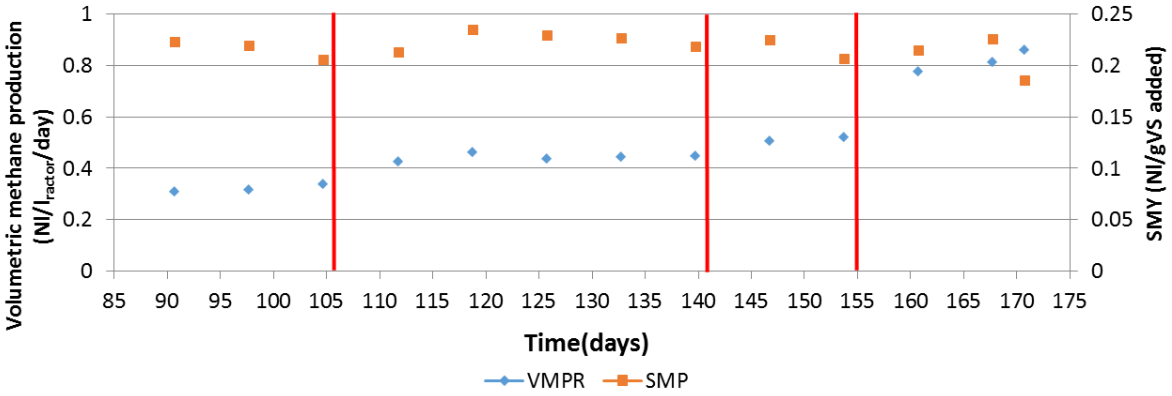

Figure K.1: Evolution of the VMPR and the SMP overtime during the semi-continuous digestion of DGS 3. The red lines represent a change in the feeding regime

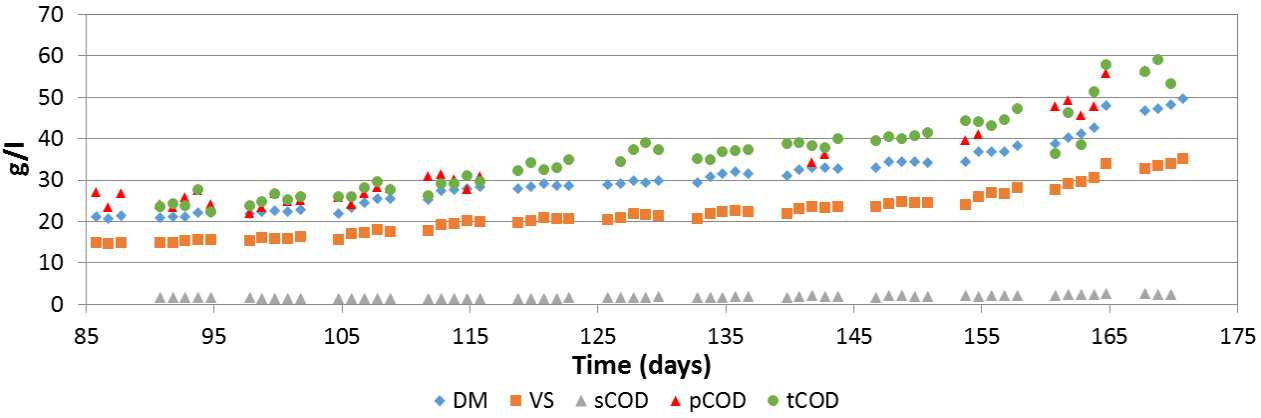

Figure K.2: Evolution of TS, VS, tCOD, pCOD and sCOD during the semi-continous digestion of DGS 3

Annex L: Results for the semi-continuous digestion of DMS 2 at increasing organic loading rate

Annex L.1: Biogas performance

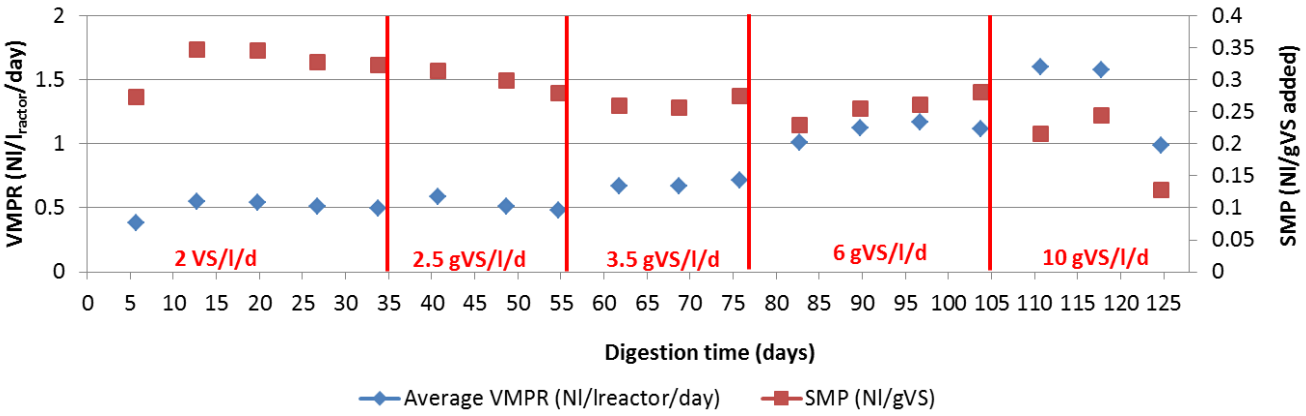

Figure L.1: Evolution of the VMPR and the SMP overtime. The red lines represent a change in the feeding regime

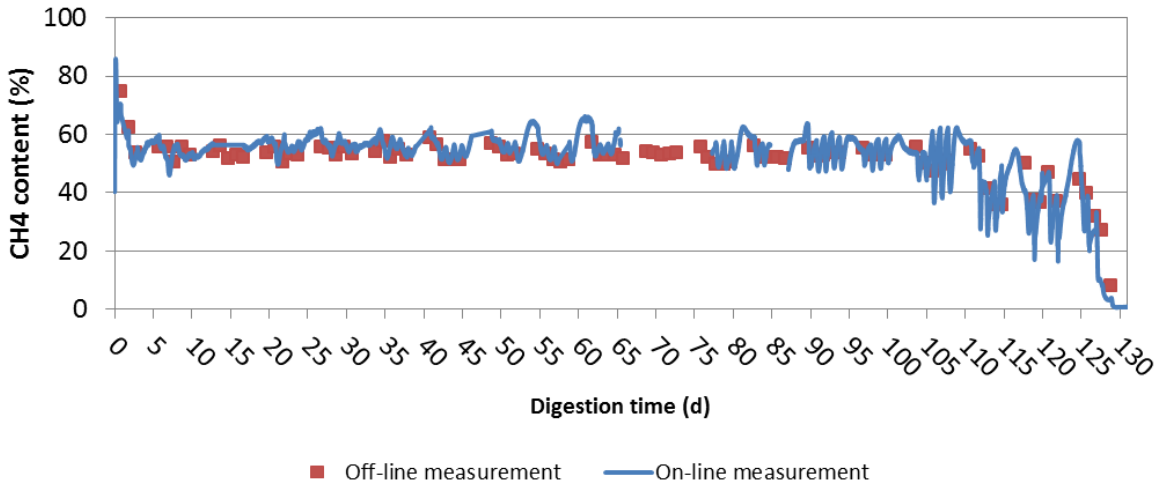

Figure L.2: Comparison of the evolution of CH_4 content measured on-line and off-line

Annex L.2: Evolution of intermediary products and stability

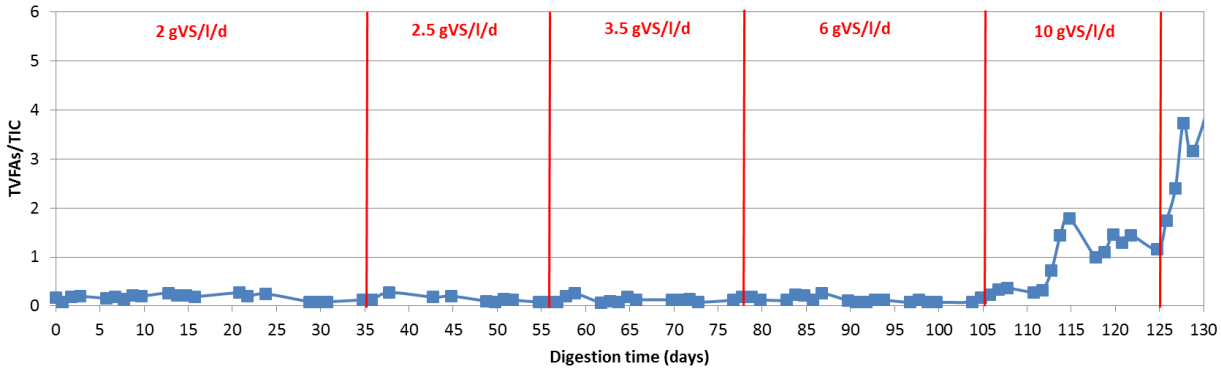

Figure L.3: Evolution of the TVFA/TIC ratio with increasing OLR during semi-continuous mono-digestion of maize silage

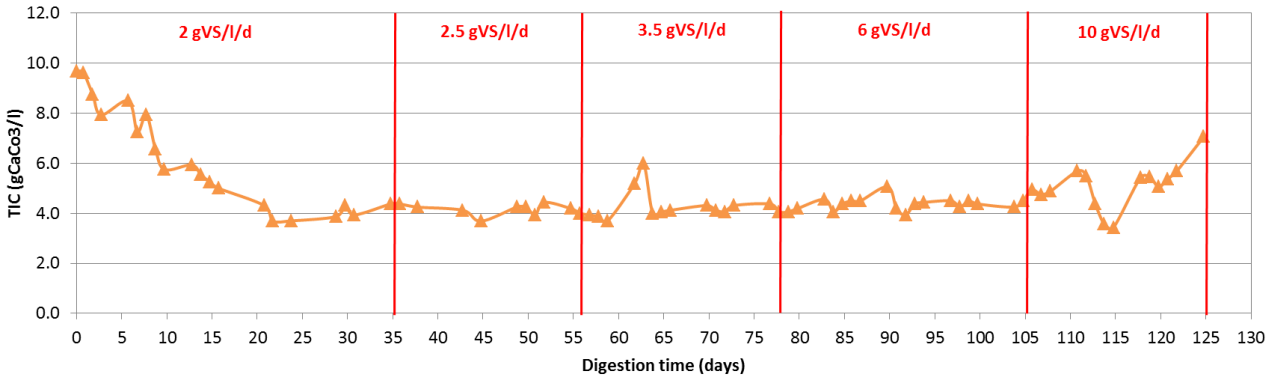

Figure L.4: Evolution of the TIC ratio with increasing OLR during semi-continuous mono-digestion of maize silage

Annex M: Results for the batch experiment with acetate and propionate

Two sets of batch experiments were implemented, for acetate and propionate respectively. Each set counts with 4 and 3 assays respectively, each with a different spiking concentration: 0.5 g/l, 1g/l, 2 g/l, and 4g/l. Each assay, which runs at mesophilic conditions, counts with 6 PET 1l reactors with 750g of inoculum and one control ("blank") reactor without addition of substrate running in parallel. Two reactors were connected to gasometers (to measure gas quantity and quality), one for online pH monitoring (Quadroline pH 296 with SensoLyt SEA and PtA, WTW), one for sampling and measuring VFA concentration (by means of the GC), one to be connected to the micro-sensor (AMT, Germany) for measuring dissolved H_2 and finally one connected to Bluesense online gas sensors (Sensor PA H2, Sensor PA CH4 and Sensor PA CO2, Bluesense). The reactors were inoculated with pre-acclimatized inoculum from Beckerich agricultural biogas plant in Luxembourg and run in series.

Figure M.1 shows the methane content in the biogas (top), the MPR (centre) and the methane yield (bottom), for the acetate (left) and the propionate (right) trial, measured off-line.

As regards the methane content in the biogas, for the acetate trials, it ranged from 70% up to 90%, which was quickly achieved after 2 days of digestion. For the propionate experiments, the methane content ranged from 50% up to 87%, which was achieved only at the end after progressive increase. The evolution in the content was almost identical for all OLs and for both series, except in the case of the propionate experiment with an OL of 4 g/l, which could present some inhibition.

For both series, there was an increase of the maximum production rate value and time achieved with increasing OL. It is interesting to mention that in the case of the acetate experiments, 2 peaks instead of 1 were systematically measured with 1 day interval for all OL. As regard the methane yield (expressed as $Nl_{CH4}/gCOD_{added}$), it clearly showed the impact of increasing the OL for both series, which lower slopes with increasing loading. The results showed higher yield for the propionate experiments but also suggested higher sensibility to overloading.

Using the stoichiometric conversion according to the following equations and applying the Buswell formula, it was possible to determinate the theoretical methane volume in each case, which is presented in Table M.1.

$CH_3CH_2COO^- + 3H_20 \rightarrow CH_3COO^- + HC0_3^- + 3H_2 + H^+$

$CH_3COO^- + H_20 \rightarrow HC0_3^- + CH_4$

The calculated achieved potential after 4 days of digestion was considerably lower that it could be expected, probably due to set-up and measuring error due to rapid foaming in the beginning of both experiments.

The recovery rates were satisfactory for both sets of experiments, with the lowest value for the Ac^- experiment with the OL of 0.5 g/l, with 84.4%. The relatively small volume produced, made it difficult to the measurement of the gas composition (given the limitations of the current measuring material in terms of the minimum volume required) and increased the possible error of the measurements.

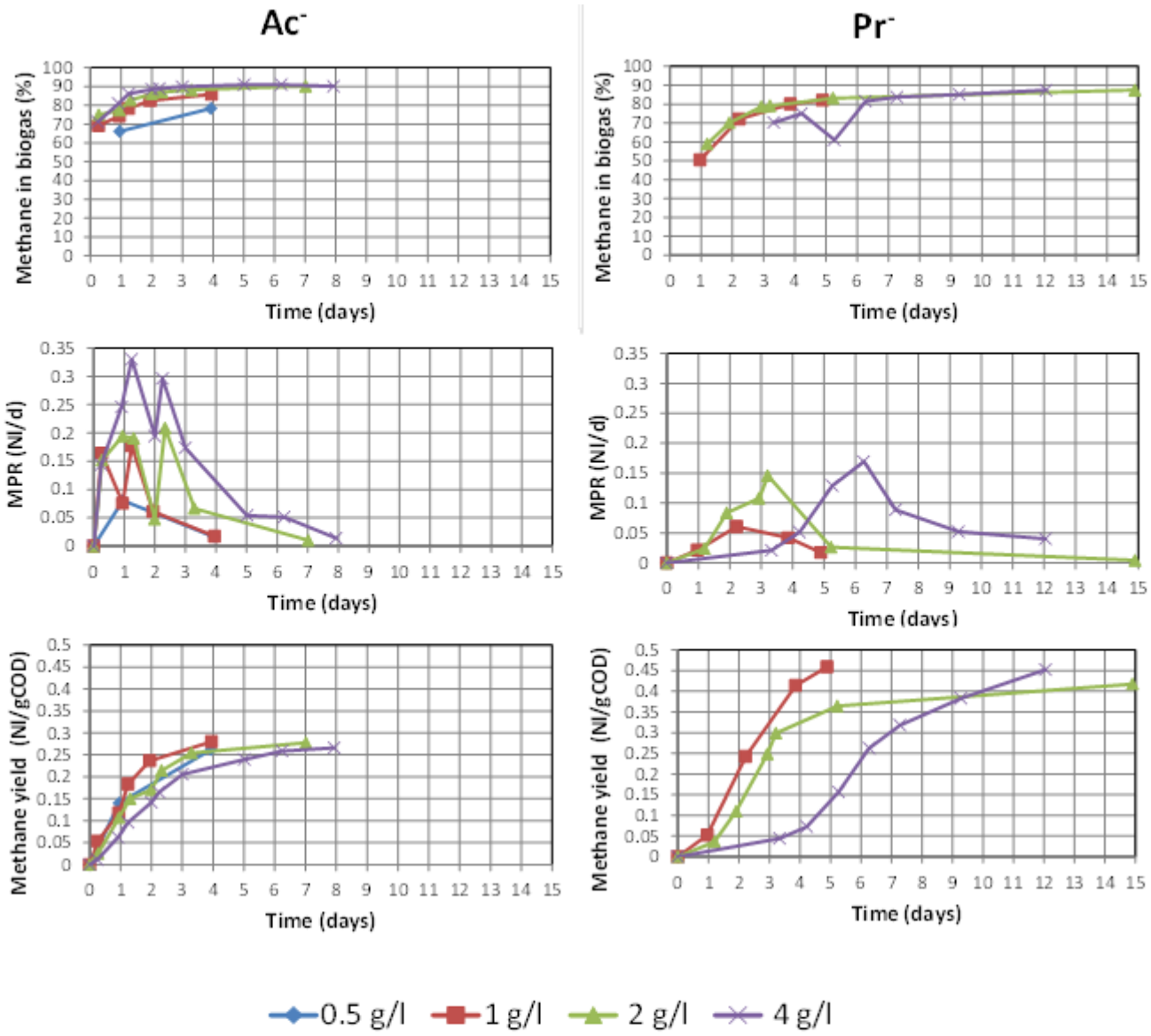

Figure M.1: Evolution of the methane content in the biogas (top), the MPR (centre) and the methane yield (bottom) for the Acetate (left9 and propionate batch experiments

Table M.1: Theoretical (calculated with the Buswell formula) and experimental methane volumes for the acetate and propionate trials

	Acetate			Propionate		
	Experimental volume (Nl)	Theoretical volume (Nl)	Recovery (%)	Experimental volume (Nl)	Theoretical volume (Nl)	Recovery (%)
0.5g/l	0.11	0.12	84.4%	0.18	0.19	98.6%
1g/l	0.22	0.25	90.3%	0.34	0.37	89.7%
2g/l	0.45	0.50	89.5%	0.73	0.75	97.2%
4g/l	0.85	1.00	85.8%			

The evolutions of HAc and HPr concentrations are presented in Figure M.2 for the different OLs tested. It can be observed:

- Digestion time increases with OL. While the total uptake of the acetate took almost 1 day for the OL of 0.5 g/l and 2 for the OL of 1 g/l, it took 3 days for the 2 g/l, and almost 6 for the highest OL of 4 g/l.
- The propionate seemed to present slower uptake rate than acetate, and also slower with increasing OL. This could also reflect the higher sensibility to inhibition, possibly due to increased partial pressure of H_2 in the gas phase.
- The measured evolution in the concentrations suggested a good accuracy of the GC that is usually used for individual VFA determination.

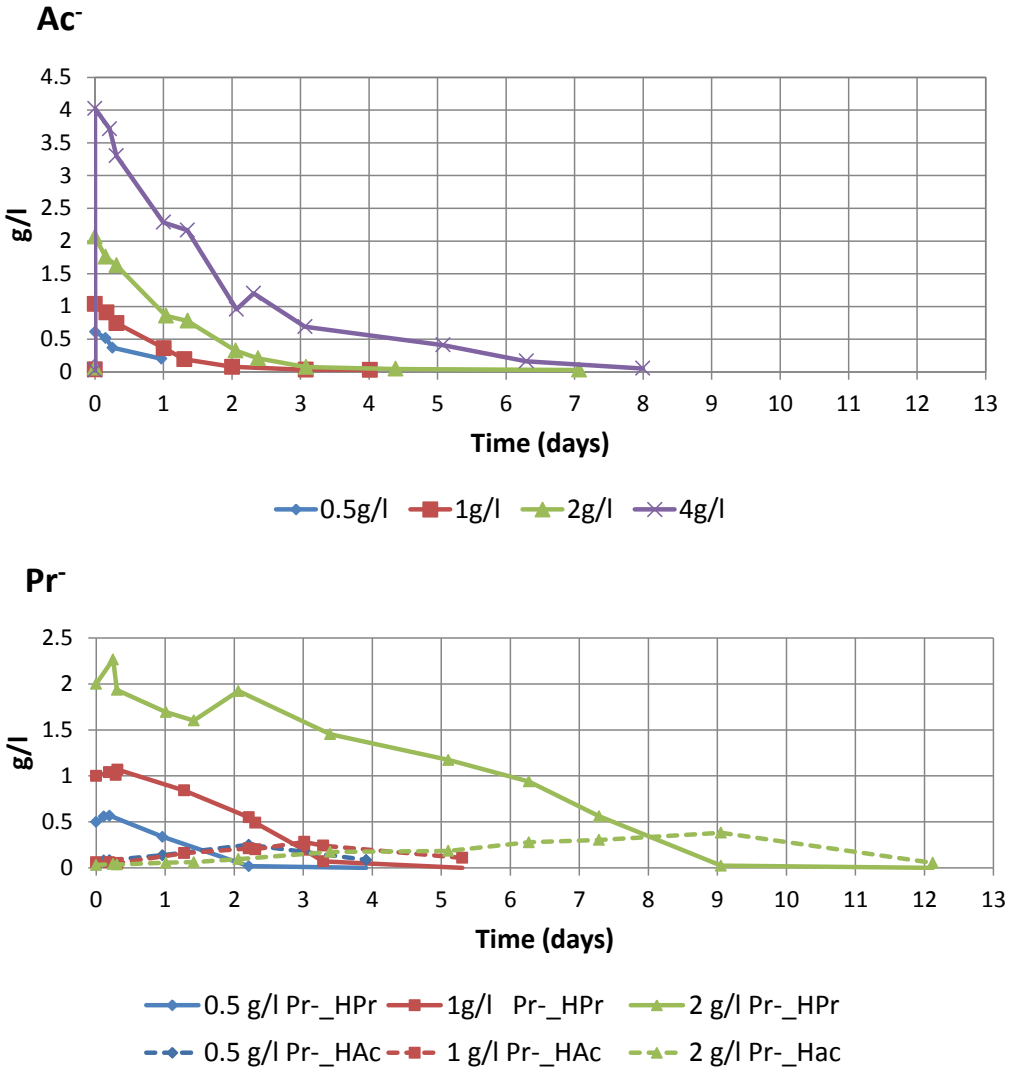

Figure M.2: Concentration evolution of Ac^- and Pr^- for the acetate (top) and propionate (bottom) assays.

The comparison of the calculated first-order kinetic constants for both set of experiments and the different OLs are presented in Table M.2. The fitting to first-order dynamics was satisfactory in all cases (lower R^2 value of 0.73). The calculated value support previous observation, namely:

- The uptake of propionate was slower than for acetate by almost 50%.
- Propionate wasmore sensible to the effects of increasing the OL.

Table M.2: Calculated hydrolysis first-order rate constants for propionate and acetate

	Acetate		Propionate	
	k (d^{-1})	R^2	k (d^{-1})	R^2
0.5g/l	0.8	1	0.51	0.88
1g/l	0.87	0.95	0.35	0.89
2g/l	0.65	0.94	0.18	0.73
4g/l	0.5	0.96		

Annex N: Results for the co-digestion experiments with grass and maize silages

Annex N.1: Co-digestion of grass and maize silages for batch conditions

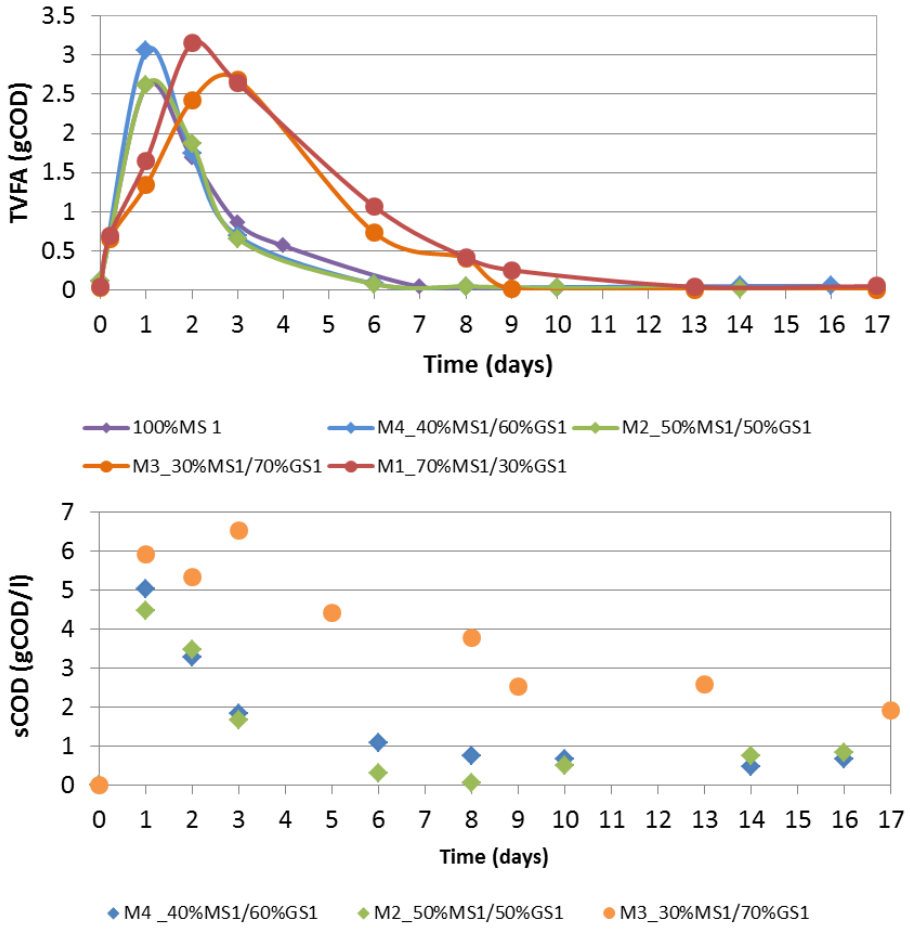

Figure N.1: Variation of TVFA (top) and sCOD (bottom) concentrations over time

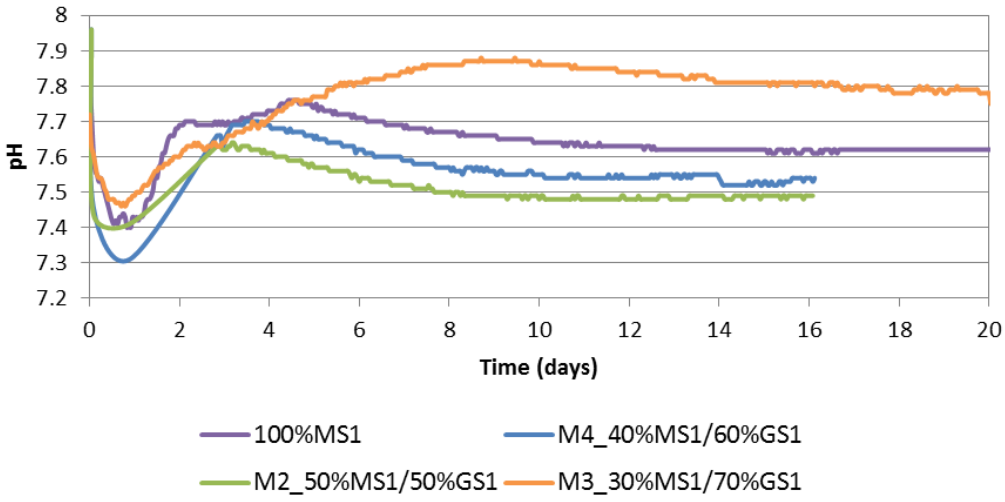

Figure N.2: pH evolution during co-digestion of selected mixtures tested

Annex N.2: Co-digestion of grass and maize silages in semi-continuous feeding mode for an OLR of 2gVS/l/d

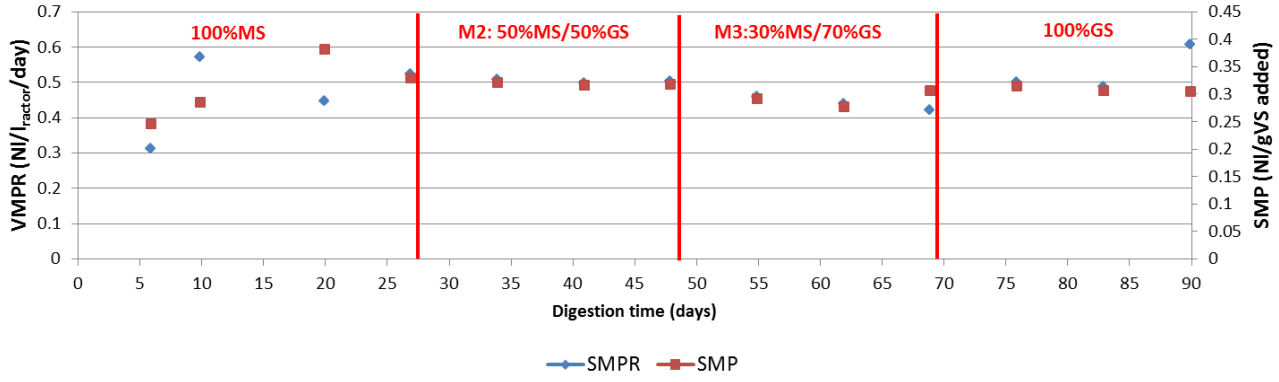

Figure N.3: Evolution of the VMPR and SMP during semi-continuous co-digestion of maize and grass silages silage

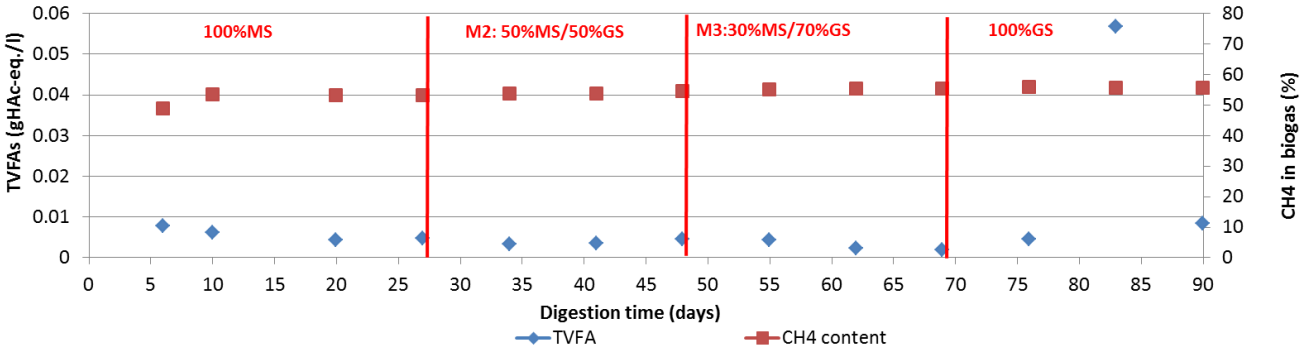

Figure N.4: Evolution of the TVFA and the CH_4 content in the biogas overtime. The red lines represent a change in the feeding regime

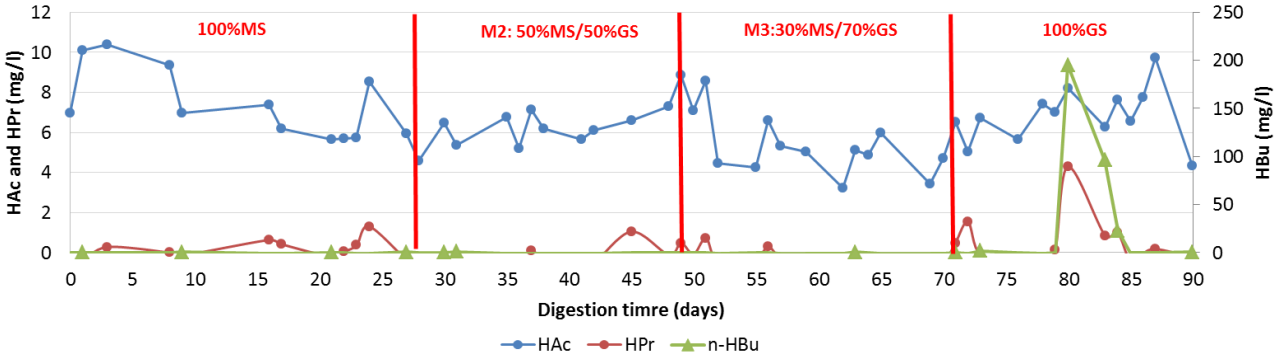

Figure N.5: Evolution of the HPr and HAc concentration (left axe) and the n-HBu (right axe) overtime in the digestate. The red lines represent a change in the feeding regime

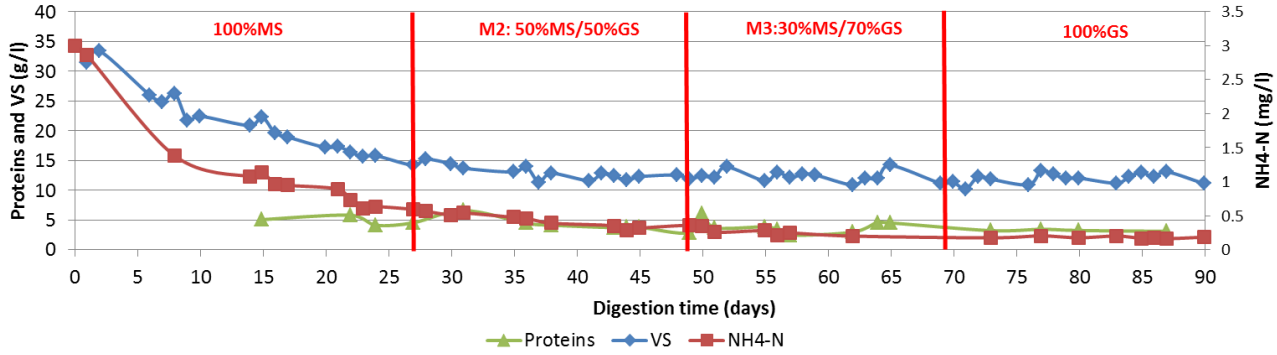

Figure N.6: Evolution of the proteins concentration, the VS and the NH_4^+-N overtime in the digestate. The red lines represent a change in the feeding regime

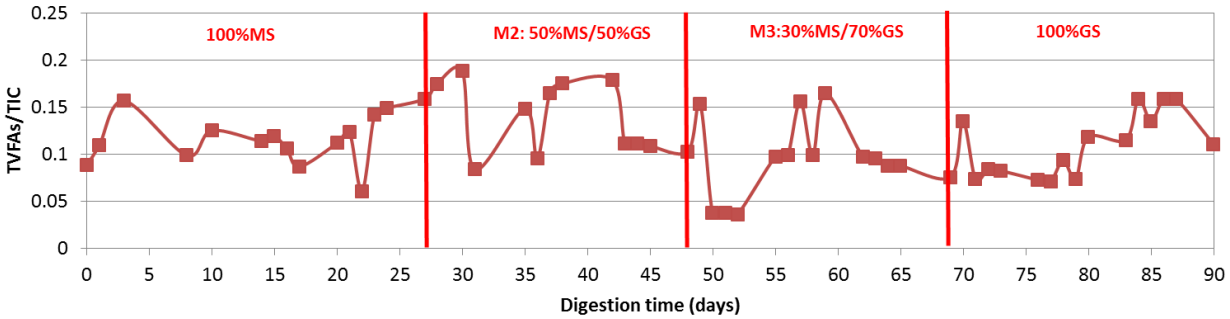

Figure N.7: Evolution of ratio TFA/TIC overtime in the digestate. The red lines represent a change in the feeding regime

Annex O: Results for the batch experiments with cellulose, starch, and glucose

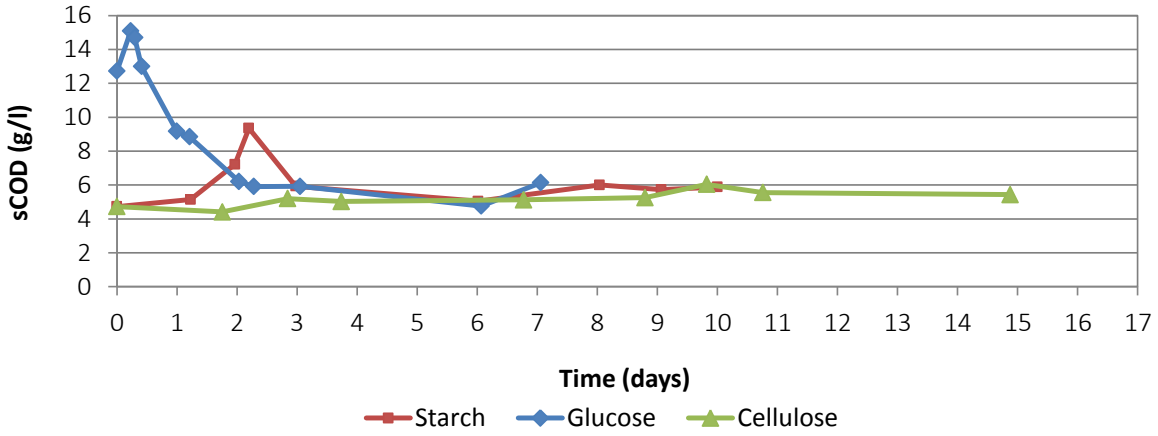

Figure O.1: Evolution of the sCOD concentration during batch digestion of cellulose, starch and glucose

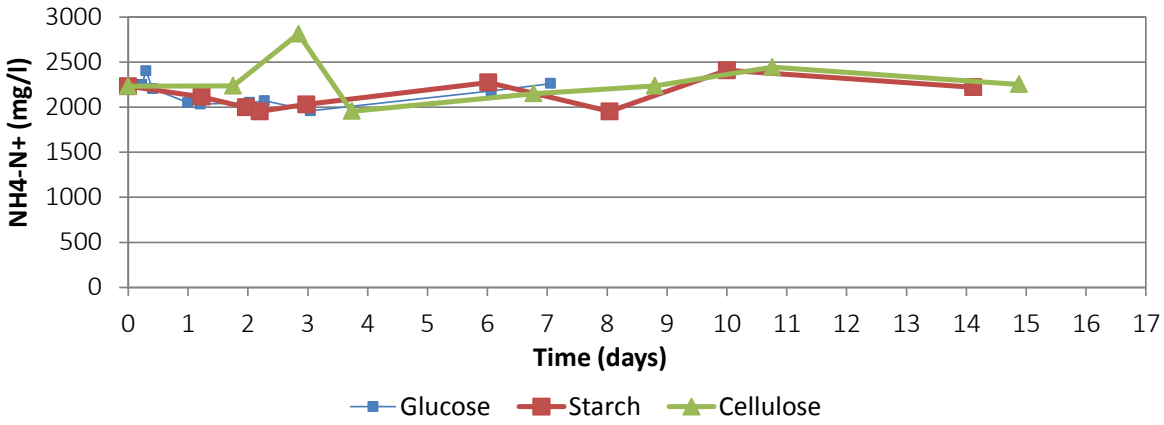

Figure O.2: Evolution of the NH_4^+-N concentration during batch digestion of cellulose, starch and glucose

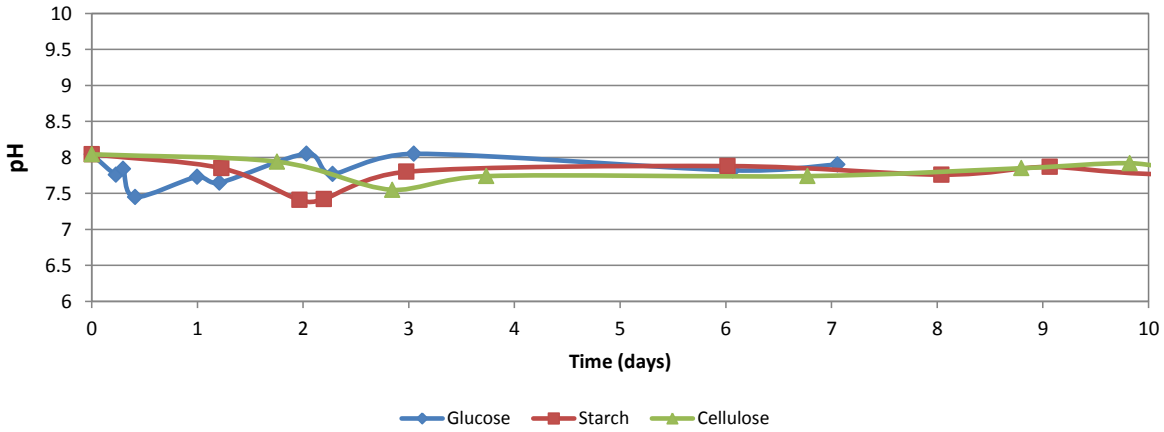

Figure O.3: Evolution of the pH during batch digestion of cellulose, starch and glucose

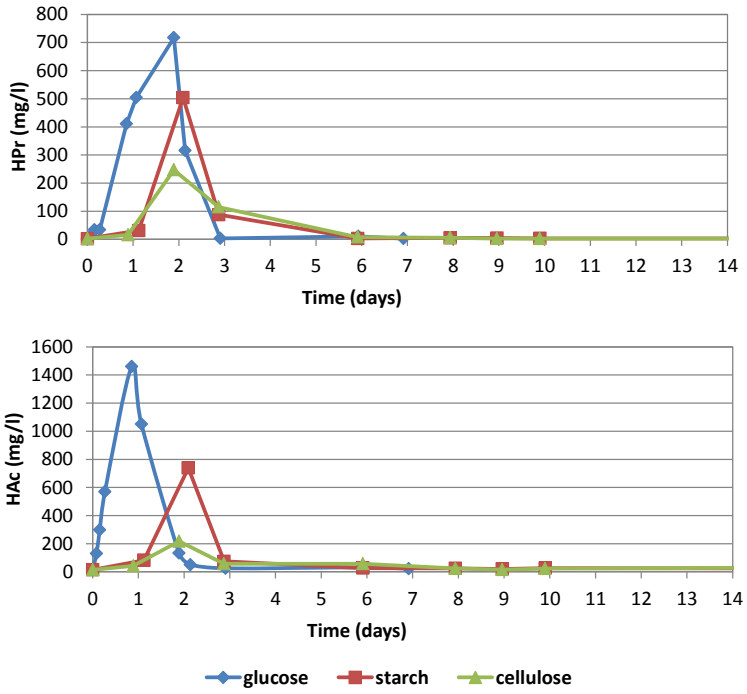

Figure O.4: Evolution of HAc (bottom) and HPr (top) during digestion of glucose, starch and cellulose

Annex P: Results for digestion of maize silage in a two stage semi-continuous system

Annex P.1: H_2 producing reactor (first stage)

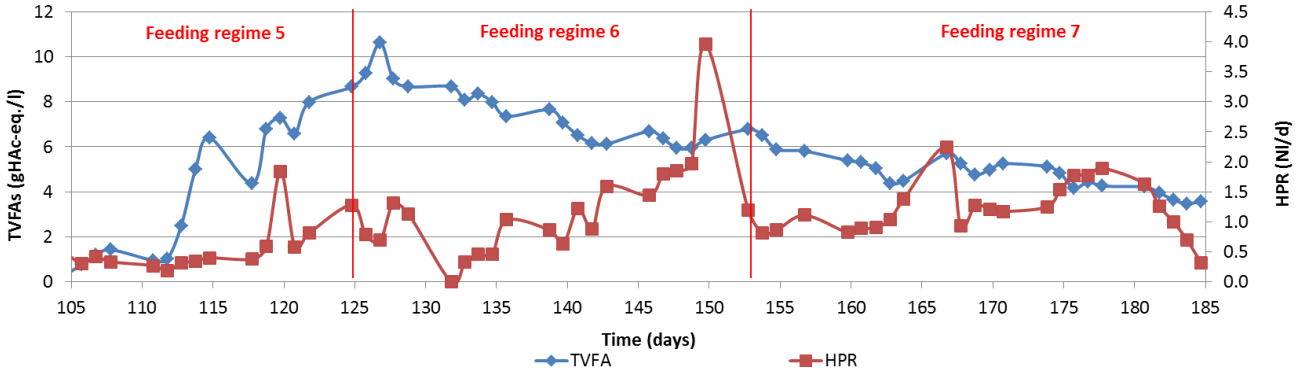

Figure P.1: Evolution of the daily concentration of TVFA (in gHAc-eq./l) (left axis) and the HPR (right axis)

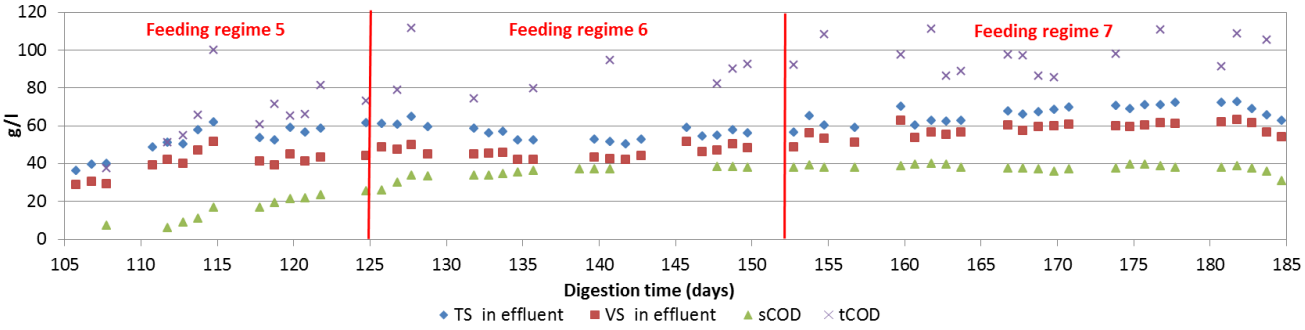

Figure P.2: Evolution of TS, VS, tCOD and sCOD for regimes 5, 6 and 7

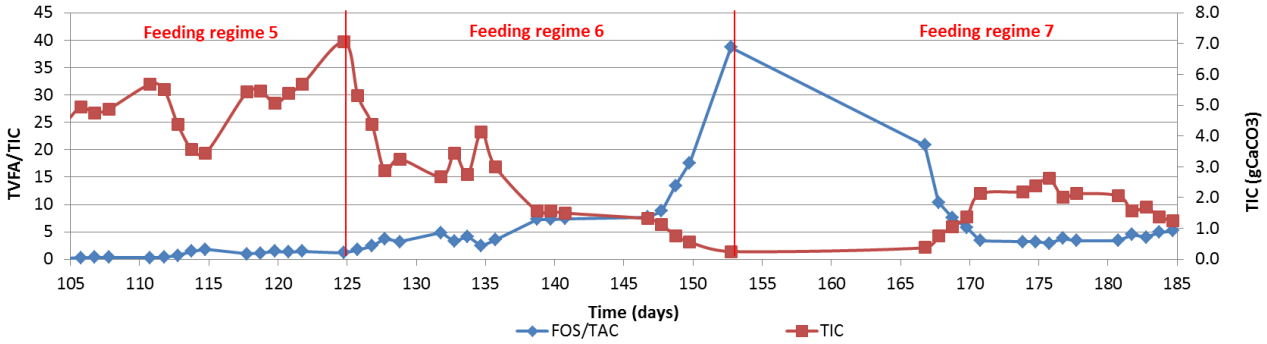

Figure P.3: Evolution of the TIC (i.e. TIC) (right axis) and the ratio TVFA/TIC (left axis) during digestion for regimes 5, 6 and 7

Annex P.2: CH_4 producing reactor (second stage)

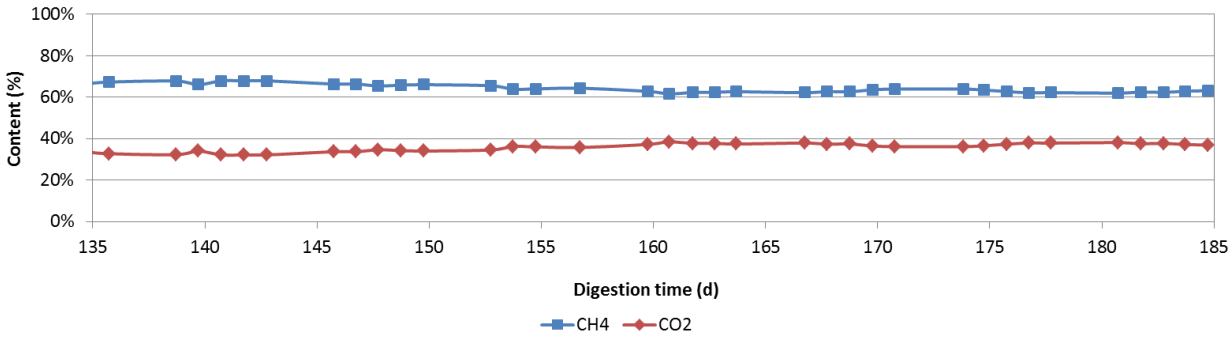

Figure P.4: Evolution of the CH_4 and CO_2 content in the biogas (off-line measurement)

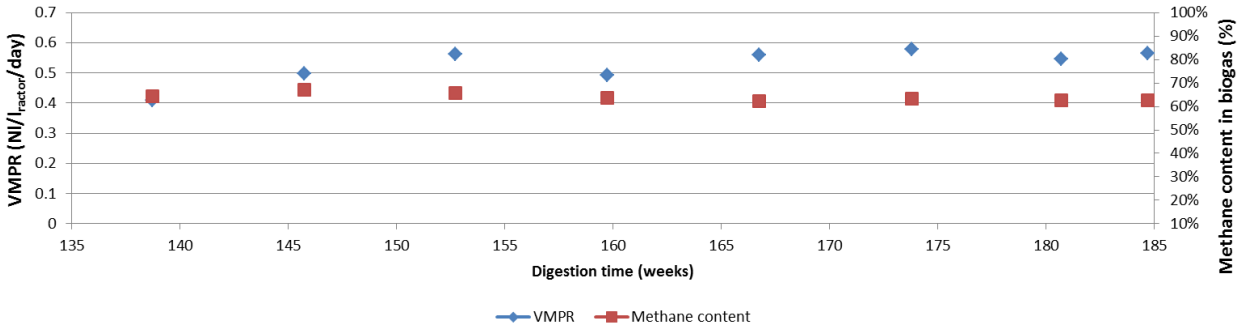

Figure P.5: Evolution of the weekly averages for the VMPR (left axis) and the CH_4 content in the biogas (right axis)

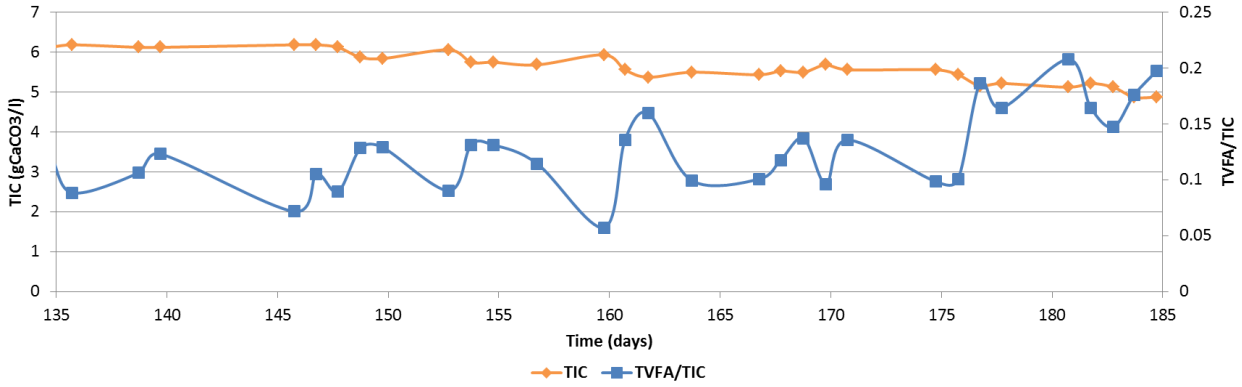

Figure P.6: Evolution of the TIC (blue and the ratio TVFA/TIC during digestion

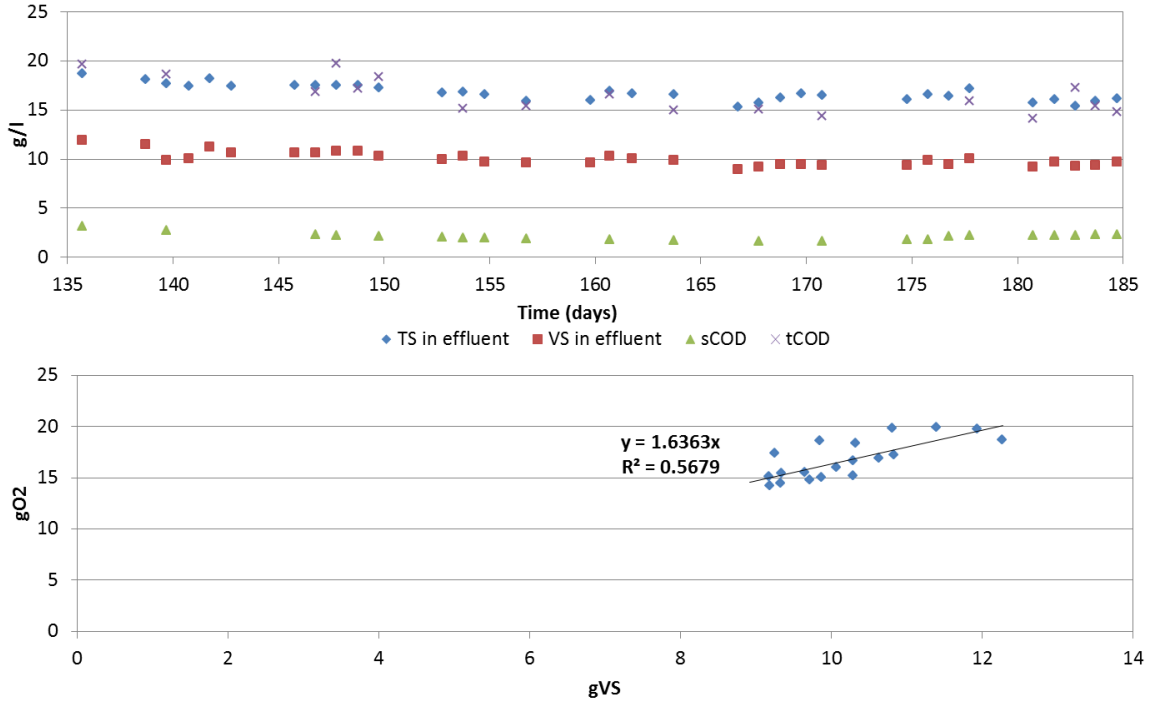

Figure P.7: Evolution of TS, VS, tCOD and sCOD during digestion (top) and correlation between COD and VS (bottom)

Annex Q: Sensitivity analysis

Annex Q.1: Ranking of mean absolute sensitivities for Lignogas-SIM model

Table Q.1: Sensitivity ranking (in red the 6 highest values for each variable)

	S_ac	S_ch4	S_co2	S_h2	S_hco3_ion	S_h_ion	S_IN	S_pro	S_mo	X_ac	X_c	X_ch	X_h2
	[gCOD/l]	[gCOD/l]	[M]	[gCOD/l]	[M]	[M]	[M]	[gCOD/l]	[gCOD/l]	[gCOD/l]	[gCOD/l]	[gCOD/l]	[gCOD/l]
km_ac	4.10E-01	8.63E-03	2.74E-03	1.13E-09	6.36E-03	3.11E-08	1.42E-04	2.67E-05	1.36E-05	2.71E-02	9.14E-04	3.22E-05	7.48E-05
kdis	1.34E-01	5.64E-03	2.01E-03	5.91E-08	2.42E-03	1.96E-08	6.96E-05	3.27E-02	1.92E-02	2.75E-03	3.31E-01	8.16E-03	4.10E-03
Y_ac	1.77E-01	3.67E-03	1.16E-03	1.14E-09	3.11E-03	1.30E-08	8.26E-04	6.57E-05	7.59E-05	1.30E-01	5.06E-03	1.78E-04	5.06E-04
km_mo	5.21E-02	1.01E-03	3.30E-04	1.25E-07	1.02E-03	4.81E-09	7.11E-05	2.26E-02	5.29E-02	2.63E-03	4.62E-04	2.06E-05	4.17E-03
Y_mo	6.43E-02	1.86E-03	6.59E-04	7.53E-08	2.75E-03	7.68E-09	2.66E-03	1.62E-02	2.70E-02	1.10E-02	1.63E-02	5.73E-04	7.39E-03
Ks_ac	5.57E-02	1.11E-03	3.54E-04	7.18E-10	8.66E-04	4.06E-09	1.87E-05	9.68E-06	3.32E-06	3.53E-03	1.22E-04	4.56E-06	8.58E-05
km_pro	3.35E-02	6.86E-04	2.08E-04	5.48E-08	1.63E-04	1.77E-09	2.70E-05	5.43E-02	5.48E-06	5.85E-04	1.82E-04	6.43E-06	1.88E-03
Ks_mo	1.62E-02	3.91E-04	1.31E-04	3.76E-08	3.09E-04	1.65E-09	2.43E-05	7.05E-03	2.03E-02	7.73E-04	1.58E-04	5.69E-06	1.30E-03
Y_pro	1.06E-02	3.18E-04	1.02E-04	1.60E-08	2.91E-04	1.03E-09	3.07E-04	1.51E-02	2.81E-05	1.10E-03	1.88E-03	6.60E-05	1.45E-03
Y_h2	6.36E-03	2.89E-04	9.67E-05	1.08E-07	5.18E-04	1.19E-09	5.68E-04	9.96E-03	6.16E-05	6.31E-04	3.48E-03	1.23E-04	8.87E-02
kdec_xmo	1.74E-03	2.18E-04	8.49E-05	3.37E-09	4.27E-04	3.15E-10	4.55E-04	3.05E-04	7.50E-04	2.42E-03	1.28E-02	4.48E-04	1.47E-03
km_h2	1.28E-02	2.86E-04	9.35E-05	2.75E-07	7.30E-05	6.95E-10	1.34E-05	2.02E-02	6.61E-06	2.53E-04	8.25E-05	2.90E-06	1.34E-03
kdec_xac	1.48E-02	2.10E-04	6.02E-05	8.89E-10	3.27E-04	8.87E-10	1.45E-04	6.23E-05	6.18E-05	3.84E-02	4.20E-03	1.48E-04	4.54E-04
khyd_ch	4.63E-03	2.22E-04	8.09E-05	5.91E-09	9.48E-05	7.56E-10	7.02E-06	1.58E-03	2.84E-03	4.85E-05	4.90E-05	1.28E-02	1.74E-04
Ks_h2	7.81E-03	1.64E-04	5.62E-05	1.97E-07	4.19E-05	4.25E-10	9.42E-06	1.30E-02	9.71E-07	1.39E-04	5.71E-05	2.03E-06	9.76E-04
Ks_pro	6.86E-03	1.41E-04	4.30E-05	1.08E-08	4.18E-05	3.98E-10	6.00E-06	1.23E-02	1.39E-06	1.35E-04	4.02E-05	1.50E-06	4.16E-04
kdec_xh2	5.67E-04	5.14E-05	1.97E-05	7.36E-09	1.07E-04	7.13E-11	1.15E-04	3.97E-04	4.60E-05	6.11E-04	3.17E-03	1.11E-04	3.09E-02
khyd_pr	1.08E-03	5.79E-05	2.11E-05	1.30E-09	2.22E-05	1.91E-10	1.64E-06	3.69E-04	6.58E-04	1.11E-05	1.14E-05	4.02E-07	4.37E-05
kdec_xpro	1.00E-03	3.52E-05	1.24E-05	1.81E-09	7.26E-05	5.54E-11	7.75E-05	1.51E-03	3.12E-05	4.16E-04	2.14E-03	7.51E-05	2.87E-04
Ks_IN	1.65E-03	3.86E-05	1.23E-05	9.56E-10	2.87E-05	1.43E-10	9.57E-07	3.32E-04	1.96E-04	1.17E-04	6.05E-06	2.31E-07	2.68E-05
khyd_li	2.17E-04	3.02E-06	1.06E-06	3.22E-10	4.27E-06	1.75E-11	3.04E-07	7.35E-05	1.30E-04	2.45E-06	2.16E-06	7.61E-08	1.16E-05

Table Q.2: Sensitivity ranking (in red the 6 highest values for each variable) (continuation)

	X_I	X_li	X_pr	X_pro	X_mo	G_ch4	G_co2	G_h2
	[gCOD/l]	[gCOD/l]	[gCOD/l]	[gCOD/l]	[gCOD/l]	[gCOD/l]	[M]	[gCOD/l]
km_ac	8.57E-04	1.48E-06	7.45E-06	6.75E-05	5.83E-04	2.75E-01	4.29E-03	3.24E-05
kdis	3.49E-02	3.74E-04	1.89E-03	1.96E-03	2.83E-02	2.01E-01	3.15E-03	7.12E-05
Y_ac	3.86E-03	8.14E-06	4.11E-05	3.26E-04	2.84E-03	1.16E-01	1.81E-03	1.67E-06
km_mo	2.67E-04	9.47E-07	4.78E-06	6.47E-04	6.88E-03	3.42E-02	5.11E-04	6.82E-04
Y_mo	1.30E-02	2.63E-05	1.33E-04	4.51E-03	4.51E-01	6.55E-02	1.03E-03	1.05E-04
Ks_ac	1.13E-04	2.09E-07	1.06E-06	9.08E-06	7.67E-05	3.56E-02	5.54E-04	1.78E-05
km_pro	1.75E-04	2.95E-07	1.49E-06	2.94E-03	1.16E-04	2.10E-02	3.26E-04	1.79E-05
Ks_mo	1.02E-04	2.61E-07	1.32E-06	2.07E-04	2.48E-03	1.36E-02	2.04E-04	2.11E-04
Y_pro	1.47E-03	3.03E-06	1.53E-05	5.03E-02	1.08E-03	1.03E-02	1.60E-04	1.32E-06
Y_h2	2.76E-03	5.64E-06	2.85E-05	5.16E-04	2.02E-03	9.86E-03	1.51E-04	4.51E-05
kdec_xmo	1.15E-02	2.06E-05	1.04E-04	9.51E-04	1.16E-01	8.48E-03	1.33E-04	1.50E-06
km_h2	3.82E-05	1.33E-07	6.73E-07	1.13E-03	2.64E-05	9.09E-03	1.46E-04	1.61E-04
kdec_xac	3.52E-03	6.77E-06	3.42E-05	2.95E-04	2.58E-03	6.04E-03	9.43E-05	2.30E-07
khyd_ch	5.35E-05	8.05E-08	4.07E-07	5.64E-05	1.08E-03	8.04E-03	1.26E-04	1.12E-05
Ks_h2	1.94E-05	9.33E-08	4.71E-07	7.22E-04	1.51E-05	5.35E-03	8.79E-05	1.32E-04
Ks_pro	3.84E-05	6.90E-08	3.49E-07	6.11E-04	2.56E-05	4.35E-03	6.74E-05	1.06E-05
kdec_xh2	2.90E-03	5.10E-06	2.58E-05	2.58E-04	2.09E-03	1.97E-03	3.07E-05	4.06E-07
khyd_pr	1.22E-05	1.84E-08	2.96E-03	1.29E-05	2.50E-04	2.10E-03	3.30E-05	3.87E-06
kdec_xpro	1.94E-03	3.45E-06	1.74E-05	2.09E-02	1.40E-03	1.24E-03	1.94E-05	1.33E-07
Ks_IN	5.09E-06	1.06E-08	5.36E-08	1.75E-05	2.27E-05	1.24E-03	1.93E-05	3.28E-06
khyd_li	2.78E-06	5.87E-04	1.76E-08	2.55E-06	4.93E-05	1.00E-04	1.66E-06	1.44E-06

Annex Q.2: Evolution of the sensitivity functions for different variables with respect to parameters identified as sensitive for Lignogas-SIM model

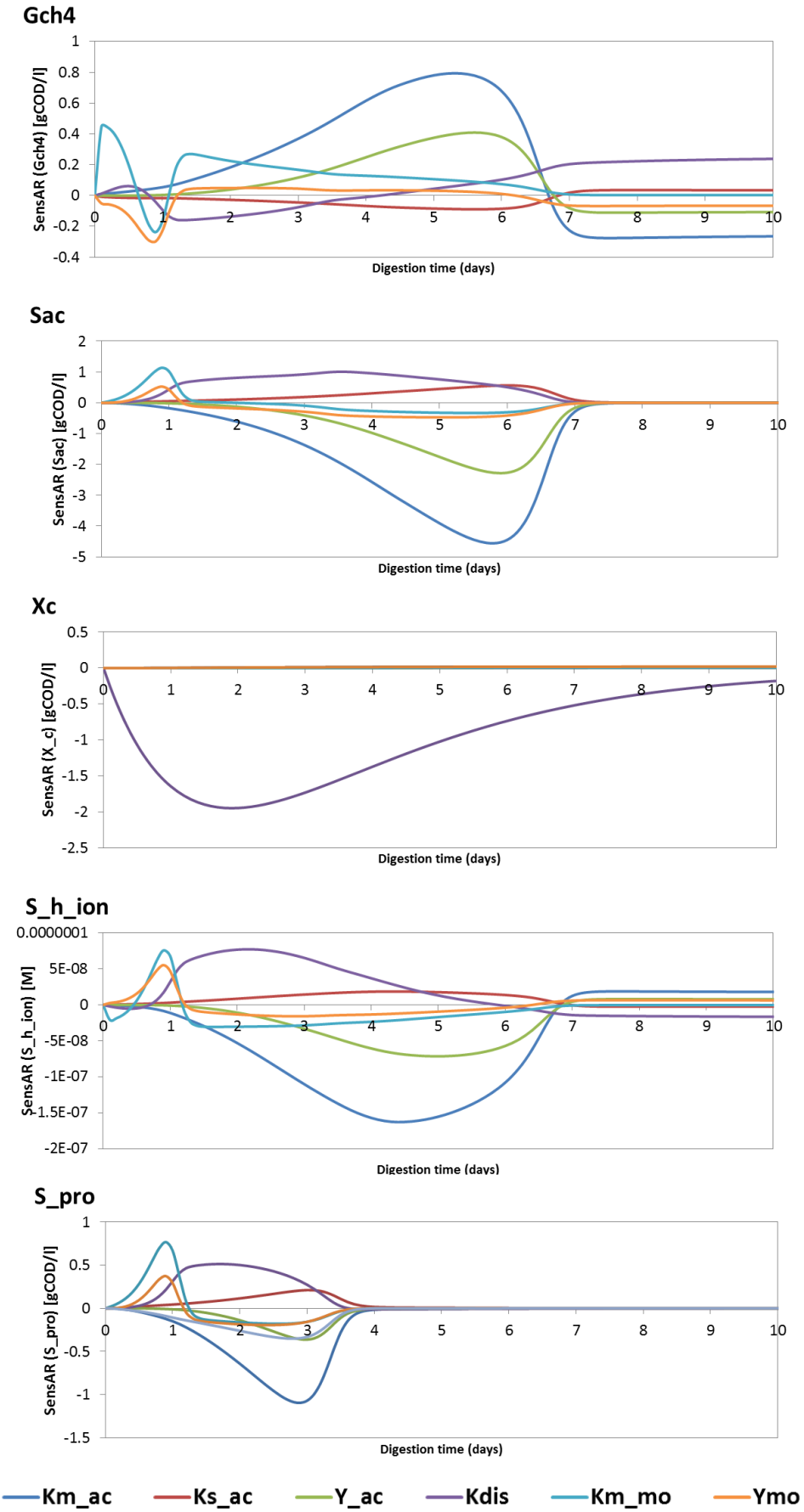

Annex Q.3: Ranking of mean absolute sensitivities for Lignogas model

Table Q.3: Sensitivity ranking (in red the 6 highest values for each variable)

	S_aa	S_ac	S_bu	S_ch4	S_co2	S_fa	S_h2	S_hco3_ion	S_h_ion	S_IN	S_pro	S_su	S_va	X_aa	X_ac	X_c
	[gCOD/l]	[gCOD/l]	[gCOD/l]	[gCOD/l]	M	[gCOD/l]	[gCOD/l]	M	M	M	[gCOD/l]	[gCOD/l]	[gCOD/l]	[gCOD/l]	[gCOD/l]	[gCOD/l]
kdis	1.76E-03	1.05E-01	7.12E-03	9.42E-03	3.45E-03	5.48E-03	8.18E-08	1.70E-03	4.24E-18	4.76E-04	2.24E-02	1.45E-02	2.78E-03	3.96E-03	1.54E-02	3.05E-01
kdis_bio	8.10E-05	5.58E-04	9.04E-05	2.16E-05	7.88E-06	2.93E-04	8.37E-10	1.52E-04	1.10E-26	1.60E-04	5.67E-05	3.25E-07	8.16E-05	1.64E-03	2.06E-04	7.96E-10
khyd_ch_s	1.14E-06	5.05E-03	3.85E-04	5.57E-04	2.04E-04	1.32E-05	8.60E-09	1.07E-04	3.73E-23	7.56E-06	1.28E-03	2.78E-03	5.29E-05	3.24E-05	5.61E-04	2.69E-06
khyd_li	4.42E-08	1.60E-04	1.27E-06	2.20E-05	8.12E-06	3.87E-04	1.54E-10	3.22E-06	2.17E-27	3.71E-07	4.87E-06	6.37E-06	2.41E-07	1.41E-06	1.53E-05	1.56E-10
khyd_pr	3.07E-04	8.95E-04	2.83E-04	1.69E-05	6.94E-06	2.87E-06	1.48E-09	1.93E-05	6.31E-26	2.60E-05	1.96E-04	7.32E-07	2.16E-04	2.24E-04	1.41E-04	4.55E-09
KI_h2_c4	3.29E-05	3.68E-02	2.20E-01	1.83E-03	6.26E-04	3.13E-04	4.21E-08	1.40E-03	1.04E-24	2.15E-04	3.97E-03	3.21E-07	6.79E-02	7.52E-04	8.81E-03	7.52E-08
KI_h2_fa	1.84E-08	8.14E-05	4.74E-07	3.27E-06	1.24E-06	2.05E-04	6.57E-11	1.39E-06	2.68E-26	1.43E-07	2.25E-06	7.12E-10	1.33E-07	5.60E-07	1.24E-05	1.93E-09
KI_h2_pro	1.75E-07	8.71E-04	2.06E-05	3.94E-05	1.34E-05	8.54E-06	2.43E-09	9.76E-06	3.90E-26	1.04E-06	1.68E-03	9.69E-09	5.67E-06	3.70E-06	4.94E-05	2.81E-09
KI_nh3_ac	2.01E-06	3.23E-03	5.40E-06	1.47E-04	4.99E-05	2.40E-05	2.17E-09	6.71E-05	9.74E-26	1.60E-05	1.39E-05	1.84E-08	3.48E-06	3.18E-05	2.91E-03	7.02E-09
km_aa	3.81E-03	1.38E-03	4.29E-04	3.69E-05	1.35E-05	5.37E-06	2.57E-09	2.34E-05	1.08E-25	2.38E-05	2.43E-04	1.12E-06	3.20E-04	2.38E-04	1.27E-04	7.80E-09
km_ac	6.19E-05	1.10E-01	1.64E-04	5.04E-03	1.72E-03	7.33E-04	6.56E-08	2.24E-03	3.20E-23	4.94E-04	5.04E-04	4.71E-07	1.09E-04	9.58E-04	8.88E-02	2.31E-06
km_acetox	4.60E-05	1.30E-01	9.11E-04	5.69E-03	1.94E-03	6.71E-04	1.24E-07	1.97E-03	4.57E-23	3.76E-04	6.55E-03	9.88E-07	3.50E-04	9.96E-04	6.30E-02	3.29E-06
km_c4	1.45E-06	8.97E-03	1.36E-02	8.32E-05	2.91E-05	2.96E-05	1.14E-08	9.14E-05	8.16E-25	1.12E-05	1.84E-03	1.05E-07	5.51E-03	4.60E-05	8.26E-04	5.88E-08
km_fa	1.08E-06	2.58E-03	1.25E-05	1.01E-04	3.82E-05	1.39E-02	2.45E-09	4.65E-05	1.01E-25	9.05E-06	7.31E-05	1.56E-08	4.73E-06	3.32E-05	4.65E-04	7.28E-09
km_h2	2.60E-06	1.29E-02	3.21E-03	4.44E-04	1.48E-04	2.26E-03	3.39E-07	1.01E-04	1.22E-23	1.50E-05	2.07E-02	1.36E-07	1.01E-03	6.52E-05	1.12E-03	8.81E-07
km_pro	3.82E-06	1.93E-02	3.44E-04	8.35E-04	2.80E-04	1.77E-04	4.59E-08	2.08E-04	2.95E-23	2.20E-05	4.18E-02	1.72E-07	1.17E-04	9.47E-05	1.65E-03	2.13E-06
km_su	1.22E-05	3.75E-02	5.98E-03	1.78E-03	6.54E-04	3.56E-04	1.66E-07	7.72E-04	1.26E-22	7.66E-05	1.56E-02	4.30E-02	7.15E-04	1.50E-04	2.66E-03	9.08E-06
Ks_aa	3.56E-03	1.17E-03	3.72E-04	2.67E-05	9.83E-06	4.37E-06	2.09E-09	2.01E-05	1.96E-24	2.21E-05	2.17E-04	9.65E-07	2.79E-04	2.14E-04	1.21E-04	1.41E-07
Ks_ac	1.47E-05	2.08E-02	3.54E-05	8.71E-04	2.99E-04	1.57E-04	1.60E-08	4.43E-04	2.42E-24	1.16E-04	8.67E-05	1.42E-07	2.38E-05	2.25E-04	2.10E-02	1.74E-07
Ks_acetox	2.11E-05	5.04E-02	3.30E-04	2.08E-03	7.09E-04	2.64E-04	4.57E-08	7.65E-04	1.76E-23	1.71E-04	2.24E-03	1.66E-06	1.26E-04	4.34E-04	2.88E-02	1.27E-06

Table Q.4: Sensitivity ranking (in red the 6 highest values for each variable) (Continuation)

	S_aa	S_ac	S_bu	S_ch4	S_co2	S_fa	S_h2	S_hco3_ion	S_h_ion	S_IN	S_pro	S_su	S_va	X_aa	X_ac	X_c
	[gCOD/l]	[gCOD/l]	[gCOD/l]	[gCOD/l]	M	[gCOD/l]	[gCOD/l]	M	M	M	[gCOD/l]	[gCOD/l]	[gCOD/l]	[gCOD/l]	[gCOD/l]	[gCOD/l]
km_c4	1.45E-06	8.97E-03	1.36E-02	8.32E-05	2.91E-05	2.96E-05	1.14E-08	9.14E-05	8.16E-25	1.12E-05	1.84E-03	1.05E-07	5.51E-03	4.60E-05	8.26E-04	5.88E-08
km_fa	1.08E-06	2.58E-03	1.25E-05	1.01E-04	3.82E-05	1.39E-02	2.45E-09	4.65E-05	1.01E-25	9.05E-06	7.31E-05	1.56E-08	4.73E-06	3.32E-05	4.65E-04	7.28E-09
km_h2	2.60E-06	1.29E-02	3.21E-03	4.44E-04	1.48E-04	2.26E-03	3.39E-07	1.01E-04	1.22E-23	1.50E-05	2.07E-02	1.36E-07	1.01E-03	6.52E-05	1.12E-03	8.81E-07
km_pro	3.82E-06	1.93E-02	3.44E-04	8.35E-04	2.80E-04	1.77E-04	4.59E-08	2.08E-04	2.95E-23	2.20E-05	4.18E-02	1.72E-07	1.17E-04	9.47E-05	1.65E-03	2.13E-06
km_su	1.22E-05	3.75E-02	5.98E-03	1.78E-03	6.54E-04	3.56E-04	1.66E-07	7.72E-04	1.26E-22	7.66E-05	1.56E-02	4.30E-02	7.15E-04	1.50E-04	2.66E-03	9.08E-06
Ks_aa	3.56E-03	1.17E-03	3.72E-04	2.67E-05	9.83E-06	4.37E-06	2.09E-09	2.01E-05	1.96E-24	2.21E-05	2.17E-04	9.65E-07	2.79E-04	2.14E-04	1.21E-04	1.41E-07
Ks_ac	1.47E-05	2.08E-02	3.54E-05	8.71E-04	2.99E-04	1.57E-04	1.60E-08	4.43E-04	2.42E-24	1.16E-04	8.67E-05	1.42E-07	2.38E-05	2.25E-04	2.10E-02	1.74E-07
Ks_acetox	2.11E-05	5.04E-02	3.30E-04	2.08E-03	7.09E-04	2.64E-04	4.57E-08	7.65E-04	1.76E-23	1.71E-04	2.24E-03	1.66E-06	1.26E-04	4.34E-04	2.88E-02	1.27E-06
Ks_c4	9.79E-07	5.46E-03	9.09E-03	4.53E-05	1.58E-05	1.50E-05	5.51E-09	5.91E-05	6.09E-25	8.34E-06	1.17E-03	1.19E-07	4.29E-03	3.30E-05	6.04E-04	4.39E-08
Ks_fa	9.89E-07	1.96E-03	9.47E-06	7.15E-05	2.72E-05	1.28E-02	1.96E-09	3.60E-05	1.40E-24	8.07E-06	5.44E-05	1.30E-08	3.72E-06	2.94E-05	3.56E-04	1.01E-07
Ks_h2	1.59E-06	7.26E-03	2.10E-03	2.54E-04	8.37E-05	1.54E-03	2.52E-07	6.22E-05	2.94E-25	1.11E-05	1.39E-02	5.94E-08	6.79E-04	4.64E-05	9.99E-04	2.12E-08
Ks_IN	1.23E-05	8.15E-04	6.39E-05	4.47E-05	1.56E-05	5.16E-05	1.14E-09	1.58E-05	4.93E-25	1.21E-06	2.15E-04	1.51E-04	2.11E-05	2.25E-06	8.24E-05	3.55E-08
Ks_pro	1.05E-06	4.63E-03	6.79E-05	2.23E-04	7.51E-05	4.11E-05	1.08E-08	6.30E-05	7.95E-25	6.29E-06	1.19E-02	9.77E-08	2.38E-05	2.77E-05	5.13E-04	5.73E-08
Ks_su	4.20E-06	1.15E-02	2.04E-03	4.19E-04	1.57E-04	1.19E-04	5.31E-08	2.32E-04	1.67E-24	2.58E-05	5.25E-03	1.76E-02	2.50E-04	6.03E-05	5.75E-04	1.20E-07
Y_aa	1.66E-03	2.99E-03	2.85E-04	9.92E-05	3.43E-05	1.76E-04	1.75E-09	3.40E-04	1.12E-25	3.55E-04	3.25E-04	3.65E-07	2.34E-04	6.72E-02	2.80E-04	8.10E-09
Y_ac	2.36E-05	3.52E-02	4.82E-05	1.56E-03	5.33E-04	2.31E-04	2.69E-08	5.48E-04	9.95E-24	1.92E-04	1.36E-04	2.55E-07	3.41E-05	5.22E-04	9.96E-02	7.17E-07
Y_acetox	7.43E-05	4.12E-02	2.60E-04	1.79E-03	6.12E-04	5.13E-04	4.25E-08	1.02E-03	8.16E-24	5.95E-04	1.70E-03	5.78E-07	1.52E-04	1.44E-03	5.32E-02	5.88E-07
Y_c4	3.41E-05	2.21E-03	4.31E-03	1.15E-04	4.13E-05	1.35E-04	3.12E-09	2.45E-04	3.32E-25	2.74E-04	4.30E-04	3.34E-07	2.11E-03	6.70E-04	2.81E-04	2.39E-08
Y_fa	6.00E-06	1.19E-04	7.01E-06	1.32E-05	5.30E-06	1.86E-03	2.03E-10	4.53E-05	1.59E-27	4.76E-05	5.08E-06	4.35E-08	6.25E-06	1.08E-04	5.95E-05	1.15E-10
Y_h2	1.20E-04	6.97E-03	1.58E-03	1.02E-04	4.18E-05	1.64E-03	1.72E-07	9.20E-04	2.06E-23	9.62E-04	1.02E-02	1.21E-06	6.04E-04	2.37E-03	2.28E-04	1.48E-06
Y_pro	2.80E-05	4.28E-03	8.98E-05	2.50E-04	8.70E-05	1.37E-04	1.13E-08	2.27E-04	9.07E-24	2.25E-04	1.03E-02	2.64E-07	5.13E-05	5.69E-04	3.95E-04	6.54E-07
Y_su	2.42E-04	3.13E-02	3.36E-03	1.67E-03	6.12E-04	1.00E-03	8.86E-08	2.01E-03	4.69E-24	1.97E-03	1.05E-02	2.15E-02	5.95E-04	5.13E-03	2.49E-03	3.38E-07

Table Q.5: Sensitivity ranking (in red the 6 highest values for each variable) (Continuation)

	X_c4	X_fa	X_h2	X_I	X_li	X_pr	X_pro	X_su	S_ch4	S_co2	S_h2
	[gCOD/l]	[gCOD/l]	[gCOD/l]	[gCOD/l]	[gCOD/l]	[gCOD/l]	[gCOD/l]	[gCOD/l]	[gCOD/l]	M	[gCOD/l]
kdis	2.69E-03	4.88E-04	1.71E-02	3.07E-02	3.71E-04	1.86E-03	1.64E-03	2.35E-02	3.17E-01	4.95E-03	3.28E-06
kdis_bio	5.53E-04	1.47E-04	7.79E-04	8.00E-11	1.64E-05	1.26E-04	1.26E-04	1.34E-05	7.23E-04	1.13E-05	3.90E-08
khyd_ch_s	6.58E-05	3.59E-06	5.87E-04	2.70E-07	2.52E-07	1.93E-06	5.95E-05	1.17E-03	1.88E-02	2.93E-04	3.09E-07
khyd_li	6.17E-07	2.72E-05	2.43E-05	1.57E-11	7.33E-04	9.49E-08	3.16E-07	2.31E-06	7.47E-04	1.17E-05	6.13E-09
khyd_pr	6.81E-05	1.33E-06	1.85E-04	4.57E-10	1.14E-07	4.22E-03	1.23E-05	1.47E-07	6.36E-04	9.94E-06	6.36E-08
KI_h2_c4	1.78E-02	7.98E-05	1.24E-02	7.56E-09	7.16E-06	5.50E-05	1.30E-03	6.13E-06	5.77E-02	9.01E-04	1.88E-06
KI_h2_fa	2.34E-07	1.46E-05	1.39E-05	1.94E-10	4.76E-09	3.65E-08	1.69E-07	4.68E-09	1.14E-04	1.77E-06	2.76E-09
KI_h2_pro	3.37E-06	8.01E-07	6.25E-05	2.82E-10	3.36E-08	2.58E-07	9.26E-05	3.10E-08	1.23E-03	1.93E-05	9.80E-08
KI_nh3_ac	1.09E-05	3.70E-06	2.49E-03	7.05E-10	4.92E-07	3.78E-06	3.07E-06	2.59E-07	4.60E-03	7.18E-05	1.05E-07
km_aa	6.46E-05	1.42E-06	1.45E-04	7.84E-10	9.80E-08	7.52E-07	9.67E-06	1.64E-07	1.24E-03	1.93E-05	1.07E-07
km_ac	3.28E-04	1.12E-04	7.59E-02	2.32E-07	1.51E-05	1.16E-04	9.25E-05	7.76E-06	1.58E-01	2.47E-03	3.07E-06
km_acetox	4.28E-04	1.22E-04	5.72E-02	3.31E-07	1.20E-05	9.24E-05	4.48E-04	8.43E-06	1.79E-01	2.79E-03	5.16E-06
km_c4	1.25E-03	5.89E-06	9.40E-04	5.91E-09	3.73E-07	2.87E-06	4.37E-05	3.84E-07	2.68E-03	4.18E-05	4.59E-07
km_fa	1.23E-05	6.60E-04	6.85E-04	7.32E-10	3.01E-07	2.31E-06	6.62E-06	2.71E-07	3.51E-03	5.48E-05	1.06E-07
km_h2	3.22E-04	1.58E-04	1.33E-03	8.85E-08	5.11E-07	3.92E-06	1.17E-03	5.18E-07	1.37E-02	2.14E-04	1.52E-05
km_pro	6.89E-05	1.96E-05	1.99E-03	2.14E-07	7.46E-07	5.73E-06	2.25E-03	8.34E-07	2.58E-02	4.03E-04	1.87E-06
km_su	3.99E-04	2.85E-05	4.45E-03	9.12E-07	2.35E-06	1.80E-05	5.01E-04	5.77E-03	6.00E-02	9.37E-04	6.13E-06
Ks_aa	5.79E-05	1.28E-06	1.42E-04	1.42E-08	9.23E-08	7.08E-07	9.12E-06	1.46E-07	9.02E-04	1.41E-05	8.83E-08
Ks_ac	7.67E-05	2.48E-05	1.82E-02	1.75E-08	3.57E-06	2.74E-05	2.06E-05	1.84E-06	2.75E-02	4.30E-04	7.78E-07
Ks_acetox	1.78E-04	4.87E-05	2.62E-02	1.28E-07	5.45E-06	4.18E-05	1.60E-04	3.67E-06	6.53E-02	1.02E-03	1.93E-06

Table Q.6: Sensitivity ranking (in red the 6 highest values for each variable) (Continuation)

	X_c4	X_fa	X_h2	X_I	X_li	X_pr	X_pro	X_su	S_ch4	S_co2	S_h2
	[gCOD/l]	[gCOD/l]	[gCOD/l]	[gCOD/l]	[gCOD/l]	[gCOD/l]	[gCOD/l]	[gCOD/l]	[gCOD/l]	M	[gCOD/l]
Ks_acetox	1.78E-04	4.87E-05	2.62E-02	1.28E-07	5.45E-06	4.18E-05	1.60E-04	3.67E-06	6.53E-02	1.02E-03	1.93E-06
Ks_c4	8.04E-04	3.89E-06	7.00E-04	4.41E-09	2.77E-07	2.12E-06	3.58E-05	2.80E-07	1.45E-03	2.27E-05	2.27E-07
Ks_fa	1.07E-05	5.76E-04	5.73E-04	1.01E-08	2.69E-07	2.06E-06	5.28E-06	2.39E-07	2.50E-03	3.90E-05	8.56E-08
Ks_h2	2.09E-04	1.06E-04	1.13E-03	2.13E-09	3.70E-07	2.84E-06	7.79E-04	3.82E-07	7.72E-03	1.20E-04	1.15E-05
Ks_IN	6.27E-06	2.68E-06	1.15E-04	3.57E-09	3.73E-08	2.87E-07	1.19E-05	2.04E-05	1.43E-03	2.24E-05	5.20E-08
Ks_pro	1.66E-05	4.97E-06	6.11E-04	5.76E-09	2.11E-07	1.62E-06	5.97E-04	2.34E-07	6.91E-03	1.08E-04	4.47E-07
Ks_su	1.48E-04	1.04E-05	1.23E-03	1.21E-08	8.04E-07	6.17E-06	1.76E-04	2.26E-03	1.43E-02	2.24E-04	1.96E-06
Y_aa	1.61E-03	7.16E-05	2.25E-03	8.14E-10	1.16E-05	8.92E-05	3.60E-04	6.99E-06	3.15E-03	4.93E-05	6.79E-08
Y_ac	1.76E-04	5.12E-05	3.21E-02	7.21E-08	6.22E-06	4.78E-05	4.51E-05	4.29E-06	4.91E-02	7.67E-04	1.29E-06
Y_acetox	5.02E-04	1.33E-04	2.37E-02	5.91E-08	1.90E-05	1.46E-04	2.05E-04	1.18E-05	5.63E-02	8.80E-04	1.84E-06
Y_c4	4.78E-02	5.65E-05	1.52E-03	2.40E-09	8.73E-06	6.70E-05	1.71E-04	5.46E-06	3.80E-03	5.93E-05	1.31E-07
Y_fa	3.60E-05	8.18E-03	2.20E-04	1.15E-11	1.51E-06	1.16E-05	8.28E-06	8.80E-07	4.87E-04	7.60E-06	9.65E-09
Y_h2	8.55E-04	2.44E-04	1.55E-01	1.49E-07	3.08E-05	2.36E-04	5.07E-04	1.94E-05	3.84E-03	5.96E-05	7.66E-06
Y_pro	1.97E-04	5.04E-05	1.54E-03	6.57E-08	7.23E-06	5.55E-05	3.85E-02	4.66E-06	8.00E-03	1.25E-04	4.68E-07
Y_su	1.36E-03	4.40E-04	1.44E-02	3.40E-08	6.33E-05	4.86E-04	3.28E-03	3.48E-01	5.62E-02	8.79E-04	3.15E-06

Annex Q.4: Evolution of the sensitivity functions for different variables with respect to parameters identified as sensitive for Lignogas model

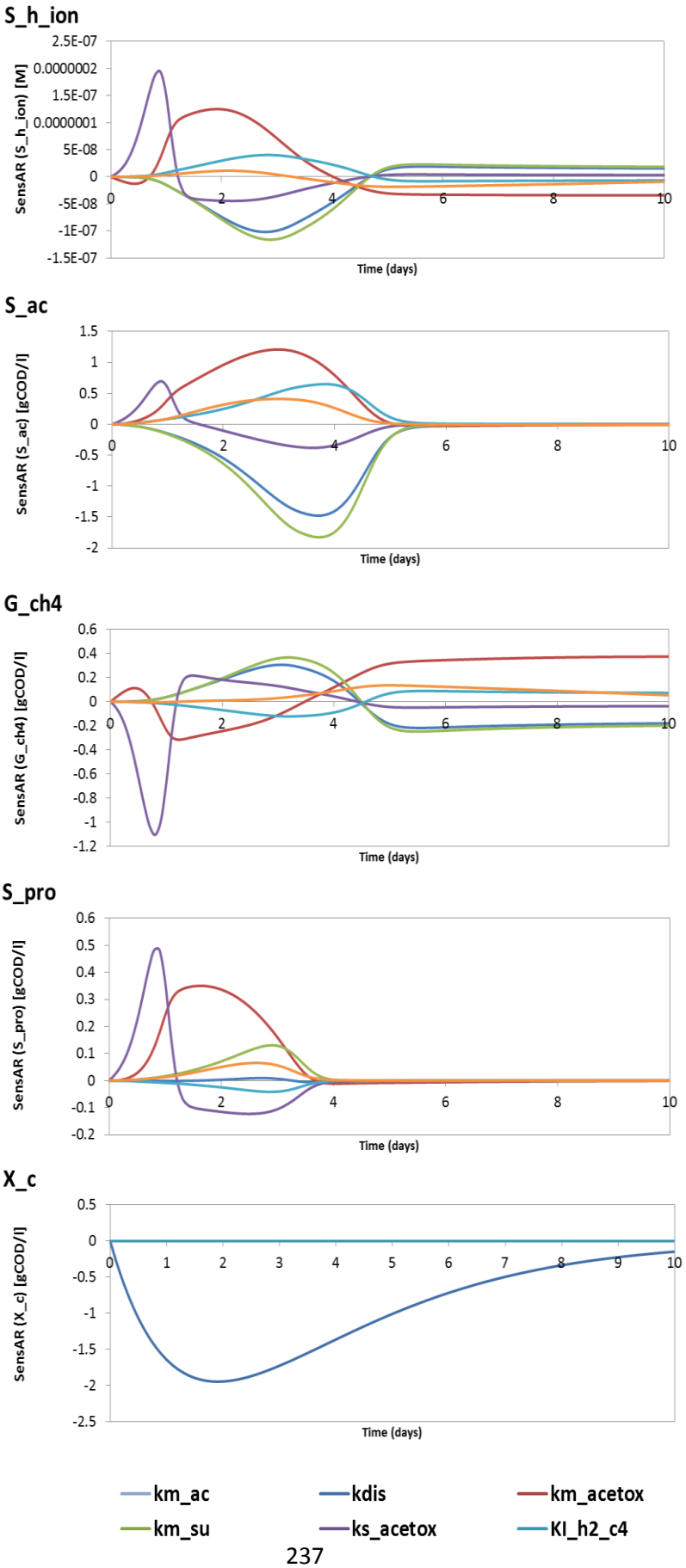

Annex Q.5: Evolution of the sensitivity functions for different variables with respect to parameters identified as sensitive for Lignogas mode when considering khyd_ch

S_h_ion

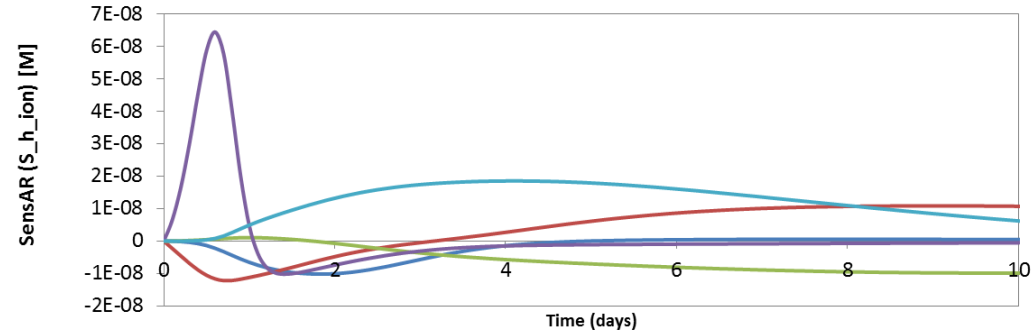

S_ac

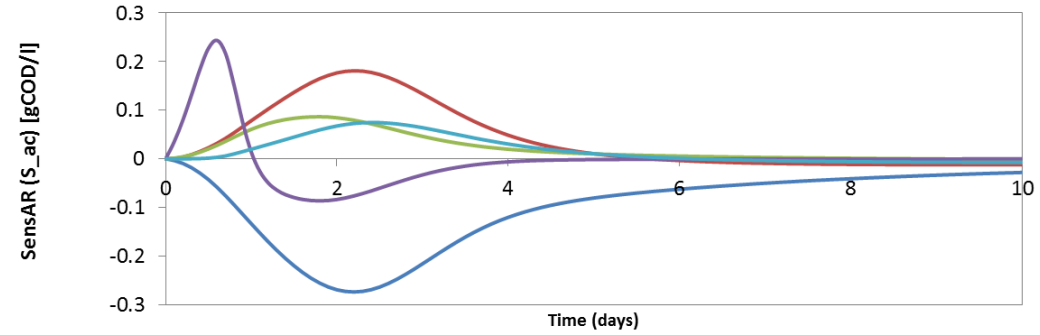

G_ch4

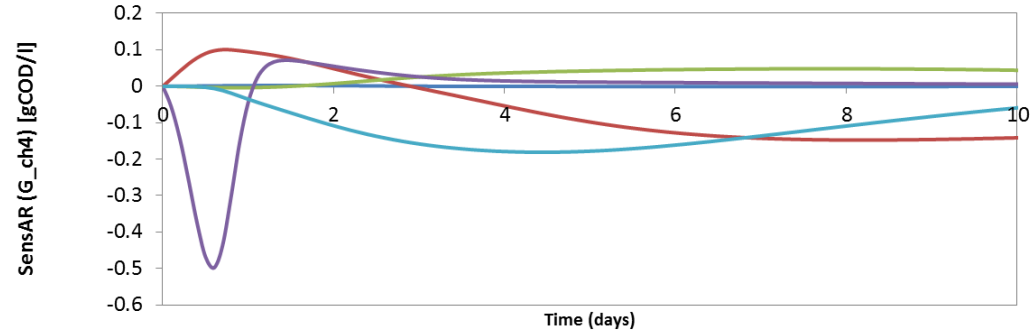

S_pro

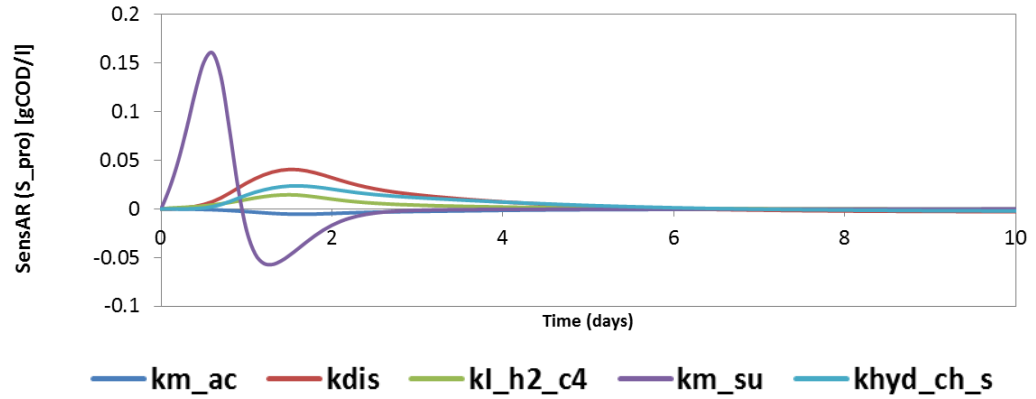

Annex R: Literature values proposed for different kinetic parameters

Table R.1: Values proposed in literature for the disintegration and hydrolysis constants for lignocellulosic material for multispecies models

Substrate	kd	Khyd_ch	Khyd_pr	Khyd_li	Operating temperature	Feeding mode	Source
Solid sub-strates	0.5	10	10	10	35	-	Batstone et al. (2002)
Grass silage	1 and 0.26	10	10	10	38	Semi-continous	Wichern et al. (2009)
Grass silage		0.14-0.5	0.8	0.14-0.5	38	Semi-continous	Koch et al. (2009)
Grass silage	1.74	0.73	0.01	0.01	38	Batch	Biernacki et al. (2013
Maize silage	0.77	0.68	0.24	0.12			
Maize silage	0.7	10	8	6	35	Batch and semi-batch	Schlattmann (2011)
Grass silage	0.5						
Rape seed oil	0.6						
Grass silage	0.02-0.05	10	10	10	37	Semi-continous	Thamsiriroj at al. (2010)
Slurry and fodder for cow		0.31	0.31	0.31	38	Semi-continous	Lübken et al. (2007)

Table R.2: Calibrated values proposed in literature for selected kinetic and stoichiometric parameters in multispecies models (operational conditions specified in Table R.1 for each reference mentioned)

Parameter	Unit	Batstone et al. (2002)	Koch et al. 2009	Wichern et al. (2009	Lübken et al. (2007)	Schlattmann (2011)
Km_ac	gCOD/gCOD/d	8	4.4	8	7.1	8
Km_pro	gCOD/gCOD/d	13	13	13	5.5	13
Km_c4	gCOD/gCOD/d	20	20	20	13.7	20
Km_fa	gCOD/gCOD/d	6	6	6	6	10
Ks_ac	gCOD/l	0.15	0.15	0.15	0.15	0.2
Ks_pro	gCOD/l	0.1	0.1	0.1	0.392	0.3
Ks_c4	gCOD/l	0.2	0.2	0.2	0.357	0.3
Ks_h2	gCOD/l	7E-E06	5.6E-E05	4.2E-E05	3.5E-E05	1.5E-E05
KI_h2_c4	gCOD/l	1E-E05	5E-E08	5.4E-E08	1E-E05	1E-E05
KI_h2_pro	gCOD/l	3.5E-E06	4.6E-E08	4.8E-E08	3.5E-E06	3.5E-E06
KI_nh3_ac	M	0.0018	0.0018	0.0089-0.01	0.0018	0.0018
pHUL_aa	-	5.5	5.5	8.5	8	7
pHLL_aa	-	4	4	6	6	5
pHUL_ac	-	7	7	7	7	8
pHLL_ac	-	6	6	6	6	6.5
pHUL_h2	-	6	6	6	6	6.8
pHLL_h2	-	5	5	5	5	5.5

Annex S: Initial conditions used for modelling

The initial conditions used for modelling the experimental data for different substrates and experimental conditions are presented in the following tables. The measured value for IN (mainly NH_4^+-N) was used for the anion concentration (S_{an}) and cation concentration (S_{cat}) was adjusted in each case according with experimental pH, as done by Ramirez et al. (2009).

Table S.1: Initial conditions (feed and inoculum) for the batch digestion of GS 1 (OL 5.99 gVS/l)

Input Substrate			Inoculum		
Ssu_f	1.02	gCOD/l	Sva_i	0.012	gCOD/l
Sva_f	0.018	gCOD/l	Sbu_i	0.002	gCOD/l
Sbu_f	0.077	gCOD/l	Spro_i	0.002	gCOD/l
Spro_f	0.002	gCOD/l	Sac_i	0.017	gCOD/l
Sac_f	0.167	gCOD/l	SIC_i	0.179	mole C/l
Xc_f	5.56	gCOD/l	SIN_i	0.027	mole N/l
			SCAT_i	0.180	M
			SAN_i	0.027	M
			SH+_ion	1.07152E-08	M

Table S.2: Initial conditions (feed and inoculum) for the batch digestion of propionate (1 g/l)

Input Substrate			Inoculum		
Ssu_f	0.00	gCOD/l	Sva_i	0.000	gCOD/l
Sva_f	0.00	gCOD/l	Sbu_i	0.001	gCOD/l
Sbu_f	0.00	gCOD/l	Spro_i	0.000	gCOD/l
Spro_f	1.514	gCOD/l	Sac_i	0.061	gCOD/l
Sac_f	0.00	gCOD/l	SIC_i	0.095	mole C/l
Xc_f	0.00	gCOD/l	SIN_i	0.053	mole N/l
			SCAT_i	0.098	M
			SAN_i	0.053	M
			SH+_ion	1.55E-08	M

Table S.3: Initial conditions (feed and inoculum) for the batch digestion of glucose (OL 7.99 gVS/l)

Input Substrate			Inoculum		
Ssu_f	8.53	gCOD/l	Sva_i	0.007	gCOD/l
Sva_f	0.00	gCOD/l	Sbu_i	0.009	gCOD/l
Sbu_f	0.00	gCOD/l	Spro_i	0.003	gCOD/l
Spro_f	0.000	gCOD/l	Sac_i	0.016	gCOD/l
Sac_f	0.00	gCOD/l	SIC_i	0.153	mole C/l
Xc_f	0.00	gCOD/l	SIN_i	0.124	mole N/l
			SCAT_i	0.156	M
			SAN_i	0.124	M
			SH+_ion	9.12E-09	M

Table S.4: Initial conditions (feed and inoculum) for the batch digestion of starch (OL 7.99 gVS/l)

Input Substrate			Inoculum		
Ssu_f	0.00	gCOD/l	Sva_i	0.007	gCOD/l
Sva_f	0.000	gCOD/l	Sbu_i	0.009	gCOD/l
Sbu_f	0.000	gCOD/l	Spro_i	0.003	gCOD/l
Spro_f	0.000	gCOD/l	Sac_i	0.016	gCOD/l
Sac_f	0.000	gCOD/l	SIC_i	0.153	mole C/l
Xc_f	10.35	gCOD/l	SIN_i	0.124	mole N/l
			SCAT_i	0.156	M
			SAN_i	0.124	M
			SH+_ion	9.06E-09	M

Table S.5: Initial conditions (feed and inoculum) for the batch digestion of cellulose (OL 8 gVS/l)

Input Substrate			Inoculum		
Ssu_f	0.00	gCOD/l	Sva_i	0.007	gCOD/l
Sva_f	0.000	gCOD/l	Sbu_i	0.009	gCOD/l
Sbu_f	0.000	gCOD/l	Spro_i	0.003	gCOD/l
Spro_f	0.000	gCOD/l	Sac_i	0.016	gCOD/l
Sac_f	0.000	gCOD/l	SIC_i	0.153	mole C/l
Xc_f	9.76	gCOD/l	SIN_i	0.124	mole N/l
			SCAT_i	0.156	M
			SAN_i	0.124	M
			SH+_ion	9.06E-09	M

Table S.6: Initial conditions (inoculum) for the semi-continuous digestion of cellulose

Inoculum		
Sva_i	0.003	gCOD/l
Sbu_i	0.009	gCOD/l
Spro_i	0.002	gCOD/l
Sac_i	0.031	gCOD/l
SIC_i	0.146	mole C/l
SIN_i	0.138	mole N/l
SCAT_i	0.149	M
SAN_i	0.138	M
SH+_ion	1.58489E-08	M

Table S.7: Initial conditions (feed and inoculum) for the batch digestion of GS 1 (OL 24 gVS/l)

Input Substrate			Inoculum		
Ssu_f	4.09	gCOD/l	Sva_i	0.006	gCOD/l
Sva_f	0.071	gCOD/l	Sbu_i	0.002	gCOD/l
Sbu_f	0.310	gCOD/l	Spro_i	0.001	gCOD/l
Spro_f	0.052	gCOD/l	Sac_i	0.011	gCOD/l
Sac_f	0.668	gCOD/l	SIC_i	0.164	mole C/l
Xc_f	22.24	gCOD/l	SIN_i	0.143	mole N/l

Input Substrate	Inoculum		
	SCAT_i	0.167	M
	SAN_i	0.143	M
	SH+_ion	9.06E-09	M

Table S.8: Initial conditions (inoculum) for the semi-continuous digestion of DGS 3 (several OLRs)

Inoculum		
Sva_i	0.001	gCOD/l
Sbu_i	0.002	gCOD/l
Spro_i	0.002	gCOD/l
Sac_i	0.011	gCOD/l
SIC_i	0.041	mole C/l
SIN_i	0.019	mole N/l
SCAT_i	0.045	M
SAN_i	0.019	M
SH+_ion	6.30957E-08	M

Table S.9: Initial conditions (inflow with substrate and inoculum) for the batch digestion of MS 1

Input Substrate			Inoculum		
Ssu_f	0.86	gCOD/l	Sva_i	0.000	gCOD/l
Sva_f	0.003	gCOD/l	Sbu_i	0.007	gCOD/l
Sbu_f	0.003	gCOD/l	Spro_i	0.017	gCOD/l
Spro_f	0.008	gCOD/l	Sac_i	0.108	gCOD/l
Sac_f	0.200	gCOD/l	SIC_i	0.145	mole C/l
Xc_f	6.93	gCOD/l	SIN_i	0.033	mole N/l
			SCAT_i	0.148	M
			SAN_i	0.033	M
			SH+_ion	1.413E-08	M

Table S.10: Initial conditions (inoculum) for the semi-continuous digestion of DMS 2 (several OLRs)

Inoculum		
Sva_i	0.000	gCOD/l
Sbu_i	0.002	gCOD/l
Spro_i	0.000	gCOD/l
Sac_i	0.015	gCOD/l
SIC_i	0.097	mole C/l
SIN_i	0.027	mole N/l
SCAT_i	0.100	M
SAN_i	0.027	M
SH+_ion	3.16228E-06	M

Annex T: Modelling results

Annex T.1: Batch digestion of GS 1

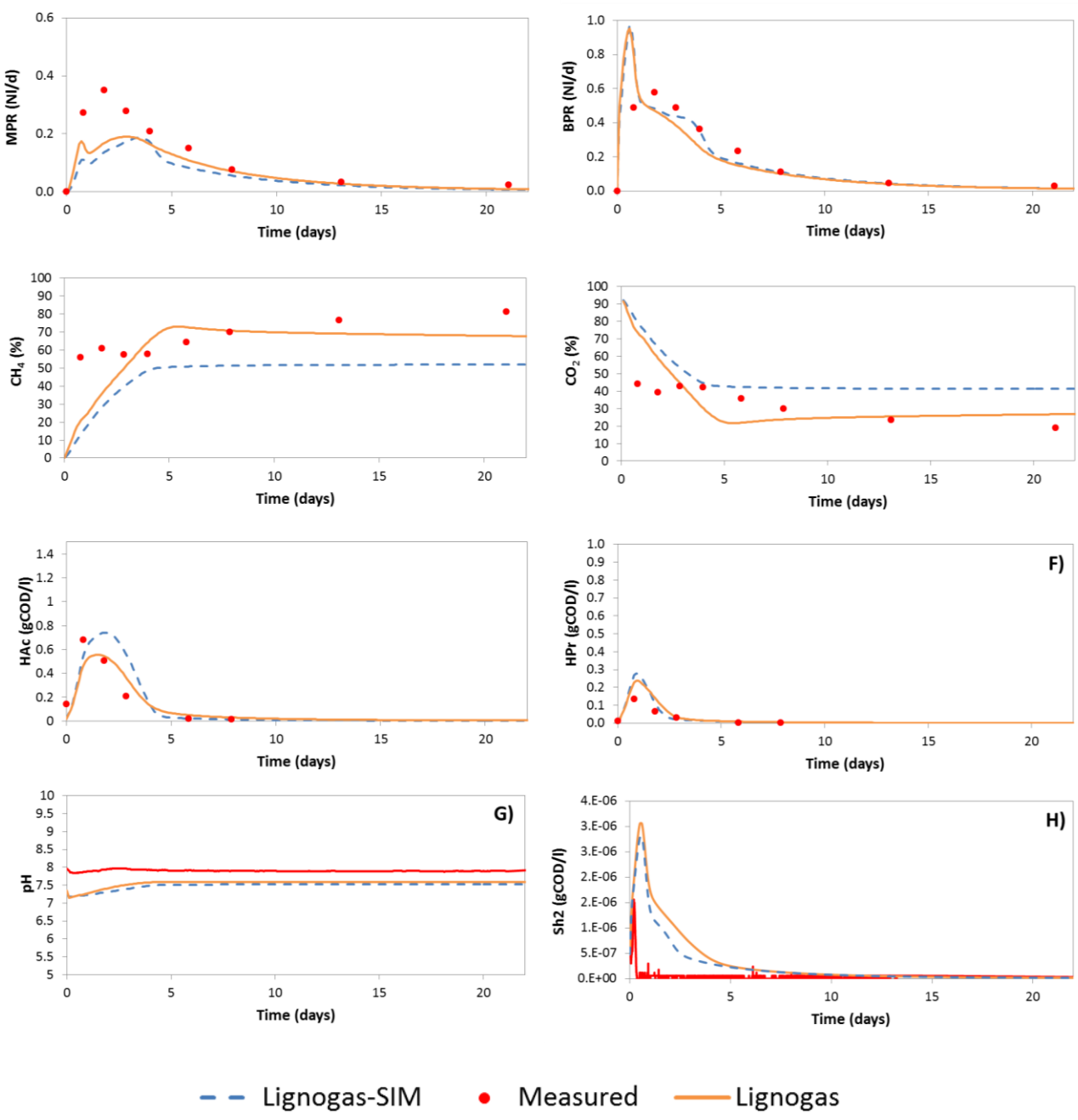

Figure T.1: Measured and modelled variables with Lignogas and Lignogas-SIM: A) MPR (in Nl/d), B) BPR (in Nl/d), C) CH_4 content (in %), D) CO_2 content (in %), E) HAc concentration (in gCOD/l), F) HPr concentration (in gCOD/l), G) pH, and H) H_2 concentration in the liquid phase (in gCOD/l)

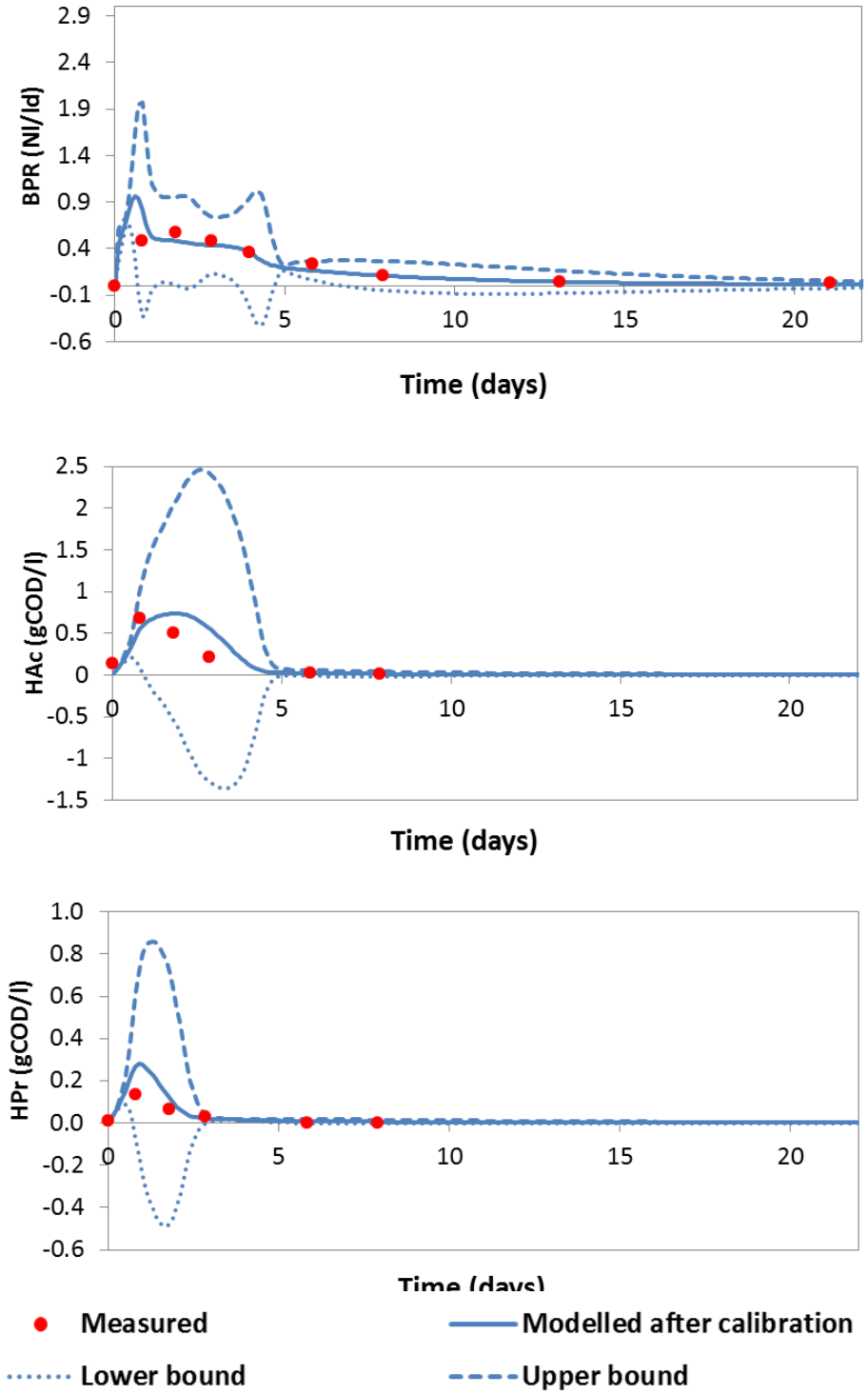

Figure T.2: Measured, modelled variables with Lignogas-SIM and error bounds for BPR (in Nl/d) (top), HAc concentration (in gCOD/l) (centre), and HPr concentration (in gCOD/l) (bottom)

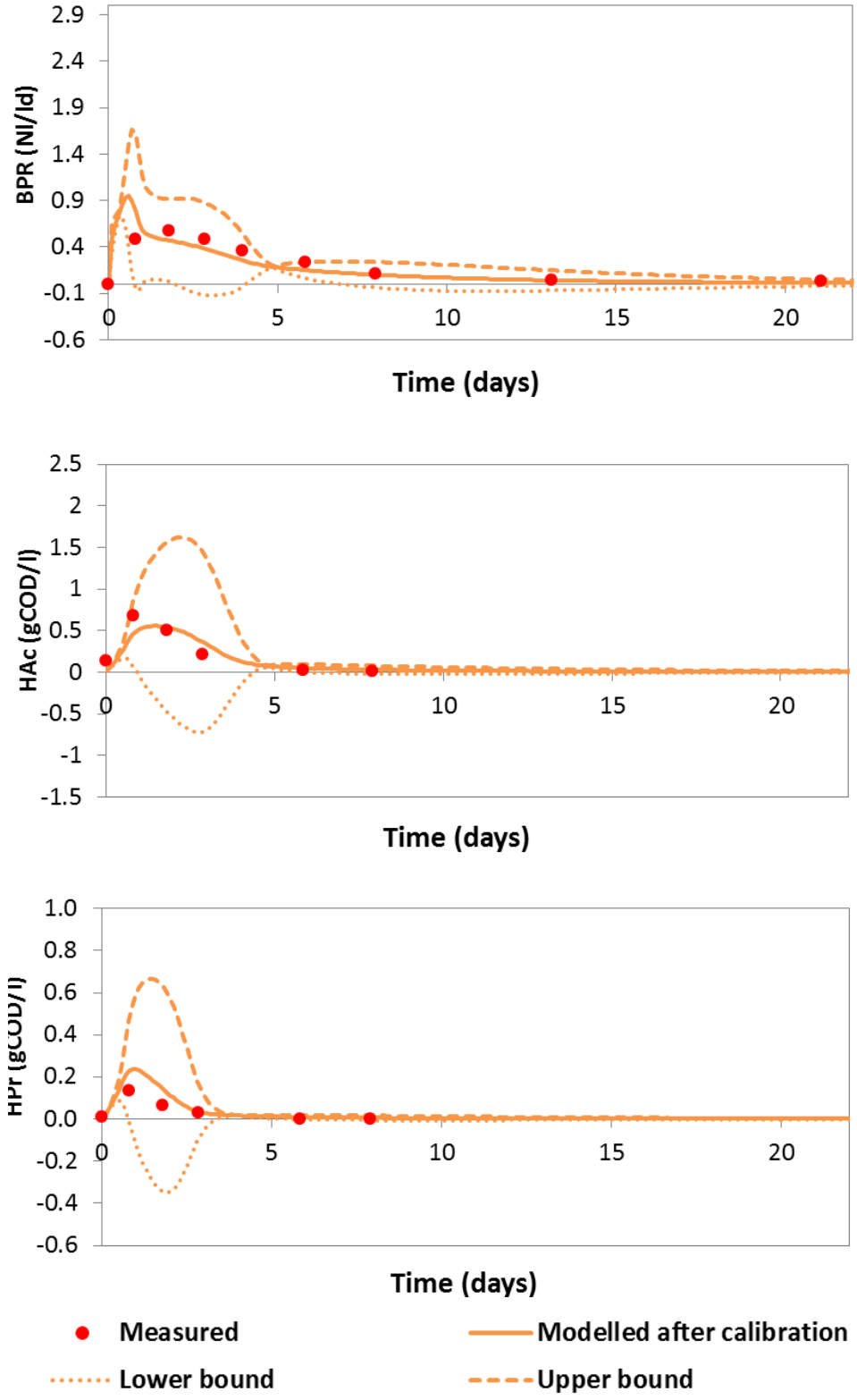

Figure T.3: Measured, modelled variables with Lignogas and error bounds (without considering the contribution from KI_h2_c4) for BPR (in Nl/d) (top), HAc concentration (in gCOD/l) (centre), and HPr concentration (in gCOD/l) (bottom)

Annex T.2: Semi-continuous digestion of cellulose

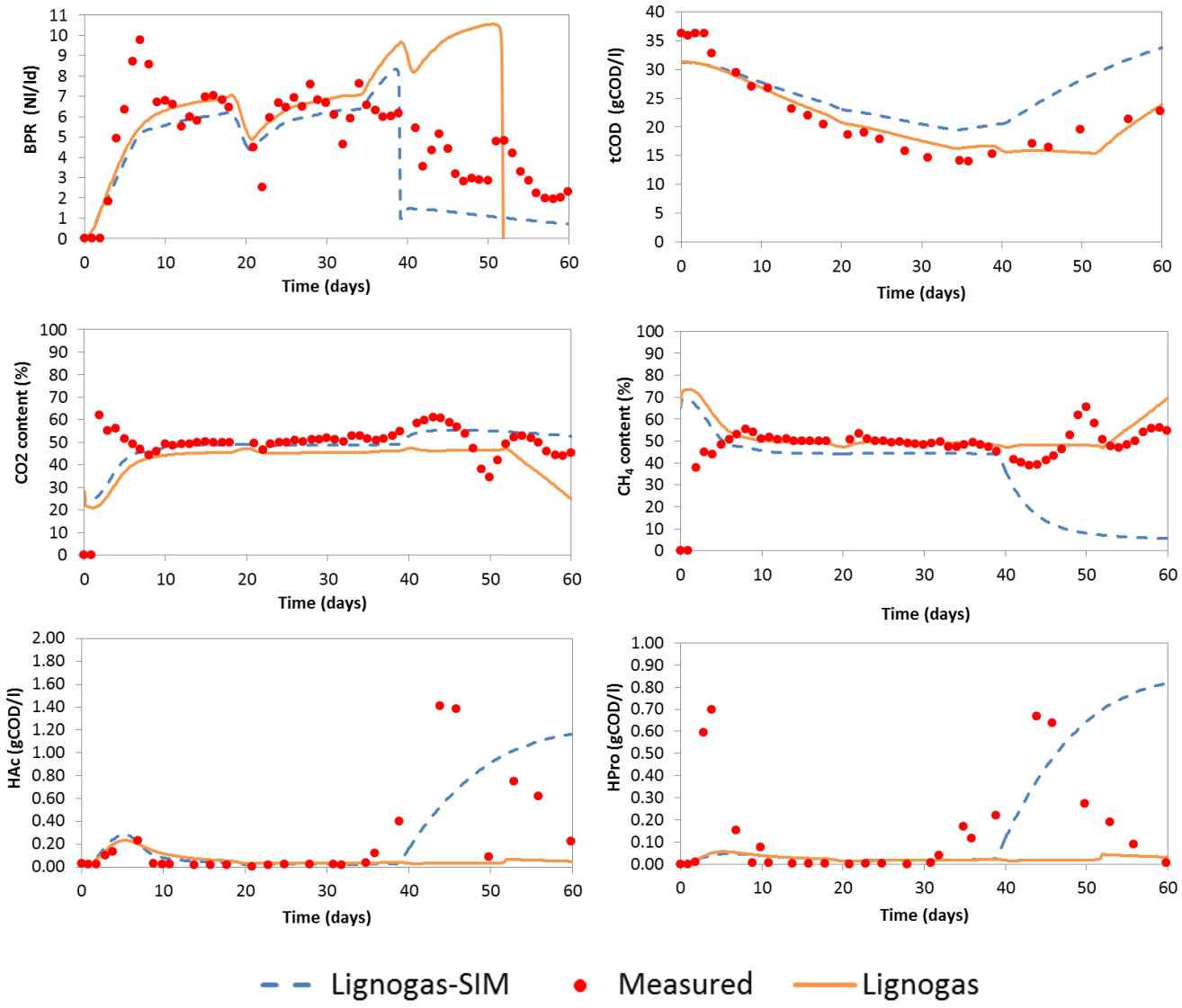

Figure T.4: Measured and modelled variables with Lignogas and Lignogas-SIM: MPR (in Nl/d), tCOD concentration evolution (gCOD/l), CH_4 content (in %), CO_2 content (in %), HAc concentration (in gCOD/l), and HPr concentration (in gCOD/l)

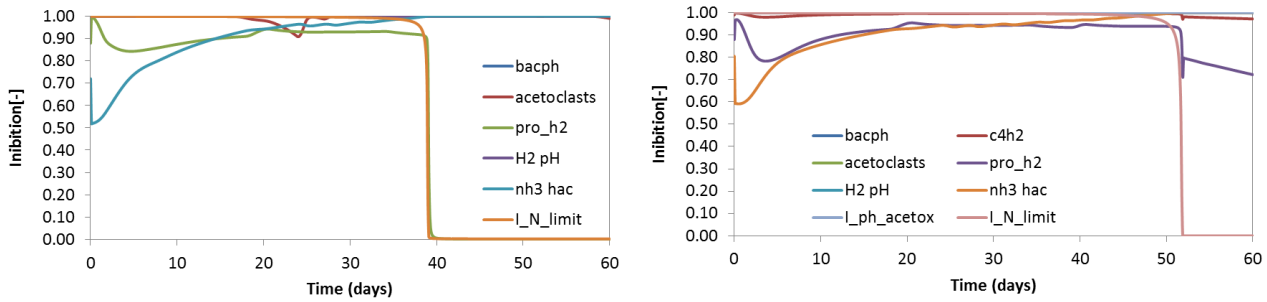

Figure T.5: Modelled inhibition function for Lignogas-SIM (left) and Lignogas (right)

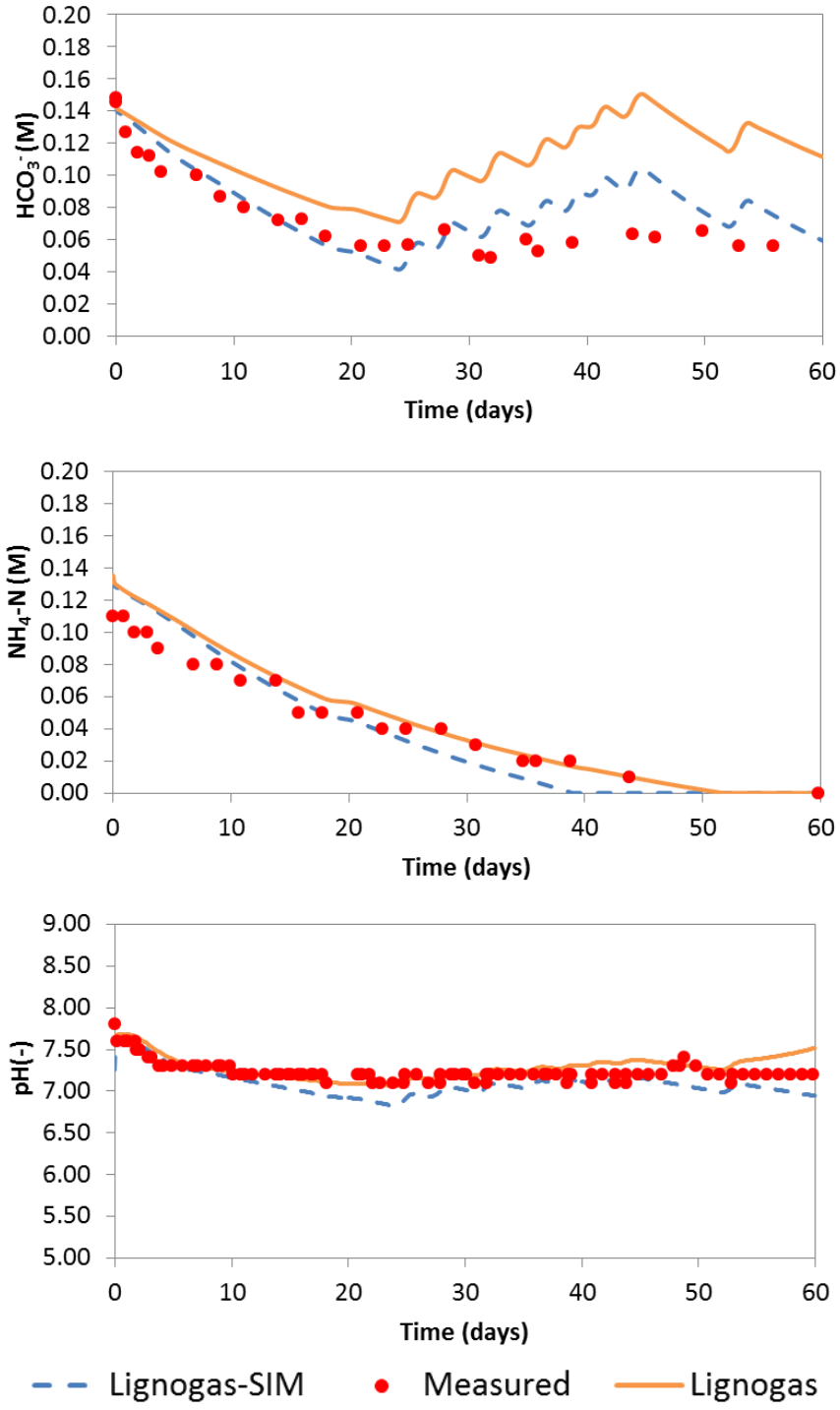

Figure T.6: Measured and modelled HCO_3^- (in moles C/l), (top), NH_4^+-N (in moles N/l) (centre), and pH (bottom) with Lignogas and Lignogas-SIM

Annex T.3: Semi-continuous digestion of DGS 3

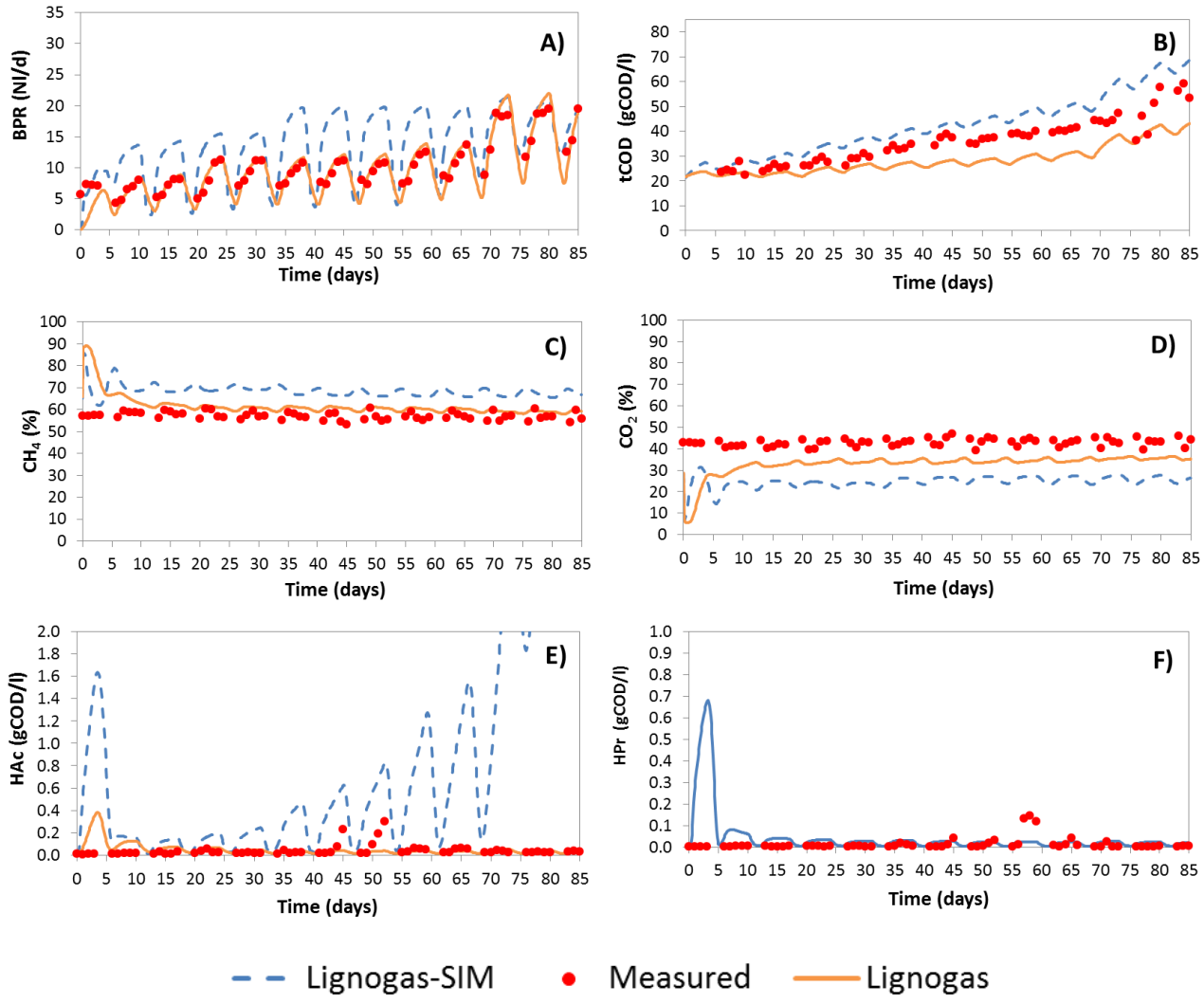

Figure T.7: Measured and modelled variables with Lignogas and Lignogas-SIM: A) BPR (in Nl/d), B) tCOD concentration evolution (gCOD/l), C) CH_4 content (in %), D) CO_2 content (in %), E) HAc concentration (in gCOD/l), and F) HPr concentration (in gCOD/l)

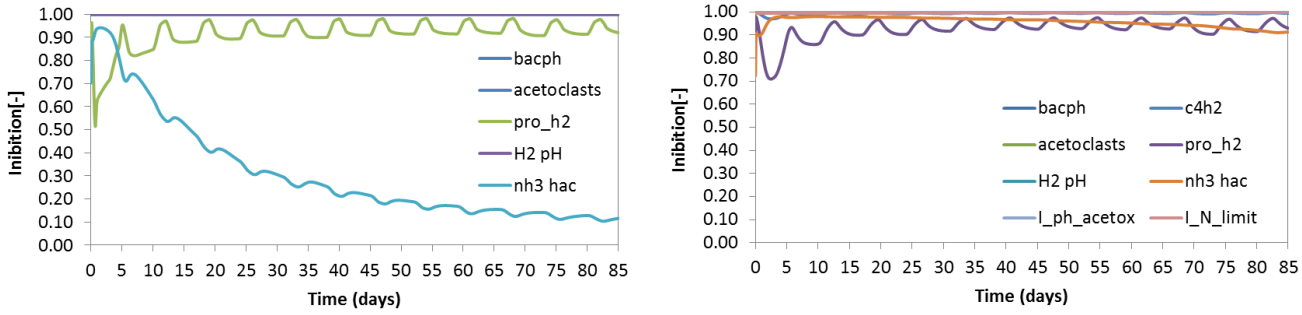

Figure T.8: Modelled inhibition function for Lignogas-SIM (left) and Lignogas (right)

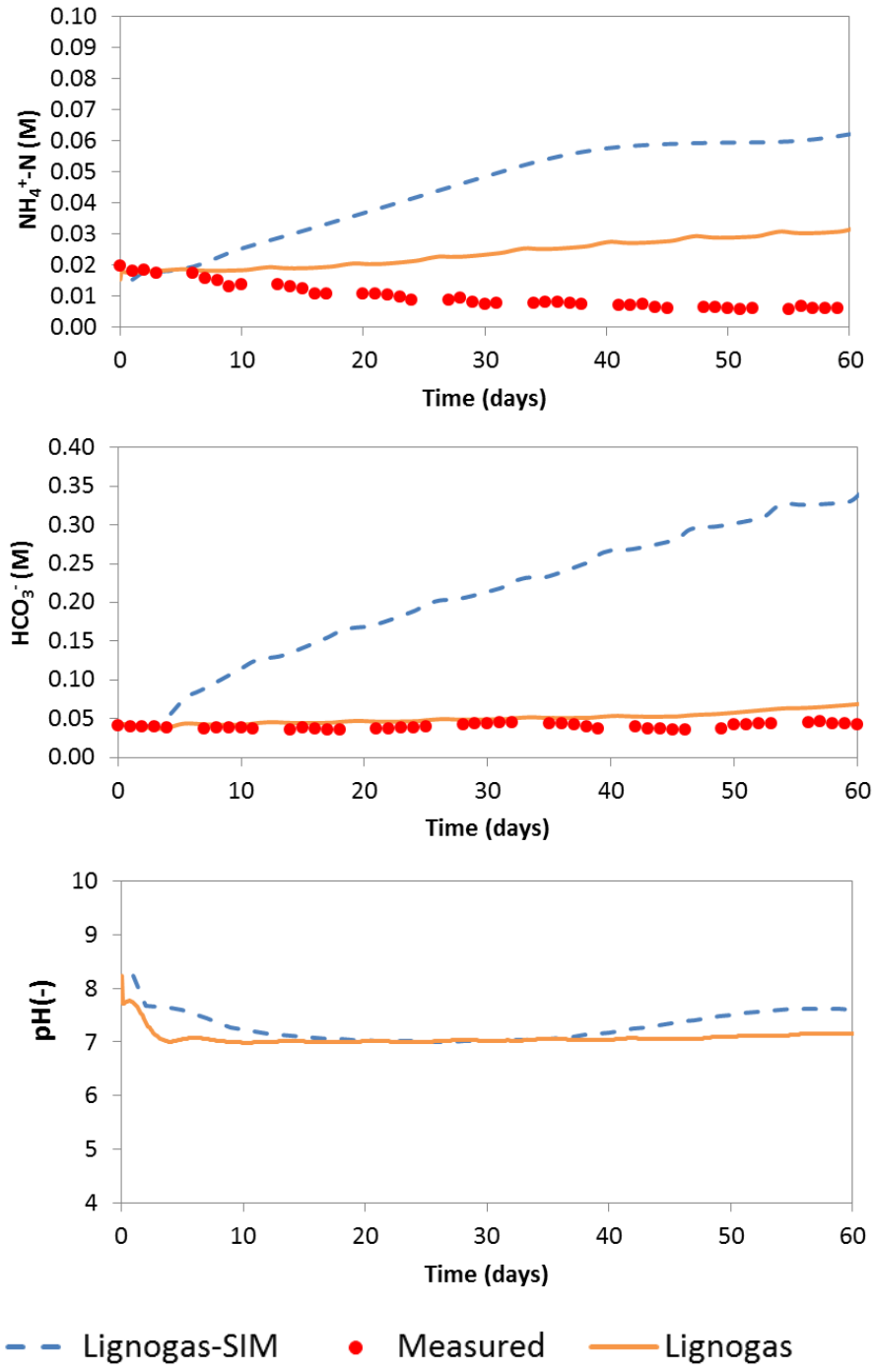

Figure T.9: Measured and modelled HCO_3^- (in moles C/l) (centre), NH_4^+-N (in moles N/l) (top), and pH (bottom) with Lignogas and Lignogas-SIM

Annex T.4: Semi-continuous digestion of DMS 2

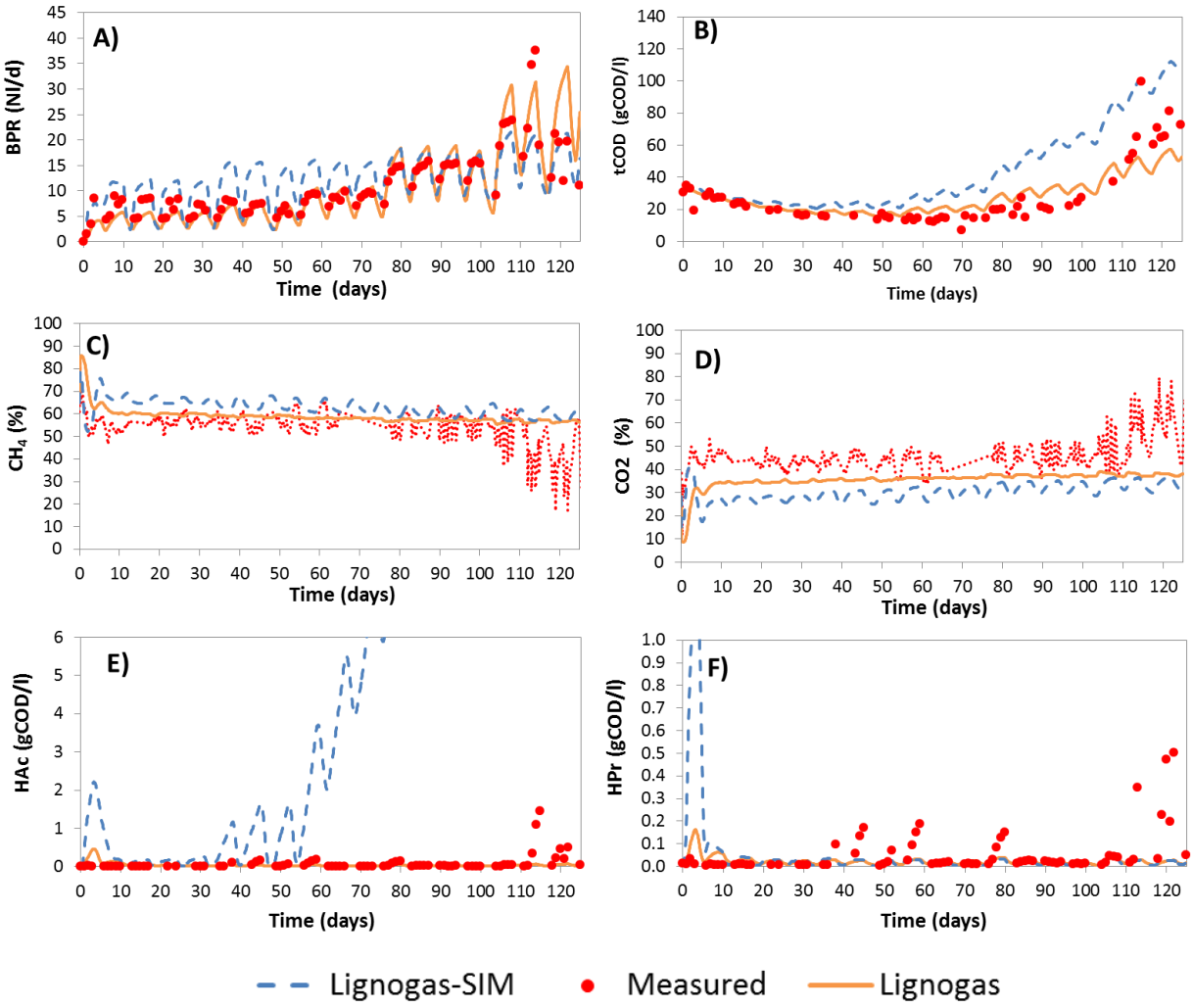

Figure T.10: Measured and modelled variables with Lignogas and Lignogas-SIM: A) BPR (in Nl/d), B) tCOD concentration evolution (gCOD/l), C) CH_4 content (in %), D) CO_2 content (in %), E) HAc concentration (in gCOD/l), and F) HPr concentration (in gCOD/l)

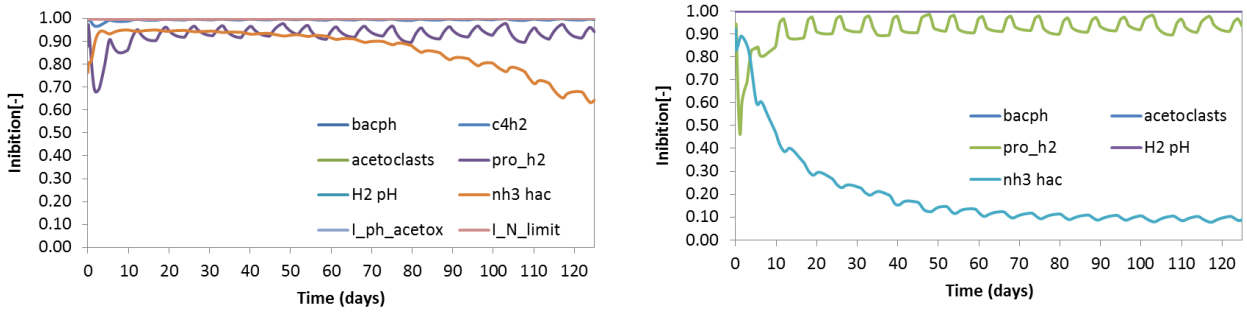

Figure T.11: Modelled inhibition function for Lignogas-SIM (left) and Lignogas (right)

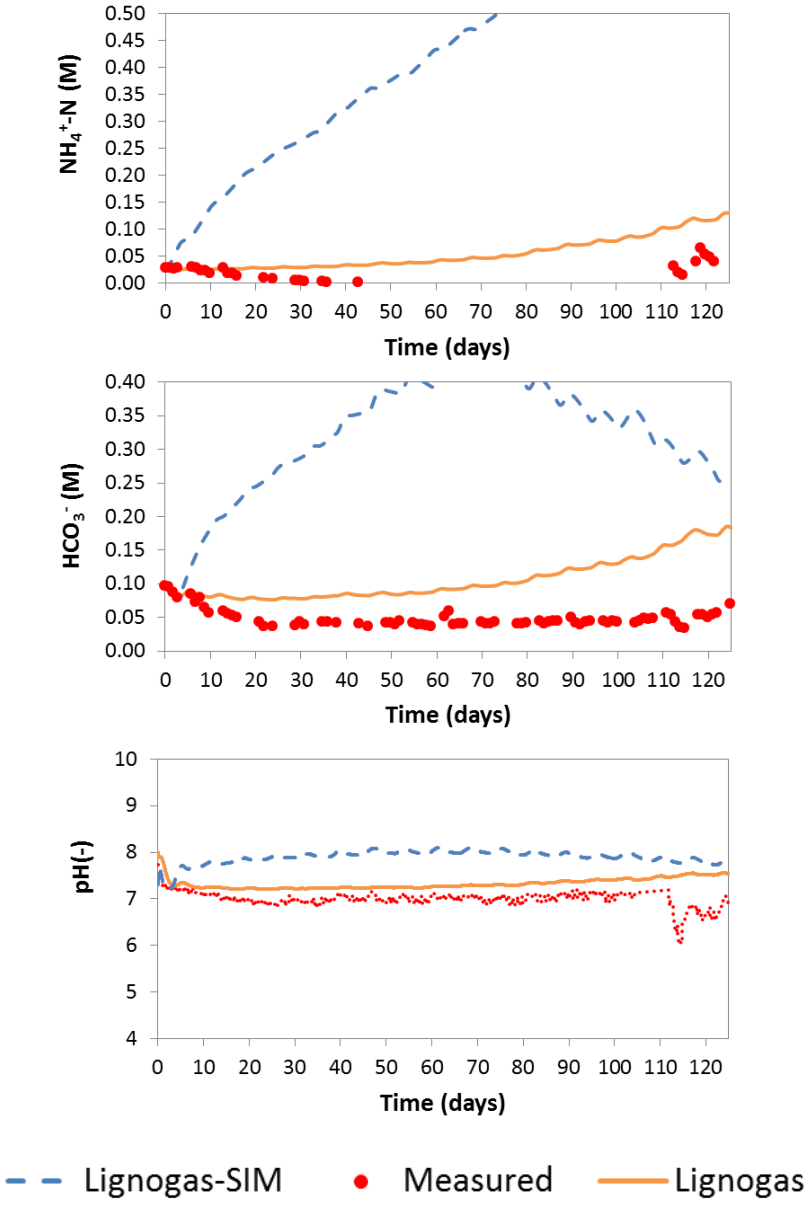

Figure T.12: Measured and modelled HCO_3^- (in moles C/l) (centre), NH_4^+-N (in moles N/l) (top), and pH (bottom) with Lignogas and Lignogas-SIM

Annex U: Probes used for q-PCR analysis (16SrDNA)

Probe	Name Set	Forward Primer Reverse Primer Sonde	Amplicon length
16SrDNA Archaeen	ARC	Archfw: ATTAGATACCCSBGTAGTCC Archrev: GCCATGCACCWCCTCT ArchTaqman: AGGAATTGGCGGGGGAGCAC	~ 273
16SrDNA Methanobacteriales	MBT	Mbacfw: CGWAGGGAAGCTGTTAAGT Mbacrev: TACCGTCGTCCACTCCTT MbacTaqman: AGCACCACAACGCGTGGA	~ 343
16SrDNA Methanomicrobiales	MMB	Mmicrfw: ATCGRTACGGGTTGTGGG Mmicrrev: CACCTAACGCRCATHGTTTAC MmicrTaqman: TYCGACAGTGAGGRACGAAAGCTG	~ 506
16SrDNA Methanosarcinaceae	Msc	Mscfw: GAAACCGYGATAAGGGGA Mscrev: TAGCGARCATCGTTTACG MscTaqman: TTAGCAAGGGCCGGGCAA	~ 408
16SrDNA Methanosaetaceae	Mst	Msaetfw: TAATCCTYGARGGACCACCA Msaetrev: CCTACGGCACCRACMAC MsaetTaqman: ACGGCAAGGGACGAAAGCTAGG	~ 164